CLASSIC UPPER PALEOZOIC REEFS AND BIOHERMS OF WEST TEXAS AND NEW MEXICO

A FIELD GUIDE TO THE GUADALUPE AND SACRAMENTO MOUNTAINS OF WEST TEXAS AND NEW MEXICO

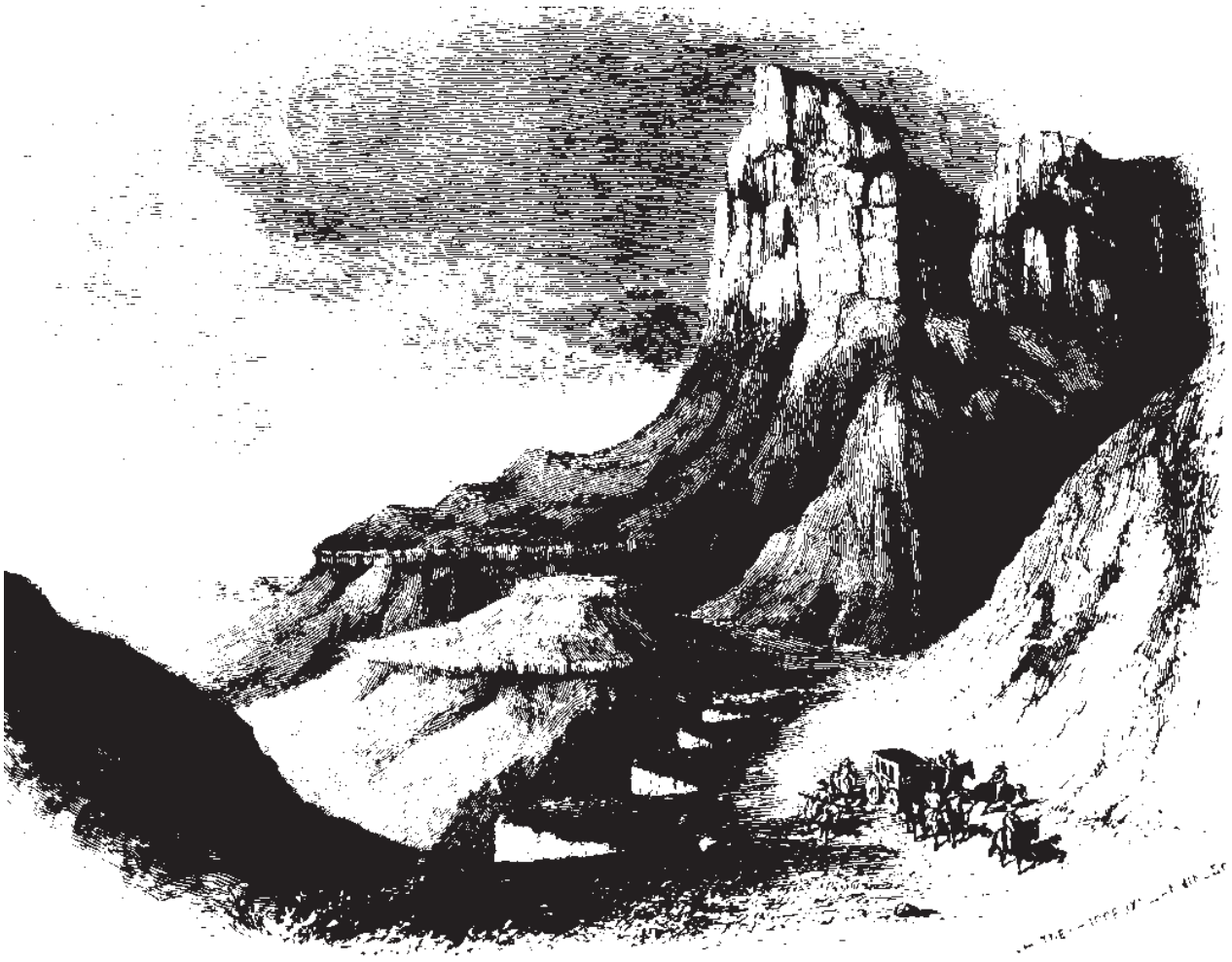

by Peter A. Scholle, Robert H. Goldstein and Dana S. Ulmer-Scholle

Cover illustration: El Capitan and Guadalupe Peak as viewed from the Guadalupe Pass area by Bartlett in 1850 on his journey by wagon from San Antonio to El Paso (from a wood-block engraving in Bartlett, 1854).

Acknowledgments

Dr. Robert Halley, although no longer an active participant in the trip and the writing of this edition of the guidebook, was instrumental in the original field seminar run for the U. S. Geological Survey and later for the American Association of Petroleum Geologists. His contributions and his generosity in continuing to allow them to be used, are greatly appreciated.

CLASSIC UPPER PALEOZOIC REEFS AND BIOHERMS OF WEST TEXAS AND NEW MEXICO

FIELD GUIDE TO THE GUADALUPE AND SACRAMENTO MOUNTAINS OF WEST TEXAS AND NEW MEXICO

By

Peter A. Scholle
New Mexico Bureau of Geology and Mineral Resources
New Mexico Institute of Mining and Technology
Socorro, NM 87801

Robert H. Goldstein
Department of Geology
University of Kansas
Lawrence, KS 66045

Dana S. Ulmer-Scholle
Department of Earth & Environmental Sciences
New Mexico Institute of Mining and Technology
Socorro, NM 87801

Open-file Report 504
New Mexico Bureau of Geology and Mineral Resources
A division of the New Mexico Institute of Mining and Technology
801 Leroy Place
Socorro, New Mexico 87801-4796

September, 2007

CONTENTS

PART I:
THE PERMIAN REEF COMPLEX OF THE GUADALUPE MOUNTAINS

PETER A. SCHOLLE

AND

DANA S. ULMER-SCHOLLE

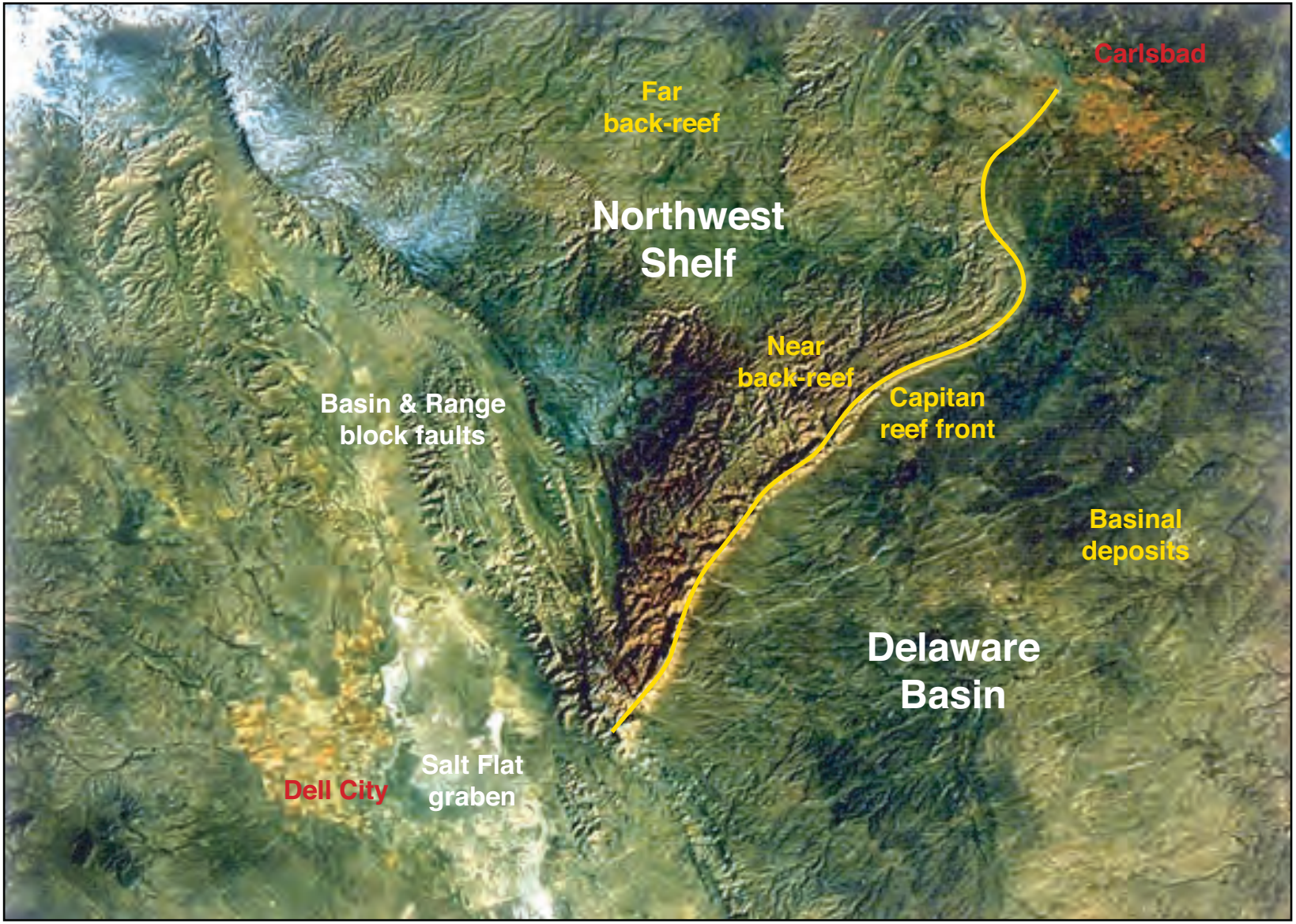

Frontpiece. Satellite view of the Guadalupe Mountains (center top). Landsat photograph was taken on January 15, 1977. Capitan reef front forms the right margin of the triangular Guadalupe Mountain block and separates the Delaware Basin (right) from the Northwest Shelf (left). This restored Permian landscape has resulted from modern dissolution of post-Capitan evaporites. The west side of the range is formed by a series of Basin and Range block faults that border the Salt Flat graben.

GENERAL SETTING

The Permian Basin region of New Mexico and west Texas provides an excellent opportunity to study the interrelationships of depositional facies, diagenetic alteration patterns, oil generation and migration and ultimately, petroleum potential and production from carbonate reservoirs. The Guadalupe and Delaware Mountains, in particular, contain some of the finest outcrops of reef and reef-related rocks in the world. It is also a region of stark, yet often spectacular, beauty and of rich history, both for Native Americans and later arrivals.

The entire depositional spectrum from far-back-reef to deep basin can be observed in outcrops of the Guadalupe Mountains and adjacent areas (Fig. 1), with little or no structural deformation and slight vegetation or soil cover. The reef complex of this region is dissected by a series of deep canyons cut approximately at right angles to the regional facies strike. These canyons, especially McKittrick and Slaughter Canyons, provide exceptional cross-sectional views of the lateral and vertical relations of depositional environments through time.

Finally, the region is rather exceptional in that, at the end of Guadalupian time, the entire suite of facies was preserved (essentially pickled) by extremely rapid deposition of evaporites (gypsum/anhydrite, halite, sylvite, and more exotic salts). These Ochoan evaporites filled the Delaware Basin remnants and even covered adjacent shelfal areas. Thus, original facies relations were preserved from extensive erosional modification, and late Tertiary uplift, coupled with dissolution of the very soluble evaporites, has led to resurrection of original (Permian) topography (Fig. 2), greatly facilitating facies reconstruction.

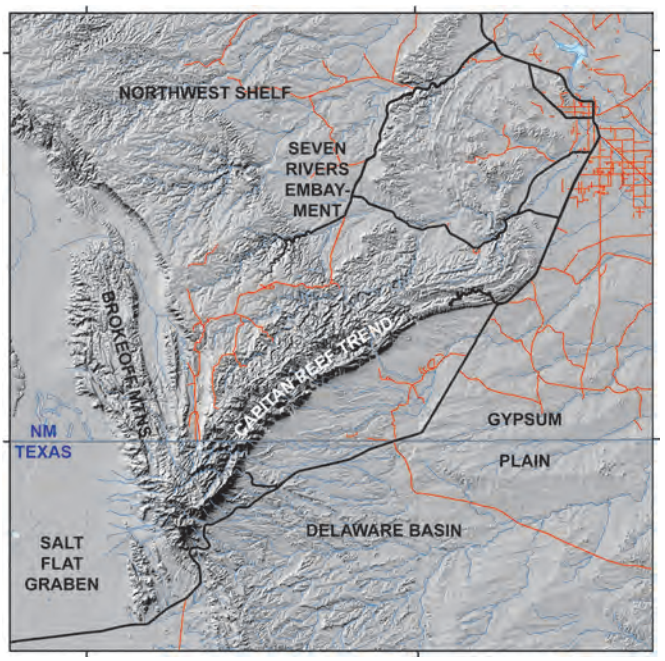

Figure 2. Modern topographic expression of exhumed depositional and structural features of the southern Guadalupe Mountains, Texas and New Mexico.

Figure 1. Photograph of the north wall of McKittrick Canyon, Guadalupe Mountains National Park showing the shelf-to basin facies of the late Guadalupian Capitan reef. Strata at top of section at far left are Yates and Tansill back reef carbonates; massive triangular cliff just to the right is last phase of Capitan reef development; strata below and to the right of the reef are steeply-dipping fore-reef talus beds which flatten and pass laterally into the deeper-water sediments of the Delaware Basin.

In addition to the advantages provided by these outcrops, the Permian Basin has a wealth of subsurface data. More than 50,000 exploration wells and hundreds of thousands of development wells have been drilled in the Permian Basin region, leading to the discovery of 4,000-5,000 oil and gas fields. All the outcrop facies of the Guadalupe, Delaware, and Glass Mountains are encountered in the subsurface Delaware Basin,

Northwest Shelf, Central Basin Platform, Midland basin (Fig. 3) and, to a lesser degree, the Marfa basin. Thus, the associations of oil and gas with specific depositional and diagenetic facies can be clearly established in this region.

PREVIOUS STUDIES

A number of classic studies have been completed on the "Permian reef complex" of New Mexico and Texas that have established an excellent stratigraphic and sedimentologic framework for the region. Three early studies (King, 1948; Adams and Frenzel, 1950; Newell et al., 1953), in particular, presented the overall outlines of our modern concept of reef-related depositional environments. Subsequent studies, including those of Dunham (1972), Esteban and Pray (1977), Harms (1974), Hayes (1964), Mazzullo and Cys (1977), Meissner (1972), Sarg and Lehman (1986a and b), Schmidt (1977), Tyrrell (1969), Ward et al. (1986), and numerous University of Wisconsin graduate students under Lloyd Pray's direction (e.g., Babcock, 1977a; Candelaria, 1982 and 1989; Crawford, 1981 and 1989; Franseen, 1985 and 1988; Rossen, 1985; Sarg, 1981 and 1989b; Yurewicz, 1976, 1977; and others) have fleshed in the details of many of the depositional environments and have contributed to our understanding of the diagenetic history of the region. In recent years, stratigraphic studies have focused primarily on large-scale sequence stratigraphic interpretations (Beaubouef et al., 1999; Kerans and Fitchen, 1995; Lindsay and Reed, 1992; Mutti and Simo, 1993; Osleger, 1998; Sarg, 1985 and 1989a; Tinker, 1998), bed-scale cyclicity (Borer and Harris, 1991; Gardner, 1991; Harris et al., 1993; Kerans and Nance, 1991; Lowenstein, 1988; Sonnenfeld, 1991), or chemostratigraphy (Colgan, 1990; Grossman, 1994; Magaritz et al., 1983; Scholle, 1995). Finally, studies of Holocene deposits in unusually arid modern settings have also contributed directly to our understanding of comparable deposits in the Permian (e.g., Kendall, 1969; Warren, 1983; Handford et al., 1984; Logan, 1987).

In spite of all this research, few areas have more unresolved geological controversies than the Permian reef complex. Every single one of the facies represented in the spectrum of basinal to far-back-reef settings has evoked a variety of opinions (discussed later) as to its origin or significance.

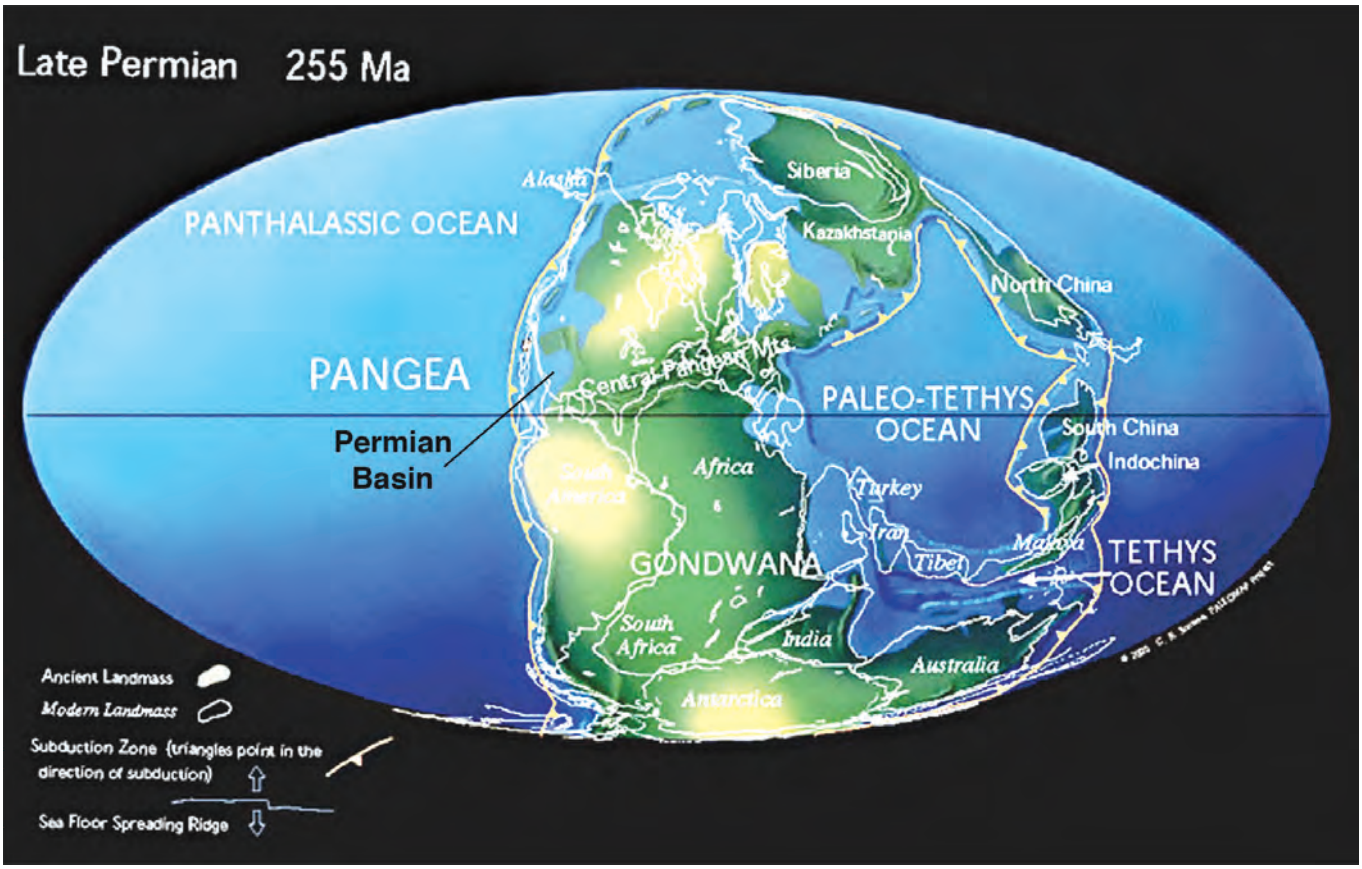

Figure 3. Continental recontruction during Late Permian (Kazanian) time. In this model, the Permian Basin lay just south of the equator and close to the western margin of the Pangean continent. Approximate present-day outlines shown for reference. (Scotese, C.R., http://www.scotese.com, PALEOMAP website, 2002).

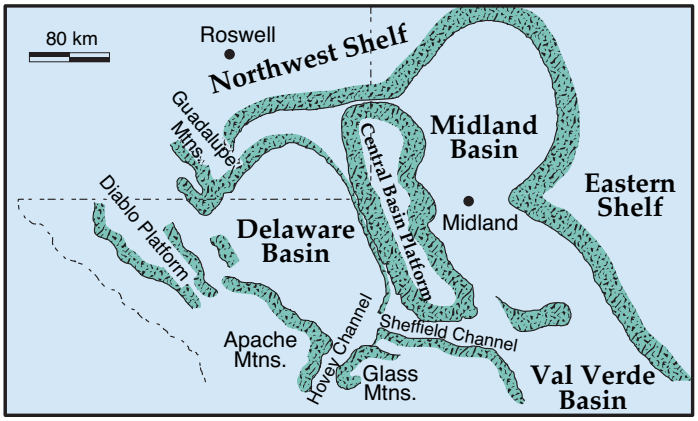

Figure 4. Major physiographic features of the Permian Basin region during early Guadalupian time. Major modern outcrop areas are also shown (Guadalupe, Diablo, Apache and Glass Mountains). Modified from Ward et al. (1986).

Thus, although the overall environmental framework of facies is generally agreed upon, much work remains to be done on specific interpretations.

STRUCTURAL HISTORY

The Permian Basin region was situated close to the western margin of Pangea during Late Permian (Guadalupian to Ochoan or, in international teminology, Guadalupian to Lopingian) time and lay about 10° north of the paleoequator of that time (Fig. 3), although the latitudinal estimate varies depending on the plate reconstruction one uses (Smith et al., 1973; Scotese et al., 1979; Irving and Irving, 1982; Scotese and McKerrow, 1990; Scotese and Langford, 1995). The region was part of the southern flank of the

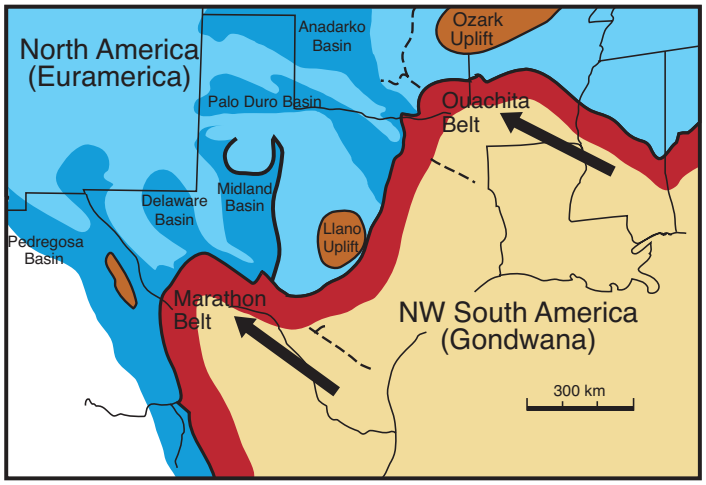

Figure 5. Diagrammatic representation of the tectonic setting of the Permian Basin. Large arrows indicate directions of major tectonic displacement (after Ross, 1986).

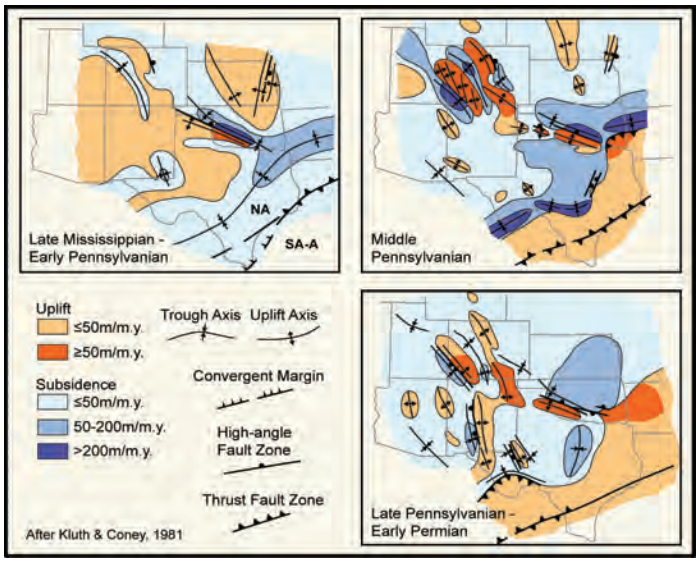

Figure 6. Paleotectonic evolution of the southwestern U.S. from the Late Mississippian to Early Permian. Adapted from Kluth and Coney (1981).

North American craton, a zone of moderate subsidence and shelfal, mainly carbonate, sedimentation until Late Mississippian time. During the late Paleozoic, the Permian Basin, along with the broader southwestern U.S. region, underwent substantial tectonism and was subdivided into a series of smaller basins and platforms (Figs. 4-6).

Some of these features formed well before the Permian; for example, there is some indication that the Central Basin Platform was already a positive topographic element during Early Mississippian time (Wuellner et al., 1986). However, full-scale initiation of the Delaware, Midland, Val Verde and Marfa basins (and associated shelfal areas) did not occur until the onset of the Pennsylvanian Ouachita-Marathon orogeny (Hills, 1984, 1985; King, 1948; Ross, 1979).

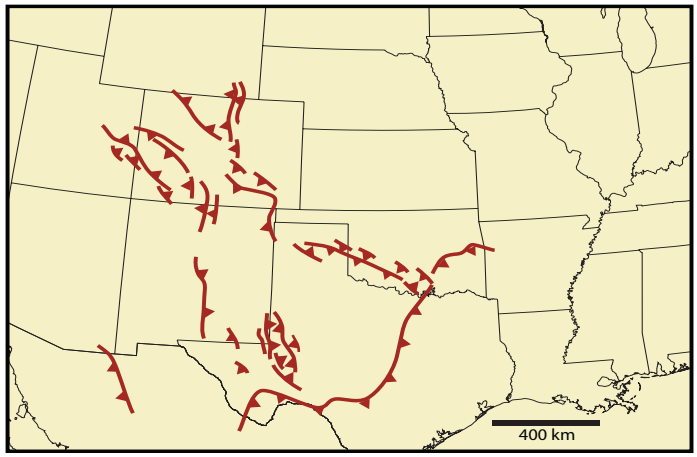

Figure 7. Distribution of Pennsylvanian Ancestral Rockies compressional structures in the southwestern U. S. (after Ye et al., 1996).

This major continental collision event, along with possible subduction along the western margin of North America established a regional transpressional regime, generated a complex foredeep trough in the Permian Basin region, and caused the rejuvenation of older, north-south to northwest-southeast oriented basins and uplifts, including the Ancestral Rockies (Kluth and Coney, 1981; Ross, 1986; Goetz and Dickerson, 1985; Yang and Dorobek, 1993, 1994; Ye et al., 1996; see Figs. 5-7). The orogeny formed the underlying control for most Late Pennsylvanian to Permian sedimentation from Texas to Colorado and led to the eventual formation of a platform-to-basin geometry similar to that seen in the Bahamas today (Ball, 1967; Ball et al., 1969; Fig. 8). The major paleotopographic features of the region are bounded by complex sets of high-angle faults that generally formed along reactivated earlier Late Precambrian to Cambrian structural lineaments (Hills, 1984; Oriel et al., 1967; Ross, 1986).

Such structures were further accentuated by differential sedimentation and regional subsidence during Permian time, resulting in the complex features shown in the cross-section of the Central Basin Platform and adjacent areas (Fig. 9). In this scenario, original structural relief was significantly accentuated by higher rates of sedimentation of shallow water carbonate deposits on structural "highs" compared with lower rates of sediment reworking into structural "lows." Thus, basins that may have been only a few tens of meters deep at the start of Permian time eventually had water depths in excess of 500 m (1,600 ft) by the close of Guadalupian time. These paleo-water-depths are reasonably well established because large-scale continuity of outcrop has allowed the physical measurement (after correction for compaction) of elevation differences between age-equivalent shelf and basin deposits.

Although these local variations in sedimentary facies and sedimentation rates existed, the Permian Basin was also subjected to broad, regional subsidence, resulting in the accumulation of between 2,100 and 4,200 m (7,000 and 14,000 ft) of Permian clastic terrigenous, carbonate and evaporite strata (McKee et al., 1967a, b). Specifically, about 3.5 km (12,000 ft) of Permian strata have been measured in outcrops from the Guadalupe Mountains, on the western side of the Permian Basin (King, 1948). In that area, the Middle Permian (Guadalupian) section, the main focus of this field trip, contains about 1 km (3,500 ft) of sediment and the overlying Late Permian (Ochoan) sequence is even thicker where it is preserved in the Delaware Basin. Considering that most current geologic timescales accord approximately 17 million years to the combined Guadalupian-Ochoan interval (Wardlaw et al., 2004), Permian average rates of basin subsidence and sedimentation were fairly high (>100-150 m/my).

The Permian Basin region was part of a stable, largely non-depositional province during Mesozoic time. Minor tectonic movements during the Laramide period, coupled with extensive uplift of the western part of the region during middle to late Tertiary Basin and Range block faulting, produced a significant (approximately 5-10°) regional east-

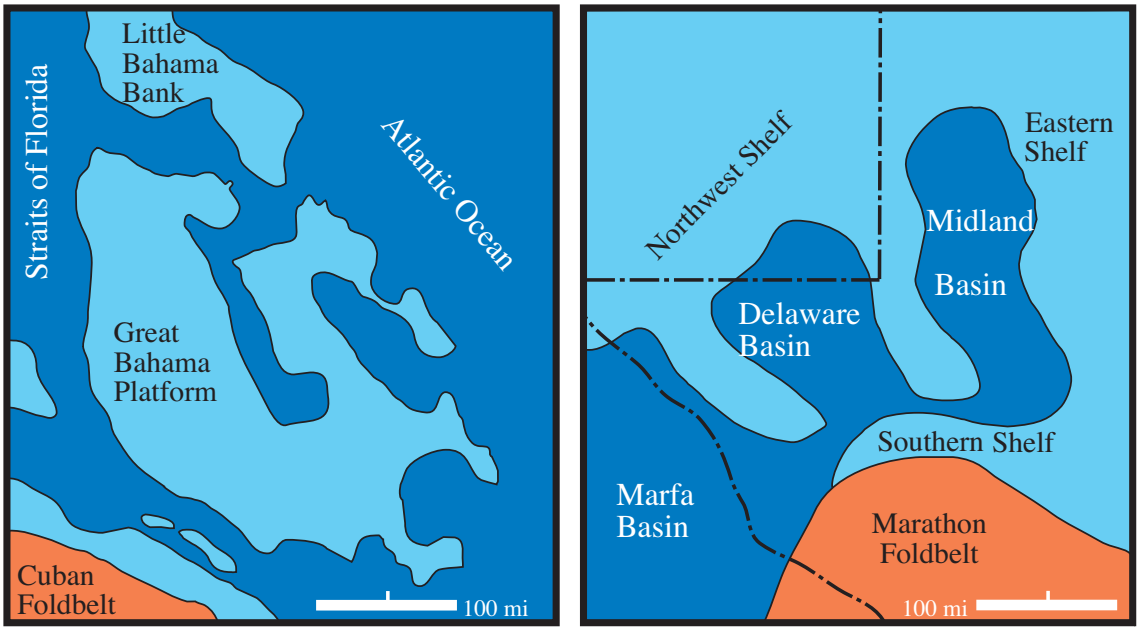

Figure 8. Comparison of the physiographies of the modern Bahama platform and the Permian Basin at equal scales; orange represents active tectonic belts; dark blue indicates deeper-water areas; light blue shows shelf areas — Bahamian basins are 1 to 4 km deep whereas the Permian ones were less than 600 m deep (adapted from Ball et al., 1969).

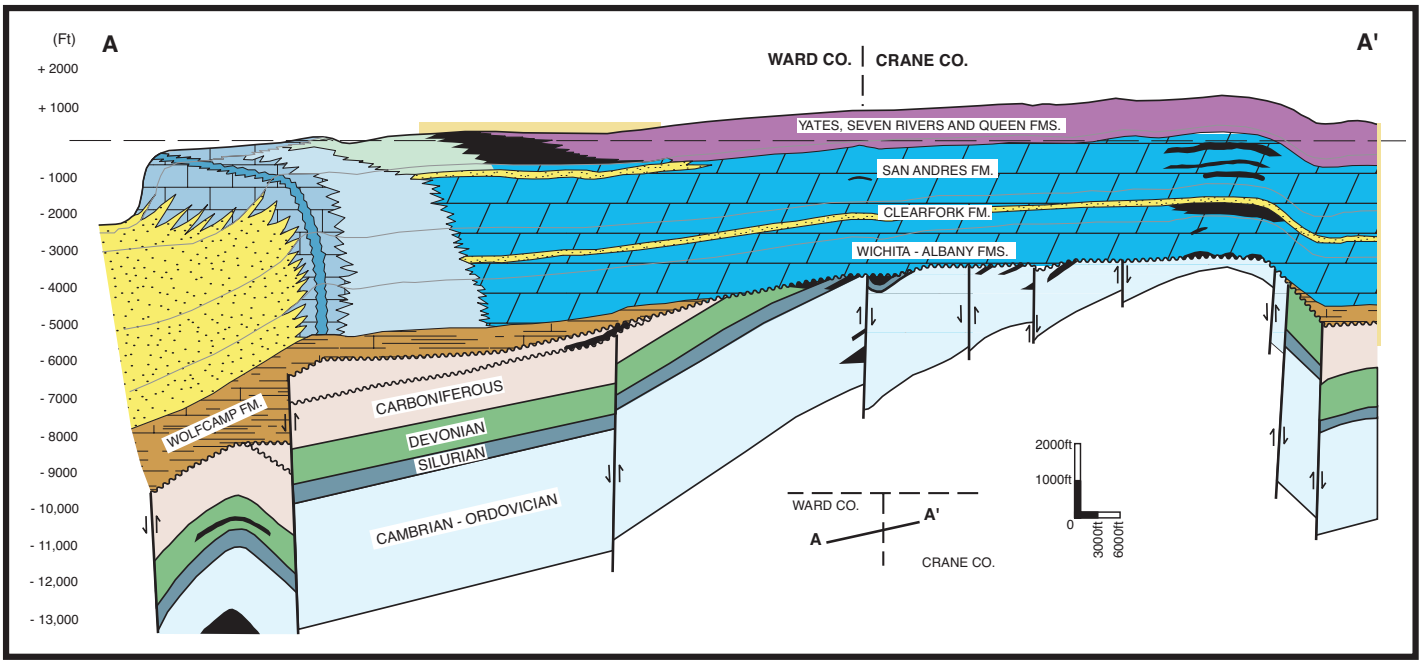

Figure 9. Cross section through the western part of Central Basin Platform showing relationship between structure and stratigraphy of Paleozoic strata. Oil fields are shown in black. Modified from Ward et al. (1986).

ward dip of pre-Tertiary strata (Fig. 10). This deformation led to erosional exhumation of original Permian topography on the western margin of the region, widespread influx of meteoric waters with renewal of deep ground-water circulation, dissolution and/or replacement of Permian evaporites, and widespread cavern formation in limestones of the Guadalupe Mountains. Tertiary uplift is directly responsible for the extensive, but scattered, exposures of Middle Permian shelf-to-basin facies along the western and southern margins of the former Delaware Basin in the Guadalupe Mountains, Apache Mountains and Glass Mountains of west Texas and New Mexico. It is also responsible for the superimposition of numerous high-angle faults and fractures on the Permian rocks of the Guadalupe Mountains, especially along the western escarpment and the Brokeoff Mountains (King, 1948) where these faults greatly complicate stratigraphic studies.

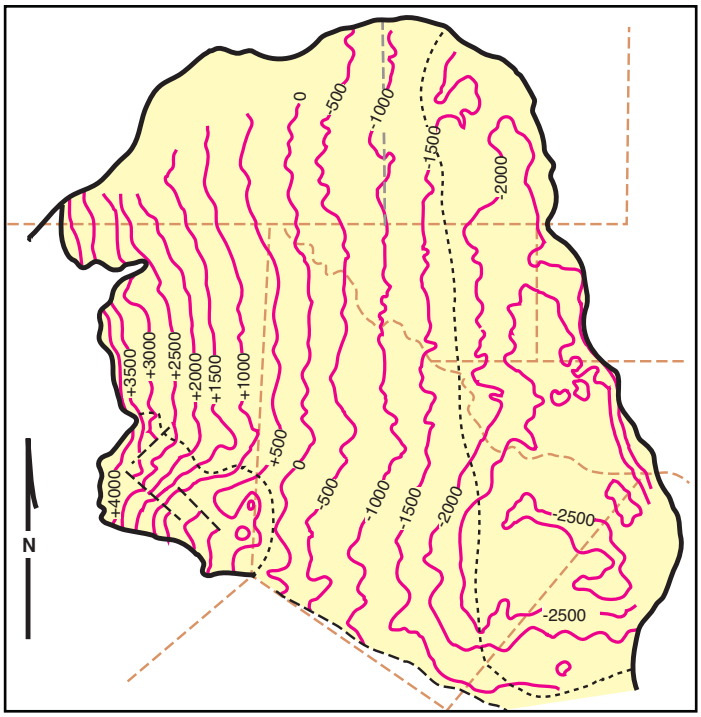

Figure 10. Structure contour map of the Delaware Basin, drawn on top of the Bell Canyon Fm. (from Grauten, 1965).

STRATIGRAPHIC SETTING AND NOMENCLATURE

The Permian reef complex is characterized by three sections of time-equivalent but lithologically very dissimilar rocks. The first facies consists of thick masses of finely laminated siltstones and sandstones with thinner, interbedded, gray to black limestones. The second facies contains massive, light-gray limestones overlying steeply bedded, partially dolomitized, blocky limestone rubble. The third zone contains tan, fine-grained, medium-bedded dolomites with interbedded evaporites and red to brown sandstone and siltstone units.

As early as the late 1920s, it was recognized that these three rock packages represent strata deposited, respectively, in basinal, shelf-margin, and shelf-interior settings

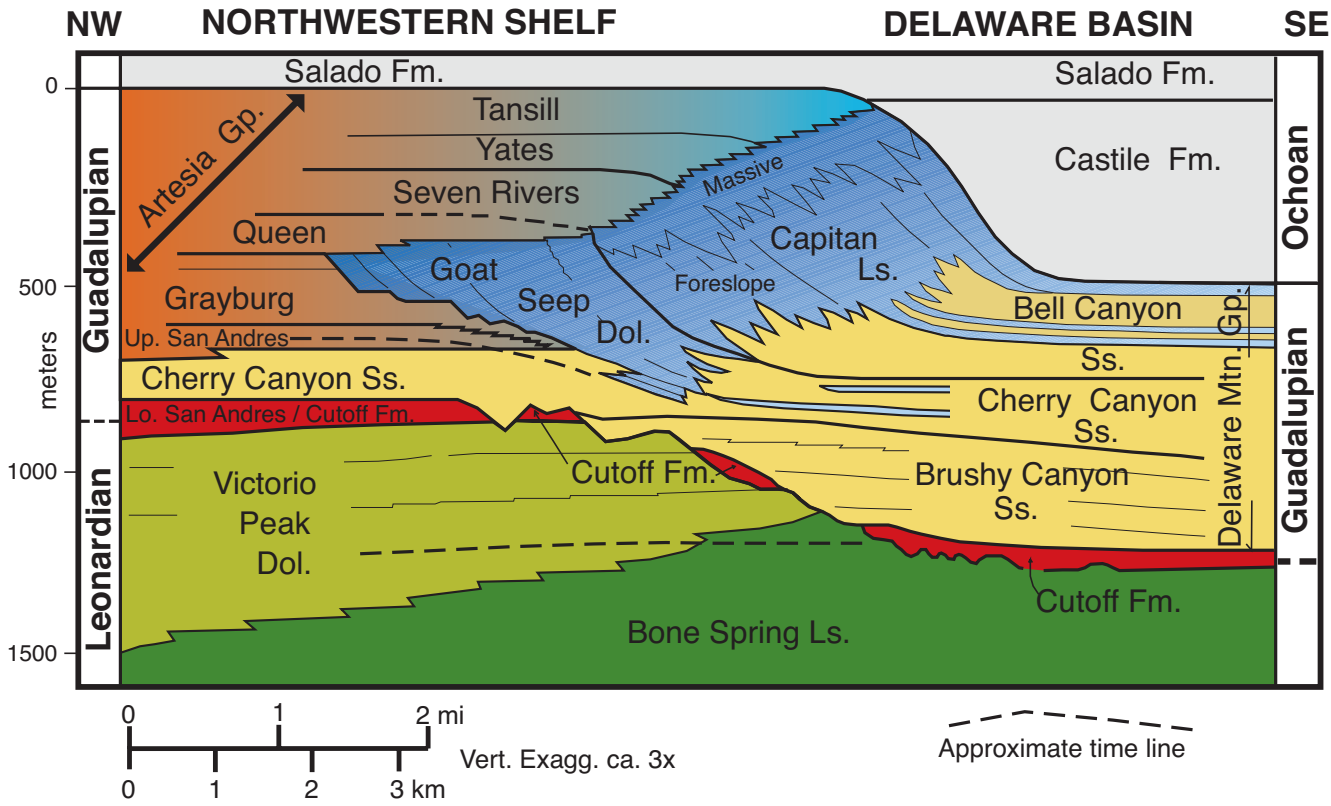

Figure 11. Stratigraphic nomenclature of the Permian rocks exposed in the Guadalupe Mountains. Modified from numerous sources including King (1948), Hayes (1964), Tyrrell (1969) and Pray (1988a).

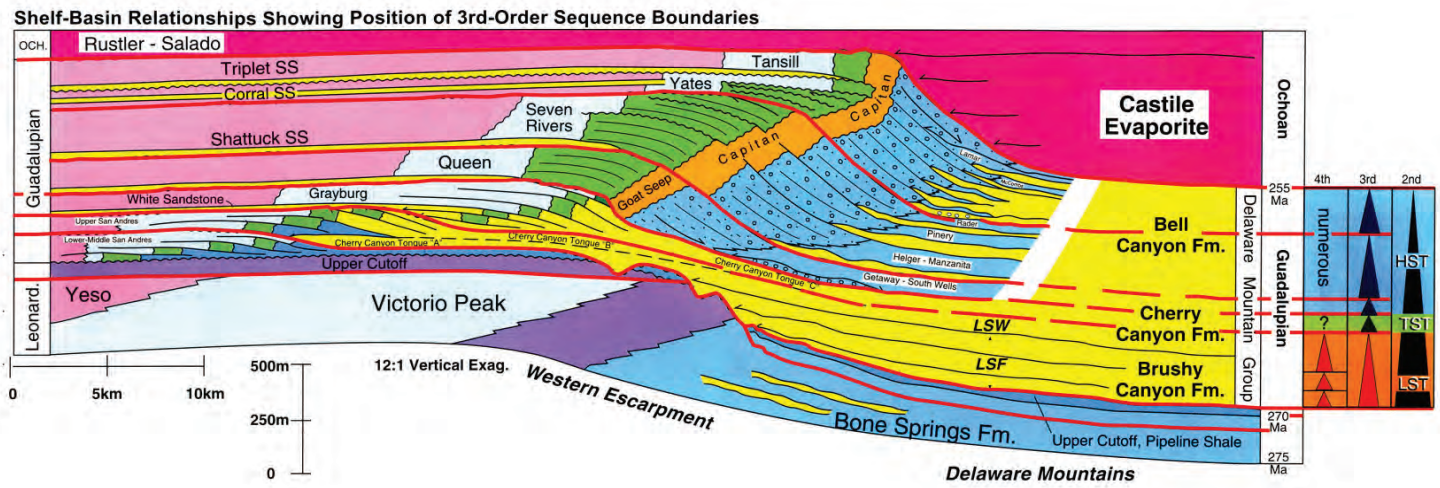

Figure 12. Simplified 2nd- and 3rd-order sequence stratigraphic framework of the Permian rocks exposed in the Guadalupe Mountains. From Beaubouef et al. (1999).

(Blanchard and Davis, 1929; Crandall, 1929; Lloyd, 1929). These conclusions were drawn largely on lithologic and structural criteria, but subsequent work (e.g., King, 1948; Newell et al., 1953; Babcock, 1977a) on faunal, floral, sedimentologic and stratigraphic aspects of these units has confirmed the initial conclusions.

The stratigraphic nomenclature used in this guidebook largely follows the standard terminology of King (1948), Newell et al. (1953), Hayes (1964), and Tyrrell (1969), as are shown in the figures below (Figs. 11, 12); thus, the nomenclature will not be discussed in much detail. Table 1 shows the regional stratigraphic terminology for the entire Phanerozoic section; Figure 11 provides the terminology for the Guadalupian of the entire area; Figure 12 depicts the sequence stratigraphic framework of that same section; Figure 13 shows the detailed nomenclature used for basin

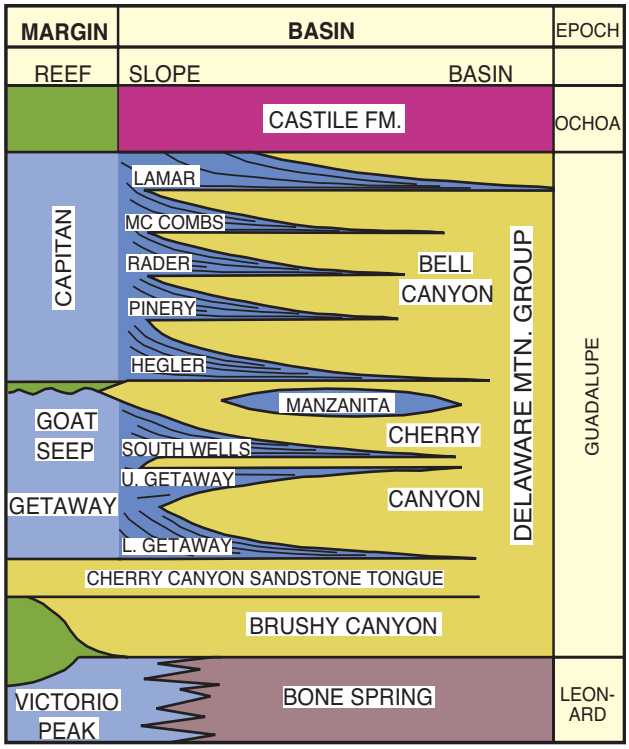

Figure 13. Diagrammatic representation of the Guadalupian shelf margin to basin stratigraphic nomenclature in the Delaware Basin region (after King, 1948).

and basin-margin strata only. All the terminology for the Leonardian to Ochoan interval reflects the structurally-influenced depositional settings in the area: shelf, shelf margin and basin. For example, strata of the upper Guadalupian Goat Seep and Capitan Formations were formed in shelf margin settings as barrier reef boundstones and associated fore-reef debris aprons. The Queen, Seven Rivers, Yates and Tansill Formations (Fig. 11) are the shelfal redbed, evaporite, and dolomite units that are age-equivalent to the Goat Seep-Capitan section. Likewise, the Bell Canyon Formation (which, along with the Brushy Canyon and Cherry Canyon formations, is part of the Delaware Mountain Group) represents the Capitan-correlative, dominantly terrigenous, basinal section. Leonardian and early Guadalupian strata show similar shelf-to basin sequences but without reefal shelf margins. Ochoan strata are dominantly evaporites that fill remnant topography enhanced by differential Guadalupian shelf-to-basin carbonate sedimentation.

Numerous authors have pointed out that cyclic sedimentation of one sort or another is widespread in the Permian Basin in Pennsylvanian as well as Permian strata (e.g., Meissner, 1972; Silver and Todd,

Table 1. Correlation of Permian sections in west Texas and southeastern New Mexico (adapted from McKee et al., 1967a).

AGE		STRATIGRAPHIC UNIT			
SYSTEM	SERIES	DELAWARE BASIN	CENTRAL BASIN PLATFORM	MIDLAND BASIN	EASTERN SHELF
Q		Alluvium	Alluvium Ogallala	Alluvium Ogallala	Alluvium Ogallala
CRETACEOUS	Gulfian				
	Comanchean	Fredericksburg Trinity Ss.	Fredericksburg Trinity Ss.	Washita Fredericksburg Trinity Ss.	Washita Fredericksburg Trinity Ss.
TR	Upper	Santa Rosa	Dockum	Dockum	Dockum
PERMIAN	Ochoan	Dewey Lake Rustler Salado Castile	Dewey Lake Rustler Salado Castile	Dewey Lake Rustler Salado	Rustler Salado
	Guadalupian	Delaware Sands: Bell Canyon	Capitan Reef: Tansill, Yates, Seven Rivers, Queen, Grayburg	Tansill Yates Seven Rivers Queen Grayburg	Tansill Yates Seven Rivers Queen Grayburg
		Cherry Canyon Brushy Canyon	San Andres	San Andres	San Andres
	Leonardian	Bone Spring	Clear Fork / Tubb Wichita	Spraberry Dean Leonard	Clear Fork Wichita
	Wolfcampian	Wolfcamp	Wolfcamp	Wolfcamp Thin to absent	Wolfcamp
PENNSYLVANIAN	Cisco	Cisco	Cisco	Cisco Horseshoe Atoll	Cisco
	Canyon	Canyon	Canyon	Canyon	Canyon
	Strawn	Strawn	Strawn	Strawn	Strawn
	Atokan	Atoka	Atoka	Atoka	Atoka Bend
	Morrowan	Morrow			
MISSISSIPPIAN		Mississippian ? ? ? Kinderhook Woodford Shale	Mississippian Kinderhook Woodford Shale	Mississippian Ls. Kinderhook Woodford Shale	Mississippian Ls. Lower Woodford Sh.
DEVONIAN		Devonian Upper Silurian Sh. Fusselman	Devonian U. Silurian Sh. Fusselman	Devonian Upper Silurian Sh. Fusselman Sylvan Shale	U. Silurian Sh. Fusselman
ORDOVICIAN	Upper	Montoya	Montoya	Montoya	
	Middle	Simpson Group	Simpson Group	Simpson Group	
	Lower	Ellenburger	Ellenburger	Ellenburger	Ellenburger
CAMBRIAN	Upper			Wilberns	Wilberns Hickory
pC					

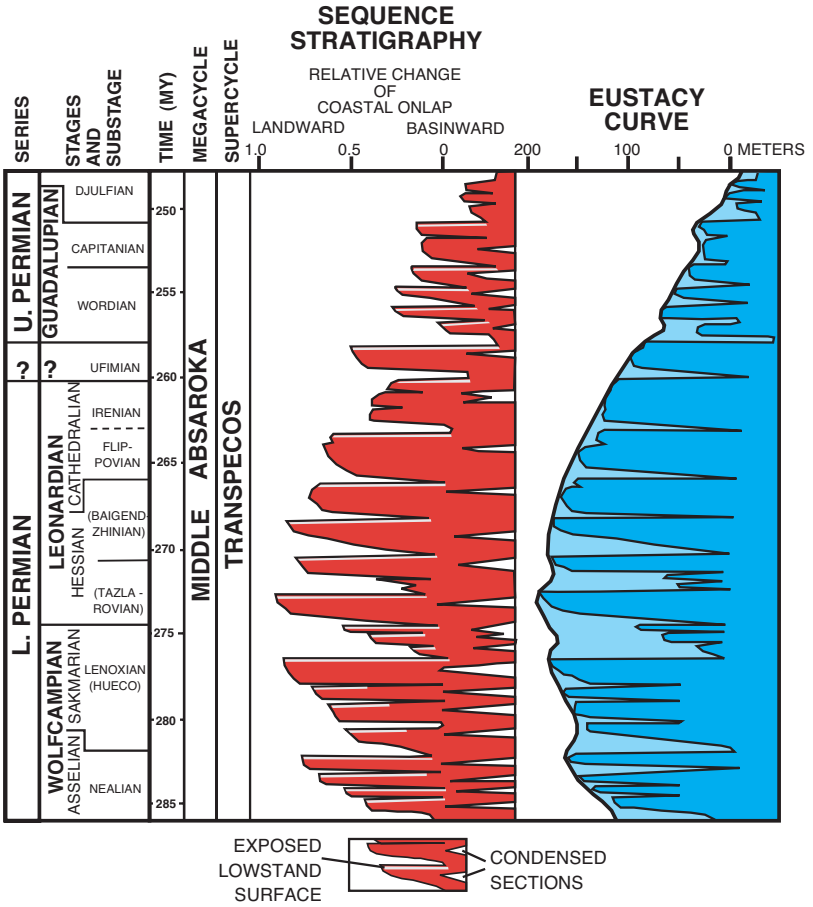

Figure 14. Inferred coastal onlap and eustacy curves for the Permian (adapted from Ross and Ross, 1987a).

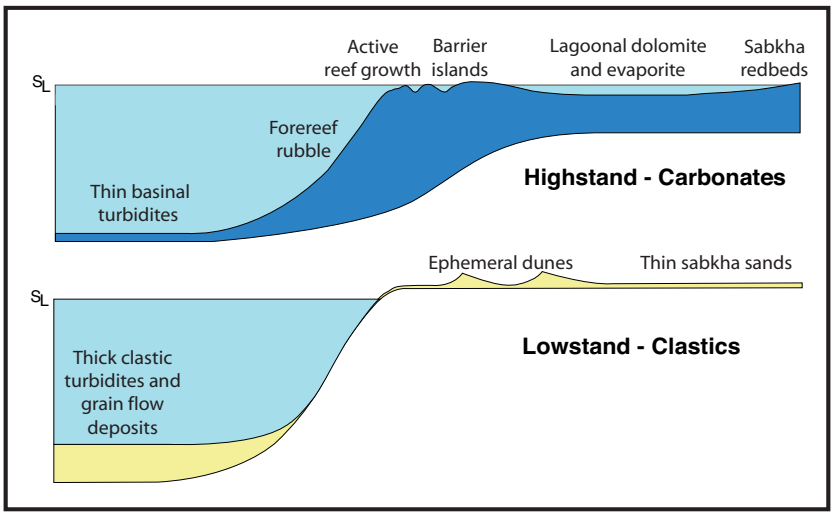

Figure 15. Diagrammatic representation of sea-level high- and low-stand deposition in Guadalupian strata.

1969; Wilson, 1972; Sarg, 1985 and 1989a; Tinker, 1998; Beaubouef et al., 1999). Cyclic sedimentation operated at a number of scales, from fractions of a meter to hundreds of meters, and such cycles were superimposed on an apparently long-term drop in sea level through much of Permian time. Broader sequence stratigraphic studies have indicated that the large-scale cycles (Fig. 14) may be world-wide in extent (Ross and Ross, 1985b, 1987b, 1988), and known Late Pennsylvanian to Permian glacial advances and retreats may have contributed to the generation of such cycles by creating periodic eustatic sea-level changes (Crowell, 1978 and 1982).

Although dating of these southern hemisphere glacial events is far from exact due to the provinciality and endemism of the floras and faunas present, recent work (Fielding et al., 2005) indicates that the late stages of continental glaciation extend into the Late Permian. Glaciations, thus, may explain several large cycles within the Guadalupian, although probably not the major regression at the close of Guadalupian time (Caputo and Crowell, 1985; Frakes and Francis, 1988; Veevers and Powell, 1987). Epeirogenic events, late orogenic deformation in Appalachian and Hercynian regions, and variations in sea-floor spreading may account for other Late Permian cycles. Moreover, regional basin subsidence patterns may have been episodic and could also have contributed to the cyclicity of sedimentation.

The concept of reciprocal sedimentation (Fig. 15) also helps to decipher a significant problem in Permian Basin stratigraphy namely, the fact that the shelf margin sequences which ring the Delaware Basin are largely carbonate (generated in-situ), yet the basinal section is composed overwhelmingly of detrital terrigenous sandstone and siltstone. How did sands move into the basin while leaving so little record in the surrounding shelf-margin facies? In the reciprocal sedimentation (sequence stratigraphic) scenario (Figs. 15 and 16), carbonate sedimentation dominated during high sea-level stands; reefs and/or grainstone shoals flourished, acting as carbonate "factories" on the platform margins; broad carbonate-evaporite lagoons occupied much of the shelf area, and thin but widespread carbonate turbidite units were deposited in the basins. Clastic terrigenous strata were either trapped in vegetated dunes or interdune flats, on

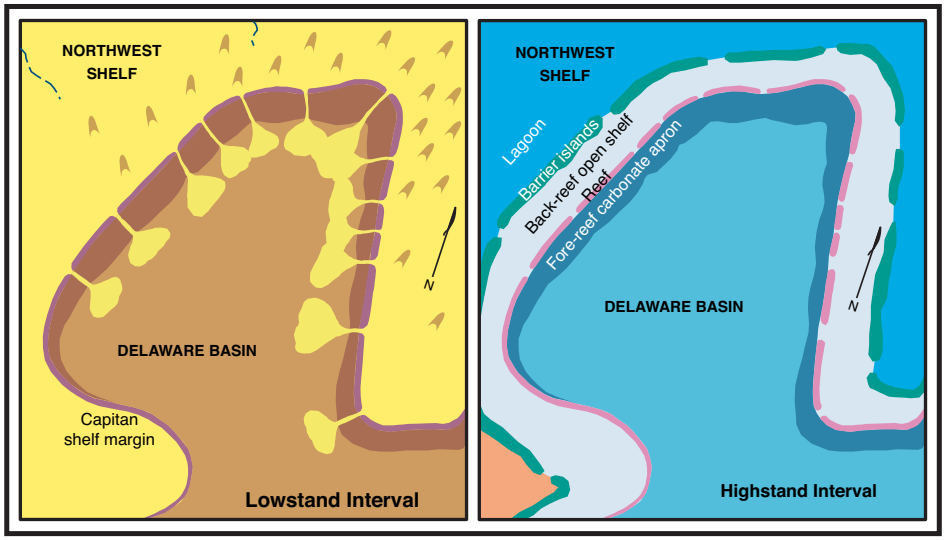

Figure 16. Diagrammatic model of reciprocal sedimentation with low- and high-stand depositional environments in the Delaware Basin.

sabkhas, or in shoreline deposits well up on the shelf. During lowered sea levels, on the other hand, eolian and fluvial (ephemeral stream) terrigenous sands and silts spread across the shelf areas, accumulated along shelf margins and eventually were transported into the basins to form thick sandstone sequences. In this concept, intervals of thick shelf sedimentation correspond with times of thin basinal deposition and vice versa. Thus, although the basin, shelf-margin and shelf-interior rock packages mentioned above are lateral time-equivalents of each other and have approximately the same overall thickness, this equivalence does not necessarily extend to smaller scale units. Laminated sandstones, which are tens to hundreds of meters thick in the basin facies, apparently have either very thin or no equivalents in the reef or back-reef sections. Likewise, reef and back-reef limestone and dolomite sequences which, again, may be tens to hundreds of meters thick on the shelf and slope, will commonly thin to less than a meter toward the basin center.

Alternatively, it is possible that some terrigenous material moved through channels or tidal passes in the barrier reef contemporaneous with carbonate sedimentation, for some lenticular sandstone beds and disseminated terrigenous sand grains have been found in shelf edge and upper slope carbonate units. Nevertheless, the cyclic distribution of both shelfal and basinal carbonate/clastic packages indicates that some degree of reciprocal sedimentation is required to explain overall sediment distribution.

A clearly defined seismic sequence stratigraphy has been developed since the mid-1980's for the Permian Basin region (e.g., Sarg, 1986; Tinker, 1998; Beaubouef et al., 1999; see Fig. 12), and it supports the concept of repeated relative sea-level variations, probably related to eustatic cyclicity on a time scales ranging from roughly a million years down to tens of thousands

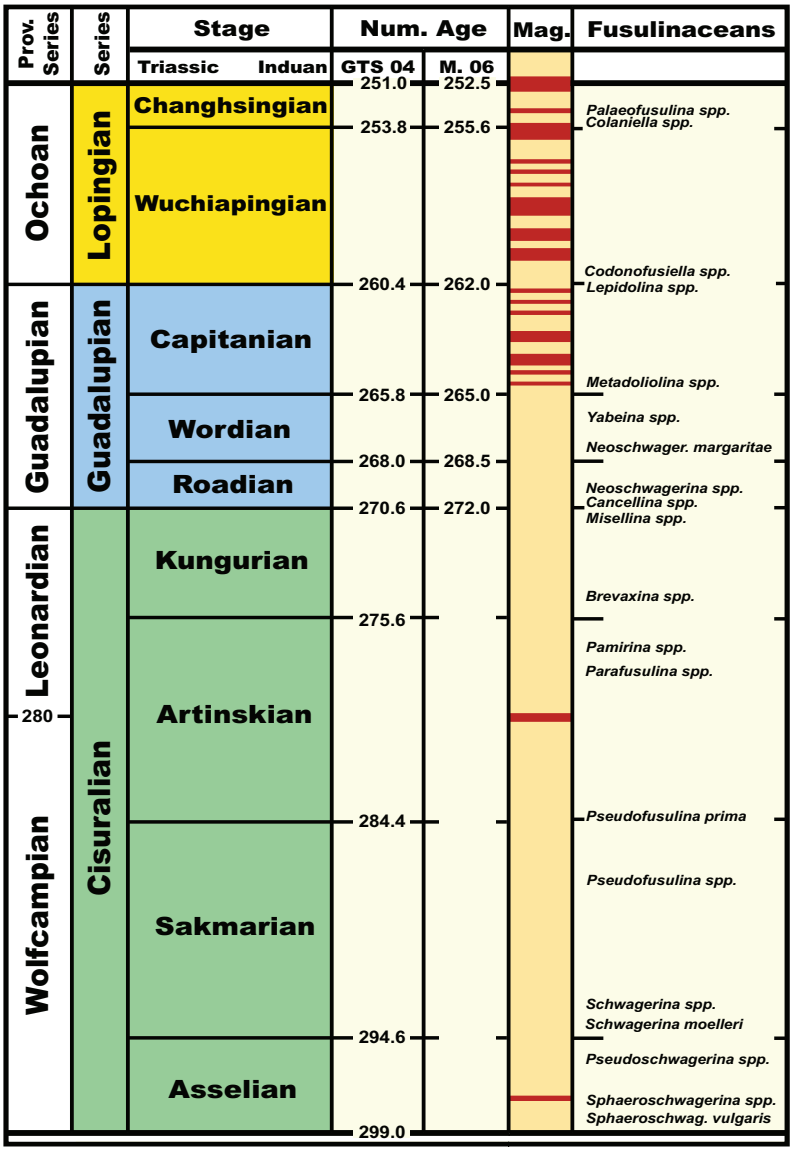

Figure 17. Comparison of southwestern U.S. provincial and international stage designations, fusulinid zones, and absolute age determinations for the Permian. Adapted from Henderson (2005). GTS 04 timescale is from Gradstein et al., 2004; N. 06 timescale from Menning et al. 2006.

of years. In addition, field mapping of seismically-defined sequences (Sarg, 1986; Ross and Ross, 1987a, 1987b; Meader-Roberts et al., 1991; Kerans and Fitchen, 1995; Kerans and Kempter, 2002) has led to the recognition of major erosion surfaces, low-stand depositional wedges, onlapping units, and other depositional features indicative of significant temporal changes in sea levels.

Depositional patterns are also controlled by long-term changes in subsidence versus sedimentation rates. When subsidence rates were high, or when sea levels were rising rapidly, facies tended to build vertically, as during the time of Goat Seep reef deposition. Conversely, with high rates of sedimentation and slow subsidence or minor sea-level rise, facies progradation was predominant. This is nicely illustrated by the Capitan reef on the stable western margin of the Delaware Basin (the Guadalupe Mountains) where the reef prograded nearly 10 km (6 mi) during Capitan sedimentation. On the more rapidly subsiding eastern margin of the same basin (the western edge of the Central Basin Platform) less than 3 km (2 mi) of progradation took place during the same interval (Ward et al., 1986). Perhaps even more dramatically, both the Midland and Delaware Basins were completely filled by extremely high rates of deposition of clastic terrigenous, carbonate, and evaporite strata. The Midland basin ceased to be a marine sedimentation site at about the time that the Capitan reef started growing around the Delaware Basin, and the Delaware Basin itself was entirely filled by very rapidly deposited (>4 km/my) evaporites during early Ochoan time.

Athough depositional cycles in the Permian Basin appear to have global controls, interbasinal and intercontinental correlations of Permian strata (Fig. 17) have proven difficult, largely because faunas in many Permian strata are strongly endemic. Furthermore, the older Permian type sections in the Soviet Union were, at least partly, in non-marine rocks. Fusulinid and conodont biostratigraphic studies have, to date, been most successful in tying together the widely dispersed Pangean Permian sections (Babcock, 1974b; Rasmussen et al., 1990; Ross, 1985a, 1987b; Wardlaw, 1987; Wilde, 1975, 1988; Henderson, 2005), but advances in both isotopic stratigraphy and sequence stratigraphy have also proved useful (Burke et al., 1982; Ross and Ross, 1988). While far too complex a problem to summarize in this guidebook, the Middle Permian (Guadalupian) strata of west Texas and New Mexico are considered to be generally correlative with the Phosphoria-Park City-Goose Egg deposits of Idaho and Wyoming, as well as the extensive Zechstein deposits in Europe.

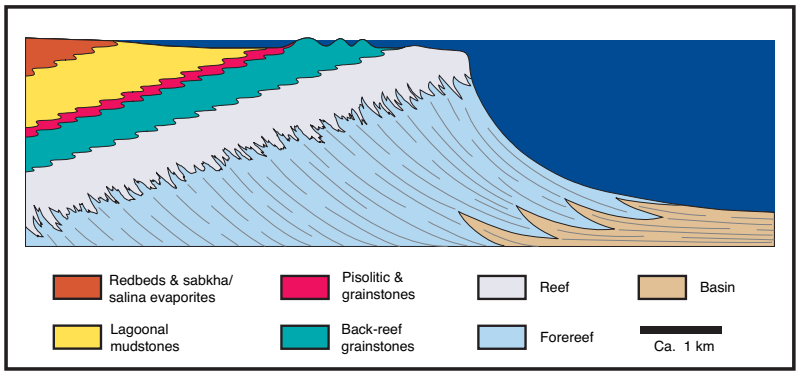

Figure 18. Shelf-to-basin spectrum of microfacies and interpreted depositional environments for the Capitan and Capitan-equivalent strata of the Guadalupe Mountains. Vertical axis is approximately 0.5 km.

DEPOSITIONAL PATTERNS

Because this discussion will examine the full suite of shelf-interior, shelf-margin, and slope to basinal strata in the Guadalupe Mountains (Fig. 18), it is appropriate to describe the general characteristics of deposits in each of those settings. More detailed descriptions of individual microfacies are also found in the road log section under the descriptions for specific outcrop stops.

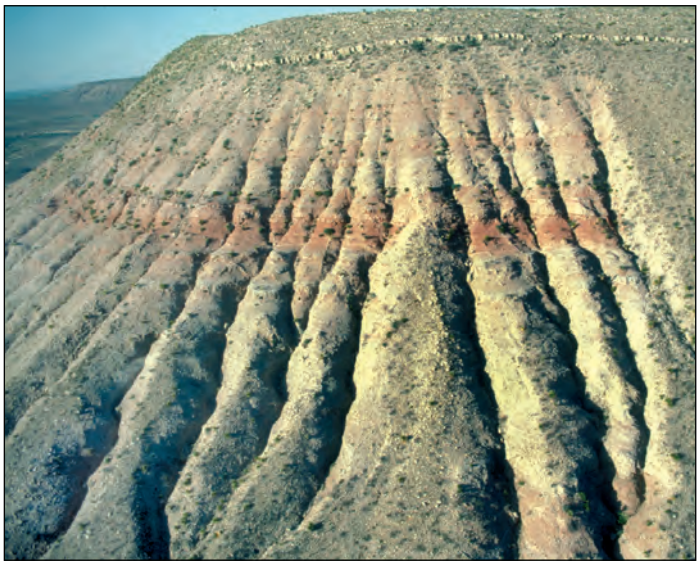

Figure 19. Seven Rivers embayment on New Mexico Highway 137 about 10 km north of the intersection with Dark Canyon road. Approximately 100-m-thick section of interstratified red siltstone and gray, massive, bedded evaporite of the Seven Rivers Formation. Note extensive gullying of the soluble evaporite and presence of capping layer of dolomicrite (Azotea Dolomite) which has preserved this outcrop from erosion.

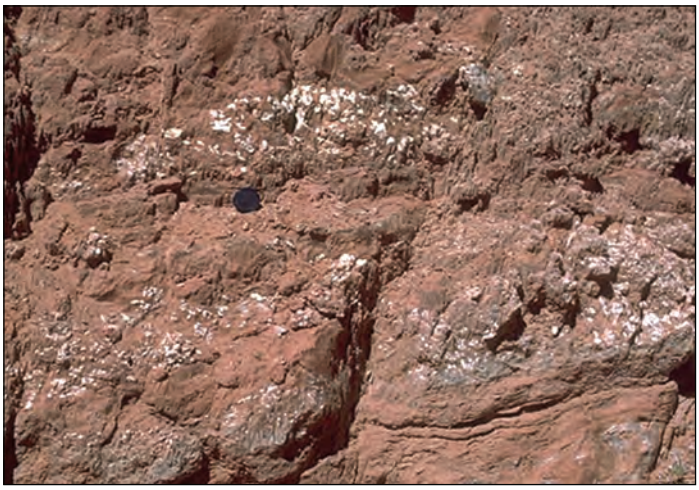

Figure 20. Red siltstone and nodular gypsum from the Seven Rivers Formation. Siltstone shows vague horizontal lamination, largely disrupted by growth of evaporite minerals. Outcrop in Seven Rivers embayment on New Mexico Highway 137, about 10 km north of the intersection with Dark Canyon road.

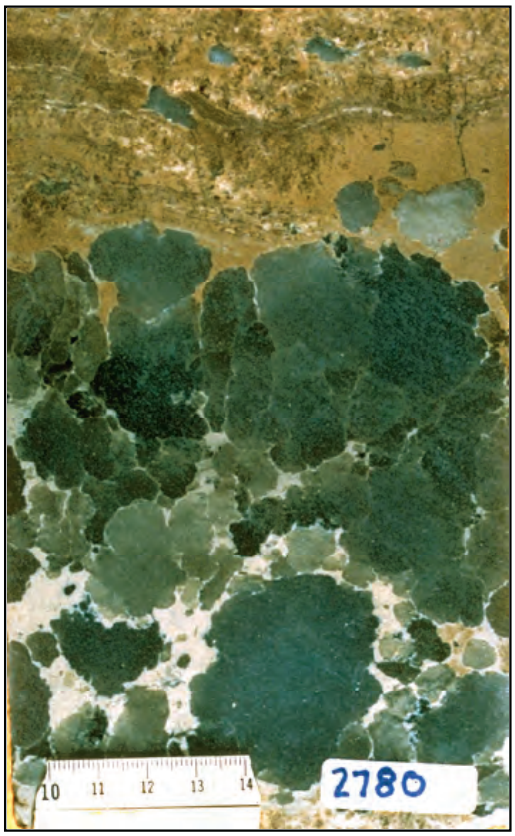

Figure 21. Core from 2,780 ft (847 m) depth in the McElroy field, eastern margin of the Central Basin Platform, Crane Co., Texas. Photograph of nodular anhydrite (dark gray) in Grayburg-San Andres strata. Light-colored material between anhydrite nodules is clayey carbonate; tan material above nodules is slightly oil-stained dolomite. Scale bar is in cm.

Shelf Interior Facies

The farthest shelfward units to be considered here are redbeds that are interpreted to have been deposited on broad, sabkha-like plains (Kendall, 1969). Clastic terrigenous detritus was derived from the north, northeast, and perhaps also the northwest, largely from remnant basement uplifts in the Ancestral Rockies and other areas. Transportation of the subarkosic sediment was probably partially accomplished through fluvial (especially ephemeral stream) processes but was more likely dominated by eolian (dune/dust storm) reworking.

The massive redbeds (Figs. 19-20), as well as thinner sandstone units interbedded in the shelf sequences, display few sedimentary structures. Evaporite nodules are common, and faint traces of horizontal lamination, adhesion ripples, low-angle cross-bed sets and similar structures can be seen locally; trace fossils are virtually absent. This is consistent with deposition on an evaporitic plain across which large dunes may have migrated, yet in which the only sediments trapped were those held by a capillary fringe above the water table (e.g., Glennie, 1970).

Beds of gypsum (or anhydrite in the subsurface) are complexly interstratified with the redbeds on their seaward margin (Fig. 20). The evaporites typically have nodular fabrics (Fig. 21) but also are found as rosettes or radiating bursts of crystals. Deposition of evaporites has been interpreted to have taken place by direct

Figure 22. Solution collapse breccia in lower part of the Seven Rivers Formation. Timing of such evaporite dissolution and collapse brecciation of overlying dolomites has been postulated as Late Permian (Dunham, 1972) but is more likely, in this case, to be Late Tertiary or Quaternary. Outcrop in western Dark Canyon.

precipitation in shallow pools or lakes (salinas) as well as through displacive nodular growth in sabkha flats (Kendall, 1969; Sarg, 1981).

Extensive dissolution of shelf evaporite beds (Fig. 22) has led to widespread solution-collapse brecciation. Although it is possible that much of this dissolution is a result of near-surface weathering during Tertiary uplift, the presence of solution breccias in age-equivalent strata in the deep subsurface makes it likely that at least some of this brecciation is of Permian age. Probably pluvial-interpluvial climatic cycles existed in association with Permian glaciations just as they did during the Pleistocene (e.g., Benson and Thompson, 1987); this may have led to alternating phases of evaporite formation and dissolution.

Seaward of the main evaporite deposits, and again complexly interstratified with the evaporites and redbeds (Fig. 19), are fine-grained, thin-bedded dolomicrites or dolomudstones (Fig. 23). These too were probably deposited in a shallow subtidal or lacustrine setting a coastal salina or a hypersaline marine lagoon (Sarg, 1981). Constituents include irregular pellets or peloids, some oncoids, calcispheres, and foraminifers, plus local microbial stromatolite boundstones. Other fossils are generally scarce to absent. The micrite matrix and allochems have been replaced, presumably penecontemporaneously, by very finely crystalline dolomite that preserved primary fabrics. Although some of these strata have considerable moldic and fenestral porosity on outcrop (Fig. 23), equivalent units in the subsurface generally are completely plugged with evaporite minerals, especially anhydrite. Such minerals rarely survive outcrop weathering, but crystal molds or calcitized evaporites are commonly found in outcropping strata on the landward side of this facies belt. This supports the idea that outcrop and subsurface strata both shared a high original percentage of evaporitic constituents.

Interbedded with these dolomicrites are numerous thin (20 cm to 2 m) beds of clastic terrigenous sand. These terrigenous units contain material very similar to that which predominates in the redbed facies—very fine sandstone and coarse siltstone with a subarkosic composition, few sedimentary structures and essentially no fossils or trace fossils. Such beds probably represent small progradational advances of sabkha-type sedimentation across the back-reef lagoonal area as a consequence of cyclic changes in climate, sediment supply or sea level. Some of the individual sandstone beds extend seaward for several kilometers but thin and eventually pinch out before reaching the shelf-margin reef facies (Candelaria, 1982, 1989). Despite their thinness and lack of continuity in a seaward direction, however, some of the more prominent sands have considerable extent parallel to the shelf edge. These form excellent marker units that have been

Figure 23. Polished slab of a laminated, fenestral, very fine-grained dolomite from the back-reef "lagoonal" facies of the Seven Rivers Formation. This fabric was most likely produced by intertidal blue-green algal stromatolites; some of the larger voids are the result of dissolution of synsedimentary evaporite crystals.

mapped over many tens of thousands of square kilometers in the subsurface as well as in surface sections.

Immediately seaward of the dolomitized carbonate mudstones lies what is probably the most controversial facies in the Permian of the Texas-New Mexico area. The "pisolite facies" is a tract, a kilometer or more wide, that persists throughout the Grayburg to Tansill section (i.e., about a kilometer of sedimentary buildup). It consists of irregularly bedded deposits of laminated, fenestral carbonate, beds of skeletal debris, and most importantly, abundant lenticular

Figure 24. Polished slab of pisolitic dolomite from the uppermost Yates Formation. Note reverse grading of grains and "fitted fabric" in which grains have interlocked boundaries produced by compromise growth of outer coatings. Slab is 8.4 cm in height.

Figure 25. Tepee structure in Tansill Formation at the parking lot of Carlsbad Caverns.

zones of pisolitic dolomite. The pisoids range in size from a few millimeters to greater than 5 cm; they commonly have a reversely graded structure, with finer pisoids at the base and coarsening upward (Fig. 24; Dunham, 1969). However, cross-bedded and unsorted pisolitic deposits are also present. Pisolitic strata typically contain some marine fossils, especially on the seaward side of the facies. Pisolitic nuclei include some marine fossils but are dominantly fragments of older pisoids. In their later stages, pisoids grow "in place", developing fitted fabrics, common or shared coatings and passing into botryoidal crusts of former aragonite "marine" cements (Dunham, 1969; Loucks and Folk, 1976; Scholle and Kinsman, 1974). The pisolite facies has been extensively replaced by very early (penecontemporaneous), aphanocrystalline dolomite crystals that clearly mimic primary fabrics. Although very porous on outcrop, this facies again shows extensive filling by evaporite minerals in most subsurface sections.

The pisolitic deposits are found in association with large (1-3 m/3-10 ft high; 10-25 m/30-80 ft diameter) polygonal features termed "tepee structures" (Fig. 25; Dunham, 1969; Kendall, 1969). These are polygonal expansion features that are marked by buckled and deformed sediments, crusts of precipitated, originally aragonitic cement (Fig. 26) and pockets of pisolitic sediment beneath and between the polygonal upwarps. Tepee structures are usually stacked; that is, they build up through a series of successive beds until they are truncated or otherwise terminated by a thin sandstone or carbonate grainstone bed.

The pisolite facies is always found as a transitional zone between fossiliferous marine grainstones, packstones, and wackestones on the seaward side and the largely unfossiliferous, evaporitic dolomicrites on the landward side. As such, the pisolite facies must represent or be associated with a long-lived barrier to water movement between open shelf and hypersaline lagoonal settings. The detailed interpretation of the environment of deposition of this unit has, however, been the subject of very diverse speculation over the years. Pisolite formation was originally attributed to marine growth of algal nodules but has been reinterpreted as a product of marine inorganic precipitation in a subtidal setting (Esteban and Pray, 1977); caliche formation in continental or coastal spray-zone settings (Dunham, 1969; Scholle and Kinsman, 1974); complex marine and brine reflux cementation (Kirkland et al., 1999a); and back-barrier, marine seepage or groundwater springs (Handford et al., 1984).

This last hypothesis (Fig. 27) appears to be a very

Figure 26. Transition from growth of free pisoids to a botryoidal cement crust in an outcrop of the uppermost Yates Formation. Last stages of pisoid precipitation occurred on the upper growth surfaces which eventually merged to form a crust of originally aragonitic cement.

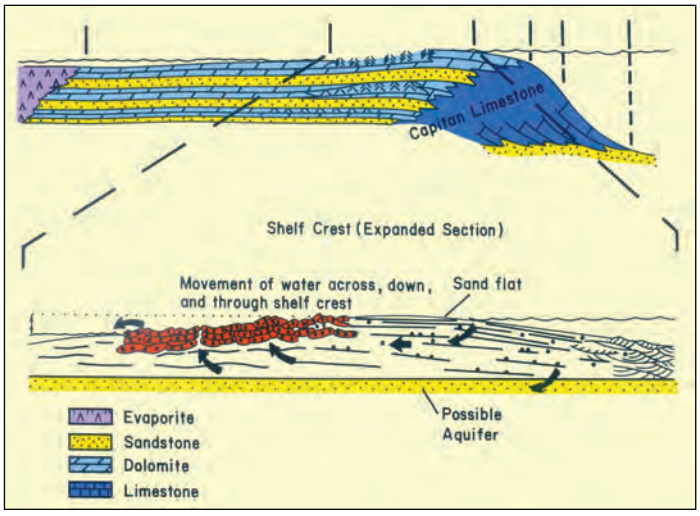

Figure 27. Diagrammatic depiction of the back-barrier salina seepage model for teepee/pisolite development in the Capitan-equivalent shelf facies. Adapted from Handford et al., 1984.

viable interpretation and is based on a number of studies of modern coastal salinas, lakes and sabkhas in southern and western Australia (e.g., Warren, 1982, 1983, 1985; Handford et al., 1984; Kendall and Warren, 1987; Logan, 1987). In the more arid settings, evaporative drawdown of lakes and lagoons that lie behind marine or eolian grainstone barrier ridges allows the constant seepage of marine waters through the barriers. This results in the formation of pisolitic, aragonite cemented crusts around the spring-like inflow areas. Continued growth of aragonite crystals leads to development of fractured, tepee-like crusts that can build up through several meters of section. In more humid or seasonally wet areas, focusing of discharge areas of rainwater seepage by a variety of features also leads to similar spring formation with equivalent aragonitic tepee-pisolite deposits (Lock and Burne, 1986). The seep-spring hypothesis, based on its modern Australian analogs, closely matches many of the observed features in the Permian pisolite belt:

1. The Permian pisolitic units are associated with a significant and persistent barrier between normal marine and hypersaline or otherwise restricted settings.

2. Pisolitic beds are associated with tepees that remain in relatively fixed positions through significant periods of time.

3. The pisoids are distributed in small pockets or patches that could represent localized seepage areas.

4. Permian sandstone units do not thin over the pisolite facies so that it is unlikely that this facies was itself an elevated barrier as required by caliche hypotheses thus a back-barrier seepage area fits the topographic constraints.

5. The Permian pisolitic units contain "marine" (formerly aragonitic) cements but are largely dolomitized. This is common in modern salina settings where marine pore fluid seeping into the basin yield aragonitic and high-Mg calcite cements and where subsequently evaporated brines produce dolomitization.

6. Cross-bedded, reworked or fossiliferous deposits should be common in a back-barrier setting that may frequently be breached by storms. Such deposits, containing rounded molluscan or fusulinid grains, are common in the Permian strata.

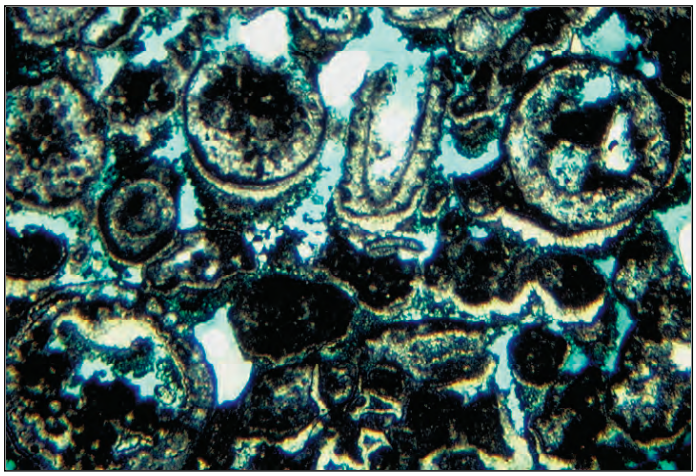

Figure 28. Thin-section photomicrograph (plane-polarized light) of a near-back-reef grainstone in the Tansill Formation. The predominant grains are *Mizzia* green algae and, in this example, the primary porosity was partially filled with an early diagenetic cement produced in the vadose zone — note slight corrosion of tops of grains and pendants or microstalactites of calcite cement below the grains. Subaerial exposure may have occurred on small islands during sedimentation or in association with a major (early Ochoan) hiatus that follows Tansill deposition. Walnut Canyon, less than 1 km west of canyon mouth, Carlsbad Caverns National Park, Eddy Co., New Mexico.

Shelf Margin Facies

The deposits that lie seaward of the pisolite zone contain a wide variety of lithologies. Generally, these strata show signs of open marine circulation, with normal or only slightly hypersaline conditions. The rocks typically are rich in marine fossils, especially fusulinids and other foraminifers, gastropods, pelecypods, green algae (Fig. 28; especially *Mizzia* and *Macroporella*), blue-green algal boundstones,

Figure 29. Low angle, seaward-dipping cross-beds in the upper Tansill Formation. These skeletal grainstones of probable beach origin overlie subtidal and lower intertidal grainstones and packstones (below base of photograph) and, in turn, are overlain by pisolitic strata. Thus, they are part of one of the many shallowing-upward sequences in this part of the section, probably associated with small barrier islands in the very near-back-reef zone. These barriers are thought to have restricted the flow of marine water from the basin onto the shelf.

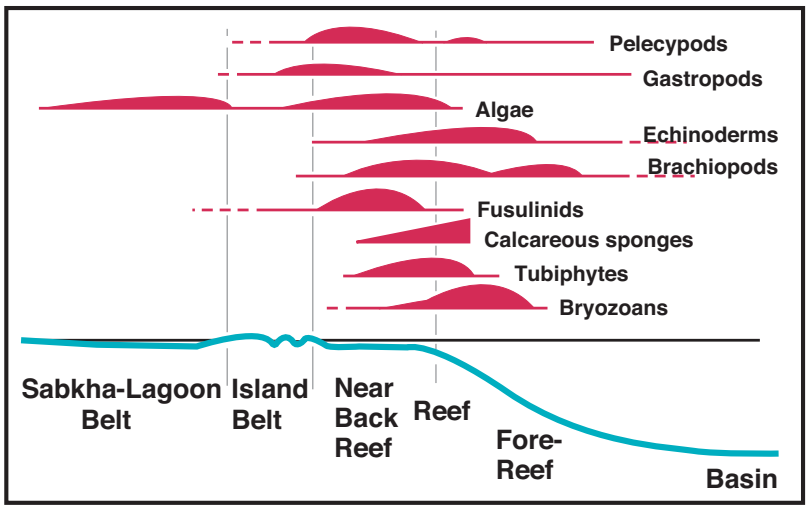

Figure 30. Distribution of the major faunal groups in the Capitan Formation and associated units (adapted from Newell et al., 1953 and Schmidt, 1977).

oncoids and other skeletal grains. Bedding is indistinct on the seaward side of the facies but becomes well defined and medium-scale on the shelfward side. Grainstones and packstones predominate, but some wackestones and algal boundstones are also present in localized areas.

Sedimentary structures vary greatly on a small scale and include several types of cross bedding; trough sets, bi-directional or herring-bone units and seaward-dipping, low-angle planar sets (Fig. 29) all are commonly observed. Fenestral fabrics, slightly pisolitic teepee structures, channels and crudely graded storm beds also are encountered. In general, shallowing-upward (subtidal to supratidal) sequences are very abundant and occur on small as well as large scales (centimeters to tens of meters).

If, as concluded previously, the pisolite barrier does not represent a topographically elevated area, then this facies, its seaward neighbor, must be such a region. The combination of varied, small-scale facies, shallowing upward sequences, marine fauna, thinning of associated sandstones and other features all indicate that the seaward part of this facies was a zone of small, coalescing sand waves and islands, perhaps with intervening tidal passes (Mazzullo et al., 1989). Quite possibly, the landward third of the facies, in which storm beds, tepees and possible soil crusts are common, represents a more continuous and more permanent low-relief barrier island facies. Whether through the presence of a single continuous marine-eolian barrier or through a series of coalescing, shifting islands, this facies acted as an overall deterrent to water movement farther landward.

The grainstone-island facies is as complex and varied from a diagenetic point of view as it is from a depositional perspective. Locally, massive marine cements occlude all porosity (especially on the seaward margin). In other cases, minor marine cement is accompanied by vadose and/or phreatic fabrics, leaching of unstable (originally aragonitic and high-Mg calcite) grains, and development of moldic porosity. This is not surprising in an area of shifting islands where small fresh-water lenses may penetrate sections that were formerly in marine pore-fluid settings. Unlike any of the shelf interior facies, however, the island belt underwent only partial dolomite replacement and relatively minor evaporite pore-filling cementation (both probably related to subsequent progradation of more shelfward units over this facies). Thus, rocks of this facies are prolific reservoirs in the subsurface both because to their inherent porosity and because of their close proximity to updip and overlying evaporite-plugged seals.

Just seaward of the grainstone-island belt lies the main carbonate-producing facies of the area,

Figure 31. A portion of the diorama of the Capitan reef produced by Terry L. Chase and displayed at the Permian Basin Petroleum Museum in Midland, Texas. This artist's conception emphasizes the framework sponges and the abundant encrusting fauna.

Table 2. Correlations between faunal and sedimentary features and depositional environments in the Middle Permian strata of the Guadalupe Mountains (data partially adapted from Newell et al., 1953 and Schmidt, 1977). Relative abundance in stratigraphic unit and/or environment is indicated by: C = common; P = present; R = rare; * indicates feature is generally or always detrital or allochthonous. Absence of any symbol indicates feature is absent or extremely rare.

FEATURE	ARTESIA GROUP			CAPITAN LIMESTONE			BELL CYN.
	Sabkha-Lagoon Facies	Pisolite Facies	Near Back-Reef Facies	Reef Crest Facies	Upper Forereef Facies	Lower Forereef Facies	Basin Facies
Fauna:							
Ostracods	P	R	P	R	R	R	R
Calcispheres	C	P	P				P
Stromatolites	P	P	R	P	P		
Dasyclad algae		R	C	R	R*	R*	
Fusulinids		P	C	R	R*	R*	P
Other Foraminifera	P	R	P	P	R	R	R
Gastropods		R	C	P	R		
Pelecypods		R	C	P			
Red Algae			P	C	P		
Echinoderms		R	C	C	P	P	R
Brachiopods			P	P	P	C	R
Calcareous Sponges			P	C	C	P*	
Hydrozoans			P	C	C		
Tubiphytes			P	C	C		
Bryozoans				C	C	P	
Ammonoids			R	R	R	R	R
Solitary Corals				P	P	R	
Phylloid Algae				C			
Siliceous Sponges						C	P
Conodonts						R	P
Radiolarians							P
Fish							R
Carbonate Rocks:							
Boundstone	P		R	C	C	P*	
Grainstone		C	C	P	P	P	
Packstone	R	C	P	P	R	C	P
Wackestone	P	P	P	P	C	C	C
Mudstone	C	P	P	R	R	P	C
Non-Carbonate Rocks:							
Shale	C						C
Siltstone	C	P	R			P	C
Sandstone	C	P	R			P	C
Organic-rich units	R					P	C
Grain Types:							
Skeletal	R	P	C	C	C	P	P
Pelletal	C	R	P	P	P	R	
Pisolitic / oolitic	R	C	P				
Intraclastic	R	P	P	C	C	P	R

Table 2. Continued.

FEATURE	ARTESIA GROUP			CAPITAN LIMESTONE			BELL CYN.
	Sabkha-Lagoon Facies	Pisolite Facies	Near Back-Reef Facies	Reef Crest Facies	Upper Forereef Facies	Lower Forereef Facies	Basin Facies
Sedimentary Structures:							
Lamination	C	R	R			P	C
Bedding	C	C	P		R	P	C
Synsedimentary fractures			P	C	C		
Channels			P	?	C	P	C
Cross-bedding		R	P		R	P	P
Graded Bedding			R		R	P	P
Collapse breccias	C				C	P	
Tepee Structures		C					
Diagenetic Features:							
Marine Cements			P	C	C	P	
Dolomitization	C	C	P		P	P	
Evaporite nodules	C	R			R	P	R
Evaporite cements	P	C	C		P	R	
Freshwater Cements	R	C	P				
Chertification					P	C	C
Late calcitized evaporites	C	C	R		C	P	R
Late-stage silica	R						
Primary Porosity	P	R	P				C
Secondary Porosity	C	R	C	R	P	R	R

the reef. This microfacies forms a sharply defined, largely continuous, shelf-margin zone that surrounds the Delaware Basin. Although the reef shows broad bends and embayments on a scale of kilometers, massive bedding and weathered or inaccessible outcrops have, in most localities, precluded mapping of smaller-scale reef structures such as channels or spur-and-groove morphology.

The Capitan reef is a zone of maximum faunal diversity (Fig. 30, Table 2). The major framework organisms in the reef complex include finger-like and platy calcareous sponges, *Tubiphytes* (a possible hydrocoralline), and bryozoans; phylloid algae locally form a subsidiary framework. The framework constituents, often still found in living position, are commonly encrusted by possible red algae and other microbial deposits (*Archaeolithoporella*, *Solenopora*, *Collenella*, and others) and are arranged in a consistent pattern of subfacies that probably reflect changing environmental conditions passing up the slope and onto the shelf (J. Babcock, 1977a, 1979; Toomey and Cys, 1977). In addition to framework and encrusting organisms, the reefs contain a wide range of ancillary organisms: echinoderms (including crinoids and echinoids), brachiopods, bivalves, gastropods, ostracods, solitary rugose corals, trilobites, and others (Fig. 31). Finally, numerous or cavity-dwelling organisms, especially cryptic sponges, have been recognized in recent years (e.g., Wood, 1999a, 1999b).

On the shelfward side of the reef, sponge-algal rubble passes into *Tubiphytes* thickets and *Mizzia* and *Macroporella* green algal grainstones with scattered bellerophont gastropods. This is very reminiscent of the sequence of microfacies across a modern Caribbean reef (e.g., Ginsburg, 1964; Multer, 1969), with coral rubble passing into sandy flats dominated by *Halimeda* green algal grainstone with grazing bellerophontid gastropods (conchs) and echinoderms.

A major factor in the formation of these late Guadalupian reefs was the massive amount of penecontemporaneous marine cementation that took place at or near the shelf margin (Mazzullo and Cys, 1977). Large and small cavities alike were rapidly filled with massive, botryoidal crusts of radial-fibrous cement (Fig. 32). The cement is partly intergrown with *Archaeolithoporella* encrustations, internal sediment, and even sessile macrofossils, all of which attest to the syndepositional nature of the cementation by originally aragonitic and/or high-Mg calcite cements. Massive marine cementation is largely confined to the reef facies, the near-back-reef grainstones, and the pisolite/tepee

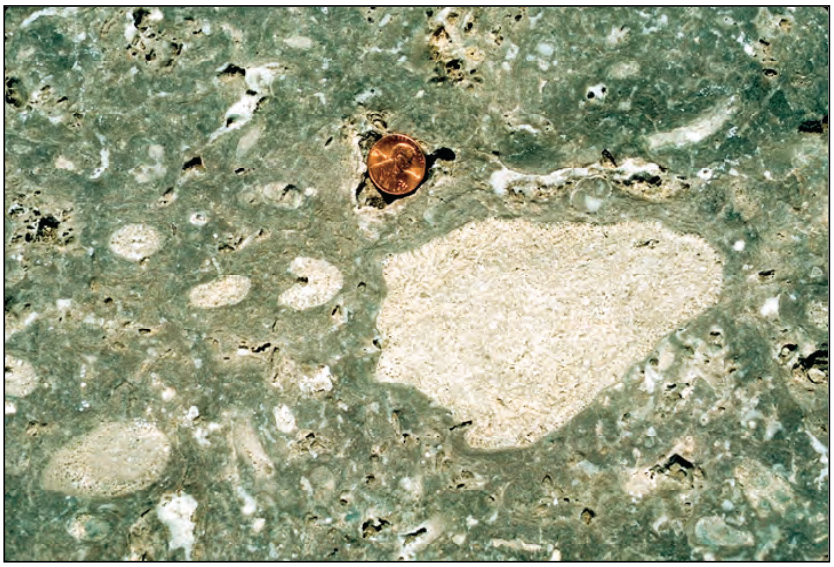

Figure 32. Capitan reef framework from mouth of Walnut Canyon. Shows large calcareous sponges (white) still in an oriented living position with long axes perpendicular to reef trend. Calcareous sponges are encrusted by *Archaeolithoporella* and marine cement (gray to black).

zone. In most cases, in the more seaward of these units, synsedimentary cementation has reduced porosity to such a degree that these units are not significant hydrocarbon reservoirs despite the fact that locally extensive fracturing has given some of these zones high permeability.

As with many ancient reefs, there has been considerable discussion over the past few decades as to whether this was a "true" ecologic reef, whether it was a continuous or discontinuous barrier, and whether it developed at the topographic crest of the shelf or in deeper water on the upper slope (Achauer, 1969; Dunham, 1970, 1972; Schmidt, 1977; Hurley, 1979; Saller, 1996). Various workers have considered the Capitan to represent an unconsolidated shelf margin skeletal bank or mound (Lang, 1937; Achauer, 1969), a true barrier reef (Newell et al., 1953; Kirkland and Moore, 1990, 1996; Kirkland et al., 1999b), or an uninterrupted slope facies (King, 1948). Others have felt that the abundance of penecontemporaneous marine cement indicated that the wave-resistant nature of the Capitan "reef" was a result of primarily inorganic rather than biological processes making this a "cement reef" rather than an "organic or ecologic reef" (Schmidt and Klement, 1971). Some have even interpreted much of the observed reef fauna as having lived within carvities of a cement reef (Wood et al., 1994, 1996; Wood, 1999).

Overall, the high biological diversity of this environment (see Table 2, Fig. 30); the abundance of framework calcareous sponges, bryozoan, and hydrocorallines; the ubiquitous presence of encrusting organisms (*Tubiphytes*, *Archaeolithoporella*, *Girvanella* and others); the remarkably high productivity of organisms generating vast masses of reef and fore-reef skeletal debris; the distinct internal faunal zonation (Figs. 33 to 35); the presence of abundant inorganic, radial-fibrous, originally aragonitic cements; and the large-scale fragmentation and disruption of fabrics by wave and current activity all are features of the Permian reef complex which are highly analogous to modern reefs.

Indeed, much of the semantic confusion over the reefal nature of the Capitan Formation revolves around the presence or absence of in-situ biological growth fabrics. That confusion is a result of trying to transfer the common definition of modern reefs as "stable, wave-resistant, frameworks" into the geologic record. The wave-resistance concept, however, is largely a misconception produced by the "fair-weather" examination of modern reefs. On a clear, calm day, when most geologists venture forth, the modern reef is truly wave-resistant, consisting of abundant, in-situ framework organisms. The day after a hurricane, however, much of this "wave resistant framework" has been smashed into rubble that accumulates within the reef or is transported into deeper water settings. Indeed, quarries in Pleistocene or older reefs show only a small percentage (typically 10-25 percent) of in-place framework organisms (e.g., Stanley, 1966).

The work of Newell et al. (1953), Babcock (1977a), and

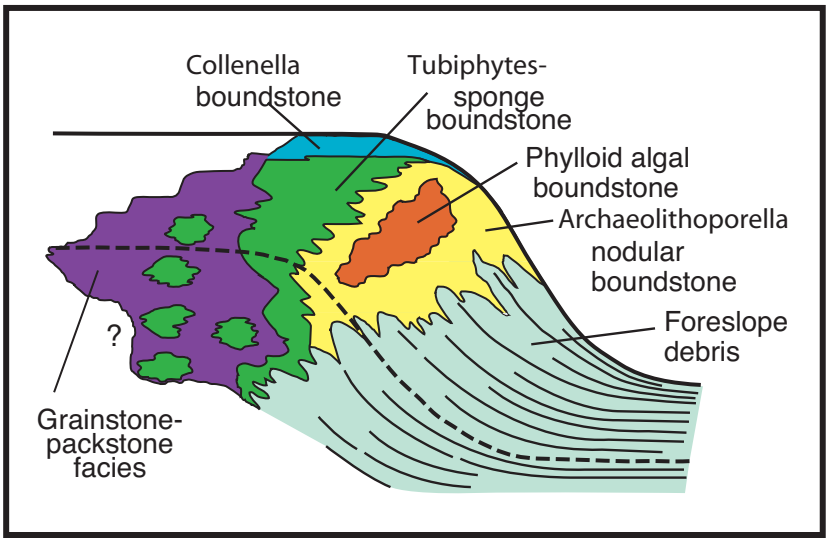

Figure 33. Diagrammatic depiction of microfacies distribution within the upper Capitan reef. Dashed line in center is an approximate time line (adapted from J. Babcock, 1977a).

Babcock and Yurewicz (1989) has established the existence of consistent faunal zonation within the Capitan reef (Fig. 33) and has demonstrated that much of the fauna is still in living position, at least in the few areas of exceptional exposure which were studied. To a considerable degree, this has demonstrated that the Capitan contains at least local "true reef" limestones, but it has also stimulated further questions about the environmental setting of the reef growth. Some have argued that the preservation of delicate, branching or plate like organisms and the presence of roll-over bedding at the shelf margin indicate that reef growth took place in somewhat deeper water on the upper slope (Hurley, 1979; Pray, 1985). One can see considerable evidence, however, of wave reworking of the most shelfward parts of the reef, with transport and rounding of blocks up to a meter across. In addition, it should be remembered that this was a small, landlocked basin with less than 160 km (100 mi) maximum fetch. Generation of waves of sufficient size to destroy a massively cemented reef would have been an exceptional occurrence, even in relatively shallow shelf-edge waters.

Regardless of semantic questions, the rapid rate of marine cementation of the reef facies, coupled with the very high rate of biological productivity, meant that during much of Guadalupian time more material was generated in the reef margin zone than could be accommodated there given limited rates of subsidence. This excess material was transported into back-reef and, volumetrically more importantly, fore-reef environments. Thus, the Capitan reef of the Guadalupe Mountains prograded seaward between five and 10 kilometers (3-6 mi) during its roughly 5 million year history, despite sitting at the margin of a nearly 600 meter (1,800 ft) deep basin. This clearly required a very large volume (and a high rate) of sediment production.

The intense penecontemporaneous cementation of the Capitan reef (Fig. 35), coupled with the fact that it prograded rapidly over 500 or more meters (1,600+ ft) of largely unconsolidated and compactible debris, led to extensive syndepositional fracturing of the cemented reef slab (Figs. 36 and 37; King, 1948). As bedding is largely absent in the massive reef facies, weathering has exposed these shelf-edge-parallel fractures that were filled with internal sediment, encrusting organisms and, most commonly, by paired

Figure 34. Phylloid algal-*Archaeolithoporella*-marine cement facies in Capitan reef in Walnut Canyon. White, curved strips are oriented phylloid algae; white-gray patches are trapped micrite and darker encrustations consist mainly of *Archaeolithoporella* and marine cement.

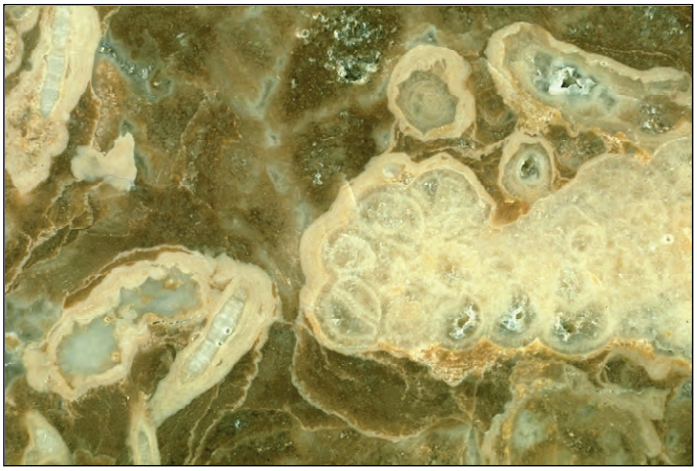

Figure 35. Polished slab with calcareous sponges, *Archaeolithoporella* encrustations, and dark brown marine cements from the sponge boundstone facies of Babcock (1977a) in Walnut Canyon.

Figure 36. Synsedimentary fracture (neptunian dike) in the Capitan reef showing parallel cement linings on opposite walls of a fracture seen in an acid-etched outcrop at the mouth of Walnut Canyon. Latest stage filling in the center of the fracture contains clastic terrigenous silt piped down from an overlying surface of transport. Fractures trend parallel to reef front and extend essentially vertically down through the reef and into upper fore-reef talus facies. These are the cause of the "spurs" seen in reef.

Figure 37. Syn-sedimentary fractures in the reef and upper slope. View north from McKittrick Canyon.

zones of marine cements on the fracture walls (Fig. 36). Clastic terrigenous sand grains and dolomitic linings are also found in some of the late-stage fillings of these fracture sets, giving evidence that terrigenous materials and hypersaline fluids indeed passed over the Capitan shelf margins. The fractures, which weather in sharp relief relative to the surrounding rock, also form the easiest way of recognizing the reef and upper forereef zone in the field (Fig. 37).

Slope and Basin Facies

One of the most volumetrically important carbonate facies in the Permian reef complex is the fore-reef talus apron. These deposits consist of steeply dipping rubble of reef, near-back-reef, and upper slope origin combined with sediment formed in-situ on the middle and lower slope. Brachiopods, fenestrate and ramose bryozoans, and echinoderms were the most common organisms to have lived on the slope (Fig. 38); siliceous sponges added significantly to the biomass only in base-of-slope settings. Slope sedimentation, however, was overwhelmingly dominated by allochthonous material transported by rock fall, grain flow, debris flow, and turbidity current processes (Figs. 39, 40). The slope facies thus consists of innumerable individual, small, allochthonous deposits that have coalesced to form a relatively uniform apron of debris (see Bebout and Kerans, 1993; Brown and Loucks, 1993a, b).

Bedding generally is distinctly visible in canyon exposures that dissect the shelf margin. Bedding angles exceed 35° on the upper slope and flatten gradually to only a few degrees as one approaches the basin floor (angles correctd by about 7° to account for Tertiary structural tilt). Individual beds vary in thickness from a few tens of centimeters to several meters and typically wedge out laterally. Much of the sedimentation was controlled by small canyons, channels or slump scars on the slope. These sites acted as sediment conduits until they were plugged by massive debris or grain flows and new channels became active. Grain-flow deposits typically contain fusulinid foraminifers and other near-back-reef material that may have passed through tidal gaps in the Capitan reef. The bulk of the sediment, however, consists of poorly sorted or unsorted reef detritus either as small fragments and individual constituent grains or larger blocks of lithified (encrusted and cemented) reef

Fig. 38 A large fragment of a fenestrate bryozoan, one of the more common organisms which colonized the Capitan fore-reef slope (north wall, McKittrick Canyon).

Figure 39. Small channel in Capitan fore-reef talus (south side of McKittrick Canyon). Floor of channel axis is lined with several thin flow units and then is plugged with a massive debris flow. Slope deposition was accomplished by a mix of rock falls, debris flows, density currents, and perhaps other processes. The middle slope, in particular, is dominated by debris flow deposits.

Figure 40. Graded turbidite of carbonate packstone to wackestone in the lower slope facies of the Capitan Formation (Permian Reef trail, north side of McKittrick Canyon). Constituent grains are mainly slope-dwelling organisms (brachiopods, bryozoans, echinoderms), many of which have been replaced by authigenic silica.

Figure 41. Thin-bedded, dark colored, subtly graded, distal turbidites (wackestone to mudstone) in lower part of the Capitan slope facies (north wall of McKittrick Canyon). Base of unit at level of acid bottle shows silicification of coarse basal material. Inter-turbidite sediment is fissile and slightly more clay-rich than associated turbidite sediment.

framework. The size of the blocks, the massive bedding, the interstitial matrix of reefal material, and the degree of diagenetic alteration commonly make it difficult to impossible to consistently differentiate Capitan reef and fore-reef strata either in the field or the subsurface where the geometric relationships of the entire shelf margin cannot be seen.

Clastic terrigenous material is scarce in middle and upper slope strata. In some horizons, well-rounded terrigenous sand grains and more angular silt grains are disseminated among the predominant carbonate constituents. Isolated terrigenous sand-filled channels are found in other sites; these channels can be up to 10 m (30 ft) thick. The lowest part of the slope, on the other hand, shows extensive interfingering of carbonate debris beds, that thin basinward, with sandstone beds which show the opposite relationship.

The slope area is just as complex from a diagenetic perspective as it is from a depositional viewpoint. Fluids from basinal and shelf sources likely passed through and mixed in this environment (Scholle et al., 1992). Compaction is extensive below the marine cemented zone at the very top of the slope. Post-depositional, moderately coarsely crystalline, selective dolomitization is very widespread and, in places, completely alters the slope strata (Melim and Scholle, 2002; Melim, 1991). Late diagenetic porosity filling by gypsum, anhydrite, kaolinite, and other minerals is commonly seen in the subsurface although on outcrop most of the evaporite minerals have been converted to coarsely-crystalline calcite or empty vugs. Directly precipitated calcite cements also are present in upper slope strata where fresh-water input has occurred (Given and Lohmann, 1986; Mruk, 1985, 1989; Scholle et al., 1992; Wiggins et al., 1993). Slope strata, either despite or because of these varied diagenetic events, form hydrocarbon reservoirs in some of the older (mainly Wolfcampian and Leonardian) sections along the edges of the Delaware and Midland basins (Wiggins and Harris, 1985; Hobson et al., 1985; Mazzullo and Reid, 1987).

Toward the base of the slope, the character of the fore-reef deposits changes significantly. Bedding becomes thinner, and more graded beds are present; furthermore, the sediment is finer grained, darker colored, more stylolitic and contains more siliceous biota than do strata from upper or middle slope settings (Fig. 41). Dolomite is largely lacking in these beds, but compaction, stylo-nodular bedding, silica replacement of calcitic fossils and chert nodule formation are important factors in the virtually complete destruction of porosity in this part of the slope.

The lower slope beds thin rapidly as they pass smoothly into the basinal carbonate sections. The Lamar Limestone (Fig. 42), the youngest of the Guadalupian basinal carbonates, for example, thins from nearly 40 m (130 ft) at the base of the slope to about 1 m (3 ft) within 15 km (10 mi) basinward. Basinal carbonates typically are very fine grained, have only traces of grading (although they probably are distal turbidites), and generally are finely laminated and dark-colored. Organic carbon contents, however, rarely exceed one percent and typically are 0.5 percent or less. These strata are mostly devoid of fauna, although a few radiolarians have been described. Burrowers and other benthic organisms are present along the basin margins but generally are lacking in the basin center areas. This provides

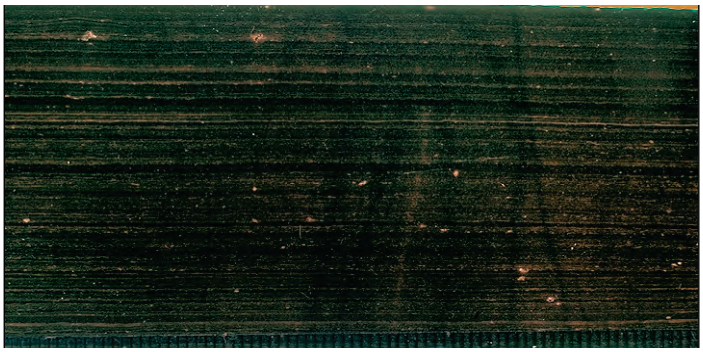

Figure 42. Polished slab of laminated, very dark colored, basinal Lamar Limestone (the uppermost member of the Bell Canyon Formation, roadside outcrop along U.S. Highway 62-180). Note excellent preservation of fine-scale lamination and lack of bioturbation in this sample from a locality about 7 km basinward from the age-equivalent Capitan reef margin.

evidence that the basin centers may have been occupied by oxygen depleted waters, perhaps dense, saline brines from the shelf (L. Babcock, 1977b).

As was noted earlier, the thin, detrital carbonate beds do not form a volumetrically important part of the Guadalupian fill of the Delaware and Midland basins. Clastic terrigenous sandstones and siltstones, transported from the shelves either through penecontemporaneous channels in the reef or during episodic events of sea-level lowering, provide greater than 90 percent of the fill (Fig. 43). These strata consist of subarkosic, very fine-grained sandstones and coarse siltstones that are compositionally very similar to the thin clastic terrigenous units found on the shelf. The coarser sand grains are generally well rounded and frosted. Carbonate grains of shelfal origin, especially fusulinid foraminifers, were entrained in the sandstone deposits and ultimately also contributed to the generation of widespread carbonate cement in the clastic units.

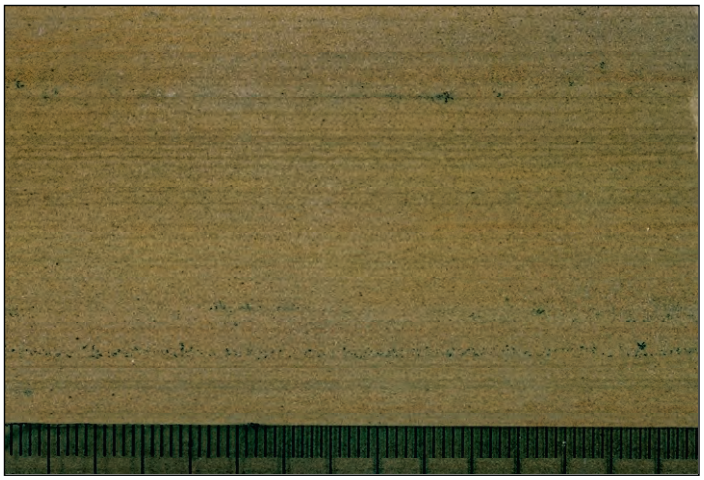

Figure 43. Polished slab of typical, finely laminated, very fine-grained basinal sandstone/siltstone. Sample from middle of Bell Canyon Formation, outcrop along U.S. Highway 62-180.

Large-scale sedimentary structures in the basinal sandstones are dominated by the sinuous channels, levees and overbank deposits typical of submarine fan complexes (Williamson, 1977). Elongate channels can be seen in outcrop where they are filled with amalgamated, generally clean and well sorted sands (Fig. 44). Slumps, flame structures and sand-injection structures are commonly associated with these channel and overbank deposits. Submarine channels have also been mapped in the subsurface, especially in the Bell Canyon Formation, where they are major exploration targets. The channel sands have porosities as high as 27% (Williamson, 1977), although the small average grain size results in low permeabilities and low oil recovery factors. In the Bell Canyon Formation, sandstones were mainly derived from the northern and northeastern sides of the basin; data are poorer for Cherry Canyon and Brushy Canyon intervals, but sediment transport there apparently was dominantly from the present-day north and northwest.

Smaller-scale sedimentary structures are dominated by horizontal lamination, although some rare small-scale channels, starved ripples, cross-bedding, flute casts and related structures also have been observed. The scarcity of structures produced by bottom currents and the predominance of horizontal lamination led Harms (1974; Harms and Williamson, 1988) to propose a "density overflow" hypothesis (Fig. 45). In this scenario, unstable, unconsolidated sands delivered to shelf settings by unspecified (presumably ephemeral stream

Figure 44. View southeast from U.S. Highway 62-180 south of Guadalupe Pass showing face of the Delaware Mountain escarpment with a series of lenticular sand-filled submarine fan channels surrounded by finer-grained interchannel (overbank) sediments. Approximately 300 m of Brushy Canyon Formation strata are exposed below the Cherry Canyon Formation carbonate ledges that cap the ridge.

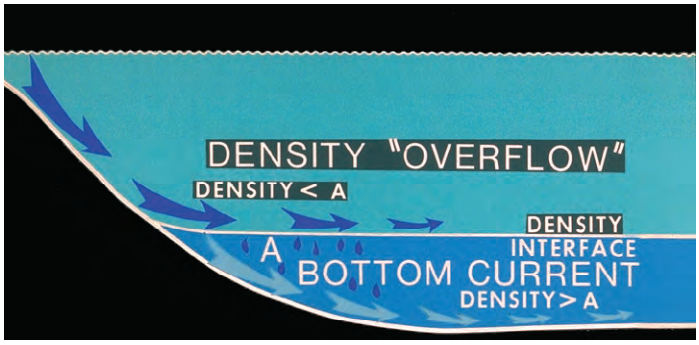

Figure 45. Harms' (1974) model of density "overflow" deposition of laminated terrigenous sediment in the Delaware Basin. Low-density sand-bearing flows were unable to displace dense, saline, basin-center brines and thus moved across the upper interface of the brines, dropping their sediment load as they lost velocity. Rarer, denser currents displaced basinal brines yielding classic traction deposits. This process could have operated during both relative high- and low-stands of sea level.

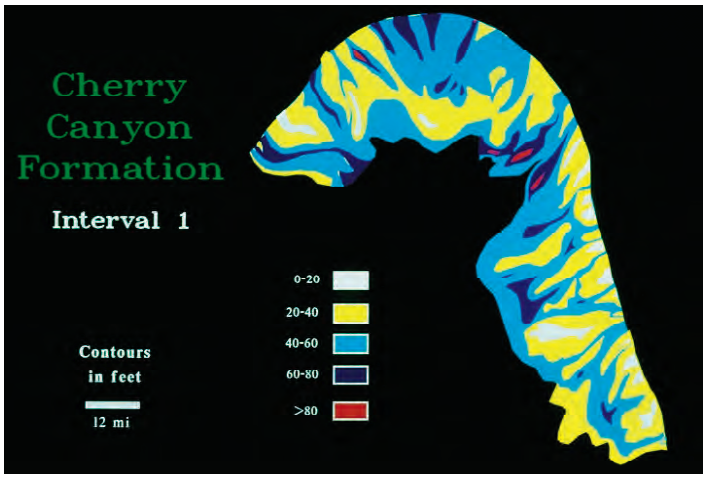

Figure 46. Isopach map showing thickness of sands in the lower Cherry Canyon Formation in the Delaware Basin. Note channelized and lobate forms of sand deposits and the presence of numerous entry points around the basin margin. This is interpreted to indicate wide distribution of sands, primarily by eolian process on shelves during lowstands with subsequent influx of those sands through numerous "lows" in shelf-margin carbonate deposits of the previous highstand (from Geisen and Scholle, 1990).

and eolian) processes were carried into the basin by salinity currents generated in evaporitic lagoons that may have been shifted close to the edge of the shelf during relative lowstands of sea level. These comparatively low-density currents transported very fine-grained sands and silts into a basin that already had dense, high-salinity brines at the base of the water column. A significant number of the saline, sand- and silt-laden currents were unable to displace the existing bottom waters and therefore flowed out across the interface between the basal brines and the less dense overlying fluids. As these "density overflows" (really interflows) slowed, entrained sediment was rained down producing a laminated deposit devoid of traction structures.

Alternatively, direct eolian input by major dust storms could have contributed laminated silts and very fine sands to much of the area of these small basins on an episodic basis (Fischer and Sarnthein, 1988). Furthermore, it is possible that some terrigenous sands passed across the shelf margins even during relative sea-level highstands, probably by transport through channels or tidal passes in the reef barrier. Discrete, terrigenous sand-filled channels are abundant in outcrop and subsurface sections of the Capitan fore-reef talus facies. These channels have not been tied to subaerial exposure horizons on the shelf and have not been shown to occur in any cyclical pattern on the slope. Thus, they may mark sites of clastic terrigenous sediment bypass through a dominantly carbonate system even during relative highstands of sea level.

Mapping of the distribution patterns of sandstones in the Delaware Basin has been undertaken in order to answer the question of episodic or continuous sand transport into the basin as well as to delineate changes in terrigenous sources through time (Fig. 46; Geisen and Scholle, 1990). The results to date have supported the concept of highly cyclical input of sands rather than continuous bypass supply. During most intervals examined, the preponderant terrigenous influx has been from the north and east of the Delaware Basin and entered through 10 or more major conduits (probably accompanied by dozens of smaller supply passages) rather than through a single channel. A northeast supply direction is reasonably consistent with expected wind patterns in the Trade Wind belt that the Permian Basin was in at that time..

Increasing hydrocarbon exploration in basinal sandstones of the Delaware Basin from the 1980s onward has led to a plethora of additional publications on the detailed geometry of depositional units in these facies. The works of Rossen and Sarg (1988), Bashman (1996), Loftin (1996), Beaubouef et al. (1999), Carr and Gardner (2000), Gardner and Borer (2000) summarize much of this work.

Within the basinal sandstones, one also occasionally finds coarse debris-flow deposits that represent catastrophic failures of parts of the shelf margin (Fig. 47). Such deposits contain huge blocks of carbonate slope debris and apparently travelled as far as 10 km (6 mi) into the basin without significant disruption of underlying unconsolidated sands. The largest of these deposits form elongate tongues of debris with volumes comparable to large modern landslides (Newell et al., 1953; Rigby, 1957).

Figure 47. Large blocks of carbonate slope material in a debris flow (the Rader slide) within sandstones of the Bell Canyon Formation at Stop II-4. The largest clasts in this part of the flow (which lies approximately 7 km basinward from the shelf margin) exceed 3 m in diameter. The deposit represents an unusually large catastrophic failure of part of the Delaware Basin margin, and its occurrence at the transition between clastic and carbonate sedimentation phases in the basin may indicate that it was associated with a sea-level change.

Figure 48. Laminated Castile Formation basinal evaporites with small crenulations that have been interpreted in several different ways: structural effects of Tertiary block faulting, anhydrite-gypsum transformation during uplift, and flowage on outcrops due to erosion of laterally adjacent deposits (roadside outcrop along U.S. Highway 62-180 about 1.5 km north of Texas-New Mexico border; Stop II-7).

Post-Capitan Sedimentation

Deposition of carbonate reefs and associated carbonate shelf sedimentation was largely terminated at the end of Guadalupian time, presumably as a consequence of increased restriction of circulation and elevated salinities in the Delaware Basin. The remnant basin was then rapidly filled by massive evaporites during Ochoan time. The first phase of filling was the Castile Formation (Fig. 48), a unit that reachs 550 m (1,800 ft) thickness in the northeastern part of the Delaware Basin. This formation consists of an unusual deposit of millimeter-scale interbedded laminae of gypsum (anhydrite in the subsurface) and organic matter plus calcite. The laminae are planar and highly continuous over much of the Delaware Basin; indeed, individual layers have been correlated for more than 100 km (Anderson et al., 1972). Approximately 209,000 lamination cycles have been counted in the Castile Formation with an additional roughly 40,000 cycles in the overlying Salado Formation. These cycles have been interpreted as varves, with the gypsum representing evaporative arid season layers and the organic matter plus calcite reflecting more normal salinity that prevailed during monsoonal summer conditions with more cloud cover and rainfall (Anderson, 2006). The laminae also have been shown to reflect Milankovitch-scale climatic variability including precession (circa 22,000 year) and eccentricity (100,000 year) cycles (Anderson, 1984). This combination of characteristics suggests that the Castile evaporites were deposited in water depths of tens to hundreds of meters (at least below wave base).

The Castile sediments filled the Delaware Basin, and evaporite sedimentation then spread across the surrounding shelfal regions. Water depths were undoubtedly much shallower at this stage and conditions became even more hypersaline with deposition of the anhydrite, halite, sylvite, and other bittern minerals of the Salado Formation. Commercial deposits of potash minerals have been exploited in these thick, last-stage fillings of the Delaware Basin and its marginal areas. Water depths during this phase were probably quite shallow, perhaps of the order of a few meters or less (Lowenstein, 1983, 1988).

Subsequent to the formation of the Salado evaporites, sedimentation in the area was dominated by nonmarine

redbed deposition that extended into the Triassic Period, completing the cycle of progressive desiccation and filling of the Permian Basin region. These evaporites preserved the geometry of the basin and provided the excellent seals needed to trap a high percentage of the oil generated from the rather sparse basinal source rocks. Finally, the removal of some of these evaporites by dissolution during the Late Tertiary has given us the spectacular present-day outcrops of the Guadalupe Mountains and its surrounding areas.

General Relations

The nature of, and the interrelationships between, the shelf-interior, shelf-margin, and basin facies are governed by a number of factors. Eustatic sea-level stands and(or) relative rates of subsidence versus sedimentation, as mentioned earlier, can lead to "reciprocal" sedimentation patterns. Ecological conditions, such as water temperature, salinity, turbidity or other factors, can affect reef formation and, thus, overall facies patterns. Indeed, just within the Permian facies of the Guadalupe Mountains region, one can see remarkable variations in microfacies patterns, especially in shelf-margin settings. Bank margins of non-reefal bioclastic calcarenite are present in some intervals (Victorio Peak and Getaway units); reefs that prograde largely horizontally out over reef talus are dominant at other times (upper Capitan unit). Yet other reefs that build up almost vertically in the section form the bank margin in the Goat Seep unit. Finally, terrigenous sand sheets cover the entire region from back-reef to basin at other times. So the discussion of facies patterns in the Permian Basin region must take into account these temporal variations in modifying factors.

The climatic setting of the Permian reef complex also had a major influence on both depositional and diagenetic processes. The region lay at the western margin of a broad alluvial plain to the west of the Appalachian mountain area. The basin was presumably connected to a major western and southern ocean by narrow channels (Figs. 4, 5). The entire region clearly had a hot and and at least seasonally very arid climate, as evidenced by the extensive back-reef evaporite deposits.

During Guadalupian and earlier time, water circulation in the Delaware Basin apparently was adequate to maintain normal marine salinity of the surface water along the bank margins. Waters penetrating deeper onto the banks were evaporatively concentrated to high salinities. Generation of heavy brines on the banks, which periodically flowed into the basin, may have contributed to euxinic, stratified water masses in the deeper parts of the Delaware and Midland Basins. Progressive restriction of the passageways between the Delaware Basin and the "open oceanic" areas to the south and west led to apparent salinity increases and extinction of reef growth in the region at the close of the Guadalupian, and continued aridity, coupled with restricted influx of marine waters, led to the completely filling the topographic depression left after Guadalupian time with evaporites. The extreme aridity of the region also had other influences. Transportation of clastic terrigenous debris was dominated by eolian processes. Equilibrium eolian deflation surfaces (sabkhas) are present in back-reef areas and dune migration may have been responsible for transport of a significant volume of sand to the shelf edge from where it could be moved into the basin, especially during lowstands of sea level. Although few dunes are preserved in the Permian Basin, large Permian dune fields have been described from areas to the north and west in Colorado, northern New Mexico, Arizona and Utah (Reiche, 1938; McKee et al., 1967a).

Aridity also presumably prevented the formation of extensive karstification during sea-level drops, allowed the development of widespread "coastal caliche" and led to the formation of hypersaline brines that may have contributed to the extensive dolomitization of back-reef carbonate sediments.

The question of relative sea-level changes, mentioned previously as part of the model of "reciprocal sedimentation," should also be examined further. Regional subsidence, local tectonic effects, eustatic sea-level stands, and epeirogenic movements all can play a role in relative sea-level stands. Other factors, such as variations in sedimentation rate, can yield apparent changes due to progradation or retrogression of shorelines. Studies by Franseen et al. (1989), Melim and Scholle (1989b), and Sarg (1985) found that a number of important, if subtle, discontinuity surfaces can be traced across the region. Subsequent studies (e.g., Kerans and Fitchen, 1995; Tinker, 1998; Beaubouef et al., 1999; Kerans and Kempter, 2002) further explored the influences of relative sealevel fluctuations and shelf exposure on both depositional and diagenetic patterns. Older ideas of "all wet" shelf sedimentation (Pray, 1977) are no longer tenable in light of these recent studies.

DIAGENETIC PATTERNS

Diagenetic features have already been discussed to some degree under the individual environments, but more generalized patterns of diagenesis in the Guadalupian section are outlined in Table 2 and Figure 49. This is a region with a relatively simple burial history (Fig. 50) consisting of rapid burial during the Permian, stability during the Mesozoic

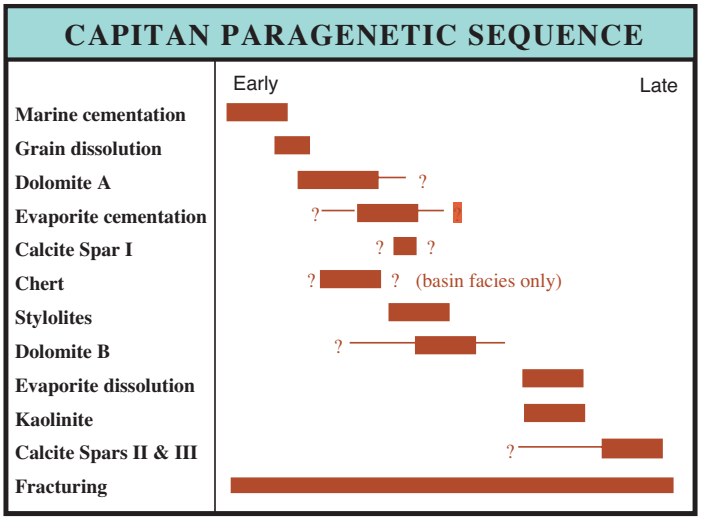

Figure 49. Diagram showing inferred relative timing of diagenetic events in the Permian reef complex.

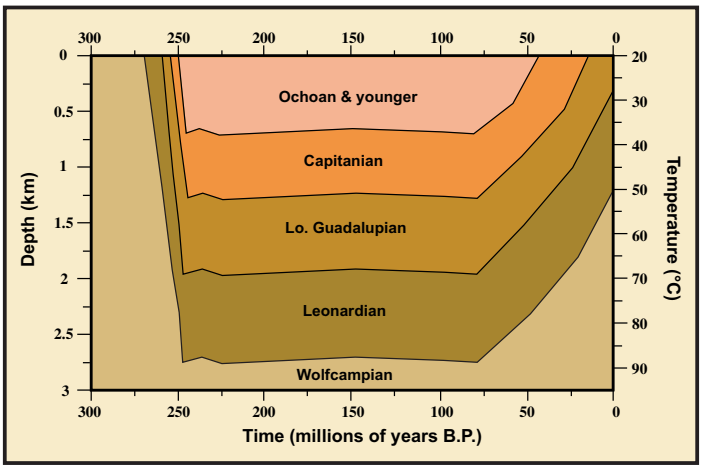

Figure 50. Burial history diagram for the Permian section in the Guadalupe Mountains. The late Guadalupian (Capitanian) interval is highlighted in orange. Note rapid burial of strata during the Permian, general stability during the Mesozoic, and extensive uplift during the Tertiary.

and part of the early Cenozoic, and then tectonic tilting and uplift during the later Cenozoic. Thus, most diagenetic alteration occurred either during the Permian (close to the surface at or near the time of sedimentation or during initial burial) or during the late Cenozoic.

The back reef province is characterized by the highest average porosities. The areas that were topographically highest (such as island facies) were frequently subjected to subaerial exposure and freshwater diagenesis. Evaporitic conditions in restricted lagoons and sabkhas led to the formation of evaporite minerals (gypsum and anhydrite). The withdrawal of these calcium sulfate minerals from the shelfal waters led to elevated Mg/Ca ratios and perhaps also to the formation of dolomitizing brines as in the modern Persian Gulf. Alternatively, but less probably, freshwater input and mixing with marine pore fluids may have led to dolomitization through "brine mixing" ("Dorag" dolomite). Thus, the back reef areas of the Permian reef complex are typified by calcareous grainstones and mudstones with a mixture of preserved primary porosity and secondary porosity related to such factors as early freshwater cementation and leaching, early dolomitization, or late (mesogenetic) dissolution of evaporite minerals.

The reef facies has very low average porosities. Small-scale permeability is very low, but large-scale permeability is quite high as a result of synsedimentary fracturing. Porosity in this facies was completely obliterated by submarine cements probably within a few tens to hundreds of

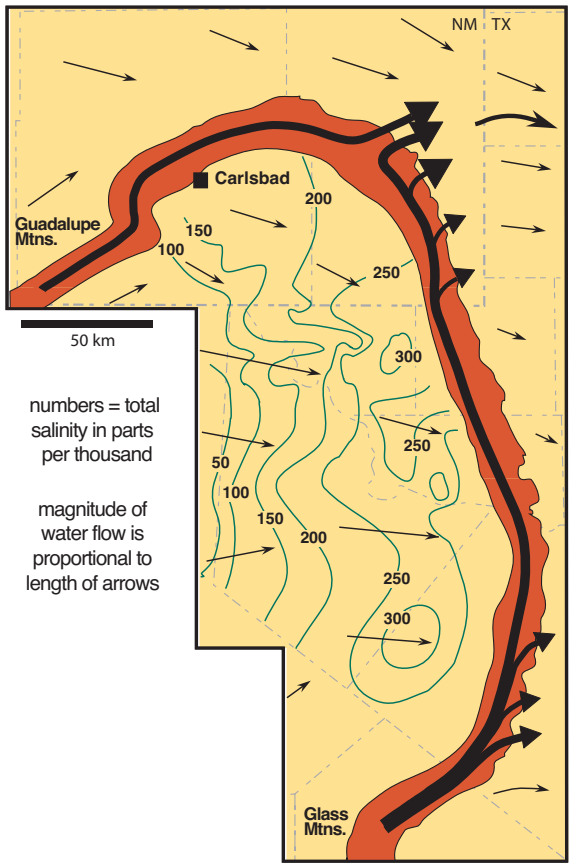

Figure 51. Diagrammatic representation of modern groundwater flow patterns and compositions in the Delaware Basin region. Arrows represent directions and volumes of water flow from recharge areas in the Guadalupe and Glass Mountains prior to the incision of the Pecos River as well as modern-day water withdrawal and oil development. Contours show concentrations of total dissolved solids in waters moving through the Capitan-equivalent Bell Canyon Formation (modified from McNeal, 1965 and Hiss, 1980).

years after the time of reef deposition (Mazzullo and Cys, 1977; Schmidt and Klement, 1971). Relatively coarse, radial, fibrous crusts of originally aragonitic cement, as well as more finely-fibrous crusts of probable high-Mg calcite, formed within open pores in these Permian reefs just as in many modern reefs (Aïssaoui, 1985; Ginsburg and James, 1976; Schroeder, 1972; see also Grotzinger and Knoll, 1995). Similar cements have also been described from Pennsylvanian-Permian reefs in other parts of the world (Davies, 1977; Davies and Krouse, 1975; Halley and Scholle, 1985; Hurst et al., 1988; Wendt, 1977). Further porosity destruction was accomplished by the infiltration of muddy, pelletal, internal sediment into remnant pores.

This type of cementation affected not just the reef-crust sediments but extended for several hundred feet down the fore-reef slope (a feature also seen in modern reefs). Thus, the upper fore-reef slope also has very low porosities. The lower half of the fore-reef talus facies has more complex diagenetic relations. Lesser amounts of submarine cementation are seen here. However, medium-crystalline, relatively late, very strongly fabric-selective dolomitization is present within this environment and has resulted in the replacement of about 1/2 of the original carbonate material in this facies. Such dolomitization has not led to significant secondary porosity in this facies, however.

The source of dolomitizing fluids may be either from the overlying back-reef facies or from the hypersaline basin waters of Castile and Salado time. Melim and Scholle (1989a) showed that multiple phases of relatively early dolomitization took place and that dolomitizing fluids moved downward mainly through solution-enlarged fractures and karstic pipes. When these fluids reached permeable fore-reef grainstones they spread laterally, selectively replacing fine-grained carbonate intraclasts, internal sediments, and fossils as well as forming dolomitic cements. At least one of these dolomite generations may have been produced by Mg-rich fluids derived from the exposure horizon between the Capitan and the Salado because the uppermost Capitan has been shown to have been replaced extensively by magnesite (Garber et al., 1990).

The toe of the fore-reef slope is characterized by compaction and silicification. Calcitic fossil fragments, especially brachiopods, bryozoans, and echinoderms, were selectively and delicately silicified by chert, chalcedony, and megaquartz. In some cases, silicification extends to aragonitic fossils or formed non-fabric-selective chert nodules that cross-cut primary textures and constituents. The source of silica most likely is from siliceous sponges and radiolarians, which lived in lower slope and (or) basinal settings.

The basin facies is typified by calcite and very subordinate quartz cementation of sandstones as well as compaction of sandstone, siltstone, shale, and carbonate beds. Porosity in the finer-grained basinal sandstones can be quite high (up to 27 percent; Williamson, 1977, p. 414) with corresponding permeabilities in the tens to hundreds of millidarcies.

Telogenetic (uplift-stage) alteration has substantially affected the region. Evaporite minerals that formed as primary precipitates or diagenetic phases were extensively hydrated, replaced, or leached during uplift (Fig. 51), both at substantial depth and at the surface (Scholle et al., 1992). Thus, calcite and silica cements found in many environments are actually evaporite replacements and much of what one sees as porosity in surface outcrops may once have been evaporite-plugged in the subsurface.

RECENT MODELS

The Permian depositional and diagenetic patterns described here can be matched quite closely in some modern settings. The basinal oceanographic conditions and the topographic configurations can be modeled in the Mediterranean, the Black Sea and the Bahamas-Florida area. The restricted circulation and partially euxinic conditions can be found, to some degree, in the Red Sea, Mediterranean and Black Sea during the Tertiary or Quaternary. The deep, relatively elongate, structurally controlled basins surrounded by steep, reefal escarpments bordering isolated platform areas, which are seen throughout the Permian Basin, are best modeled in the Bahamas (Ball et al., 1969). Likewise, the Permian facies suite of fore-reef debris, reef, back-reef rubble, near-back-reef skeletal sands and muds, islands, restricted lagoons, and finally supratidal deposits is remarkably similar to the general facies spectrum found in the Florida Keys-Florida Bay area (Ginsburg, 1964; Purdy, 1963). Yet climatically and paleogeographically, the Permian of west Texas and New Mexico was much more like the arid, continent-interior southwestern margin of the Persian Gulf than the high-rainfall, ocean-margin region of south Florida. Thus, the lagoons and sabkhas of the Trucial Coast of the Persian Gulf provide an excellent analog for the far-back-reef areas of the Permian during highstand intervals (Kendall, 1969; Shinn, 1983).

It is clear, then, that no single area today provides a full analog for the Permian Basin. Yet if we combine the climatic factors of the Persian Gulf with the tectonic-sedimentologic patterns of the Florida-Bahamas region and the hydrographic factors of the Mediterranean-Black Sea-Red Sea area, we can very closely approximate the patterns seen in the Permian.

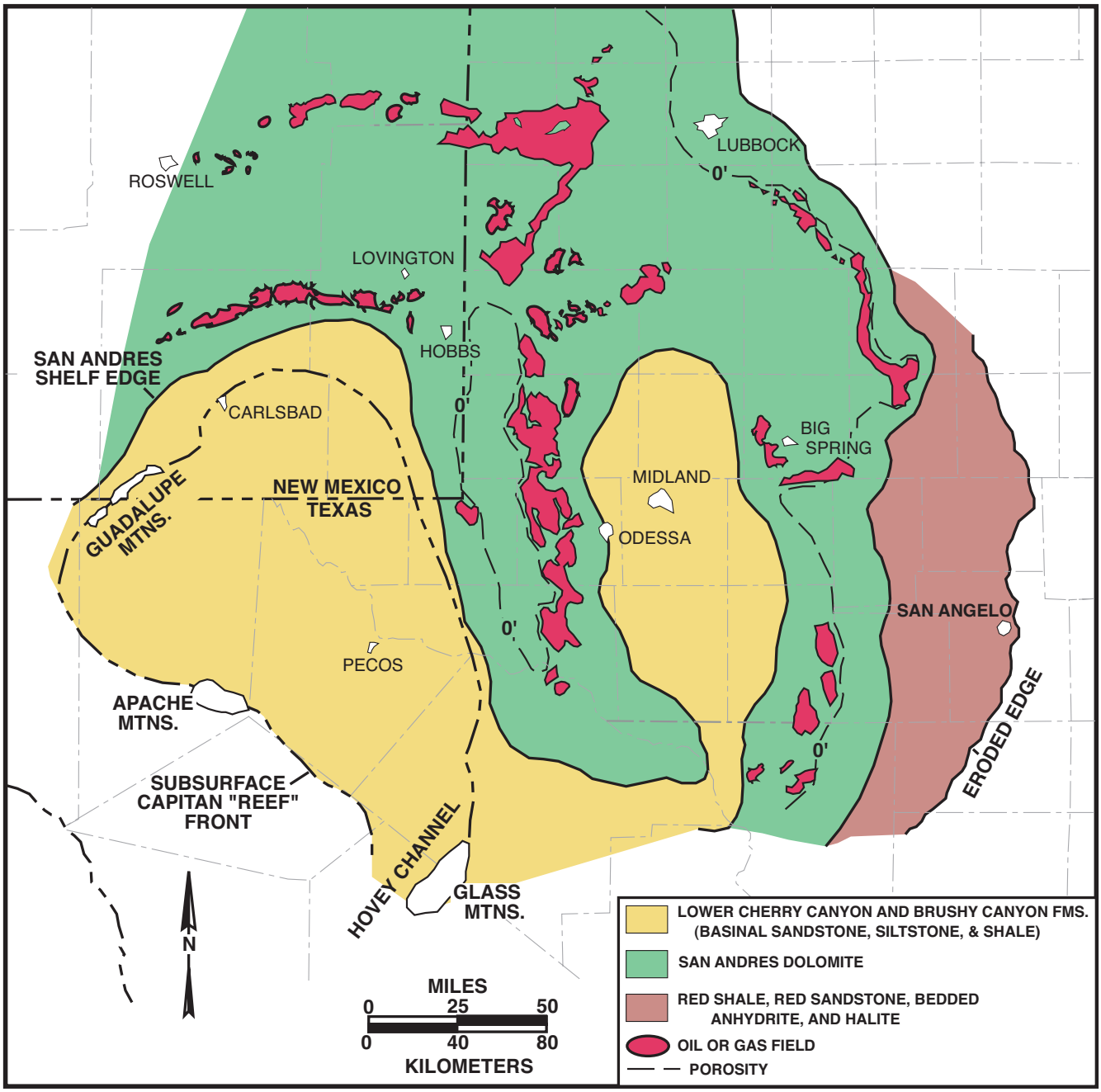

Figure 52. Inferred distribution of depositional facies in lower Guadalupian strata of the Permian Basin. Oil and gas fields producing from that interval are also shown (after Ward et al., 1986). Thin dashed line represents zero net porosity.

OIL AND GAS PRODUCTION

The Permian Basin has had hydrocarbon production for nearly 60 years and is one of the most prolific petroleum provinces in North America. As of the late 1970's, "approximately 91.6 billion barrels of oil-in-place and about 3 trillion cu m (106.2 trillion cu ft) of dissolved/associated and non-associated gas-in-place have been discovered in the Permian Basin" (Dolton et al., 1979, p. 1). Production from the Permian Basin extends from the Cambrian (Wilberns Formation) to the Cretaceous (thin carbonate units) although production from units younger than Permian is negligible. Paleozoic reservoirs produce oil from depths of less than 150 m (500 ft) to greater than 4,250 m (14,000 ft) and also produce gas from depths of less than 150 m (500 ft) to greater than 6,400 m (21,000 ft) (Dolton et al., 1979). The Permian section is mainly oil productive with greater than 65 billion barrels of oil-in-place (71 percent of the total discovered in the Permian Basin) having been discovered to date (in 2,188 pools). Non-associated gas production, on

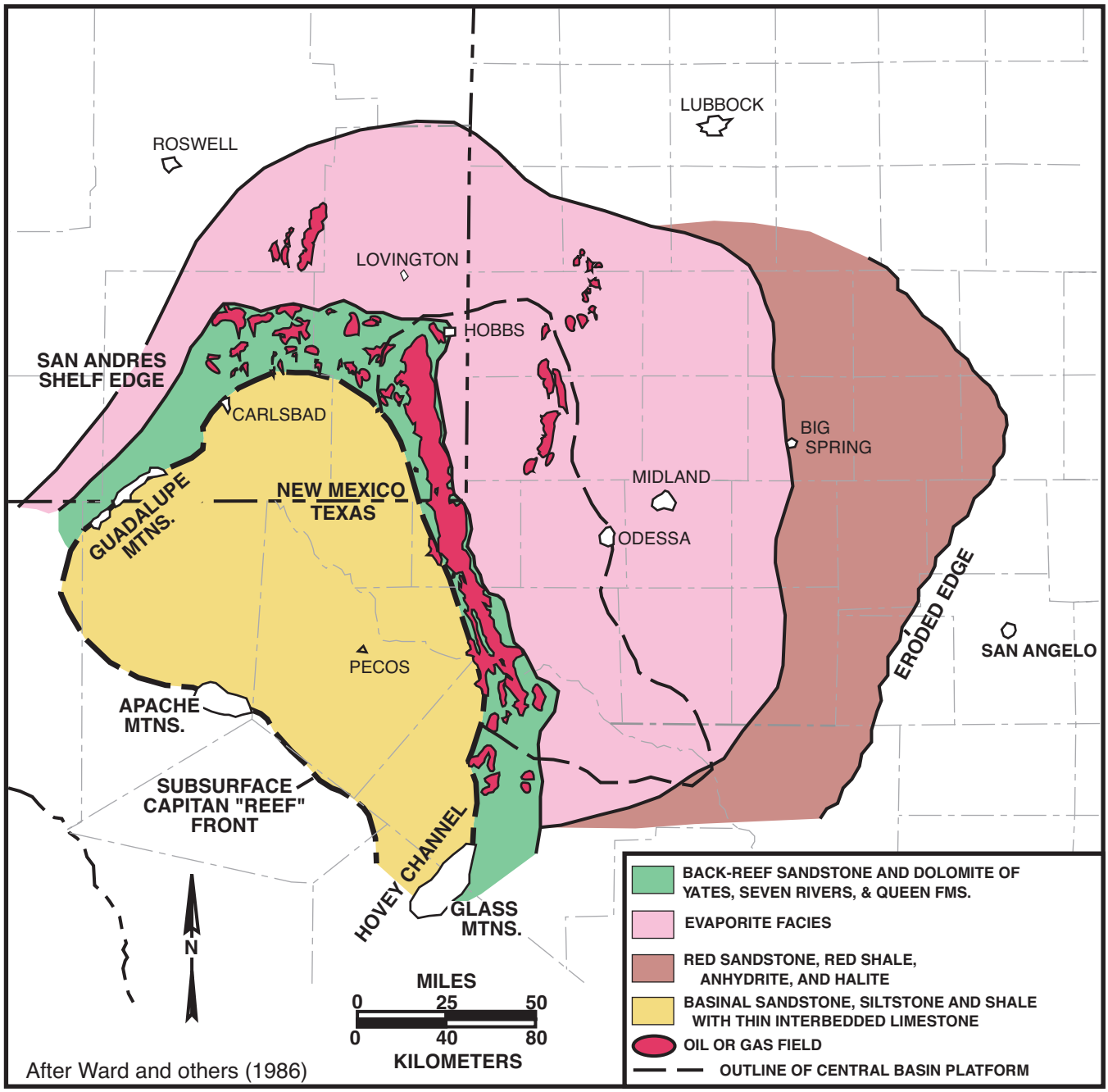

Figure 53. Inferred distribution of depositional facies in upper Guadalupian strata of the Permian Basin. Oil and gas fields producing from that interval are also shown (after Ward et al., 1986).

the other hand, comes predominantly from pre-Mississippian strata. Permian units contain only about 0.18 trillion cu m (6.3 trillion cu ft) of non-associated gas-in-place (about 13 percent of the total for the Permian Basin). However, Permian units contain 0.93 trillion cu m (32.7 trillion cu ft) of associated/dissolved gas-in-place (54 percent of the Permian Basin total) (Dolton et al., 1979).

The predominance of oil production from Permian units is clearly related to their relatively shallow burial in this region where virtually all Permian strata are found at present-day burial depths of less than 4,600 m (15,000 ft). Furthermore, virtually all production from Permian rocks comes from units at less than 3,000 m (10,000 ft) burial depths; most of it from less than 1,500 m (5,000 ft) depths (Dolton et al., 1979).

"The four provincial series of the Permian do not contain hydrocarbons in equal amounts. The largely evaporitic Ochoan rocks have accounted for only about 6 million bbls of discovered oil in-place, less than 0.01 percent of the Permian's 65 billion bbls" (Dolton, et al., 1979, p. 24).

"By contrast, the Guadalupian has accounted for 67 per-

Table 3. Cumulative oil and gas production through the year 2000 for selected stratigraphic units from the Permian Basin of west Texas and southeastern New Mexico.

PRODUCING FORMATION	NO. OF POOLS	CUMULATIVE OIL PRODUCTION (bbls)	CUMULATIVE GAS PRODUCTION (Mcf)
Bone Spring Limestone	36	10,836,946	26,107
Capitan Formation	0	0	0
Castile Formation	10	177,446	0
Delaware Mountain Group	228	147,838,929	444,186
Goat Seep Limestone	0	0	0
Grayburg Formation	173	3,257,310,434	17,265,940
Queen Formation	179	527,719,866	1,254,017,480
Rustler Formation	5	1,019,685	0
San Andres Limestone	435	3,605,905,136	36,433,294
Seven River Formation	91	921,401,640	823,028
Tansill Formation	12	229,717	0
Victorio Peak Limestone	0	0	0
Yates Formation	159	609,064,948	1,710,628,578
Yeso Formation	15	202,411,700	803,437,919
Total all Units	**1343**	**9,283,916,450**	**3,823,076,532**

cent of all Permian oil found and 62 percent of all Permian gas. The Leonardian follows with 28 percent of the oil and 32 percent of the gas. The Wolfcampian contains 5 percent of the oil and 10 percent of the total Permian gas. These amounts are directly related to the progressive development of reefs and back-reef lagoons beginning in the Wolfcampian, increasing in the Leonardian, and culminating in the development of the Capitan reef complex in the Guadalupian.

Hydrocarbon traps in Permian rocks are largely a combination of stratigraphic and structural types, although each type does occur alone. The intricate stratigraphic interfingering of lithologies responsible for trapping much of the Permian oil has resulted largely from the constantly shifting sedimentary environments. In particular, the filling of the Midland basin during the early Guadalupian (by Grayburg time) meant that oil fields on the Midland basin side of the Central Basin Platform produce mainly from San Andres-Grayburg or older reservoirs (Ward et al., 1986). Continued carbonate sedimentation in the Delaware Basin through the end of the Guadalupian resulted in the fact that oil fields on the west side of the Central Basin Platform produce largely from post-San Andres reservoirs (Figs. 52, 53).

Primary sealing mechanisms in all units are porosity and permeability barriers of carbonate, evaporite or shale, particularly updip transitions from porous limestones or dolomites to anhydrite plugged dolomites (Ward et al., 1986). Thus, maps showing facies distribution versus known oil fields (Figs. 52, 53) show a remarkably close correlation between them (Ward et al., 1986). Production is typically maximized in the near-back-reef or grainstone margin facies that underwent neither the marine cementation of the Capitan reef nor the evaporite plugging of the farther back-reef strata. A roughly 10 km wide porosity-permeability fairway thus exists that contains most of the oil fields and closely parallels the outlines of basin configurations. About 40 percent of these (Permian) reservoirs are limestone, 29 percent are dolomite and 29 percent are sandstone. Porosities range from 1.5 to 25 percent and reservoir permeabilities from 0.02 to 200 millidarcies.

"Recovery factors range from a low of 7.6 percent to a high of 47.5 percent. The fractured siltstone Spraberry reservoir of the Midland basin has a very low recovery factor, although the volume of oil in-place is the largest of any single Permian pool. The average recovery factor for the Permian System is 25 percent." (Dolton et al., 1979, p. 24).

Production totals through the year 2000 for each producing stratigraphic unit are given in Table 3, along with a grand total for all these strata in the Permian Basin region. Only units that will be seen on this field trip have been included in the table. Extensive production from age-equivalent but differently named units from the Central Basin Platform, Midland basin, and Eastern Shelf have not been listed. Data for this table was supplied by the Petroleum Data System, University of Oklahoma, Norman, Oklahoma. Similar data is

Table 4. Cumulative production of oil plays in the Permian Basin (New Mexico and Texas), listed by reservoir age. Production is through 31 December 2000 (adapted from Dutton et al., 2004).

AGE	RESERVOIR	CUM. PROD. (Mmbbl)
PERMIAN		
Guadalupian	Artesia Group platform sandstones	1,855.4
	Queen tidal-flat sandstone	179.6
	Delaware Mountain Group basinal sandstone.	351.9
	Grayburg platform, mixed carbonate/sandstone	2,239.3
	San Andres/Grayburg mixed platform deposits	2,286.5
	San Andres platform carbonates	8,394.9
Leonardian	Sprayberry/Dean submarine fan sandstone	1,287.1
	Bone Spring basinal sandstone and carbonate	70.7
	Yeso/Clear Fork restricted platform carbonate	3,297.2
	Abo platform carbonate	541.5
Wolfcampian	Wolfcamp/Leonard slope and basin carbonate	195.0
	Wolfcamp/Leonard platform carbonate	457.4
PENNSYLVANIAN	Up. Penn./Lo. Perm. slope and basin sandstone	271.4
	Penn./Lo. Perm. reef/bank/platform carbonate	3,555.5
	Penn. shelf sandstone	7.3
MISSISSIPPIAN	Miss. Platform carbonate	15.1
DEVONIAN	Devonian ramp carbonate	110.2
	Devonian deepwater chert	785.9
SILURIAN	Wristen platform and buildup carbonates	888.8
	Fusselman shallow platform carbonate	356.3
ORDOVICIAN	Simpson platform sandstone	103.2
	Ellenburger ramp carbonate	1,651.0
	Total Permian Basin Production	**28,901.0**

provided in Table 4, but hydrocarbon production is grouped by play types and includes units from the Ordovician through the Permian (see Dutton et al., 2004).

Table 3 also shows that there is absolutely no hydrocarbon production from the Capitan, Victorio Peak, or Goat Seep reef or fore-reef deposits that were tightly cemented at the sea floor shortly after deposition. The bulk of hydrocarbon production (greater than 90%) is from primary or early diagenetic secondary porosity in back reef dolomites, limestones and sandstones of the Tansill, Yates, Seven Rivers, Queen, and Grayburg Formations or the open shelf facies of the San Andres Limestone.

A second, much smaller, peak of production comes from basinal channel sandstones of the Delaware Mountain Group (particularly in the Bell Canyon Formation) and basinal limestones of the Bell Canyon Formation or Bone Spring Limestone. More significant oil reserves in basinal sandstones are found in the Midland basin. There, the Spra-

berry Formation has more than 8 billion barrels of oil-in-place. However, recovery factors of less than 10 percent indicate ultimately recoverable reserves of about 534 million barrels of oil.

Individual channels in the "Ramsey Interval" near the top of the Bell Canyon Formation are up to 30 m (100 ft) thick, 0.4 to 6.5 km (1/4 to 4 mi) wide, and 80 km (50 mi) in length (Williamson, 1977 and 1979). These channels have a very pronounced regional trend (NE-SW for the "Ramsey") that strongly controls the shape and distribution of basinal oil fields, at least in the uppermost part of the basinal sandstone section.

Overall, back-reef environments account for greater than 90 percent of all hydrocarbon production with basinal sediments accounting for the rest. Reef and fore-reef facies are totally non-productive. Clearly, penecontemporaneous and early burial diagenesis played a major role in controlling the distribution of reservoirs. Evaporite formation and dissolution, synsedimentary dolomitization, early vadose and phreatic leaching and cementation, coupled with probable early oil migration from rapidly deposited and buried, overpressured source rocks in the basins, led to outstanding reservoir characteristics on the shelf. Early submarine cementation obliterated reservoirs on the shelf edge and slope long before oil migration. Finally, some basinal reservoirs may have been preserved from compactional porosity loss by overpressuring beneath 200-1,200 m (2,000-4,000 ft) of rapidly deposited evaporites.

The source for most of this Permian oil is presumably from the euxinic, relatively organic carbon-rich, basinal sediments such as the Bone Spring Limestone and some intervals within the Delaware Mountain Group. Although these units generally have present-day organic carbon contents of less than 1 percent (King, 1948; Gawloski, 1987; Barker and Pawlewicz, 1987; Palacas, oral commun., 1978), their carbonate composition, great thickness and intervening sandy, permeable zones most likely meant that they could act as very efficient source rocks. Oil reservoired in the basinal facies, then, probably migrated only a short distance from source to reservoir. Much of the oil in the back-reef sections, however, presumably moved up-section or laterally through fractured reef sediments to get from source to reservoir. The fracturing of the reef was essentially contemporaneous with deposition (because of compaction of the thick, underlying reef talus) and thus, even syndepositional reef cementation probably did not significantly retard fluid movement. Indeed, even today, the tightly cemented reef zone has the highest permeability of any of the Guadalupian bank-to-basin facies (Motts, 1968).

The abundant up-dip and overlying evaporite seals help to explain why, although the Permian Basin is source-rock poor, it is the largest petroleum province in North America. This region has one of the highest retention rates for generated hydrocarbons of any basin in the world and, even today, oil seeps are quite scarce in the region.

Detailed discussion of individual oil fields is beyond the scope of this guidebook, but the "Atlas of Major Texas Oil Reservoirs" (Galloway et al., 1983) provides a wealth of information on area fields. Informative oil field summaries are also provided in Anonymous (1982) and Bebout and Harris (1986).

Current estimates of the volume of undiscovered hydrocarbons in-place for Permian rocks of the Permian Basin are that "at the 95 and 5 percent probabilities, 1.0 to 6.0 billion bbls of oil in-place (1.5 to 9.2% of the discovered Permian crude oil) remain undiscovered, while 0.7 to 4.1 trillion cu ft of dissolved/associated gas in-place (2.2 to 12.4% of the discovered dissolved/associated gas) remain undiscovered. Finally, 0.2 to 0.6 trillion cu ft of non-associated gas in-place (3 to 21% of the discovered non-associated gas) remain undiscovered. Most of these undiscovered in-place hydrocarbons occur above 10,000 ft (Dolton et al., 1979, p. 47).

"These undiscovered amounts will probably occur in circumstances similar to known fields and pools with respect to reservoir characteristics, seals, source beds and nature of the hydrocarbons. Traps will probably be predominantly stratigraphic. The undiscovered deposits are likely to be distributed in undrilled areas surrounded by or flanking known production. Such flanking areas are in the western part of the Northwestern Shelf, the western areas of the Delaware Basin, and the southern and western parts of the Val Verde basin." (Dolton et al., 1979, p. 47).

Studies have shown that "undiscovered pool sizes are small; only at the 5 percent probability is there a chance of occurrence of an oil pool of 16 million bbls or larger, or a non-associated gas pool of 24 billion cu ft or larger" (Dolton et al., 1979, p. 47).

CONCLUDING NOTES — ACKNOWLEDGEMENTS AND FURTHER READINGS

For further general discussions of Permian Basin depositional and diagenetic facies patterns the papers by King (1948), Newell et al. (1953), Hayes (1964), Cys et al. (1977) and Ward et al. (1986) are recommended. Other, more specific papers, can be found in the extensive bibliography on the Permian Basin region given at the end of Part I of the guidebook.

Discussions of the specific details of facies patterns and diagenesis are also presented in the road log section of this

guidebook. The log owes much to previous guidebooks (Nelson and Haigh, 1958; Anonymous, 1960, 1962, 1964, and 1969; Dunham, 1972; Pray, 1975; and Pray and Esteban, 1977). However, this guidebook has extensive additional commentary on many localities and is organized differently from previous guides. All road logs are based on continuous routes with side trips being presented as separate, supplementary logs. Thus, the trip from El Paso to Carlsbad is logged as a continuous route with the side excursions to McKittrick Canyon, Walnut Canyon and Dark Canyon-Rocky Arroyo being listed as separately logged routes. This makes the logs, we hope, easier to use on car trips.

SAFETY ISSUES

One final, but by no means secondary, word about the most important thing on this field trip — SAFETY! Please make this your number one priority. We are going to be driving on back roads and will be a long way from medical attention. There are hospitals, emergency rooms and doctors in El Paso, Carlsbad and Alamogordo but we may be hours away from these facilities when we visit remote outcrops. This area has many hazards in addition to the "normal" geologic problems of loose boulders and sharp rocks. Cacti of many types, scorpions, tarantulas and rattlesnakes are all common to the region. Remain cautious and aware of these dangers at all times (Figs. 54 and 55). Never pick up rocks without looking at what might be on, near or under them. While climbing, try to avoid reaching up onto ledges that you cannot first examine for hazards. We do carry a small first aid kit with us and thus can help, at least with minor emergencies, but let's try to avoid the major ones. Surprisingly most accidents do not involve any of the hazards described. They come from sunburn, dehydration and accidental tripping over rocks, curbs or other obstacles. So stay hydrated, alert, and careful.

Finally, much of the trip is in national parks so in addition to watching out for wildlife, you must not harm what you find. A wide detour around hazards will prove to be the best strategy in almost all cases.

Figure 54. Lechuguilla (*Agave lechuguilla*) is a plant found only in the Chihuahuan and Sonoran Deserts, almost always on limestone soils. It is NOT your friend.

Figure 55. Robert Halley, one of the early contributors to this guidebook, contemplating life and death in the Guadalupe Mountains.

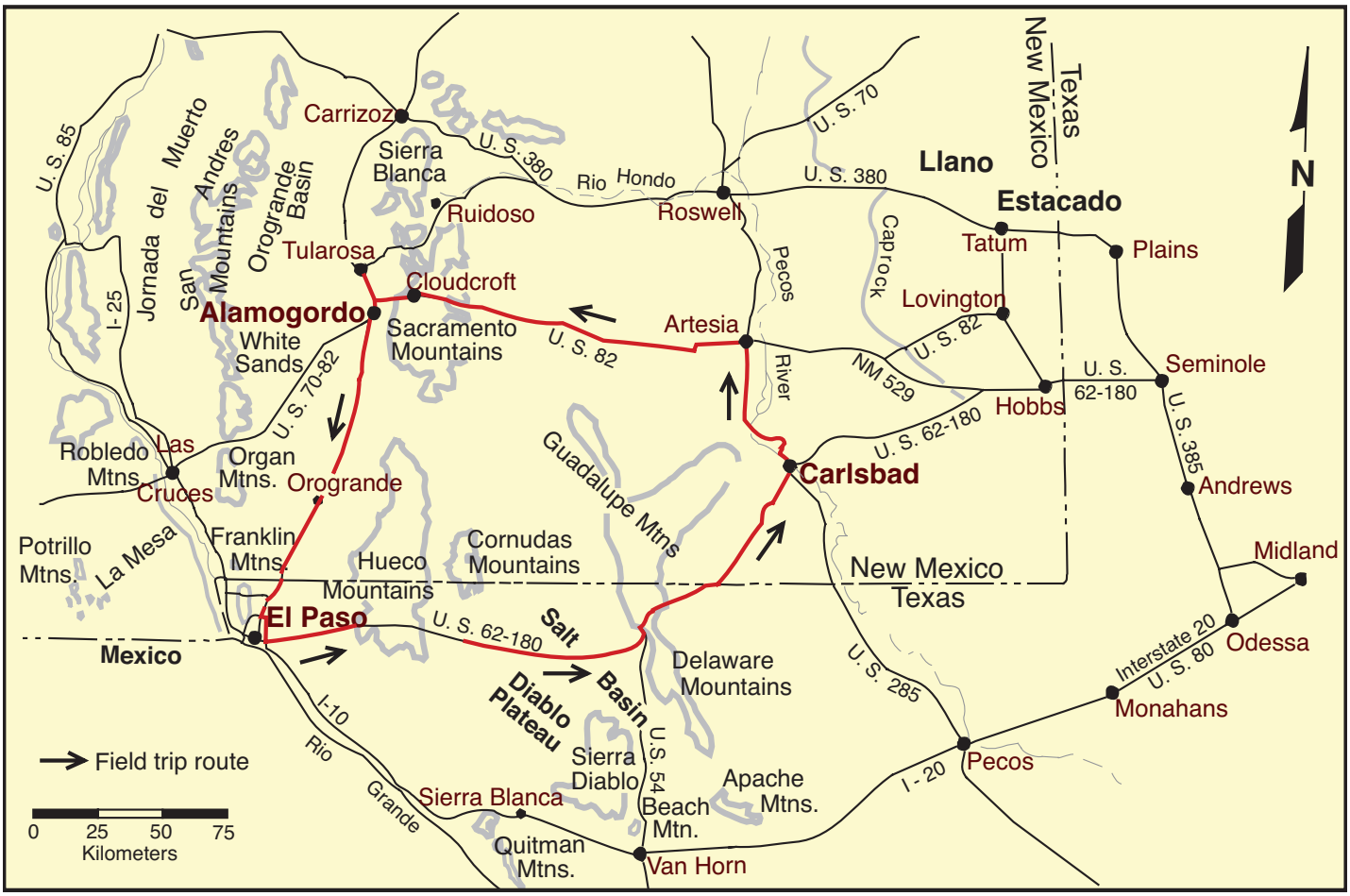

Figure 56. General field trip route. Map modified from Toomey and Babcock (1983).

EL PASO, TEXAS - CARLSBAD, NEW MEXICO GEOLOGIC ROAD LOG

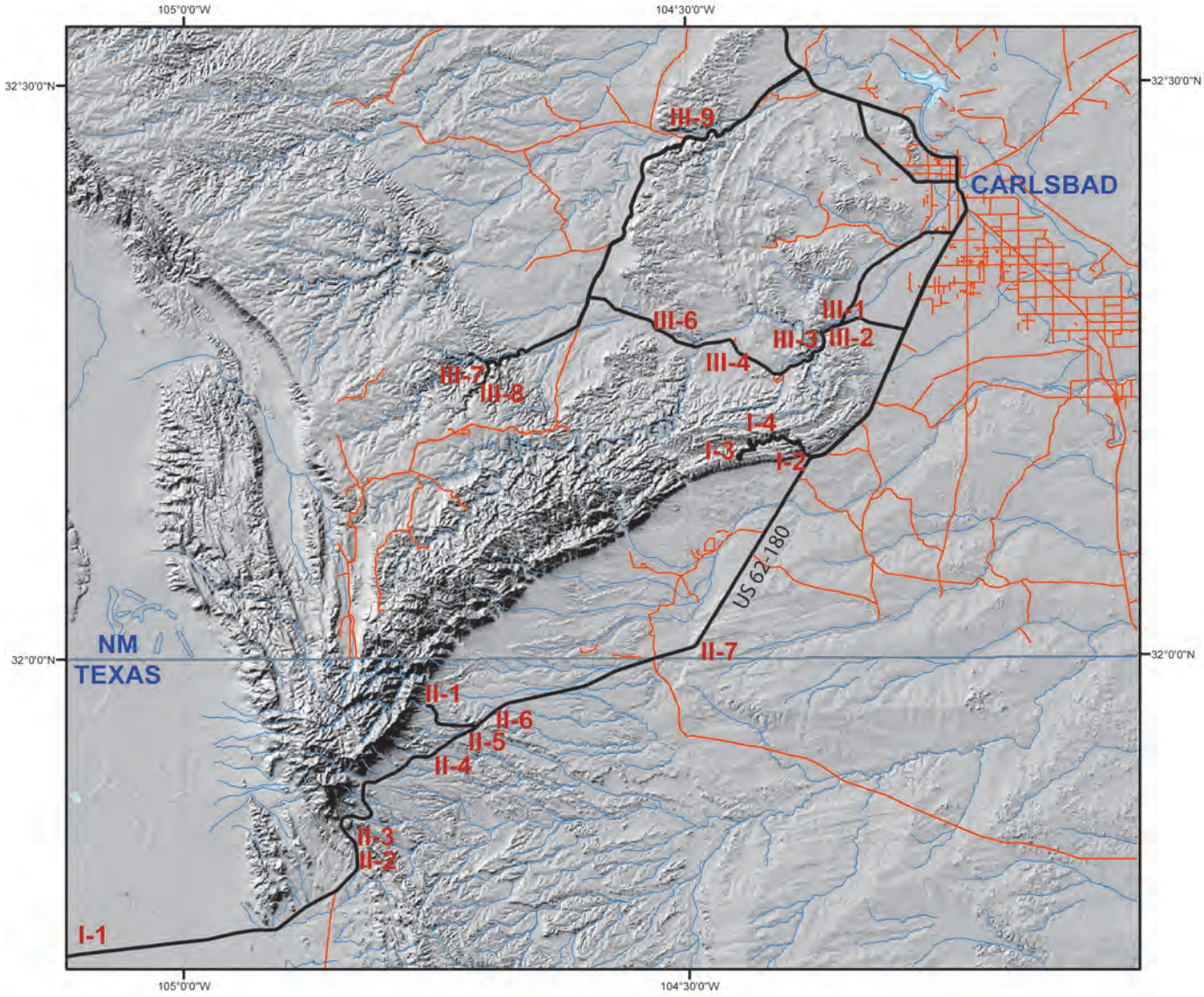

Figure 57. Approximate locations of outcrops examined on Days 1 to 3 of the field excursion. Base is from U.S.G.S. National Elevation Data set.

Mileage from previous stop	Cumul. mileage from El Paso	Cumul. mileage from Carlsbad	Location Description
			The field trip route is shown in Figure 56 and the location of stops for the next three days are given in Figure 57.
0.0	0.0	159.4	Leave El Paso Airport on Airway Rd.; turn left (heading east on U. S. Highway 62 and 180 (Montana Avenue). Behind us (to the northwest) are the Franklin Mountains, a block faulted section of Precambrian through Paleozoic strata (stratigraphic section shown in Fig. 58) steeply tilted to the west. The sections there have been summarized in a number of articles and guidebooks (Cunningham and Cromwell, 1989; LeMone, 1988; LeMone and Lovejoy, 1976; Nelson and Haigh,

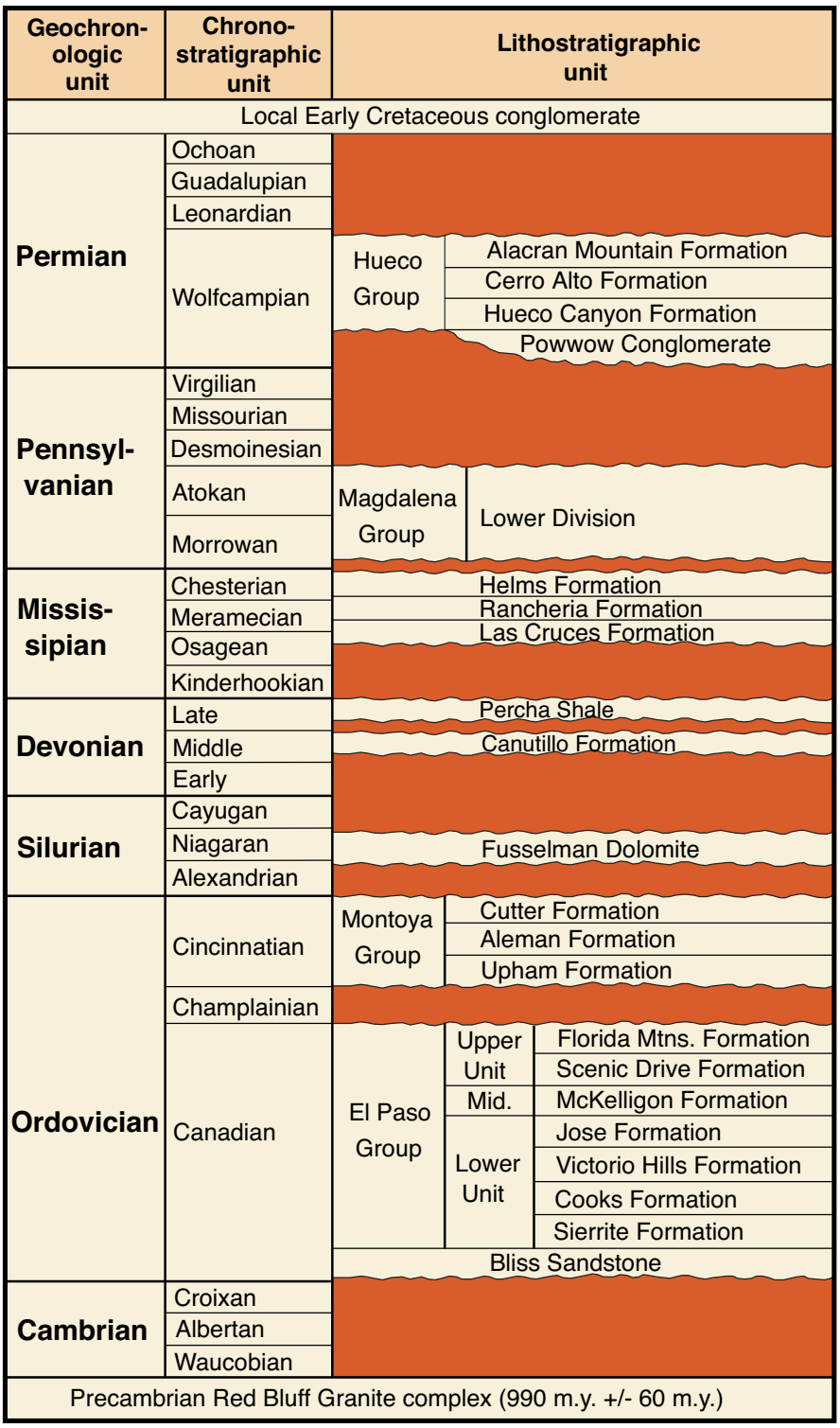

Figure 58. Paleozoic stratigraphy of the southern Hueco Mountains (modified from LeMone, 1988)

1958). Also see the description of the El Paso area and its geology at the end of the Alamogordo to El Paso road log in this guidebook.

7.1	7.1	152.3	Stabilized (vegetated) dunes of clastic terrigenous debris blown from the floor of the Hueco Bolson, the flat, intermontane basin we have been and are continuing to cross. The Hueco Bolson is one of the easternmost grabens of the Basin and Range

Province and is bounded on the west by the Franklin Mountains and on the east by the Hueco Mountains. To the north, near Orogrande (north of the Texas-New Mexico border), the Hueco Bolson is separated from the Tularosa Basin (which has completely internal drainage) by a low ridge near the town of Orogrande. The Hueco Bolson has external drainage along its southeastern side through the Rio Grande River valley. The average elevation of the Hueco Bolson is approximately 1,200 m (4,000 ft), and the basin averages 40 km (25 mi) in width and 130 km (80 mi) in length. "A ... (1967) U.S.G.S. seismic and gravity profile across the Hueco Bolson from the base of the Franklin Mountains to the base of the Hueco Mountains indicates a deep structural trough bounded on the west by a large normal fault. The maximum thickness of the Hueco Bolson fill in the center of this trough is calculated to be about 9,000 feet [2,750 m]." (McGlasson and Seewald, 1968). Details of the seismic line and supplementary gravity work were published by Mattick (1967). The bolson fill ranges in age from Miocene to Holocene; the Pleistocene deposits are particularly thick, with local accumulations of as much as 1,500 m (5,000 ft) of Pleistocene alluvial and lacustrine sediment (Strain, 1969). Surface sediments in the bolson belong mainly to the Pleistocene Fort Hancock and Camp Rice Formations that are best exposed along the Rio Grande River. The bolson forms the main aquifer for the El Paso-Juarez area. This trapped water is mainly from Pleistocene pluvial cycles and is being depleted rapidly.

1.5	8.6	150.8

El Paso city limit.

3.1	11.7	147.7

Junction with Texas FM Road 659 to Ysleta (to right) and start of two-lane section of U. S. Highway 62 and 180; continue straight ahead. The intensely block-faulted, low-relief (ca. 300-460 m; 1,000-1,500 ft) Hueco Mountains can be seen directly ahead. Precambrian to Tertiary igneous, metamorphic and sedimentary rocks are exposed in this range (Fig. 58). Cerro Alto, the highest peak, is a Tertiary syenite porphyry intrusive. The Permian (Wolfcampian to early Leonardian) section of the Hueco Mountains contains nearly 600 m (2,000 ft) of limestone and very subordinate shale. The pre-Permian sedimentary section consists of a lower interval of Cambrian to Mississippian strata (mainly limestones and dolomites) and an upper interval of Pennsylvanian limestones, shales and subordinate sandstones. The upper and lower intervals each are about 600-1,200 m (2,000-4,000 ft) thick. The lower interval shows disconformable contacts typical of stable shelf sections, whereas the upper interval contains angular unconformities indicative of the increased tectonic activity and bank-to-basin differentiation of that time.

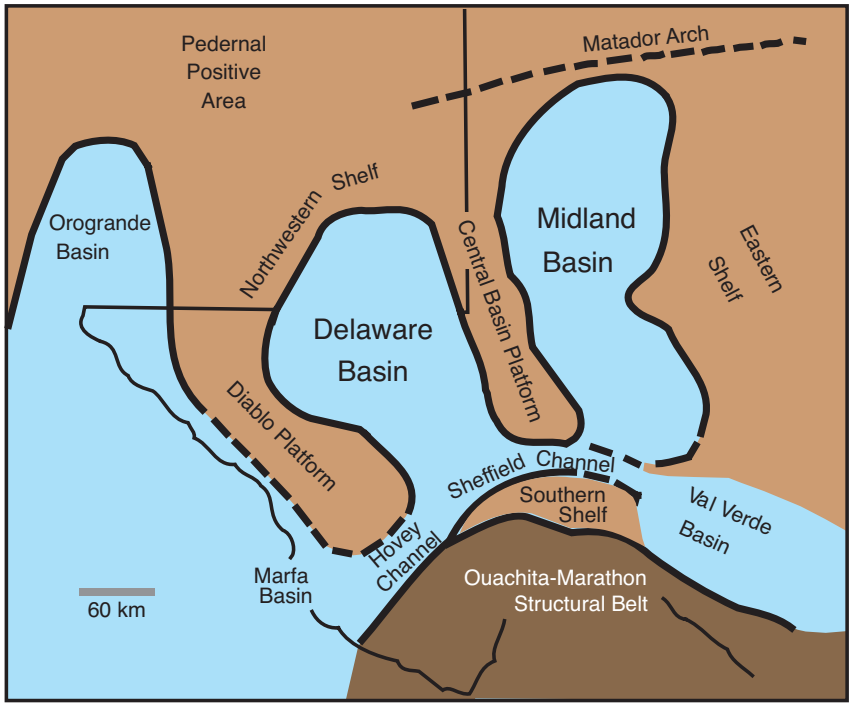

Figure 59. Major physiographic features of the Permian Basin region during early Guadalupian time. Adapted from Ward et al. (1986).

Throughout this trip, the bank-to-basin facies sequences we see will be related in one way or another to the initial, structurally controlled topographic variations generated during Pennsylvanian and Permian deformation. The folding and faulting of this period, part of the Ancestral Rockies movements, generally trends northwest-southeast. The Diablo platform, Orogrande Basin, Pedernal uplift, Northwest shelf and Delaware Basin (Fig. 59) were among the many major physiographic

			features formed during this time interval. This primary structural relief was, in most cases, strongly modified by subsequent differential sedimentation.
4.4	16.1	143.3	Loose (unvegetated) dunes deposited by winds from the northwest that lose velocity and drop sand near the base of the Hueco Mountains. The hills on the right (largely covered by dunes) are made of Wolfcampian limestones of the Hueco Group.
2.5	18.6	140.8	Quarry in Hueco Group limestone on the right. The limestone here is about 97 percent pure $CaCO_3$ and the quarry exposes a single, thin, fusulinid-rich bed about 3/4 of the distance up the rock face. The quarried carbonate is calcined and is sold as quick lime.
0.4	19.0	140.4	Lower part of Hueco Group is exposed in hill on right. The unconformable contact between the Hueco limestone and the underlying lower part of the Pennsylvanian Magdalena Limestone is exposed in the low knob at the base of the eastern slope of the hill. This unconformity is an indication of pre-Permian uplift and erosion on the Powwow anticline.
0.8	19.8	139.6	Exposures of the Mississippian Helms and Pennsylvanian Magdalena Formations in hills on left.
0.6	20.4	139.0	Quarry at 2:00 o'clock in Magdalena Limestone. The very pure (99.8 percent $CaCO_3$) limestones in this quarry, as well as those from the quarry at mile 18.6, were formerly transported to El Paso where they were calcined to CaO (quick lime).
0.3	20.7	138.7	Junction with Texas SF Road 2775 to Hueco Tanks State Park; continue straight ahead. Mounds visible in the upper parts of nearby hills are phylloid algal and fusulinid buildups in Virgilian limestones (Pol, 1988a; Harris and Simo, 2000). These are smaller than, but otherwise similar to, buildups we will examine in the Sacramento Mountains.
0.3	21.0	138.4	Hills on left are capped by Magdalena Limestone. The southeast dips visible here are on the flank of the Powwow anticline. The Jones No. 1 Sorley well, drilled a few miles west on the crest of the Powwow anticline, encountered Precambrian granites at 662 m (2,172 ft) depth. Helms Peak (elevation 1,649 m; 5,409 ft) at 2:00 o'clock is capped by limestones of the Hueco Canyon Formation unconformably overlying middle Magdalena Limestone.
0.7	21.7	137.7	Entering Powwow Canyon.
1.9	23.6	135.8	Roadcut in middle Magdalena Limestone.
0.5	24.1	135.3	Roadcut in middle Magdalena Limestone.
0.8	24.9	134.5	Roadside park on left. The unconformity at the base of the Permian is clearly visible directly ahead. On the western side of the Hueco Mountains this unconformity cuts down to the Ordovician El Paso Limestone. In the outcrop directly ahead, the unconformity is between the Pennsylvanian Magdalena Limestone and the basal Hueco Group.
0.4	25.3	134.1	Roadcut in upper 40 m (130 ft) of Magdalena Limestone.
0.3	25.6	133.8	Roadcut in basal part of the Permian Hueco Group (including the poorly exposed Powwow Conglomerate and the overlying upper member of the Hueco Canyon Formation). The Powwow Conglomerate varies locally in thickness, but is about 10 m (30 ft) thick in this area. It contains red shales, siltstones and chert- and limestone-pebble conglomerates. Another redbed interval (the Deer Mountain Shale) occurs near the top of the Hueco Group. These redbeds are considered to be the southern tongues of the thick, mainly redbed Abo Formation and the clastic units of the Laborcita Formation that are seen in the Sacramento Mountains (Candelaria, 1988; Pol, 1988b). The Lower Permian paleogeography of the region is shown in Figure 60 — this locality (as well as the ones we will examine in the Sacramento Mountains) lay just to the west of the Pedernal-Orogrande positive element and thus had extensive terrigenous influx from the east. The uplift was greater to the north so that the non-marine, terrigenous components of the Lower Permian rocks increase sig-

nificantly northward.

Detailed field guides to the geology of the Hueco Mountains have been published (Meader-Roberts, 1983; Robichaud and Gallick, 1988; Harris and Simo, 2000) and should be consulted for further information.

0.2	25.8	133.6	Roadcut in Hueco Canyon Formation, mainly shelfal limestones containing scattered phylloid algal plates, fusulinid foraminifers, mollusks and other shallow marine fauna with considerable micritic matrix.
1.2	27.0	132.4	Hueco Inn on left. Continued Hueco Group outcrops for next 12 miles.
8.7	35.7	123.7	Forty Mile Hill (elevation 1,654 m; 5,427 ft). Leaving Hueco Mountains; emerging onto Diablo Plateau.
3.1	38.8	120.6	Roadside rest area on left with view of numerous extrusive and intrusive igneous features to the north and northeast in the Cornudas Mountains. The central, high volcanic cone is San Antonio Peak (2,140 m; 7,020 ft).
13.3	52.1	107.3	Limestones of Hueco Group in roadcut.
4.7	56.8	102.6	Road on Lower Cretaceous Campagrande Formation.
0.5	57.3	102.1	Junction with Texas Ranch Road 2317; continue straight ahead. Molesworth Mesa, which lies to the south, is capped by Cretaceous Trinity-Fredricksburg sediments.
1.9	59.2	100.2	Mountains at 9:00 o'clock are the Sierra Tinaja Pinta, a breached laccolith. The anticlinal structure in the center is composed of Bone Spring Limestone and is flanked by sediments of the Yeso Formation.
5.0	64.2	95.2	Junction with Texas Ranch Road 1111; continue straight ahead.
6.1	70.3	89.1	The Antelope Hills, containing basal Cretaceous sandstones cut by a Tertiary sill,

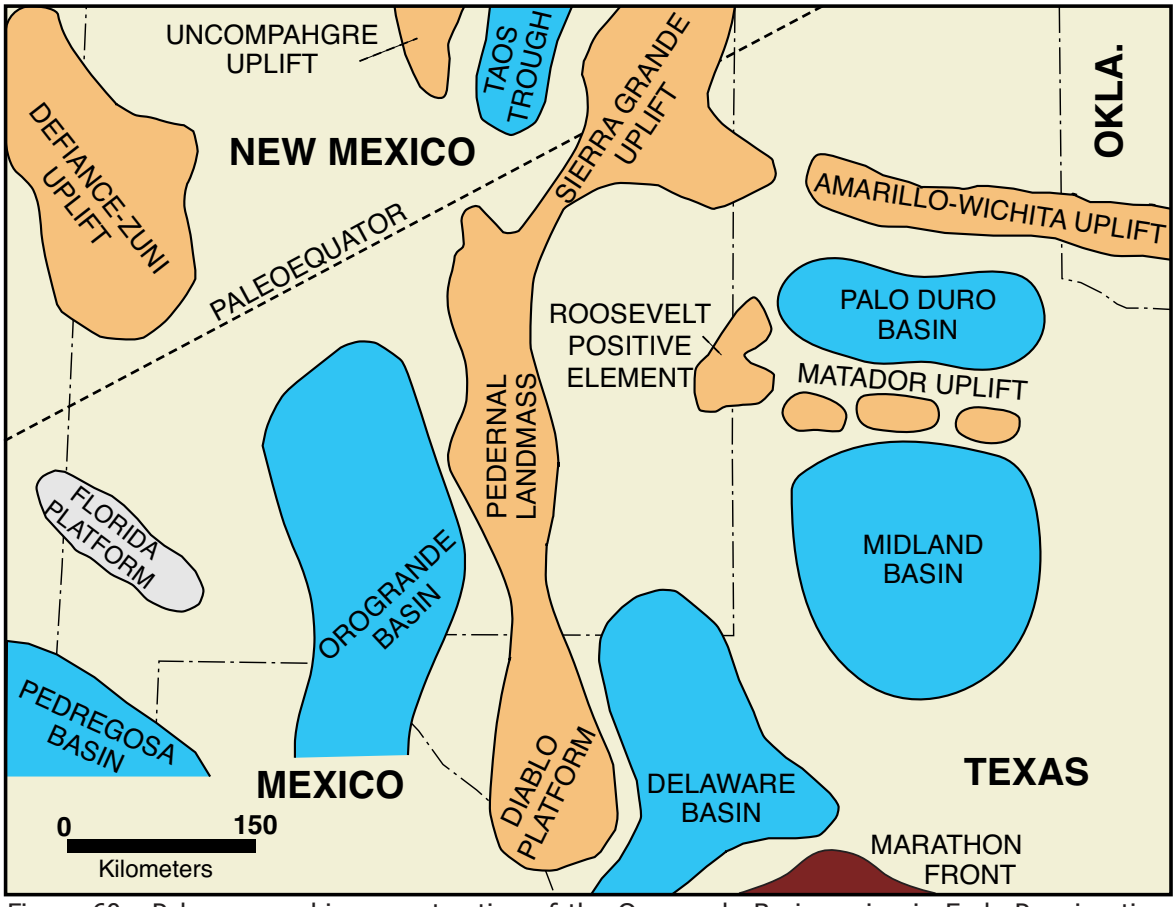

Figure 60. Paleogeographic reconstruction of the Orogrande Basin region in Early Permian time (modified from Candelaria, 1988 and Pol, 1982).

			are visible at 3:00 o'clock.
2.7	73.0	86.4	Road is on Bone Spring Limestone.
1.5	74.5	84.9	Junction with Texas Farm Road 1437 to Dell City on left; continue straight ahead. Dell City is a farming community in the Salt Flat Bolson, which has grown up as a consequence of the development of wells drawing Pleistocene(?) ground water from the bolson-fill. Rapid depletion of the water supply (use greatly exceeds recharge) and increasing soil salinities indicate a short or very expensive continued existence for agriculture in this region. For more details on the hydrology of the basin, see Nielson and Sharp (1985).
0.1	74.6	84.8	Road crosses basal Cretaceous sandstones and passes into Bone Spring Limestone.
6.5	81.1	78.3	Los Alamos Hills can be seen to the south of the highway in foreground. Leonardian to basal Guadalupian rocks are exposed here.
1.0	82.1	77.3	Junction with Texas FM Road 1576 to Dell City. Turn left for view stop.
0.25	82.35	77.05	**STOP I-1. West face of Guadalupe and Delaware Mountains**. When viewing is completed, turn around and return to U. S. Highway 62-180.

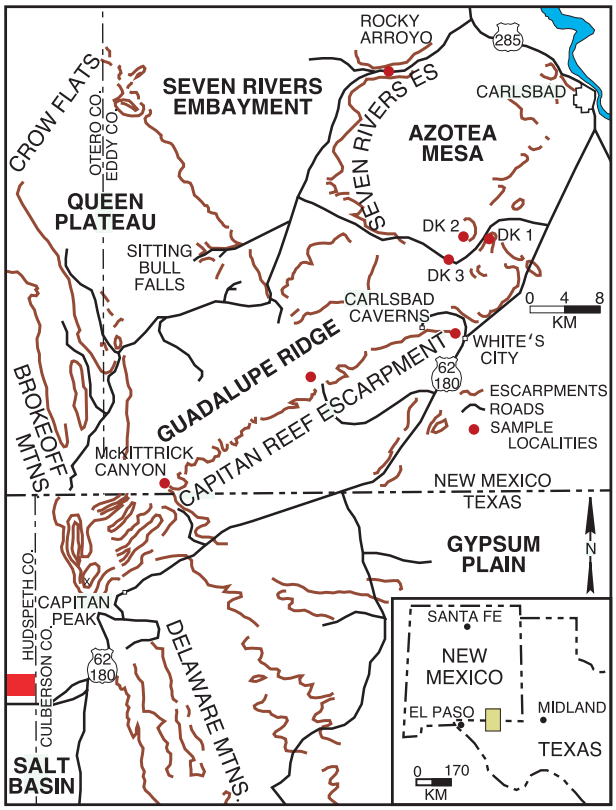

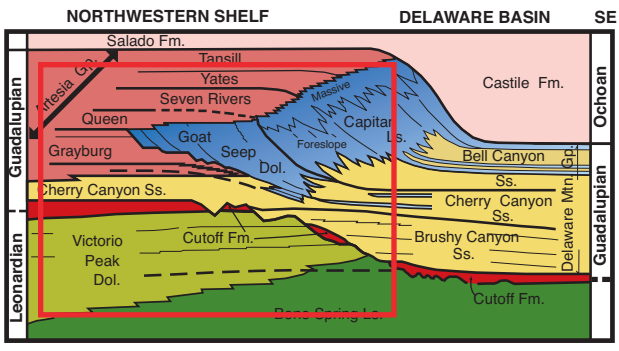

This location provides an excellent view of the Guadalupe and Delaware Mountains and the Salt Flat Bolson (in which we are now standing). We can see a magnificent panorama including the Middle Permian section of the Guadalupe Mountains, about 32 km (20 mi) to the northeast. This roughly 1,500 m (5,000 ft) escarpment is formed by a major north-south trending normal fault system that marks the eastern boundary of the Salt Flat Bolson. To the northwest and west we can see the Cornudas Mountains, Cerro Diablo and Sierra Tinaja Pinta, a series of Tertiary igneous plugs and lava flows. To the south lies the Sierra Diablo range which is terminated by the Babb flexure zone, a monocline at its northern end. The Sierra Diablo range exposes mainly Leonardian Victorio Peak Formation carbonates and older units. Middle Permian (Guadalupian) limestones and sandstones of the Cherry Canyon Formation compose the two mesas to the north of the Babb flexure. Also visible beyond these mesas is Sierra Prieta, an exhumed Oligocene nepheline syenite intrusive. To the southeast, Middle Permian strata, primarily basinal sandstones of the Brushy Canyon and Cherry Canyon Formations, are visible in the elongate face of the Delaware Mountain escarpment.

Because the Guadalupe Mountains are the major focus of this portion of the field trip, let us take a closer look at that range (Figs. 61, 62). Although the topography of the eastern side of the Guadalupe Mountains is almost entirely defined by the largely undeformed primary facies distributions and thickness variations of the Guadalupian strata, the western face is completely controlled by Tertiary normal faults (Fig. 62). Thus, on the western side, strata with a northeast-southwest facies strike are obliquely transected by a swarm of northwest-southeast or north-south trending faults. Furthermore, we are viewing the faulted exposure obliquely from our current vantage point, which makes accurate geologic observation even more difficult.

For reference purposes, let us name the major peaks on the Guadalupe Mountain skyline. From south to north these include the massif of El Capitan (elevation 2,462 m; 8,078 ft), Guadalupe Peak (the

highest point in Texas at 2,667 m; 8,751 ft), Shumard Peak (about 2,545 m; 8,350 ft), an unnamed spur off Shumard Peak (about 2,545 m; 8,350 ft), Bartlett Peak (2,595; 8,513 ft), and Bush Mountain (2,644 m; 8,676 ft). The massive, light colored rocks, which compose the upper parts of El Capitan, Guadalupe, and Shumard Peaks, are Middle Permian (Capitanian) limestones and dolomites of the Capitan Formation (Figs. 11, 61). Most of this mass is fore-reef talus that dips steeply (up to 35°) to the southeast, into the basinal sediments of the Delaware Basin. The top of Guadalupe and nearby peaks, however, have true Capitan reef facies and even back-reef sediments. The Capitan reef and fore-reef strata undoubtedly once extended several kilometers further south and southeast in this region but have been trimmed back by subsequent erosion. To the north, Bartlett Peak is capped by the oldest exposed Capitan reef limestones which overlie rubble of the Goat Seep reef. The area to the north of the Bush Mountain contains the main reef-massif of the Goat Seep as well as age-equivalent back-reef calcarenites and terrigenous sandstones (Queen and Grayburg), which stand out clearly as vegetated zones on the mountain slope. "At Guadalupe Peak the smooth slopes below the Capitan are Cherry Canyon and Brushy Canyon sandstones. North of Shumard Peak, the upper part of the Cherry Canyon grades into Goat Seep reef. A tongue of Cherry Canyon sandstone continues northward under the Goat Seep reef and grades into small reefs and reefy lime banks in the southern Brokeoff Mountains, and into bedded back-reef rocks in the central Brokeoff Mountains. There Boyd has measured approximately 600 feet (180 m) of beds which he calls the San Andres Formation, and Frenzel, considers to be lower San Andres. . .The rugged cliffs outcropping below the Delaware sand slopes are cut from the dark-bedded Bone Spring Limestone of Leonard age. Between El Capitan and Shumard Peak, the top of the Bone Spring Limestone rises over 1000 feet (300 m) and this defines the Bone Spring flexure described by King. Below Shumard Peak the upper part of the Bone Spring has changed to the gray Vic-

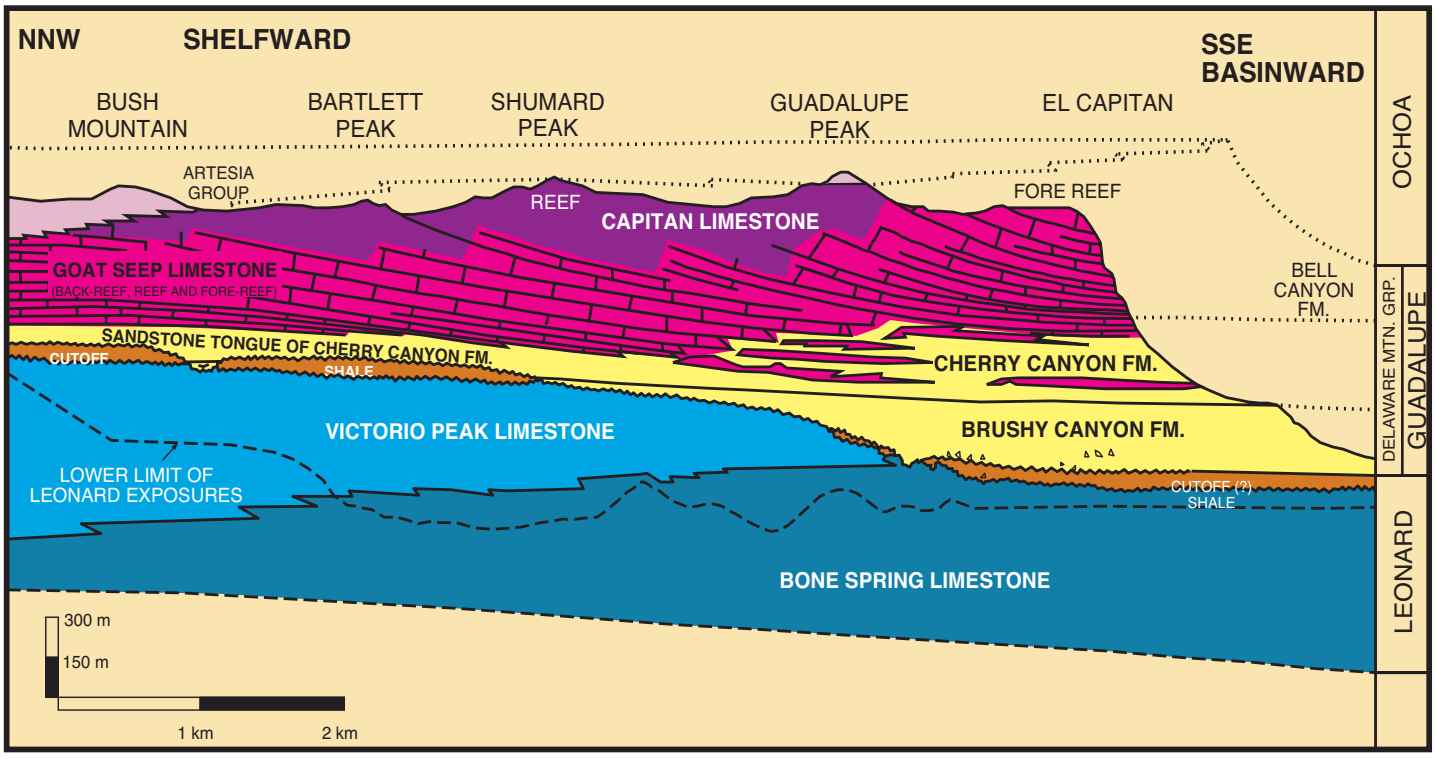

Figure 61. Diagrammatic section of the west face (southwestern end) of the Guadalupe Mountains, Texas. This approximates the view east-northeast of Stop I-1 on the trip (after King, 1948, 1967).

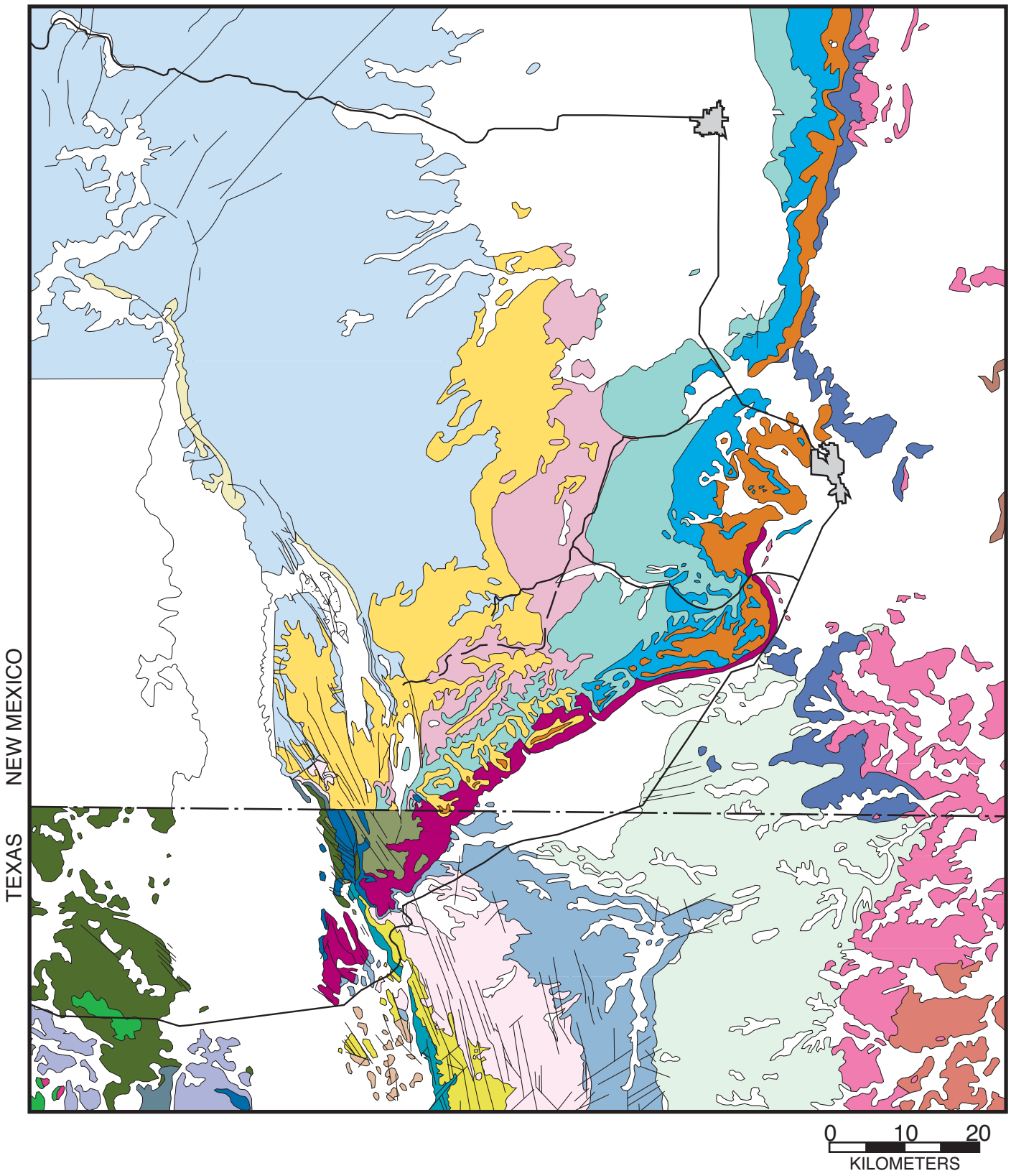

Figure 62. Generalized geologic map of the Guadalupe Mountains region (adapted from Barnes, 1968; Boyd, 1958; Kelley, 1971; King, 1948; Motts, 1962b). Legend is on facing page.

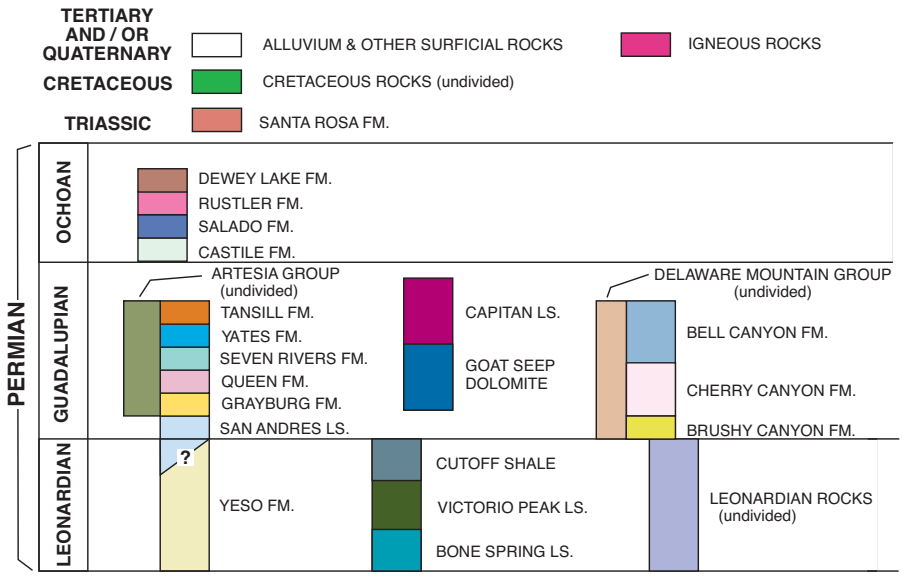

Figure 62. Continued, map legend.

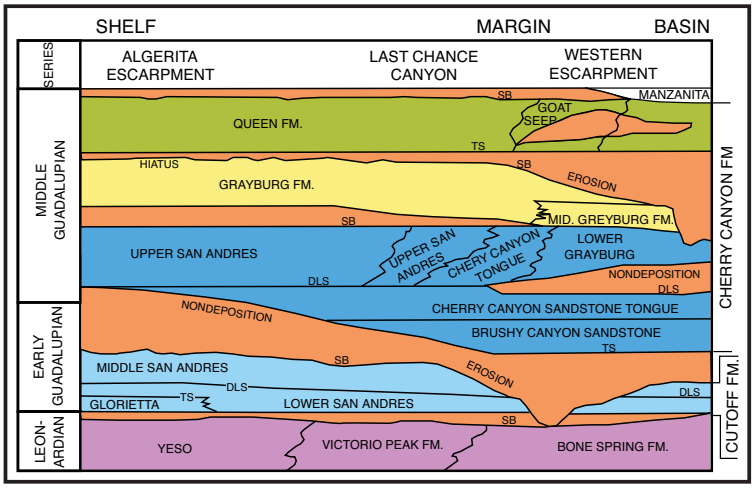

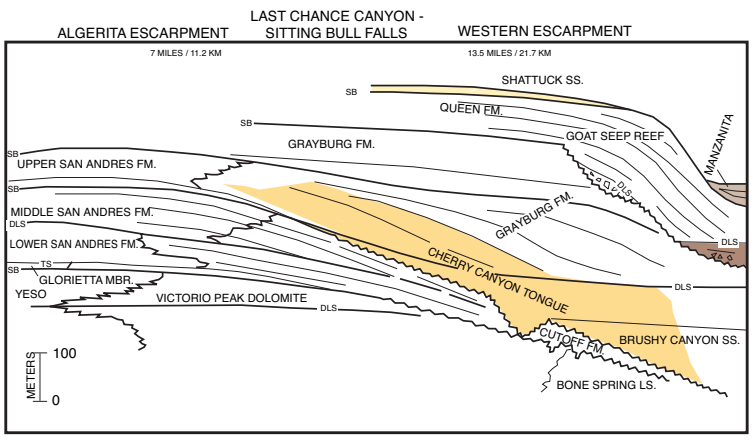

Figure 63. Late Leonardian-middle Guadalupian age stratigraphic units in the western Guadalupe Mountains. Major stratal surfaces include sequence boundaries (SB), downlap surfaces (DLS) and transgressive surfaces (TS) (from Sarg and Lehmann, 1986a).

torio Peak..., a reefy lime-bank facies. The Brushy Canyon sandstone onlaps the Bone Spring flexure and is absent in the slope below Bartlett Peak" (Anonymous, 1960, p. 50).

The bulk of the strata just described are considered to represent just two major phases of progradational basin filling according to McDaniel and Pray (1967). The Victorio Peak Dolomite and the underlying Bone Spring Limestone form the older (Leonardian) phase. This sequence represents at least 3-5 km (2-3 mi) of basinal infilling and progradation of shelf facies during the accumulation of about 300 m (1,000 ft) of section (McDaniel and Pray, 1967). "The Leonardian bank margin was eroded in latest Leonardian and/or in early Guadalupian time, and a major transgression of basin facies dark carbonates (Cutoff shaly member of King) brought basinal environments far to the north, overlapping Leonardian basin, basin margin, and shelf deposits alike" (Pray, 1975, p. 5). Presumably this transgression was a consequence either of major regional subsidence or of eustatic sea-level rise. This transgression was followed by the second major cycle of progradation, represented by Goat Seep and Capitan reef complexes. These units built the Guadalupian shelf edge outward several kilometers by filling in a basin of 300 to 550 m (1,000 to 1,800 ft) depth with steeply dipping, reef-derived debris beds that are clearly visible at the southern end of the Guadalupe escarpment. It is the upper part of this progradational sequence that will occupy much of our attention on this trip.

More recent work on outcrops and seismic data by Franseen (1989), Pray (1988a, 1988b), Crawford (1988); Sarg (1985), Sarg and Lehmann (1986) has shown a somewhat more complicated picture (Fig. 63; see also Fig. 12). In these models, significant unconformities (sequence boundaries) are found both above and below the Cutoff Formation, erosional dissection is seen on the top of the Grayburg slope and shelf edge section, and another sequence boundary is interpreted to exist near the top of the Queen Formation (Figs. 64, 65). The nature of many of these unconformities, whether subaerial or submarine, is still actively debated.

All authors agree, however, that there is a major change in the nature of carbonate sedimentation visible in the upward progression of units. Carbonate sedimentation of the Victorio Peak, San Andres and Grayburg strata was characterized by "ramp" develop-

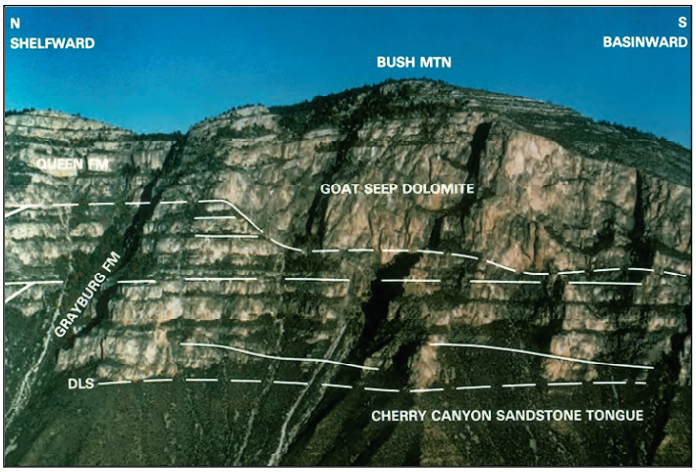

Figure 64. Low-angle oblique aerial photograph of the west face of the Guadalupe Mountains with Bush Mountain in center of photograph. Note downlap of Grayburg strata on the Cherry Canyon Sandstone Tongue as well as major erosional (or slump) scar, which forms the contact between the bedded Grayburg shelf carbonates and the massive Goat Seep reef. Roughly 700 m of section are exposed in this view. DLS = Downlap surface. Photograph taken from an elevation of approximately 2 km (1.2 mi) looking east-northeast. Courtesy of Exxon-Mobil Inc.

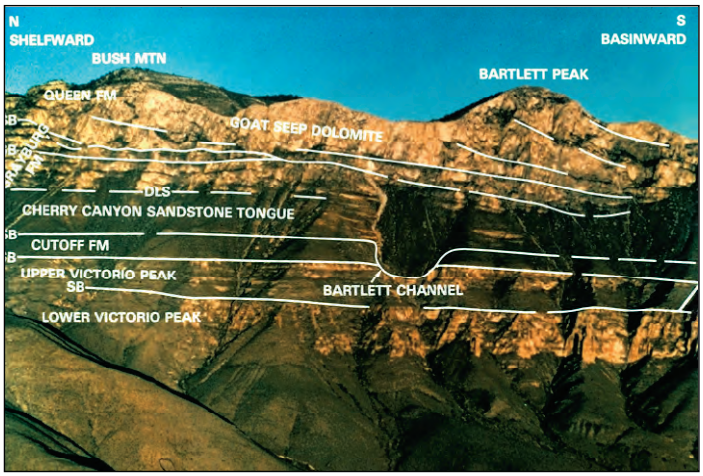

Figure 65. Interpreted view of the western escarpment of the Guadalupe Mountains. Note the downlap of the Grayburg strata on the Cherry Canyon Sandstone Tongue, the erosional contact between the bedded Grayburg shelf carbonates and the massive Goat Seep reef, and the large erosional channel cut into the Cutoff and Victorio Peak Formations. Roughly 700 m (2,300 ft) of section are exposed in this view. DLS = Downlap surface; SB = Sequence boundary. Courtesy of Exxon-Mobil Inc.

ment with an unbarred, gentle transition from shelf to basin (Pray, 1988b; Wilson, 1975). Younger units, on the other hand, show steep, reefal margins with slope angles up to 35°.

0.25	82.6	76.8	Turn left on U.S. Highway 62-180 to continue road log towards Carlsbad (or turn right to return to El Paso).
0.8	83.4	76.0	Crossing northern extension of East Diablo fault with the Salt Flat Basin downthrown on the eastern side.
2.7	86.1	73.3	Historical marker near site of former spring-fed oasis (Crow Springs) and a relay station of the Butterfield Overland Stage. The Butterfield Mail route (see cover illustration) was established in 1858 and passed through the area of Guadalupe Pass (Pine Springs). This was part of a trail that extended from Memphis and St. Louis to San Francisco (Adams, 1988). This particular part of the route lasted only about one year before the route was shifted southward to the approximate track of the present Interstate 10 through the Davis Mountains. The entire operation of the Butterfield Overland Mail was halted by confederate action in the Civil War. While it operated, however, it provided remarkably fast (25 day) and reliable service over its nearly 4,500 km (2,800 mi) route (Adams, 1988). The 180 km/day (120 miles/day) travel rate was especially remarkable considering the hostile, rugged country traversed and the fact that only three cities (El Paso, Tucson, and Los Angeles) lay on the route. Fares were rather high ($200 westbound; $100 eastbound), but the service was fully booked throughout its short history. As you enjoy your ride in air-conditioned comfort along this highway, think about 25 straight days and nights of bouncing across this rocky countryside in a stage coach.
1.5	87.6	71.8	**OPTIONAL STOP I-1a. Center of Salt Flat graben and playa.** The Salt Flat graben (Fig. 66), the easternmost basin of the Basin and Range province, formed in middle to late Tertiary time. The basin is about 100 km (60 mi) long and 16 km (10 mi) wide and has been the site of continuous alluvial, fluvial,

Figure 66. A photograph from the International Space Station (ISS006-E-45457) showing the Salt Flat graben and surrounding areas. The surface of the salt flats are white due to gypsum and halite precipitation on the dry playa lake surfaces. These salts are derived from dissolution of evaporites in nearby Permian rocks. Image courtesy of Earth Sciences and Image Analysis Laboratory, NASA Johnson Space Center (http://eol.jsc.nasa.gov).

and lacustrine sedimentation since the middle Tertiary. The sediment thickness in the basin is probably a few thousand meters. Basin margin sediments include coarse gravels and sands alternating with clays derived from the weathering of the adjacent mountains (especially the Guadalupe and Sierra Diablo ranges). Because there is no natural outlet for the basin, all drainage is internal and sediments become finer-grained toward the basin center. Several major aquifers are present within the basin fill, and are currently being exploited for irrigation in areas such as Dell City to the northwest.

Modern saline playas occur in the Salt Flat area of Texas and the Crow Flat area of New Mexico and Texas, in the topographically lowest parts of the basin (elevations about 1,100 m; 3,630 ft). These playas form in a region of low rainfall (about 23 to 25 cm/yr average; 9 to 10 in/yr) and high evaporation (about 200 cm/yr; 80 in/yr; Dunham, 1972). Thus, groundwater, which stands near the playa surface, is drawn upward and is evaporated. These ground waters have percolated through nearby evaporite-bearing Permian strata and thus are highly charged with dissolved solids that are further evaporatively concentrated, leading to elevated salinities (exceeding 250-300 ppt). These high salinities restrict vegetation and allow eolian deflation of the fine-grained playa precipitates. Pits excavated in the playa sediments reveal firm, but not hard, fine-grained, laminated, non-fossiliferous lacustrine material. Modern gypsum and halite are the dominant evaporite minerals, but calcite, aragonite, and dolomite also are found in the playa sediments, either as primary or secondary minerals (see Friedman, 1966; Dunham, 1972, and Hussain and Warren, 1988 for further details). C^{14} age dating and geological mapping of basinal units indicate that much of the sediment found at the surface today may be relict from a larger Pleistocene pluvial lake (King, 1948; Dunham, 1972). Dark sediment layers are very organic-rich, averaging 51 percent TOC (Hussain et al., 1988; Hussain and Warren, 1985). Eolian deflation has piled up some of the primary and secondary minerals from this sediment (mainly gypsum) as dunes along the eastern margins of the playa area.

Halite has been mined from the surface of the playa in areas to the south of the road although halite is not preserved to any extensive degree in buried sediments. This salt was a highly valued commodity in the 1880s and was used for food preservation, final curing of hides, and other purposes. It was such a valuable substance that it was hauled by mule- and ox-drawn vehicles for many hundreds of miles over the southwest trail to Fort Quitman, then to San Elizaro, Franklin (now El Paso), Paso del Norte (now Juarez), and on to Chihuahua City. Disputes between Mexican and American mining interests in the area led to the El Paso Salt War of 1877. The conflict culminated in the battle of San Elizaro (then the county seat of El Paso County). Improved(?) food preservation techniques and more economical sources of salt have eliminated the relatively small-scale mining in this area although some salt was still "mined" into the 1950s.

			On the south side of the road, the Paso-Tex oil pipeline can be seen sitting on trestles; on the north side of the road the El Paso Natural Gas pipeline to the Pacific Coast is buried beneath playa sediments.
0.8	88.4	71.0	Gypsum-bearing dunes derived from deflation of the nearby playa surface. These gypsum dunes extend for long distances north and south of the road. This is one of the largest accumulations of reworked gypsum in the U.S., albeit far smaller than those at White Sands National Monument (just northwest of this area).
2.2	90.6	68.8	Eastern edge of the Salt Flat Basin.
0.8	91.4	68.0	Folded and downfaulted blocks of Middle Permian on the left.
1.2	92.6	66.8	Beacon Hill on the left is composed of Capitan Limestone that sits atop Rader Limestone at the base of the hill. This is the southern end of the Patterson Hills which consist of complexly faulted and folded Middle Permian limestones. Farther north are the Brokeoff Mountains.
0.5	93.1	66.3	El Paso Natural Gas Co. Guadalupe compressor station on the left.
0.3	93.4	66.0	Roadcut in Bell Canyon Formation.
0.4	93.8	65.6	Roadcut in Bell Canyon Formation.
0.3	94.1	65.0	Roadcut in Cherry Canyon Formation; note greenish bentonite beds.
1.0	95.1	64.3	Roadcut in downfaulted Bell Canyon Formation.
0.8	95.9	63.5	Roadcut in Cherry Canyon Formation. The Patterson Hills to the left are capped by Capitanian-age limestone.
0.6	96.5	62.9	Roadcut in Cherry Canyon Formation exposing contact with Brushy Canyon Formation at east end of outcrop.
0.5	97.0	62.4	Junction with Texas Highway 54 to Van Horn on right. Keep left for Carlsbad.
0.3	97.3	62.1	**OPTIONAL STOP I-1b. Southern tip of the Guadalupe Mountains.**

The excellent view of the south end of the Guadalupe Mountains here shows the clear relations between reef, fore-reef and basinal facies (Figs. 61, 67). Ahead and to the right, is the escarpment of the Delaware Mountains composed of Brushy Canyon and Cherry Canyon basinal sediments (mainly sandstones and siltstones). The Delaware Mountain ridge is capped by the resistant Getaway Limestone, which is exposed near the radar station visible at the top of the cliff (note numerous wind turbines lining the ridge further to the south). The Getaway Limestone Member occurs at a level about 30-60 m (100-200 ft) above the base of the Cherry Canyon Formation and, in this area, is a very fossiliferous, gray to black, turbiditic limestone (Harris and Wiggins, 1985). Note the abundance of lenticular, channelized bedding in the Brushy Canyon and basal Cherry Canyon sections exposed in the Delaware

Figure 67. Oblique aerial photograph of El Capitan and the southern end of the Guadalupe Mountains. Note the gentle regional east-northeast tilt of all strata due to Tertiary uplift and the lateral transition from massive (largely dolomitized), steeply dipping Capitan reef talus at top center to nearly flat-lying Delaware Mountain Group clastics to the right (toward the former Delaware Basin). Those clastics also underlie the carbonate cliffs of El Capitan, demonstrating progradation of the Capitan shelf margin over older, flat-lying beds of basinal Brushy Canyon Formation sandstones. Photograph from King (1948, plate 1).

Mountains escarpment. This entire sequence was apparently deposited in water depths of at least a few hundred meters by a combination of density currents, mass flows, localized slumps and perhaps even contour currents. Much of the darker material visible in the cliff face represents relatively fine-grained overbank or non-channelized flows. The lighter-colored, lenticular sediments are coarser-grained, massive, channel-fill sandstones. Finally, at the very base of the escarpment, a dark ledge of the basinal Bone Spring Limestone is exposed.

To the left we can see the great mass of Capitan Formation carbonate that forms the upper part of El Capitan. The Capitan strata in this face are virtually completely dolomitized (which accounts for this prominent erosional remnant) and represent a forereef debris facies that is time equivalent to the Hegler, Pinery and Rader Members of the Bell Canyon Formation. Below the massive (300-460 m; 1,000-1,500 ft thick) carbonate, gently sloping deposits of the Cherry Canyon Formation are evident. "The three distinctly visible ledges represent in ascending order the three basinal limestone tongues of this formation named Getaway, South Wells, and Manzanita" (K. W. Klement, in Anonymous, 1969, p. 18). The rest of the lowermost slopes of El Capitan are composed of Brushy Canyon Formation.

The lateral flattening of dips from El Capitan to the Delaware Mountains is not a result of deformation, but rather represents a primary facies transition from reef to basin. The thick, steeply dipping, rubbly limestones of the fore-reef facies thin rapidly toward the basin so that 30 or more meters (100+ feet) of reef limestone may be time equivalent to a 0.3-2 m (1-6 ft) thick limestone in the center of the Delaware Basin. The color change from the light colored, largely oxidized beds of the reef and fore-reef to the dark colored, organic carbon-rich, dysoxic to anoxic basinal facies can also be seen in these exposures.

The great thicknesses of basinal sandstones (about 1,070 m or 3,500 ft of Delaware Mountain Group), although derived from the shelf, have only thin sandstone equivalents in the back-reef facies and are virtually absent in the reef itself. In part, this may reflect the fact that much of the basinal sandstone was apparently transported from the north and northeast. The sands moved across the northern shelf as well as the Central Basin Platform (the Midland Basin was filled by then) from sources in the Pedernal Massif and the Arbuckle and Wichita uplifts (Berg, 1979; Bozanich, 1979; Hull, 1957; Watson, 1979). Thus, much of the sand influx may have been funneled through gaps in the reef or back-reef islands in areas not currently exposed in outcrop. There is evidence, however, that some sand also moved across the northwestern part of the basin margin along which we are now standing. This evidence includes submarine channel orientations, stratigraphic relations of basinal sandstones and fore-reef carbonate rocks, and the presence in outcrop of numerous, if thin, back-reef and fore-reef sandstone beds.

Thus, in all probability, another explanation must be sought for the inverse relationship of thick carbonate and thin sandstone units on the shelf and thin carbonate and thick sandstone units in the basin. As discussed in the introduction, Silver and Todd (1969), Meissner (1972) and Wilson (1972) all proposed concepts of reciprocal sedimentation to explain these observations. This model suggests that the carbonate sediments were deposited during high eustatic sea-level stands. During these times, the shelf areas had massive carbonate buildups that maintained the shelf edge at or near sea level, and terrigenous sands were largely trapped in back-reef lagoons or in continental basins and dune fields. The evaporitic conditions led to the formation of saline bottom-waters and a density-stratified basinal water column. This, in turn, led to largely euxinic, sediment-starved conditions on the floor of the basin.

During lower sea-level stands, on the other hand, eolian and ephemeral fluvial(?) transport of large volumes of well-sorted arkosic sand to the shelf edge provided a supply of unconsolidated material to the shelf edge and upper slope. From there, the sands were reworked into the basin by a variety of gravitationally-driven current mechanisms. Subsequent transgression in the next cycle removed virtually all traces of sand from the tightly cemented shelf-edge limestones.

0.7 98.0 61.4 Dirt road with locked gate on north side of highway leads to west face of Guadalupe Mountains (Williams Ranch). For field guides to this area, see Pray (1988b). Keys must be obtained from the National Park Headquarters and this unimproved road requires high clearance, preferably four-wheel drive, vehicles.

0.7 98.7 60.7 **STOP II-2. Cutoff Formation outcrop.**

This outcrop, faulted at its northern end, exposes the Cutoff Formation (Williams Ranch Member), a dysaerobic slope facies limestone deposited over an older, eroded Victorio Peak shelf margin (Lambert et al, 2000). This Early Guadalupian (Roadian) limestone, formerly misidentified as part of the upper Bone Spring Limestone, represents a gentle ramp slope that extended into water depths of the order of a hundred meters from the adjacent shelfal areas that lay roughly 20 km to the northwest of this area. The Cutoff Fm. is marked by several pronounced submarine unconformities at its base, as well as within the formation and at its top. These all indicate episodes of strong current action that channelized and oversteepened this slope setting and led to extensive submarine mass movement.

At this locality, we can see typical, dark gray to black, cherty, interbedded limestones and calcareous shales —these are the dominant lithologies of the lower slope/basinal part of the Cutoff Fm. Fossils, especially small ammonites, can be found at this locality, but are generally restricted to isolated, granular or calcarenitic beds. Bedding surfaces in the basinal Cutoff Formation are generally wavy and show evidence of soft-sediment deformation (mainly slumping with overturned folds). Both the limestone and the shale

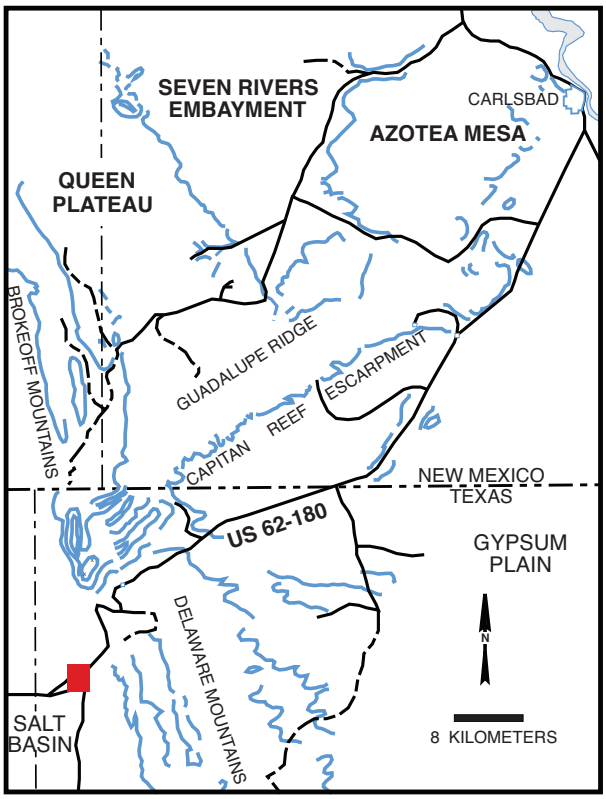

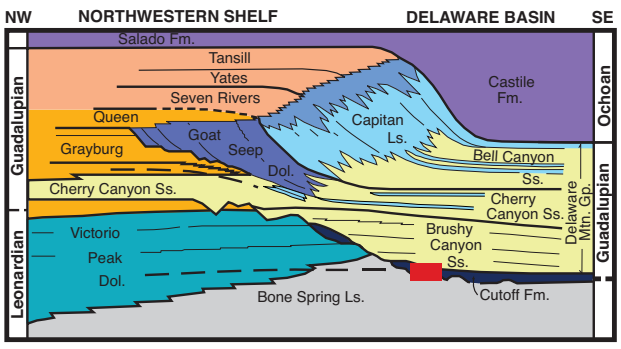

Figure 68. View north from U.S. Highway 62-180 just south of Guadalupe Pass. View of the southern end of the Guadalupe Mountains (El Capitan). The massive, mainly fore-reef carbonates of the Capitan reef complex (background) overlie flat-lying, basinal sandstones of the Brushy Canyon and Cherry Canyon Formations.

units contain considerable amounts of organic matter and may have acted as source rocks within this basin. Indeed, trapped oil can be found even on outcrop in small cavities in these rocks (Barker and Pawlewicz, 1987; Gawloski, 1987; Hills, 1984). It is also visible as oil-filled inclusions trapped in some of the fracture-filling calcite crystals (look for bands of white, followed by black spar in the fractures). Freshly broken pieces of this rock also emit a strong smell of hydrocarbons.

0.4	99.1	60.3	Roadcut in Brushy Canyon sandstone.
0.5	99.6	59.8	Well exposed, lenticular sandstone channel deposits of the Brushy Canyon Formation are visible in the distance on both the left and right sides (Figs. 44 and 68).
1.6	101.2	58.2	**STOP II-3. Brushy Canyon Formation basinal channel sandstone outcrop.** BE CAREFUL, TRAFFIC IS VERY HAZARDOUS AT THIS OUTCROP!

An exposure of basinal Brushy Canyon Formation, the lowest unit in the Delaware Mountain Group. The feature of special interest at this locality is the exposed margin of a submarine channel (Fig. 69). Such channels are common in this formation and, at least in this area, generally trend northwest-southeast, that is, perpendicular to the nearby shelf margin. At this locality, we can see dark-colored, graded, relatively fine-grained sandstones, siltstones and shales in thin beds with some soft-sediment deformation features (Fig. 70). These beds are abruptly cut by a fairly uniform, thick-bedded, sandstone-filled channel. Both types of sediments were clearly soft, even fluid, at the time of deposition, as shown by the fact that the channel margins are extensively deformed by sand injection. Channel cutting and filling most likely were separate events, perhaps separated by considerable time. That is, the channel was cut, acted as a sediment conduit for some time, and then was filled and abandoned. Evidence for this comes from the commonly observed shale drapes and rip-up clasts that lie between the cut channels and the multiple episodes of later sand fillings (Harms, 1974; Harms and Williamson, 1988).

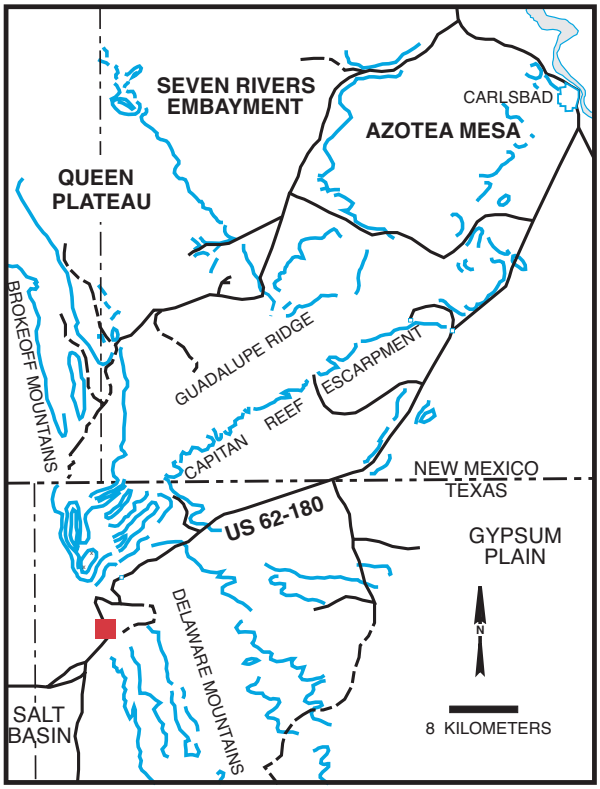

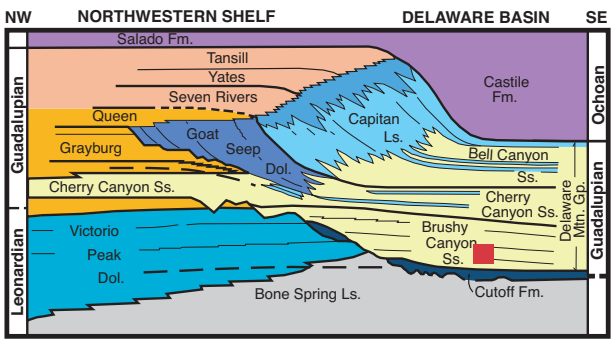

Figure 69. Margin of Brushy Canyon Formation submarine fan channel incised into "overbank" sediments. Sandstone fill of channel shows amalgamation of several flow units as well as flowage and injection of sand into the surrounding strata of the channel walls.

Figure 70. Overbank and channel deposits associated with a submarine fan in the Brushy Canyon Formation. Note soft sediment deformation in the overbank siltstones and shales. Upper part of outcrop shows part of a sand filled channel that cross-cuts and overlies the overbank deposits.

Figure 71. Polished rock slab showing a fusulinid-rich basinal sandstone in the basal Cherry Canyon Formation. The fusulinid foraminifers were derived from a shelf margin that lay to the northwest of this site (probably close to Last Chance Canyon).

Hayes (1964), Jacka et al. (1968), Payne (1979), Berg (1979), Williamson (1977 and 1979), Bashman (1996), Kerans and Fichen (1997) and other authors have interpreted these or similar deposits as part of larger submarine fans and/or as part of a basinally-restricted lowstand (but still deep-water) wedge of siliciclastic sediment (Rossen, 1985; Rossen and Sarg, 1988). The graded, finer-grained sediments are considered to be interchannel or overbank turbidity-current deposits. The cut and fill, massive, amalgamated sandstones are interpreted as part of an anastomosing system of fan channels, eventually abandoned or filled by multiple episodes of sand transport, possibly by grain flows (Watson, 1979). Harms (1974), on the other hand, proposed that the finer-grained sediments were deposited by density overflows (Fig. 45) that dropped suspended sediments as they moved out over density interfaces within the water column rather than at the sediment-water interface. The channels were cut, according to Harms, by saline and cold density currents (rather than turbidity currents) that formed on the shelf. The sand fillings of the channels were also laid down by density currents. For a much more detailed description of the modern microfacies and sequence stratigraphic interpretation of this and other basinal units, see Beaubouef et al. (1999).

In any case, these large (commonly more than 0.8 km/1-2 mi wide and 15-30 m/ 50-100 ft thick) channelized sandstones, surrounded by lower permeability siltstones and shales, represent potential stratigraphic traps for hydrocarbons. Large submarine fan lobes have also been developed as reservoirs. This is especially true because of the close spatial association of the sandstones and underlying basinal source rocks. Indeed, exploration efforts to date have located hundreds of oil or gas fields that produce from Delaware Mountain Group channel-sandstone reservoirs — these exploration efforts are aided, in part, by the advent of horizontal drilling. Early production from the Delaware Basin was mainly from Bell Canyon reservoirs, but by 2006 Brushy Canyon output accounted for nearly 15 percent of New Mexico's oil production (see Tables 3 and 4).

0.5	101.7	57.7	Roadside rest areas on left and right. Excellent views of El Capitan and the Delaware Mountain escarpment with numerous sand-filled channels (Fig. 44). Bank-to-basin transitions of the Capitan Limestone and its equivalents are well shown.
0.7	102.4	57.0	Roadcuts in sandstones and siltstones of the Brushy Canyon Formation.
0.4	102.8	56.6	**OPTIONAL STOP II-3a. View along the Delaware Mountains escarpment.** Supeerb view of the mountain front to the right. Outcrops on the left consist of basal Cherry Canyon Formation sandstones with oriented fusulinid foraminifers that were reworked into the Delaware Basin from the adjacent Northwest Shelf (Fig. 71). Several of the beds in this interval show distinct grading and well-defined flute casts on their bases, both evidence of probable turbidity current trans-

portation. In thin section, one sees compaction of the sandstones, minor quartz overgrowth cement, extensive calcite cementation, numerous fine-grained carbonate clasts mixed with well-rounded and well-sorted quartz and feldspar grains. The detrital carbonate grains show intense pressure solution embayment, especially where they are in direct contact with the less soluble quartz or feldspar grains

0.3 103.1 56.3 An enigmatic Brushy Canyon-Cherry Canyon contact is exposed in this outcrop. The contact strikes N 30°E and dips at about 17° to the southeast. This relationship has been variously explained as a fault contact, the erosion surface of a large submarine channel, or a large and coherent slide mass (Fig. 72). Note the abundant high-angle faults in the outcrops in this area. They generally have only minor offsets (although a few have 30 m (100 ft) or greater throw) and are part of the Tertiary block fault system that marks the western boundary of the Guadalupe and Delaware Mountains.

0.3 103.4 56.0 **OPTIONAL STOP II-3b. Shales, siltstones, and sandstones of the Cherry Canyon Formation.**

A number of interesting sedimentary features including a large channel, graded beds, flame structures, ripple marks (Fig. 73), slump folds and abundant horizontal lamination are found at this stop. Aa for the Brushy Canyon section, evidence is present for the involvement of both traction and suspension processes in the deposition of these units. The Cherry Canyon Formation is about 300 m (1,000 ft) thick in this area and thickens to about 400 m (1,300 ft) in the subsurface sections measured to the east. Isopach maps of sandstone thickness between regional basinal marker shales (Fig. 74) show basinal sediment lobes and channels with numerous discrete input points that lay mainly to the north and northeast. This conforms with predicted wind directions in the mid-Permian trade wind belt.

Organic carbon-rich shales and limestones within the Cherry Canyon Formation may have acted as source rocks for a significant part of the oil in the Permian strata of the Delaware Basin. Most workers, however, believe that these strata have never been heated to the threshold of oil generation (that is, they are thermally immature to submature).

0.4 103.8 55.6 Roadcut in Tertiary-Quaternary alluvium.

0.4 104.2 55.2 Thin-bedded Cherry Canyon Formation exposed on right. Excellent views of El

Figure 72. A large, shale-lined, low-angle channel or slide in the sandstones and siltstones of the basal Cherry Canyon Formation.

Figure 73. Laminated sandstones and starved ripples in Cherry Canyon Formation. The latter structures, like most traction current features, are fairly rare in Delaware Basin Group sandstones. Folded knife is about 8 cm long.

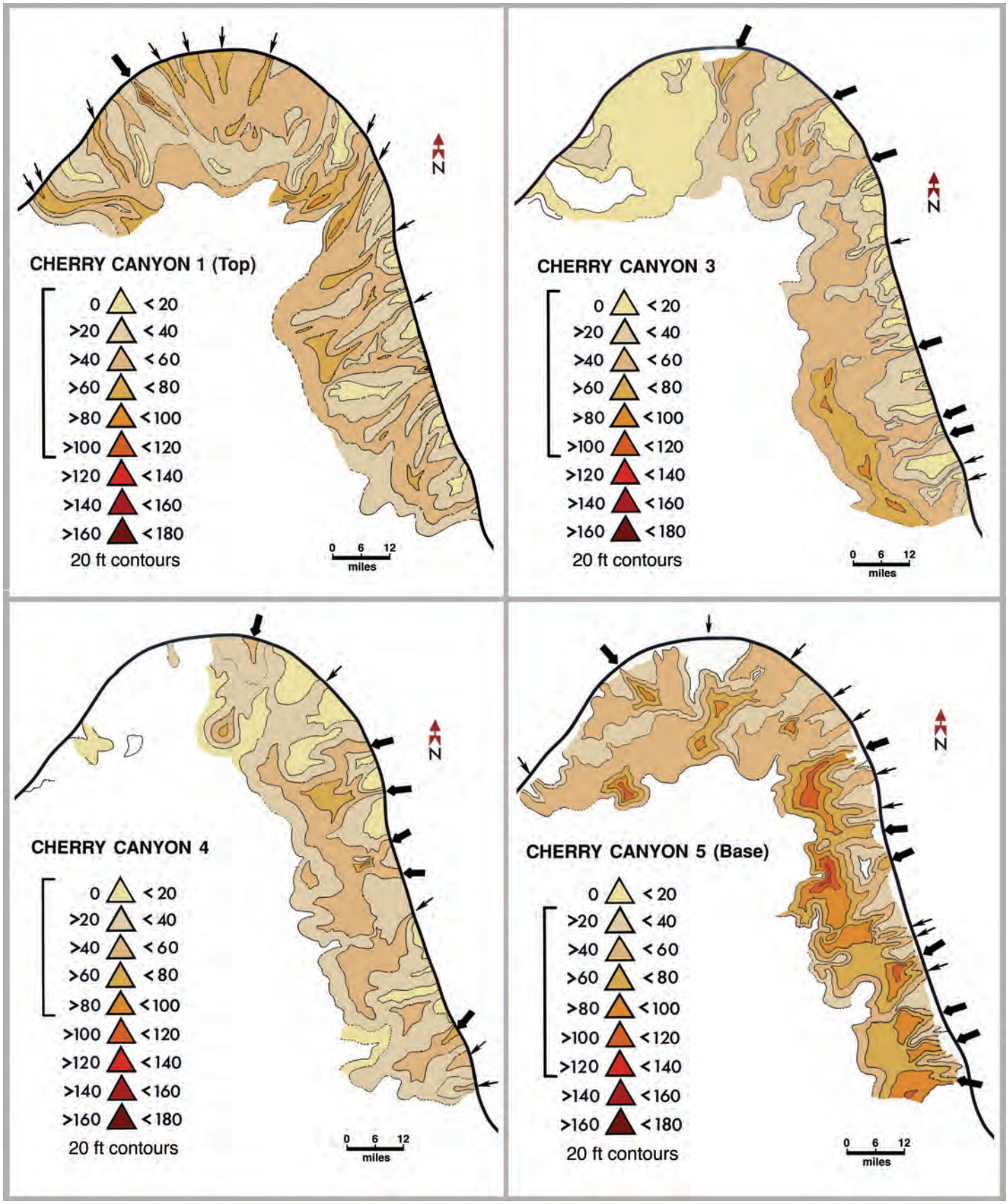

Figure 74. Isopach maps of sand thickness in four intervals of the Cherry Canyon Formation. Note multitude of probable input points for turbidite transport of sands. Adapted from unfinished M.S. thesis (see Giesen and Scholle, 1990).

Capitan from this area (Fig. 75).

1.0	105.2	54.2	Rest area on left.
0.4	105.6	53.8	Fault zone. Graded carbonate beds within the Cherry Canyon Formation.
0.7	106.3	53.1	Crest of Guadalupe Pass (elevation 1,736m; 5,695 ft). Pine Springs Canyon and Guadalupe Mountains National Park Visitor's Center on left — trails lead from here to the top of Guadalupe Peak, El Capitan, and other scenic, geologically interesting sites. The former site of the Pine Springs camp and gas station is just ahead on the right, along with the remarkably unattractive National Park Service housing tract.

Figure 75. El Capitan with the Permian Capitan forereef dolomites and limestones and underlying basinal sandstones at the south end of the Guadalupe Mountains. (OK, this is in Texas, but most of the range is in New Mexico, and it clearly was a mistake to put this part in Texas).

Guadalupe Mountains National Park opened in 1972. In 1978, approximately 60 percent of the park was designated as wilderness area, precluding any large-scale development. The establishment of the park resulted, in large part, from the concern and generosity of Wallace Pratt, one of the first geologists of the original Humble Oil and Refining Co. (later Exxon), who lived for many years in the McKittrick Canyon area. Pratt first saw the area in 1921 and by 1937 had amassed a 16,000 acre ranch. Pratt's gift to the government of 5,632 acres of land, mainly in and around McKittrick Canyon, was the first concrete step toward the formation of this park. He also donated his home ("Ship on the Desert") and a stone cabin in McKittrick Canyon. Additional land was purchased from J. C. Hunter and other ranchers, so that the park currently includes 86,416 acres.

The cliffs to the left (10:00 o'clock) are composed of Guadalupian basinal facies from the base to the middle of the slope; that is overlain by a thick zone of fore-reef rubble, which, in turn, is capped by a thin zone of preserved reef limestone. The Getaway Limestone is visible in hills on the right, and overlying strata of the Cherry Canyon Formation are present in the slopes ahead and to the left. The greenish outcrops in these slopes (for example on Nipple Hill, directly ahead) contain thin, intercalated bentonite beds and silty shales in the Manzanita Limestone Member of the Cherry Canyon Formation. Numerous small faults are present here, as in most of the outcrops we have passed in the last 15 to 25 km (10 to 15 mi).

The remaining walls of a waystation for the short-lived Butterfield Overland Mail route are located on the left. As with other parts of this route, the station was abandoned in 1859, but not before supplying some exciting stagecoach rides through Guadalupe Pass. Route engineers built a rough, unpaved road down the pass, using a route close to the one followed by the later U. S. Highway 62-180 (but not the current route of that highway). Waystations such as this one provided changes of horses (or mules in this area) as well as brief (20 minute) meal stops for drivers and passengers (Adams, 1988).

1.3	107.6	51.8	Guadalupe Mountains National Park Frijole Station on the left.
1.3	108.9	50.5	Exposures of Cherry Canyon Formation sandstone just below the South Wells Limestone Member.
0.8	109.7	49.7	Quaternary fanglomerates in roadcuts.
0.5	110.2	49.2	Roadcuts in Cherry Canyon Formation. The South Wells Limestone Member is present at the top of this exposure and consists of thin-bedded sandstone and thin, lenticular, brachiopod-bearing limestones. The limestone beds range in thickness from 10 cm to a meter (4 in to 3 ft) and are generally micritic. The intercalation of thin limestones and sandstones tends to lower the erosional resistance of this unit, and therefore it does not form a prominent scarp. This is not true of the other limestone members of the Cherry Canyon Formation, however.
1.0	111.2	48.2	Descending off the Rader Ridge. The ridge is capped by the Rader Limestone Member of the Bell Canyon Formation (the third named member up from the base

of the formation). We are now going through the upper part of the Cherry Canyon Formation.

0.2 111.4 48.0 Nickle Creek Station on the left. The pale greenish, bentonitic beds of the Manzanita Limestone Member are visible at 11:00 o'clock, about half way up the hill. Overlying limestones are the Hegler and Pinery members of the Bell Canyon Formation.

0.8 112.2 47.2 Roadcut in Manzanita Limestone. The Manzanita is between 30 and 45 m (100 and 150 ft) thick in this area. This unit, part of the Cherry Canyon Formation, predates formation of the Capitan reef and thus passes under most of the mountain section to the west. The unit probably correlates with the upper part of the Queen Formation on the shelf and the Goat Seep reef at the shelf margin.

Manzanita, by the way, means "little apple" in Spanish, and the unit was named for a red-barked tree we will see at a number of stops on the trip. Unfortunately the tree was misidentified and really is a Texas madrone (*Arbutus texana*), a heath that is related to the manzanitas (Reid et al., 1988).

0.3 112.5 46.9 **STOP II-4. Rader submarine slide.**

BE CAREFUL, HAZARDOUS TRAFFIC AT THIS OUTCROP!

The section here shows a major submarine slide deposit at the base of the Rader Member of the Bell Canyon Formation, with additional turbidites and debris flows in the overlying section (Nestell et al., 2006). The south end of the outcrop consists of laminated sandstones and siltstones of an unnamed member of the Bell Canyon Formation (Fig. 43). Near the top of this sandstone is a conglomerate zone with limestone blocks set in a sandstone matrix (Fig. 47). The limestone clasts are very poorly sorted and range from pea-sized pebbles to car-sized boulders. The clasts are non-dolomitic, generally light-colored limestones derived mainly from the Capitan upper fore-reef environments (Lawson, 1989a, b). Above this zone of bouldery rubble is a thick, graded bed of similar, but finer grained, carbonate clasts with carbonate matrix and cement. This, in turn, is capped by a series of thin-bedded, fine grained, dark-colored limestones that are typical of the basinal limestone members of the Bell Canyon Formation.

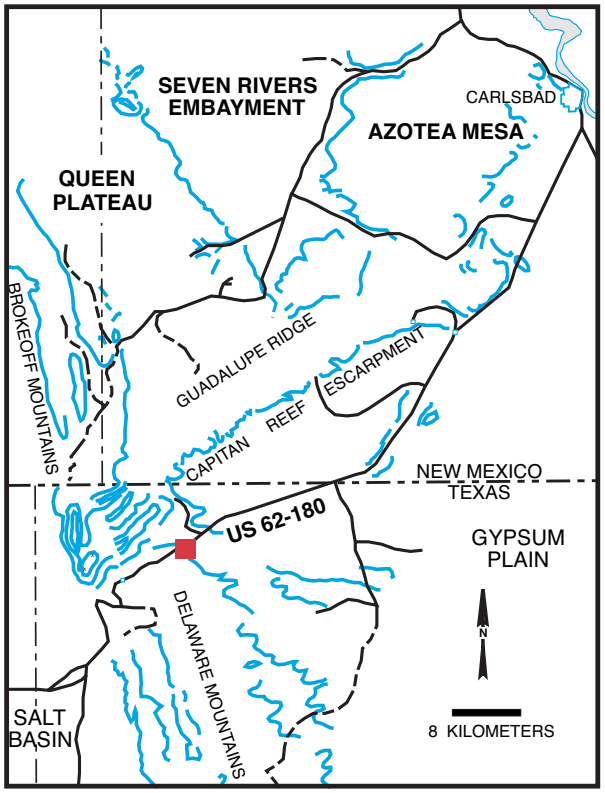

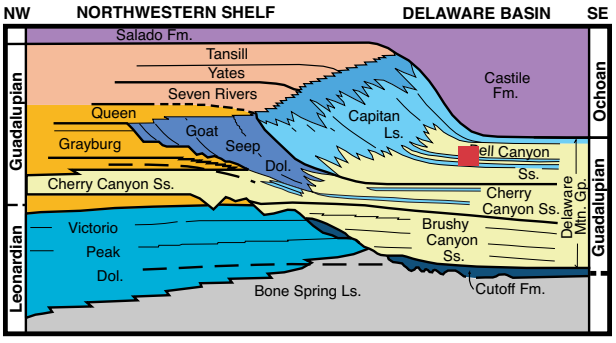

The mechanism of transport of the limestone clasts probably is largely as a submarine slide or debris flow. The volume of material involved is comparable to that of large, documented,

subaerial landslides (Newell et al., 1953, p. 77). As with subaerial landslides, there is relatively little disturbance of underlying soft sediment substrates. The incorporation of sandstone matrix with limestone boulders and the channelized or abruptly terminated lateral margins of the slides indicate that there was some erosion and inclusion of the underlying Bell Canyon sandstone in the slide. But there may also have been some plowing, subsidence, or foundering of the large, heavy, limestone blocks into the underlying sands. The event that triggered the slide also, apparently, led to the generation of a turbidity current that deposited the thick graded bed that overlies the slide. This association appears to be a common one and has even been observed in modern submarine slides (Heezen and Drake, 1964).

The Rader Limestone Member has a total thickness of about 4.5 m (15 ft) in this area, and about 3 m (10 ft) is exposed at this outcrop. The unit thickens to a maximum of about 36 m (120 ft) within about 5 km (3 mi) as one approaches the basin margin (to the northwest).

0.1	112.6	46.8	Roadcuts in Rader Limestone.
0.5	113.1	46.3	**STOP II-5. Bell Canyon Formation sandstones.** BE CAREFUL, HAZARDOUS TRAFFIC AT THIS OUTCROP!

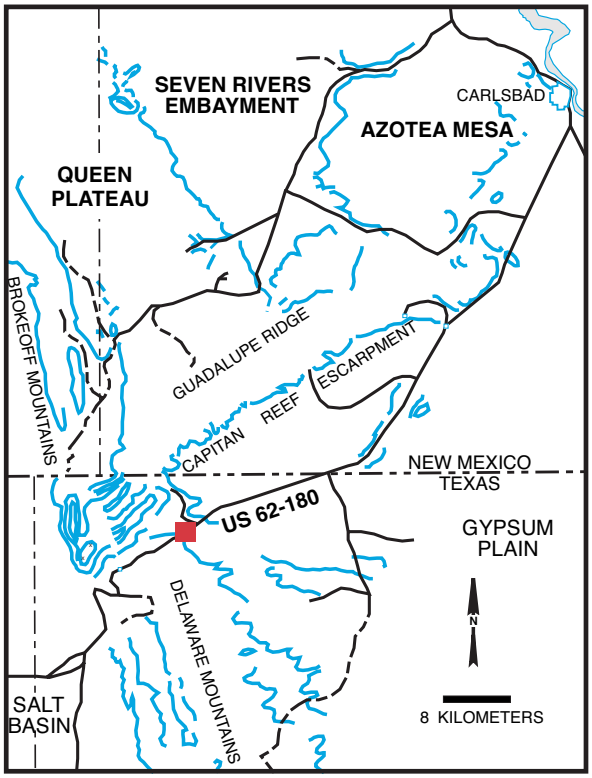

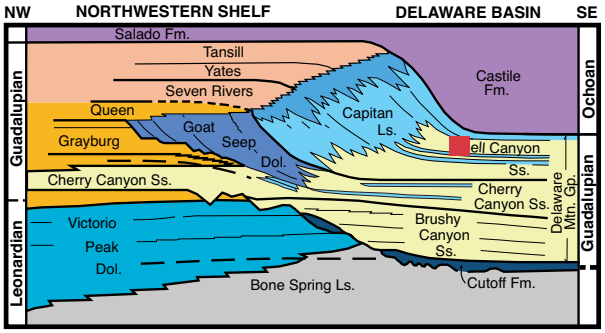

Well-sorted, subarkosic siltstones of the Bell Canyon Formation showing remarkable uniformity of bedding and horizontal lamination (Fig. 43). The Bell Canyon Formation is about 210 m (700 ft) thick at its type locality, but has been reported to be as thick as 260 m (860 ft) in subsurface sections (Hayes, 1964, p. 14). As with the other basinal sandstone units of the Delaware Mountain Group, the depositional mechanisms of the Bell Canyon siltstones and sandstones have been extensively debated. The abundance of horizontal lamination and the apparently euxinic conditions in the basin center lend credence to the idea of density overflows and suspension deposition of much of the sand and silt (Fig. 45). On the other hand, the presence of numerous subparallel erosional channels, many of them oriented from northeast to southwest but many others also oriented perpendicular to the nearest shelf margin (Fig. 76), indicates that sea floor erosion, transportation and deposition by long-lived density underflows, turbidity currents or grain flows were also important.

Fischer and Sarnthein (1988) provided an alternative explanation in which the laminated siltstones are dominantly the product of eolian dust fallout. Lamination, in this scenario, may be the product of alternating periods of dust transportation and high biological productivity in an upwelling zone. The concept of eolian transport fits well with inferred mechanisms of sand transport in Permian shelf areas. Furthermore, the Permian basinal siltstones are texturally similar to modern and Pleistocene marine dust deposits off the west coast of the Sahara (Fischer and Sarnthein, 1988). The coarser sandstones, found mainly in channelized deposits in both the Delaware Basin and the west Africa shelf, are produced by the coarser dunes moving to the shelf margin during lowstands, generating turbidites that retransport material into deeper waters (Sarnthein and Diester-Haass, 1977).

More than 100 oil and gas fields have been discovered in the Bell Canyon Formation as of 1979 (Tables 3 and 4). These “are

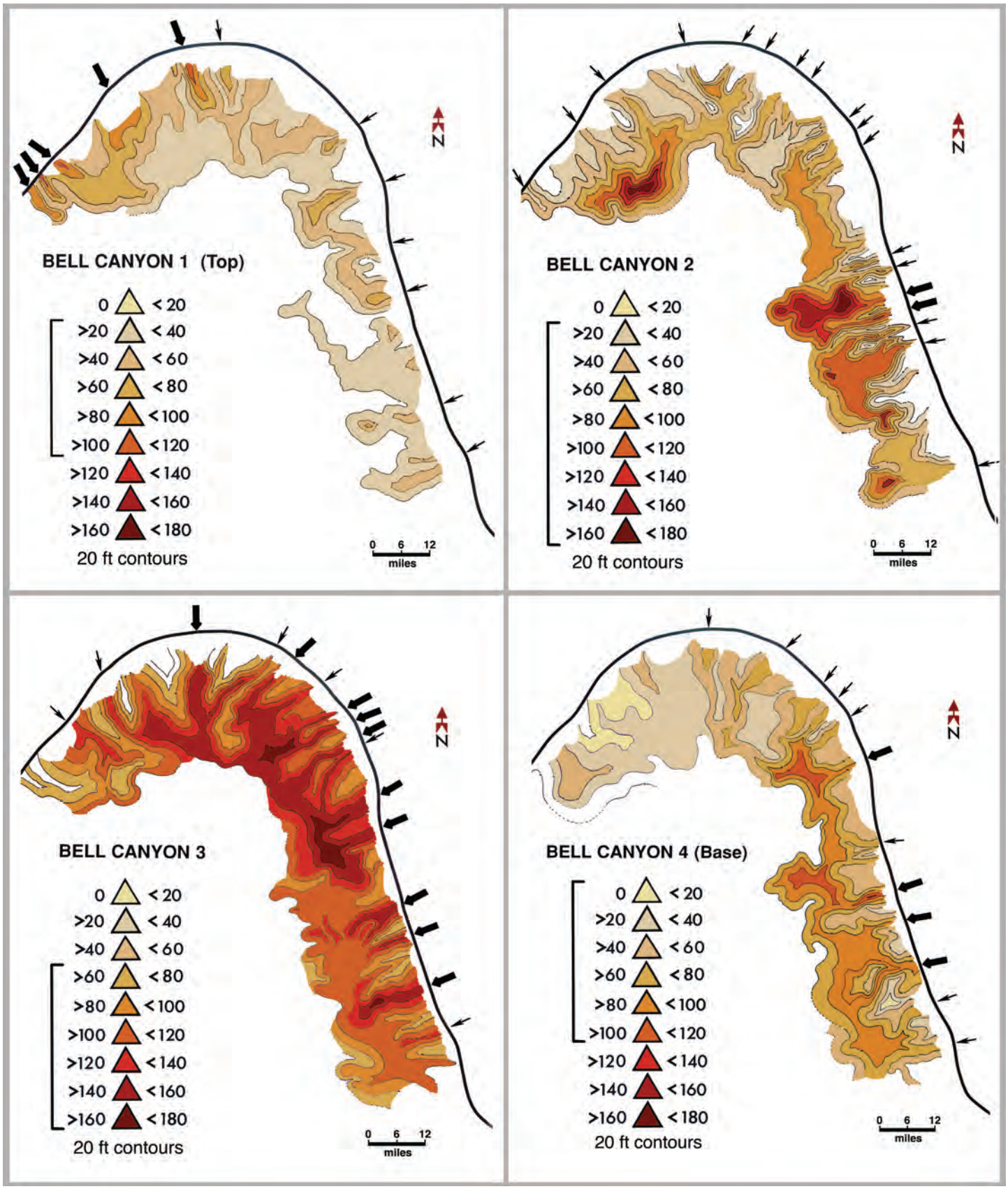

Figure 76. Isopach maps of sand thickness in four intervals of the Bell Canyon Formation. Note temporal shifts of probable input points for turbidite transport of sands. Adapted from unfinished M.S. thesis (see Giesen and Scholle, 1990).

stratigraphic-hydrodynamic traps which occur where sandstone-filled channels are incised into less permeable interchannel sandstone" (Williamson, 1979, p. 39). These channels are as much as 8 km (5 mi) wide, 30 m (100 ft) deep, and 80 km (50 mi) long and the shape and orientation of these channels clearly controls the size, trend, and productivity of oil and gas fields. Thus, only the thick, channelized, coarser-grained sandstone (of the type seen at Stop II-3) are productive; the finer-grained siltstones seen at this stop generally have permeabilities too low for commercial oil production.

0.7	113.8	45.6	Entrance to McKittrick Canyon day-use area of the Guadalupe Mountains National Park on the left. Use McKittrick Canyon supplementary road log and the associated Stop II-1 (McKittrick Canyon Permian Reef trail) description for this area.
0.1	113.9	45.5	The escarpment ahead is formed by the Lamar Limestone Member of the Bell Canyon Formation.
1.0	114.9	44.5	**STOP II-6. Lamar Limestone Member basinal carbonates.**

BE CAREFUL, HAZARDOUS TRAFFIC AT THIS OUTCROP!

This section exposes basinal, black, laminated limestones and shales (Fig. 42) of the Lamar Limestone Member, the youngest named member of the Bell Canyon Formation. Subtle features indicative of turbidite redeposition of platform-derived, fine-grained carbonate sediment are visible (e.g. micro-grading and reworking of tiny fragments of shelf- and slope-derived fossils). The Lamar is sparsely fossiliferous at this locality, with some fusulinids (including *Yabeina*), small ammonoids, brachiopods and other organisms.

The Lamar Limestone becomes darker and contains more organic carbon toward the basin center; indeed, all benthic organisms are absent from these basin-center sediments. Conversely, the unit becomes lighter colored and more fossiliferous toward the basin margin. It seems, therefore, that euxinic conditions were largely restricted to the deepest parts of the Delaware Basin (Babcock, 1977b). In this area, relatively near the basin margin, a moderately diverse fauna, which includes burrowing bivalves, siliceous sponges, holothurians and conodonts, is evidence that conditions here were not uniformly anaerobic (Babcock, 1977b). Yet the evaporite crystal casts found on many bedding surfaces (Fig. 77), the organic carbon-rich sediment and the widespread preservation of very fine-scale lamination all indicate that largely dysaerobic, evaporitic bottom waters occupied this region during much of Lamar time. Presumably, poorly oxygenated conditions were periodically relieved by input of turbidity currents bringing sediment-laden, oxygenated waters down-slope into the basin. These events were probably accompanied by short-lived but widespread colonization of the basin floor by benthic organisms.

Submarine mass movements (synsedimentary slides and slumps) are indicated by the large-scale contortions and thickness variations seen in many of the beds. Brown and Loucks (1988, p. 10) have interpreted even larger-scale features at this outcrop as the base of a very large debris slide that occupies the entire upper part of the outcrop.

The lateral thickness variations of the Lamar Limestone follow a familiar pattern of basin-margin to basin-center change.

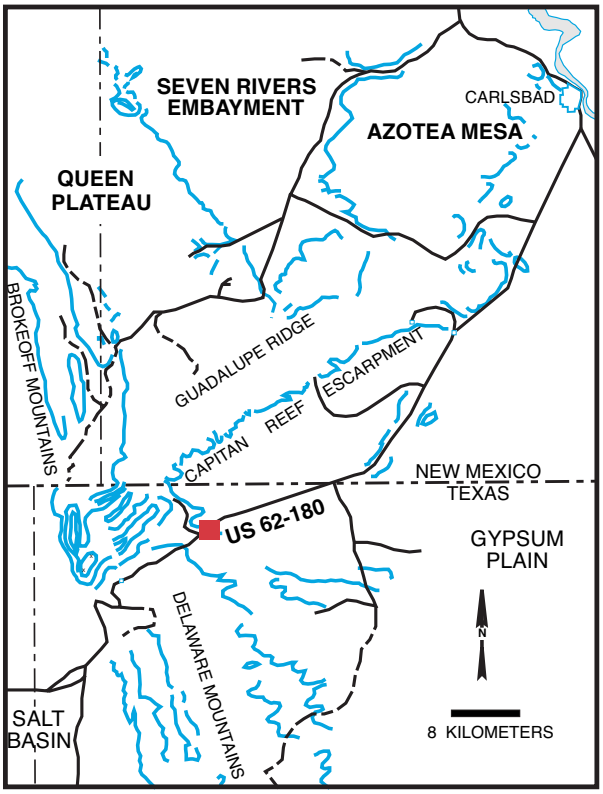

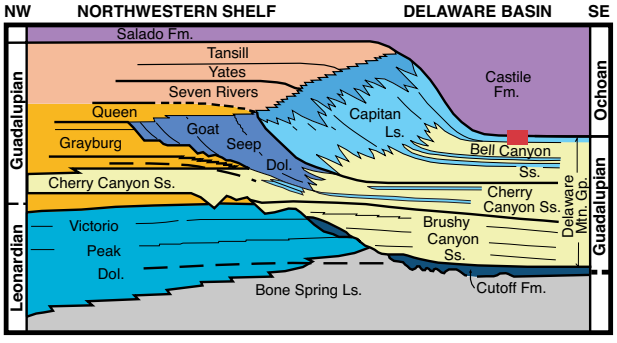

Figure 77. View of bedding plane of Lamar Limestone. Note abundance of evaporite crystal casts — these indicate hypersaline conditions in the basin center either during or immediately following Lamar sedimentation. This is also supported by paleoecological studies on the unit. Coin is 1.8 cm in diameter.

The Lamar thins from 90 m (300 ft) along the Capitan slope, to approximately 6-9 m (20-30 ft) in this area (about 7.2 km or 4.5 mi from the shelf margin), to as little as 2 m (6 ft) in outcrops about 27 km (17 mi) from the basin edge, and eventually to less than a meter (ca. 2 ft.) of silty shale in subsurface sections near the basin center (Babcock, 1977b; Tyrrell, 1969).

The Lamar Limestone Member is the youngest limestone unit in the Guadalupian part of the Delaware Basin. As such, it is a lateral facies equivalent of the uppermost part of the Capitan Limestone on the shelf edge and the Tansill Formation in back-reef, shelf-interior areas. A thin sandstone occurs between the clearly Guadalupian Lamar Limestone and the overlying Ochoan Castile Formation. Its exact stratigraphic affinities are still somewhat unclear (see, for example, Reid et al., 1988 and Wilde and Rudine, 1996) although Wilde et al. (1999) have recently provided a formal designation for the "post-Lamar beds" as the "Reef Trail Member of the upper Bell Canyon Formation." See Brown (2006) for further descriptions of this locality.

1.2	116.1	143.0	Roadside rest area on right. Excellent exposures of reef and fore-reef deposits can be seen to the southwest. The exposed part of the reef becomes progressively older toward the south. The crest of the reef at the southern end of its outcrop (near Guadalupe Peak) is approximately 300 m (1,000 ft) lower stratigraphically than the reef exposed at Walnut Canyon, about 40 km (25 mi) to the north of this location. This implies that the face of the reef has been eroded back by at least 0.8 km (1/2 mi) in the southern Guadalupe Mountains region.

There is still some scientific dispute about the nature of the transition from shelf to basin along the Guadalupe Mountain front. Hayes and Gale (1957) and Hayes (1964) mapped the mountain front zone without any faulting. Kelley (1971; 1972), on the other hand, placed a fault with an estimated 60-120 m (200-400 ft) displacement along the front.

7.9	124.0	35.4	Straight ahead lies the solution escarpment of the Castile evaporites. We are driving on a surface of Quaternary gravels that lie on the basal limestone and shale unit of the Castile and on the Lamar Limestone.
1.4	125.4	34.0	Junction with Texas Ranch Road 652 on the right. Continue straight ahead.
0.1	125.5	33.9	Texas-New Mexico state line. Welcome to New Mexico.
1.6	127.1	32.3	Notice the difference in vegetation on the gravel surface on which we are now driving versus that on the hills of Castile gypsum and anhydrite directly ahead.
0.5	127.6	31.8	**STOP II-7. Castile Formation Ochoan evaporites.** BE CAREFUL, TRAFFIC IS VERY HAZARDOUS AT THIS OUTCROP!

Excellent exposures of the Castile Formation in deep roadcuts. This unit is the oldest true Ochoan sediment in the region, and it conformably overlies the Guadalupian Bell Canyon Formation. The Castile is entirely confined to the Delaware Basin and does not extend onto the adjacent shelf areas. It overlies a thin, limestone and siltstone/shale zone that may be a lateral facies equivalent of the

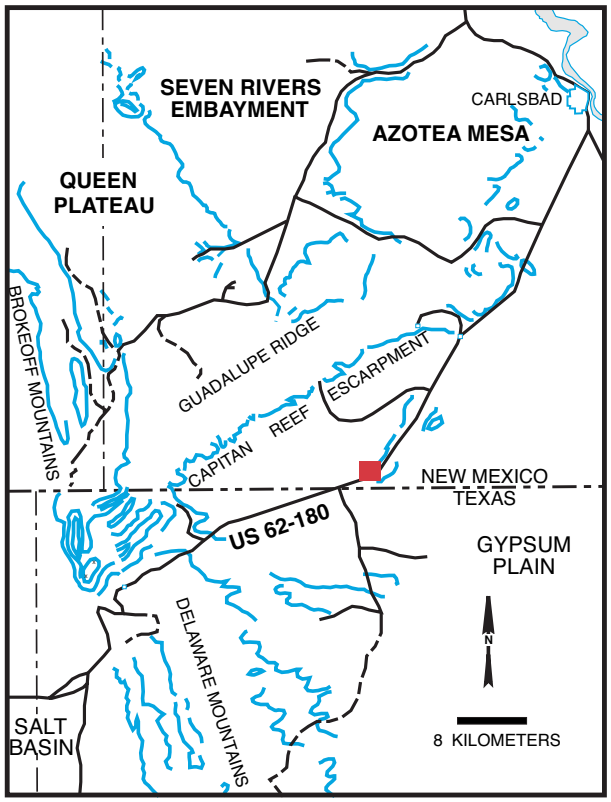

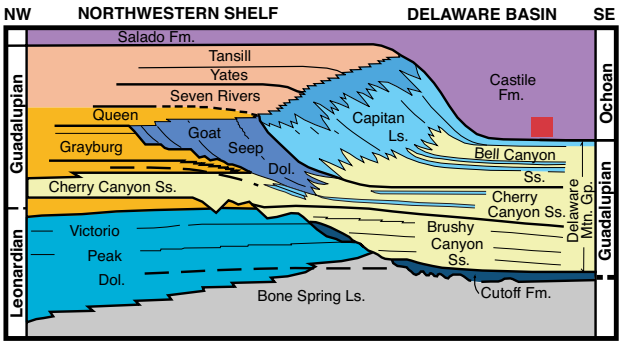

very youngest part of the Capitan and Tansill Formations or may slightly postdate those units (see discussion in previous stop, II-6, description). The bulk of the Castile Formation itself consists of a thick section of laminated anhydrite with intervals of laminated halite. The Castile Formation has been reported to reach a maximum thickness of 470 to 550 m (1,550 to 1,800 ft) in subsurface sections that thicken toward the northeastern part of the Delaware Basin (King, 1948, p. 89).

The Castile Formation grades conformably upward into the Ochoan Salado Formation; the Salado contains laminated halite, anhydrite, sylvite, polyhalite, and even more soluble evaporite minerals (Fig. 78). The extreme solubility of its components means that the Salado does not generally appear in outcrop. Indeed, in this area much (or all) of the Salado may have been removed by erosion. The Salado does, however, form a wedge of sediment that thickens toward the northeast to a maximum of greater than 600 m (2,000 ft) (Anderson et al., 1972, p. 82). In the northeastern part of the Delaware Basin, the Salado is extensively mined for potash minerals and hosts an active nuclear waste repository, the Waste Isolation Pilot Plant (WIPP). Unlike the Castile, the Salado Formation extends beyond the borders of the Delaware Basin onto the surrounding shelf areas where it generally lies directly on Guadalupian carbonate rocks. The Salado Formation, in turn, is unconformably overlain by the dolomitic Upper Permian Rustler Formation, the Dewey Lake Redbeds and younger units. The pre-Rustler unconformity shows extensive Permian tilting and erosion for, in places (particularly the southwestern part of the region), it has completely removed the Salado, allowing the Rustler to lie directly on the Castile Formation or Guadalupian carbonate rocks.

The onset of Castile evaporite deposition coincided closely with the termination of reef growth around the Delaware Basin margin. It is not clear whether this is a causal or coincidental relationship. Eustatic sea-level drop, tectonic movements, reef growth, or other factors could have increased the restriction of influx of normal marine water into this already partially barred basin. This, coupled with the extreme aridity and high evaporation rates in the area, may have led to drastic increases in the salinity of basin water, the associated killing of the salinity-sensitive reef organisms and the eventual start of evaporite deposition. It must be emphasized that although the changes in depositional patterns at the Guadalupian-Ochoan transition were dramatic, the causes of these changes may have been considerably more subtle. Strongly evaporitic conditions existed throughout Guadalupian time, as apparently did hypersaline stagnant bottom waters in the basin. Marine influx from the south was certainly present during Guadalupian time to maintain normal

Figure 78. Underground mine-wall view of evaporite deposits, including halite, sylvite, polyhalite and other bittern minerals, in the lower part of the Salado Formation. Duval potash mine, east of Carlsbad, Eddy Co., New Mexico.

Figure 79. Laminated Castile Formation basinal evaporites. Dark laminae are calcite plus organic matter; light laminae are gypsum. Laminae are considered to be varves (annual layers reflecting variations between more evaporitic and less evaporitic seasons). The coin is 1.9 cm in diameter.

or near-normal marine conditions in the surface waters of the Delaware Basin.

This influx must have continued through much of Ochoan time, if in a somewhat more restricted form, to supply the salts of the Castile and perhaps also some of the Salado Formations (other parts of the Salado have more terrestrial and/or lacustrine compositions). Thus, it appears most likely that it was a gradual change in marine water supply versus evaporative water removal that led to the abrupt shift from carbonate to evaporite sedimentation, presumably when a critical salinity level was reached. This gradual, but not perfectly continuous, salinity transition apparently continued through Ochoan time, leading to deposition of anhydrite, then halite and sylvite, and eventually the true bittern salts found in the northeastern Delaware Basin (Holt et all., 2006; Lowenstein 1983 and 1988).

The Castile Formation, then, represents an evaporite filling of the approximately 550 m (1,800 ft) deep basin remaining at the end of Guadalupian time. Although there may have been some drop in basinal water levels, most of the Castile clearly was deposited in deep water (at least below wave base) as indicated by the absence of shallow-water sedimentary structures in most intervals and the presence of fine-scale lamination. The laminae consist of regular (although variable thickness) alternations between white anhydrite laminae and darker laminae containing a mixture of organic matter (circa 1.5 percent average) and calcite (Fig. 79). The anhydrite-calcite couplets typically are 1-5 mm in thickness throughout most of the Castile Formation (Anderson et al., 1972, p. 73). On outcrop, the anhydrite may have been altered to gypsum (this locality has both gypsum and anhydrite exposed according to S. D. Kerr in Dunham, 1972). The laminations have remarkable lateral continuity, as one might expect for deeper-water evaporites, and individual laminae have been traced for more than 110 km (70 miles; Anderson et al., 1972; Dean and Anderson, 1978). In a few instances, however, layers of coarse, reworked sulfate, nodular sulfate, or bottom-nucleated crusts were noted (Kendall and Harwood, 1989; Leslie et al., 1993). These crusts were interpreted as shallow-water deposits that may have formed during times of extreme evaporative drawdown; Kirkland (2003) provided an alternative explanation based on rare events of thermal overturn of the basinal waters leading to bottom-nucleation in deep waters. Other nodular zones, however, may reflect recrystallization during burial and uplift (Fig. 80).

The laminations of the Castile Formation (as well as those in the uppermost Bell Canyon and Salado Formations) have been interpreted as seasonal varves (Udden, 1924; Anderson et al., 1972). The calcite and organic-matter layers represent periodic (annual?) freshening of the water and the development of plankton blooms. The anhydrite layers represent restricted, more evaporitic conditions (Kirkland et al., 2000; Kirkland, 2003). Although that has in the past been interpreted as summer evaporative/winter freshening cycles, more recent studies interpret the freshening to result from summer monsoonal conditions (Anderson, 2006). Considering the

Figure 80. Laminated and nodular Castile Formation basinal evaporites. These nodules are probably secondary features, perhaps resulting from the >1km of burial to which the unit was once subjected. Hammer at left for scale.

basinal nature of the depositional setting, the obvious aridity, and the prior influx of clastic terrigenous material (e.g., Kessler et al., 2001), it seems odd that the Castile-Salado evaporites contain virtually no detrital windblown silt. It is possible that the alkaline waters may have dissolved much of the original silt influx. On the other hand, if so much silica dissolved, then where are the expected siliceous precipitates or silica replacements?

Approximately 260,000 calcite-evaporite cycles have been counted in the uppermost Bell Canyon-Castile-Salado sequence (about 220,000 in the Castile Formation alone). This implies extremely rapid deposition of thousands of feet of evaporites in the Delaware Basin, a common situation with major evaporite deposits. The Castile cycles provide one of the longest continuous climatic records from any time interval in the Phanerozoic. The record of "varve" thicknesses has been analyzed in great detail (Anderson, 1982, 1984, 1991; Anderson and Dean, 1995; Anderson and Kirkland, 1988) for cyclicities. Major peaks were found in the range of 20,000 and 100,000 years, indicating that Milankovitch-scale climatic variations were active during deposition of the unit; shorter-scale cycles were found as well.

The microfolding that has contorted a number of intervals in the Castile at this outcrop (Fig. 48) clearly is post-depositional and has been interpreted to represent volume changes due to hydration and/or dehydration reactions during burial and/or uplift. Recent, detailed measurements on these structures have indicated that both small- and large-scale fold axes trend N30-50°W. This direction is parallel to the trend of Tertiary faulting in this area (Anderson and Kirkland, 1988), and the folds, therefore, are likely to be late-stage, compressional, structural features rather than early, soft-sedimentary or later hydration structures. See Alexander and Watkinson (1989) and Watkinson and Alexander (1993) for additional discussion of possible causes.

The evaporite filling of the Delaware Basin is largely responsible for the spectacular exposures of the Guadalupian facies that we see on this trip. The complete plugging of the "hole" left at the close of Capitan reef growth and the subsequent, Tertiary, removal of that plug have left us with resurrected Guadalupian topography and facies relations in this area.

The Castile and Salado evaporites may also have had a major impact on the oil and gas distribution in the Permian Basin. The rapid burial of basinal source rocks to depths sufficient for oil and (or) gas generation is one probable effect. It is quite possible that compactional geopressuring of the basinal sediments resulted from the rapid deposition. This may have eventually aided the early migration of hydrocarbons from the basin, before deep burial and destruction of porosity in potential shelf reservoirs. Overpressuring and early oil migration may have been significant factors in the excellent hydrocarbon productivity of the Permian Basin region. The early oil movement may also explain why primary porosity and early diagenetic porosity modifications, rather than later diagenetic porosity types, are so important in many Permian Basin reservoirs. In any case, the extensive blanketing of both shelf and basin by an impermeable cover of evaporites clearly provided an outstanding hydrocarbon seal for the entire region and explains why this area is North America's largest petroleum producing region.

The name of the Castile Formation, by the way, comes from the Spanish word for the castle-like (or tepee-like) structures that can be seen in the distance at the surface of this unit. These are calcitized pipes of former gypsum that weather in relief. The limestone, which retains the laminated fabric of its gypsum precursors, is thought to have formed as a result of the action of sulfate-reducing bacteria metabolizing the calcium sulfate and hydrocarbons leaking from underlying reservoirs. The process produces calcium carbonate and hydrogen sulfide; the latter has been altered locally to economic sulfur deposits through the influx of oxidizing groundwaters (see Brown and Loucks, 1988b).

1.9	129.5	29.9	Note hummocky, solution-generated topography on top of the Castile evaporite. These are the Yeso Hills. Extensive gypsum karst, with some large cave systems, is found in this area (see Land et al., 2006 for guidebook to this area).
1.1	130.6	28.8	White's City visible directly ahead in the distance. The valley to the left is developed on the uppermost Bell Canyon strata (Lamar and post-Lamar beds). The Capitan reef escarpment can be seen plunging to the north beneath Ochoan and younger sediments as a consequence of structural tilting. To the south, the reef rises higher and higher on the skyline to the point where it has been removed by erosion. The buildings at the entrance to Carlsbad Caverns can be seen on the ridge top at about 11:00 o'clock.
0.2	130.8	28.6	Dirt road on right leads to a small quarry in the Castile evaporite — here, the gypsum has been very coarsely recrystallized and yields beautiful crystals, many over a foot across.
1.0	131.8	27.6	Zone of Quaternary rubble probably derived from dissolution of upper Castile or Salado evaporites. Several thin, weathered, basaltic igneous dikes cut the evaporite section in this area.
1.4	133.2	26.2	Roadside rest area on left.
1.2	134.4	25.0	At a point approximately 90 m (300 ft) east of the highway, loose boulders of Lower Cretaceous (Commanchean) limestone have been described by W. B. Lang (1937) who interpreted them as fragments of widespread Cretaceous cover downdropped and preserved in solution pipes cut into the Ochoan evaporites.
1.5	135.9	23.5	Entrance road to Slaughter and Rattlesnake Canyons and the Slaughter Canyon Cave on left. Both Rattlesnake and Slaughter Canyon have excellent exposures of the late Guadalupian Capitan fore-reef, reef and back-reef facies (see Pray and Esteban, 1977). The view from the south wall of Slaughter Canyon (where the entrance to Slaughter Canyon Cave is located) to the north wall provides an excellent view of the progradation (and up-building) of reef and back-reef facies in the upper Capitan and associated Yates and Tansill strata. Continue straight ahead.
0.3	136.2	23.2	Highway continues on Castile Formation. The mouth of Slaughter Canyon is visible at about 8:00 o'clock; the mouth of Rattlesnake Canyon can be seen at about 9:00 o'clock. The northwest-southeast trending Huapache Monocline crosses the Capitan reef front between these two canyons.
1.8	138.0	21.4	Quaternary gravel in roadcut.
3.3	141.3	18.1	Beautiful downtown White's City. Junction with New Mexico Highway 7 to Walnut Canyon and Carlsbad Caverns on left. See separate Walnut Canyon supplementary road log for information on reef and back-reef localities in this canyon that leads up to Carlsbad Caverns. Continue on U.S. Highway 62-180 to Carlsbad, New Mexico.
5.0	146.3	13.1	Bridge over Jurnigan Draw. Rustler Formation red beds can be seen in middle distance on right.
0.2	146.5	12.9	Junction with New Mexico Highway 396 on right. The hills to the left are composed of Capitan reef and Tansill backreef limestone. The Black River oil field is

			located to the right; the field produces 42 API gravity oil from sandstones and siltstones just beneath the Lamar Limestone member of the Bell Canyon Formation at about 600 m (1,950 ft) depth. Most hydrocarbon production in this area that is located close to the highway, however, is from Pennsylvanian units.
1.5	148.0	11.4	Roadcut in Rustler Formation.
0.7	148.7	10.7	Roadcut in Rustler Formation.
2.6	151.3	8.1	Junction with Dark Canyon Road on left near the Dark Canyon Antiques and General Store building. The hills to the west are composed of Tansill Formation near-back-reef limestones and dolomites. The one-well Dark Canyon oil field lies about 0.8 km (1/2 mi) to the west. Completed in 1952, the field produced from a 3.3 m (11 ft) pay zone in Delaware Mountain sandstone at 572 m (1,876 ft) depth. The well continued to produce for many years at 10 to 12 BOPD. Continue straight ahead for Carlsbad. See supplementary Dark Canyon-Sitting Bull Falls-Rocky Arroyo road log for route to left.
1.0	152.3	7.1	In the foreground to the left are the Frontier Hills composed of Ochoan Rustler Formation sediments that dip southeastward into the Delaware Basin. The Rustler Formation in this area consists of dolomite, red beds, fine-grained sandstones, and minor gypsum. The Rustler overlies the Salado Formation in the Delaware Basin but lies directly on the Capitan Limestone in the ridge west of the Frontier Hills.
1.8	154.1	5.3	Carlsbad city limit. The town was first settled in 1888 (originally named Eddy after its founder, it was renamed Carlsbad in 1899). Charles Eddy, by the way, also founded Cloudcroft and Alamogordo, towns we will pass through and that are in or near the Sacramento Mountains to the northwest. The town of Eddy was sited here because of the Pecos river and the agricultural potential along its flood plain, although the mineral springs along the river eventually also led to a significant tourist industry as well as the renaming of the town after Carlsbad, a famous mineral spa city in the Czech Republic. Carlsbad, New Mexico, has since become an important county seat, a center for the regional potash mining industry, a significant tourist area (due to its proximity to Carlsbad Caverns), and a base for WIPP site operations (an operational/experimental facility for disposal of government-generated, transuranic radioactive wastes).
1.3	155.4	4.0	Quaternary caliche exposed in pits on right.
0.4	155.8	3.6	Caverns City Air Terminal (Carlsbad municipal airport) entrance on left. The Hackberry Hills to the west are composed mainly of Tansill dolomites and upper Yates dolomites and sandstones, both back-reef facies equivalents of the upper part of the Capitan reef. The reef itself is completely buried beneath younger sediments in this area. The back-reef equivalents are exposed only because of the gentle (approximately 5 degree) eastward dip of the Guadalupian strata in this area.
2.5	158.3	1.1	Roadway Inn on right.
0.3	158.7	0.7	Ocotillo Hills located to the northeast.
0.7	159.4	0.0	Junction with U.S. Highway 285 to Pecos, Texas on the right.

El Paso-Carlsbad road log ends.

Sunset at the south end of the Guadalupe Mountains.

Sunset at a Permian Basin drilling site.

McKITTRICK CANYON (GUADALUPE MOUNTAINS NATIONAL PARK) GEOLOGIC ROAD LOG

Mileage	Cumul. Mileage	Location Description
0.0	0.0	Junction of U. S. Highway 62-180 with paved road to McKittrick Canyon day-use area (mileage 113.8 on El Paso-Carlsbad road log). Turn west on McKittrick Canyon road. Most of this road is cut in the McCombs to Rader interval of the Bell Canyon Formation. The cliffs on the right (north) are capped by the Lamar Limestone Member.
0.4	0.4	The view ahead is directly into the steeply dipping Capitan fore-reef talus deposits.
1.6	2.0	Junction with side road (locked gate) that leads to Wallace Pratt's former home, the oil tanker-shaped "Ship on the Desert." The view to the northwest shows the exhumed Delaware Basin margin, largely stripped of its evaporite filling. The reef-massif is characterized by an apparent lack of bedding and a strongly developed vertical joint pattern that trends parallel to the reef front. These were penecontemporaneous growth faults probably produced by compaction of the 450-600 m (1,500-2,000 ft) of largely unconsolidated reef talus over which the reef was prograding. The penecontemporaneous formation (and filling) of the joints is shown by the fact that locally one finds specialized Permian fauna lining fracture walls. The joints are also filled with submarine, originally aragonitic (now calcitic) cement crusts, Permian siltstones, soil crusts and local dolomite. Steeply dipping fore-reef deposits are visible down-slope from the reef, and these form a smooth transition to the nearly flat-lying toe-of-slope and basinal deposits seen at the base of the escarpment.
2.0	4.0	Outcrops of massive, fine-grained, toe-of-slope deposits of the Lamar Limestone on the left. Large-scale lenticular bedding is clearly visible. Although largely composed of micritic limestone, these deposits contain a significant reefal fauna. Thus, they were originally interpreted as bioherms formed in deep water (depths probably in excess of 500 m; 1,600 ft; Newell et al., 1953). However, recent studies of the Florida Straits and similar areas have shown that such deposits can be produced by a combination of down-slope reworking of reefal debris, along-slope transport and deposition by contour currents, and submarine cementation (Mullins et al., 1981; Neumann and Ball, 1970; Neumann et al., 1977). Thus, these lenticular deposits may be analogous to the "lithoherms" of the Florida-Bahamas region.
0.3	4.3	**STOP II-1. McKittrick Canyon Visitor's Center.** This stop is entirely on National Park land, and collecting samples, even of loose rock material, is NOT allowed. We will be hiking for about 3-5 hours. Be sure to bring sunscreen and plenty of liquids to drink. We will walk up the canyon for a short distance (about 3/4 km; 1/2 mi) following the trail marked for "Pratt's Lodge" and then return via the streambed; we will then hike up the Permian Reef trail that was cut in the early 1980s on the north side of McKittrick Canyon. We will be undertaking an approximately 350 m (1,200 ft) climb on this well graded but rocky trail, so please wear sturdy hiking boots. Finally, the difficulty of the terrain and the size of the group make it imperative that we all stay on the clearly marked trail and remain together as a group. PLEASE, DO NOT WANDER OFF ON YOUR OWN OR IN SMALL SUBGROUPS. We will keep the pace slow enough so that all can keep up. The purpose of this stop is to examine the toe-of-slope and fore-reef facies transitions of the Capitan Limestone and its equivalents. Although it would be more pleasant if this facies change could be seen without resorting to a strenuous climb, this is not possible. It should be remem-

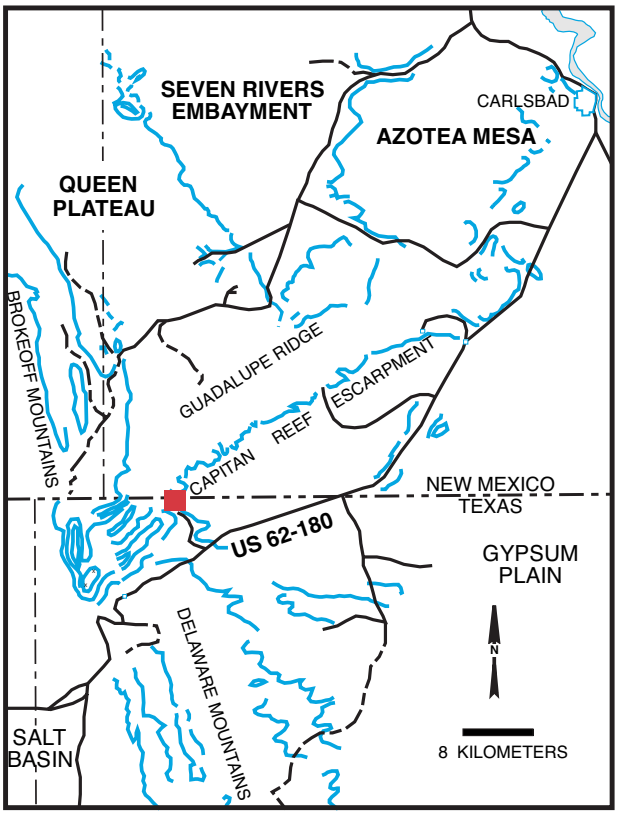

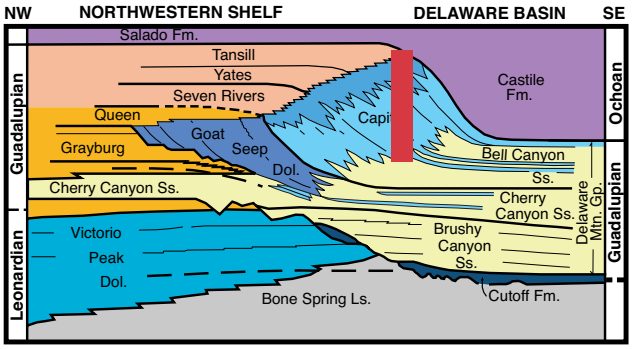

Index map for Stop II-1

bered that the facies transition is one that took place on a 30 degree slope over a vertical distance of more than 400 m (1,300 ft); thus, the vertical component is an important one. Also, these facies are exposed only in areas south of White's City and are easily accessible only in Rattlesnake, Slaughter and McKittrick Canyons. All three areas require extensive climbing, and McKittrick Canyon provides the easiest access coupled with excellent lateral exposure.

Our upward climb will take us across a number of different Bell Canyon units (Fig. 13). We start at the level of the Rader Limestone and cross several unnamed Bell Canyon sandstone units and the McCombs Limestone before reaching the Lamar Limestone. We will then ascend essentially on a Lamar-Capitan dip-slope and view the lateral changes in Lamar to slightly post-Lamar (Tansill-equivalent) talus facies (Fig. 81). For a short interval, just below the massive triangular spur of reefal material, we will be in slightly older, Yates-equivalent strata (Bebout and Kerans, 1993).

We start our walk on the Pratt Lodge trail in slope alluvium with some outcrops of the McCombs Member but soon reach the thin-bedded, dark-colored, micritic carbonate rocks of the Rader Limestone in the stream bed. Bryozoans and brachiopods are the most commonly seen megafossils in the Rader carbonates. Chert nodules and silicified (originally calcitic) organisms abound (Fig. 82) with the silica having been derived from dissolution of opaline silica in siliceous sponges and radiolarians that lived or accumulated in the down-slope area. In other areas of the Permian Basin, equivalent strata have yielded even more spectacularly silicified fauna (Fig. 83; see Cooper and Grant, 1972, 1974, 1975, 1976a and b, 1977).

Another significant macroscopic diagenetic feature visible in the limestones is compactional deformation around fossils, concretions, nodules or allochthonous blocks (Fig. 84). Thin- to medium-bedded graded carbonate turbidites, channels filled with cross-bedded reef- and slope-derived debris and large blocks of reef limestone also can be seen locally in these beds.

As we move up-stream, we will see thick packages of fine-grained, well-sorted sandstone and siltstone interbedded between the Rader and McCombs limestone members. The sandstones are compositionally identical to the thin, back-reef sandstone and siltstone units we will see at other localities. In addition, several large carbonate blocks of reef and upper slope material can be seen within the sandstones — these represent rock falls or slides on the fore-reef slope (Fig. 84). One must take care, however, to distinguish Permian from Holocene deposits, because the stream bed is also lined with patches of well-cemented fluvial gravels of modern origin.

The sandstones locally contain fist-sized crystal-lined cavities. These are interpreted as replaced evaporite nodules that formed diagenetically within the basinal sands from dense, meso- or hyper-saline brines that refluxed downward from overlying back-reef evaporitic lagoons. The evaporites precipitated at the base of the slope and were later dissolved, probably during uplift and meteoric water influx.

The up-slope interfingering of discrete, basinward-dipping Permian sandstone and carbonate units indicates that both were derived from the adjacent shelf. The sandstones also show extensive evidence of down-slope current transport including large-scale trough cross-bed-

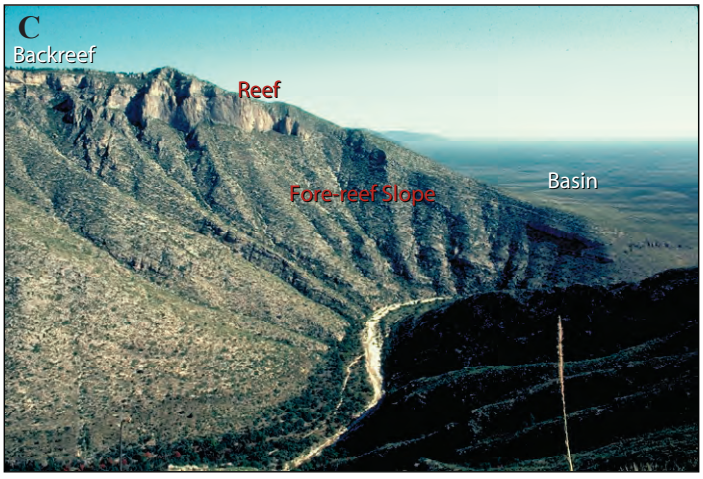

Figure 81. Panoramic views of shelf-to-basin sedimentary facies of the late Guadalupian Capitan reef complex. A. Composite photo of north wall of McKittrick Canyon, Guadalupe Mountains National Park; B. Composite photo of Slaughter Canyon, Carlsbad Caverns National Park; C. Detailed view of mouth of McKittrick Canyon (north wall), Guadalupe Mountains National Park. Strata at top of section at far left are Yates and Tansill back reef carbonates; the upper part of the massive triangular cliff just to the right is last phase of Capitan reef development; strata below and to the right of the reef are steeply-dipping fore-reef talus beds that flatten and pass gradually into the deeper-water sediments of the Delaware Basin. Views A and B courtesy of Charles Kerans (Kerans and Fitchen, 1995; Kerans and Kempter, 2002).

Figure 82. Selectively silicified fauna in base of slope deposits in the Rader Limestone (McKittrick Canyon). Silica source mainly was from siliceous sponge spicules; replaced grains are mainly calcitic skeletal fragments including the prominent brachiopod, *Leptodus americanus*, at the left. Coin is 2.4 cm in diameter.

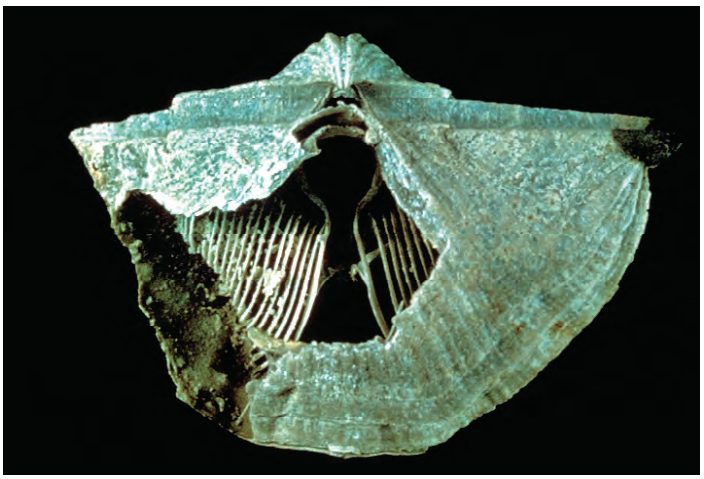

Figure 83. Selectively silicified spiriferid brachiopod from slope facies deposits. Note remarkable fidelity of preservation of delicate ornamentation and internal spiralia. This sample is from the Glass Mountains in Brewster Co., Texas.

Figure 84. A large block of reefal limestone reworked into the base-of-slope facies of the Bell Canyon Formation from the south side of McKittrick Canyon. Note compactional drape of finer-grained sediments surrounding the lithified reef block.

Figure 85. Stylonodular bedding in fine-grained, lower slope limestones (wackestone to mudstone) in the transition zone between the Capitan Formation and the Lamar Limestone on the Permian Reef trail. The initial low permeability of these sediments precluded dolomitization or extensive evaporite cementation. The absence of fresh water exposure and cementation in these deep-water deposits led to extensive mechanical and chemical compaction during burial diagenesis and ultimately yielded this bedding style that is characteristic of Paleozoic slope and basin carbonates.

ding, channels, ripple marks, and other features. Just a few hundred meters farther up-slope, the sandstones become thinner and eventually pinch out entirely. The carbonate units, on the other hand, become progressively more massive and coarser-grained in an up-slope direction (Fig. 81).

Return via the trail (or the stream bed) to the geology trail that departs from just east of the stream valley near the Visitor Center. An excellent guidebook (Bebout and Kerans, 1993) exists for this trail and sign posts with numbers (some now missing) refer to this guide.

The Permian Reef Geology Trail initially rises rapidly through consolidated stream gravels and dark-colored, very fine-grained limestones of the Lamar Member of the Bell Canyon Formation. Note the abundance of chert nodules (common only in this toe-of-slope setting, occasional debris beds, and burrowed limestones. These beds dip basinward at angles of 7 to 10°, just a few degrees steeper than the regional dip. Turn left (upslope) at the trail junction of the Permian Reef and Geology Loop trails. Do NOT take the trail marked "Geology Loop." After taking a small left-hand jog at the second junction with the Geology Loop trail, we will pass cliffs of lower slope Capitan-Lamar transition beds. Moving upslope through these strata you will be able to see generally dark-colored limestones that are thin-bedded (Fig. 41) or have irregular stylonodular bedding (Fig. 85). Some graded beds and intensely bioturbated limestones are also visible. Lack of early cementation in these strata led to extensive porosity loss during burial as a consequence of both chemical and mechanical compaction.

After passing through a deep cleft in the rocks (with a diverse flora including prickly pear, ocotillo, Texas madrone and scrub oaks), you will pass medium-bedded Lamar-Capitan limestones with superb fining-upward (graded turbidite) fabrics (Fig. 40). Much of the reworked slope and reef fauna in these detrital beds has been selectively replaced by silica (chert and chalcedony). At the first sharp switchback in the trail, note the massive bedded unit that has highly irregular (lenticular bedding). This is the first of many debris flow units we will see along the trail. Most debris flows fill laterally-restricted slope channels and thus have highly

Figure 86. Fore-reef breccia, including large clasts of marine-cemented *Archaeolithoporella*-sponge boundstones derived from up-slope reef facies. Outcrop on the north wall of McKittrick Canyon.

lenticular bedding (Fig. 39); many are also closely associated with turbidite deposits. The carbonate grains in these deposits are clearly recognizable as reef- and slope-derived skeletal fragments (Fig. 86), and large (up to small house-sized) blocks typically show reefal fabric. The fact that this is primarily reef rubble is clear from the abundance of original framework producing organisms, such as calcareous sponges and bryozoans, organic encrustations (*Archaeolithoporella*) and massive synsedimentary marine cements. In most areas, these debris-flow units have little obvious internal organization of the clasts. In the short stretch leading to the second trail switchback, you should be able to see some surfaces with excellent reefal fabrics. In addition, there are sharply bounded areas (especially well displayed at the second switchback) with lighter tan, more crystalline carbonate with numerous patches of coarse, sparry calcite. The diagenesis of these irregularly-shaped, highly altered zones is complex. Many of the detrital clasts of calcareous debris underwent submarine cementation in their original environment of formation. Subsequent alteration in the down-slope depositional environment included extensive selective dolomitization (the tan-colored material), leaching of aragonitic grains, brecciation (Fig. 87), and medium-crystalline calcite "cementation".

The dolomitization of the Capitan slope is highly variable on both local and regional scales (Melim and Scholle, 1999, 2002) — farther south, near El Capitan and Guadalupe Peak, nearly 100 percent of the slope material has been dolomitized, but in this area, less than 50 percent of the rock has been replaced. Likewise, coring of equivalent Capitan slope facies farther north

Figure 87. In-situ brecciation of partially dolomitized, fine-grained carbonates in Capitan upper fore-reef slope from the north wall of McKittrick Canyon. It has been postulated that this brecciation occurred in association with subsurface removal of evaporite cements and prior to filling of remnant pores with coarse, telogenetic, sparry calcite cement. Outcrop on the north wall of McKittrick Canyon.

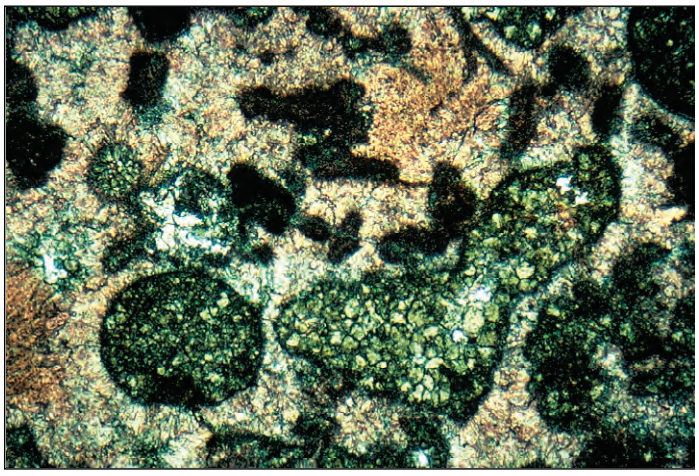

Figure 88. Photomicrograph of an Alizarin-stained thin-section of a block of Capitan reef-derived material in upper fore-reef talus from the north wall of McKittrick Canyon showing selective replacement of originally micritic clasts by medium crystalline dolomite. The abundant marine cements (stained pink) were not dolomitized. Dolomitizing fluids are thought to have been derived from overlying evaporitic settings (Guadalupian or Ochoan) — fluids flowed through syndepositional fractures in the reef and dispersed through the more permeable units in the fore-reef slope.

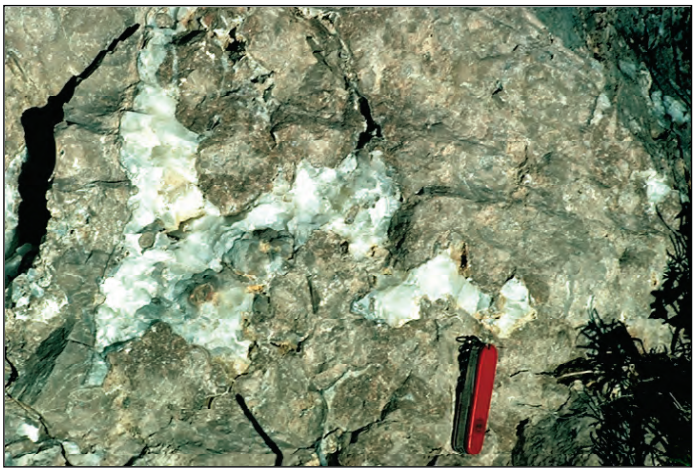

Figure 89. Large, partially connected, sparry calcite filled vugs in the upper part of the Capitan fore-reef talus facies from the north wall of McKittrick Canyon, Guadalupe Mountains National Park. Such vugs may reflect solution-enlargement resulting from an influx of meteoric pore fluids prior to evaporite cementation and burial.

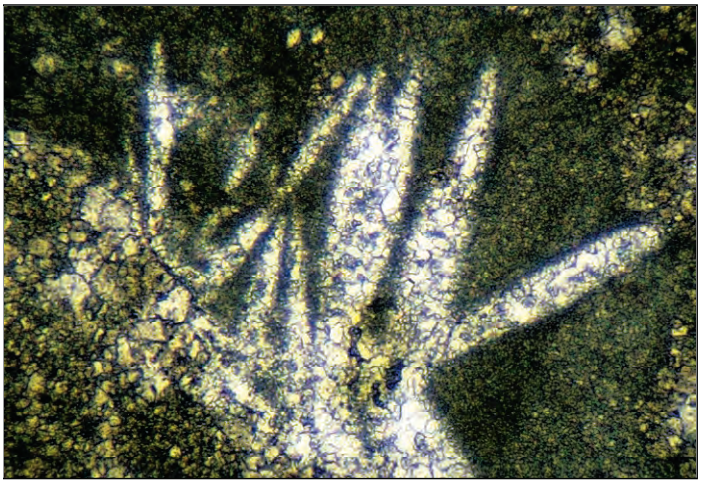

Figure 90. Thin section photomicrograph (plane-polarized light) showing sparry calcite pseudomorphing elongate, precursor displacive anhydrite crystals in the Capitan fore-reef talus facies (geology trail on north wall of McKittrick Canyon).

and east (the PDB-04 well on the northern margin of the Delaware Basin) showed a completely dolomitized reef and forereef section (Garber et al., 1989).

Dolomitization selectively affects finer-grained primary constituents (Fig. 88) and typically is distributed in sharply bounded rock bodies. Vertical, synsedimentary fracture systems and/or solution-enlarged pipes and fractures apparently funneled shelf-derived brines deep into the fore-reef debris. Permeable slope deposits then served as supplementary conduits for lateral movement and selective replacement and/or cementation by these brines (Melim and Scholle, 1989a). At least two generations of dolomite have been identified.

The dolomitized zones are generally associated with coarse, sparry calcite (Fig. 89) and vermicular kaolinite (dickite), both of which form pore filling cements. Although the coarse calcites have long been interpreted as simple burial cements (e.g., Mruk, 1985, 1989), subsequent work has indicated that they are replacements of massive evaporites which once plugged most fore-reef porosity (Scholle et al., 1992). The precursor evaporites (Figs. 90, 91) were removed during Tertiary uplift, a time in which surface-derived meteoric fluids were able to penetrate deep into the subsurface from recharge sites in the Guadalupe Mountains. Thus, evaporite minerals are common and calcite spar is scarce to non-existent in still deeply buried sections of the Capitan Formation. The Capitan forereef strata in the PDB-04 well represent an intermediate stage of alteration between the calcitized outcrops and the unaltered deeply-buried strata of the Central Basin Platform. The PDB-04 samples have some preserved anhydrite, common anhydrite relicts within poikilotopic gypsum (Fig. 92) and numerous open voids (Fig. 93) formed by evaporite dissolution (Garber et al., 1989; Scholle et al., 1992).

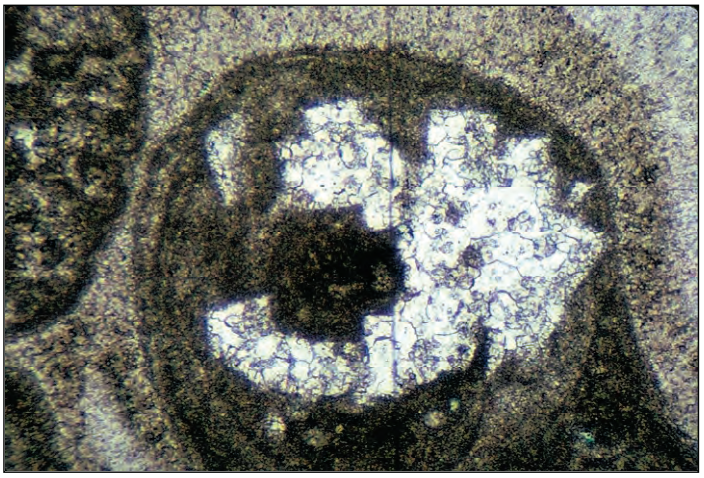

Figure 91. Photomicrograph (plane-polarized light) showing calcite pseudomorphing "stair-step" anhydrite crystals that replaced part of an ooid. Sample is from the intermediate- to near-back-reef facies of the Yates Formation from Rattlesnake Canyon, Carlsbad Caverns National Park.

The intense and varied early diagenesis precluded significant compaction in these units, but grain fracturing is common (Fig. 87), probably as a result of subsurface leaching and local collapse. Porosity in outcrop is quite low, but

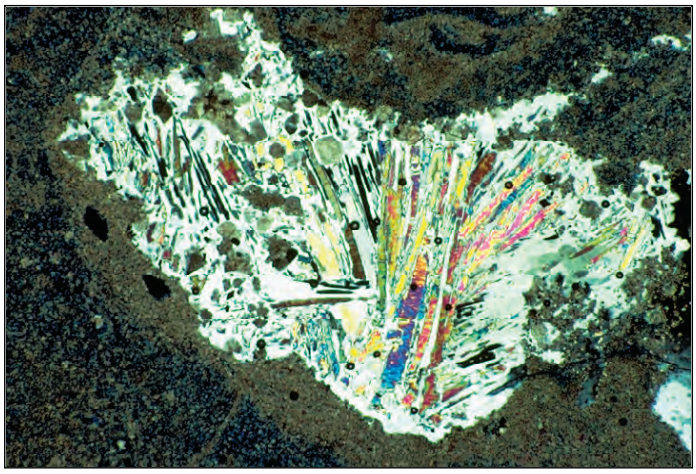

Figure 92. Thin-section photomicrograph (cross-polarized light) of evaporite-plugged porosity in Capitan fore-reef facies. Note partial conversion of anhydrite (high birefringence colors) to gypsum (gray) — this is thought to be related to modern-cycle uplift and groundwater flow. Sample from 3,282 ft (1,000 m) depth in Gulf/Chevron PDB-04 well on Northwestern Shelf of Delaware Basin, 30 km ENE of Carlsbad, Eddy Co., New Mexico.

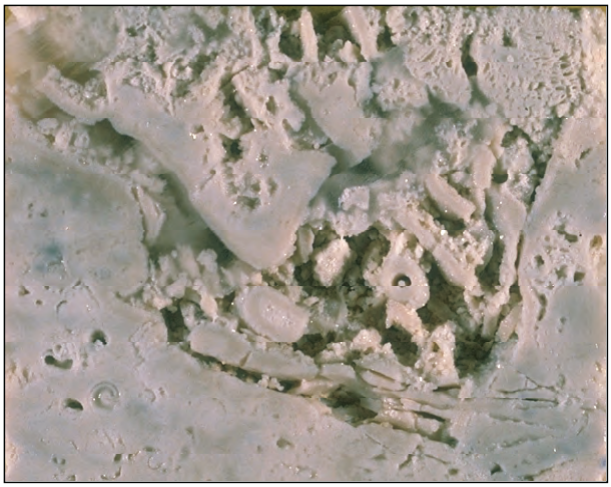

Figure 93. Core photograph of fractured reef-fore carbonate rock. Extensive open porosity probably resulted from dissolution of earlier anhydrite and gypsum cements that filled pores and fractures. Indeed, some fracturing may result from dissolutional removal of cements while the rock was under considerable overburden stress. Sample from 2,282 ft (696 m) depth in Gulf/Chevron PDB-04 well on Northwestern Shelf of Delaware Basin, 30 km ENE of Carlsbad, Eddy Co., New Mexico.

production has been obtained from comparable dolomitized slope facies in the Bone Spring Formation (e.g., Wiggins and Harris, 1985).

As we continue to climb the trail, there are few markers on which to hang a usable trail guide. In general, however, note the increasing size of debris, steepening dips, and lighter color of the debris. Furthermore, large clasts containing extensively encrusted reefal fabrics become more and more dominant upslope, at least until the upper 3rd of the slope. Most of the clasts represent allochthonous blocks of debris, ranging from gravel to house-sized. Indeed, some blocks may simply be too large to recognize — this makes picking the exact level of transition to truly in-situ lithified and encrusted reef fabrics virtually impossible. Reef growth, algal encrustation and inorganic (submarine) cementation extends into water depths of a hundred meters or more (several hundred feet) in many modern tropical reef areas, and similar patterns are to be expected in the Permian. Thus, although the zone of major faunal growth and diversity lay up-slope from the highest point we will ascend to, some in-situ growth of upper forereef organisms (especially bryozoans; Fig. 38), algal encrustations, and submarine cementation presumably extended down-slope at least into the upper part of the talus areas we are crossing.

Just before and just after the next major switchback (far up the trail, just below the sheer, triangular Capitan face), note the numerous beds of fusulinid grainstone (Fig. 94). These channelized debris flows were derived from the near-back-reef shelf detritus that probably bypassed the reef through tidal passes or channels (Harwood, 1989). The uppermost

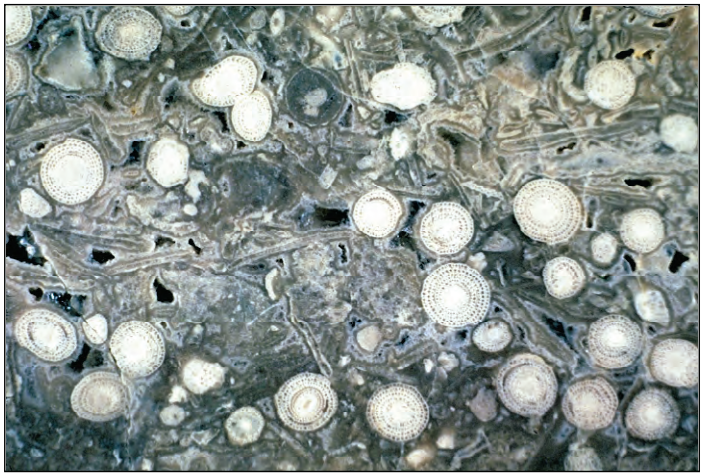

Figure 94. Polished slab of fusulinid (foraminiferal) grainstone on the upper part of the Capitan fore-reef slope on the north wall of McKittrick Canyon. These fusulinids (as well as the subsidiary green algae, intraclasts and other grains) were derived from shelf margin and near-back reef settings and were transported by grainflow and density current processes.

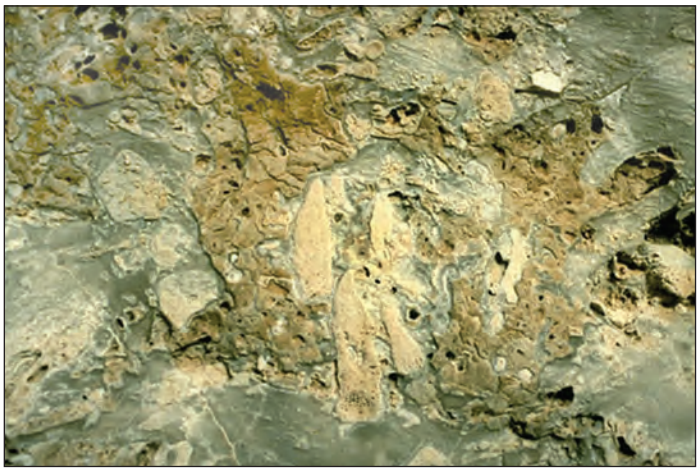

Figure 95. A rock surface showing a cluster of cryptic (cavity-dwelling) sponges. These sponges typically grew from the roof of cavities downward. The sponges in the center cluster are 3-4 cm long (Middle Permian, Guadalupian, Capitan Formation., McKittrick Canyon Reef trail). Photograph courtesy of Brenda Kirkland George.

part of the slope facies dips very steeply (more than 35° in places) and clearly contains more grainstones than beds in the mid-slope area. This may result from the fact that coarse, blocky rubble may simply not come to rest on such steep, smooth slopes. In modern environments, as in the Permian reef, the steepest slopes are either sediment free or sand-covered, whereas the coarser debris moves to mid-fan settings (e.g., James and Ginsburg, 1979).

Above the bedded Capitan talus lies a massive, nearly completely unbedded zone of the Capitan reef-massif, best seen directly above us (Fig. 81C). The massive character is a consequence of both the original skeletal framework with its sponge framework, encrusted (boundstone) fabric, and massive, penecontemporaneous cementation that completely pervaded the reef and obliterated most primary porosity. Some of these reef fabrics are seen on the last stretch of trail we will traverse — the zone just below (or the lower part of) the massive triangular face. This zone is still several hundred feet below the crest of the reef. We do get into rocks showing sponge-algal-cement boundstones, and these may represent spurs of reef that extended well down the steep fore-reef slope. Numerous examples of framework sponges can be seen as one climbs through this section, although some cryptic (cavity-dwelling) sponges (Fig. 95) also are visible here. The undeniable presence of such non-framework sponges has caused some workers (Wood et al., 1994, 1996; Wood, 1999 a and b) to question the importance of sponges as framework builders in the Permian reef complex, a conclusion that most other workers dispute.

As we climb this final long straight stretch of trail, we can look back to the south and southwest and get a better perspective on the true bedding relationships in the area. Unfortunately, the best perspective is from the south toward the face we are climbing, but even the panorama of the north wall of McKittrick Canyon can be useful. The bulk of the sediments that make up the lower 3/4 of the south wall of McKittrick Canyon (as well as the cliff we have climbed) consists of Capitan fore-reef debris. In many areas, particularly near the transition to the reef, the steep dip (nearly 30° after structural correction) of these rubble beds is apparent. The gradual flattening of those dips to the near-horizontality of the basinal Bell Canyon sediments is equally apparent as one traces individual beds basinward. Indeed, the uppermost basinal limestone (the Lamar) can be traced as a virtually continuous bed from basin to shelf as it rises more than 500 m (1,700 ft).

Although particularly well developed at its eastern end, the reef massif can be traced continuously toward the west. In this direction, the reef passes lower and lower in the section but continues to overlie thick, reef-talus deposits. Thus, from this vantage point we can see that the Capitan reef built upward nearly 300 m (1,000 ft) during the time in which it prograded out over its own debris; the debris, furthermore, filled in a basin of between 400 and 500 m (1,300 (1,600 ft) water depth.

The ratio of reef rubble to in-situ reef is extremely high, a fact noted by many workers. As pointed out by Dunham (1972), however, this is not a surprising situation. In modern reef-forming areas, the zone of significant reef growth is narrow, both laterally and vertically. The active growth zone is but a thin veneer on the upper and frontal edge of the reef platform. Much of this in-situ material is eventually broken up by storms and reworked down the fore-reef slope. New organisms grow in the reef crest area only to be reduced to rubble as well. Vast quantities of material are formed within the reef zone, but only a small fraction of this volume remains in that environment. Most is swept away into fore-reef or back-reef settings. Thus, the vast amounts of

rubble visible in the Capitan complex are not a valid piece of evidence to deny the existence of a true reef in this area. Rather, the rubble serves as evidence that the shelf edge was occupied by a faunally diverse assemblage of organisms with remarkably high rates of sediment production.

Above and to the west of the Capitan reef-massif, a wedge of flat lying, well bedded, back-reef sediments (Tansill and Yates Formations) can be seen (Fig. 81A). The wedge thickens to the west where older strata are exposed. The carbonate beds (mainly green algal-fusulinid grainstones) of the near-back-reef Tansill and Yates Formations can be seen to pass into and over the Capitan reef-massif and perhaps even to spill over onto the slope in front of the reef. This may be an indication that reef growth ceased before the end of carbonate sedimentation in the area. In that case, the final phase of shelf-edge deposition would have been marked by unconsolidated skeletal sand shoals rather than a barrier reef. The trail we are on extends through the reef and well up into the back-reef strata but, because of time constraints, we will stop near the fourth switchback. At this point you can see excellent reefal fabrics, plus considerable calcite-filled, solution-enlarged porosity, that may be indicative of a period of meteoric exposure of the reef (Given and Lohmann, 1986).

In summary, our 350 m (1,150 ft) climb has taken us through five distinctive facies: a toe-of-slope zone consisting of laminated, dark, thin-bedded limestones and interfingered sandstones; a lower slope zone consisting of medium-scale turbidites with matrix-rich debris flows; a mid-slope zone of coarse debris flows and slides with large blocks of reef debris; an upper slope zone of fossiliferous grainstones; and a transition to in-place reef.

We will now walk out on the large rock spur just east of the fourth trail switchback (a major turn that takes the trail behind, or north of, the triangular massive wall) to better see the regional setting. From this vantage point, one can see a superb vista to the north and northeast (Fig. 37). It shows present-day topography that nearly matches that of late Guadalupian time. Back-reef sediments mark the upland surface of the Northwestern Shelf; Capitan reef sediments, characterized by their vertical, strike-parallel jointing, delineate the upper margin or rim of the Delaware Basin; steeply dipping slope deposits compose the flanks of the escarpment; and flat-lying basinal deposits of the upper Bell Canyon Formation compose the floor of the present basin to the east-northeast (the Delaware Basin). The exhumation of this Permian topography is entirely a consequence of the evaporite filling of the remnant Delaware Basin in Ochoan time, and its subsequent dissolution during the Tertiary.

Note the “rollover” or “fall-in” of the bedded Tansill back reef deposits into or over the late Capitan shelf margin deposits (Fig. 37). This relationship has been used to argue for a slightly down-slope site for the main Capitan reef growth. It may, however, rather reflect down-to-the-basin syn- and post-depositional subsidence and/or faulting (see discussions in Saller, 1996, and Longley, 1999). In addition, the overtopping of the reef with bedded strata may indicate that rising salinities near the end of Capitan deposition (and prior to sedimentation of the Castile-Salado evaporites) terminated reef growth while still allowing formation of grainstone shoals at or near the shelf break.

If one turns from the northern view to the east and southeast, a series of cuesta scarps formed by the various limestone members of the Delaware Mountain Group are visible. These culminate in the major escarpment of the Delaware Mountains, capped by the Getaway Limestone.

We now descend the trail following the same route, will eat lunch in the parking lot by the McKittrick Canyon visitor center, and then will retrace our route back to U.S. Highway 62-180.

Turn right for El Paso or left for Carlsbad at mileage 113.8 on the El Paso-Carlsbad road log.

McKittrick Canyon road log ends.

A tarantula taking a close look at a partially silicified limestone in McKittrick Canyon.

WALNUT CANYON (CARLSBAD CAVERNS) GEOLOGIC ROAD LOG

Mileage	Cumul. Mileage	Location Description
0.0	0.0	Junction with U. S. Highway 62-180 and New Mexico Highway 7 in White's City, New Mexico at mileage 141.3 (reverse mileage 18.1) on El Paso-Carlsbad road log. Take NM Highway 7 toward Carlsbad Caverns.
0.5	0.5	**STOP I-2. Capitan reef to back-reef transition at mouth of Walnut Canyon.** Park vehicles on paved pull-off on the right side of the road in front of the Carlsbad Caverns National Park entrance sign. This stop is partly on National Park land and partly on private land. Collecting is not permitted within the National Park without a valid permit, and you should get permission to access the eastern part of the outcrop that is privately owned.

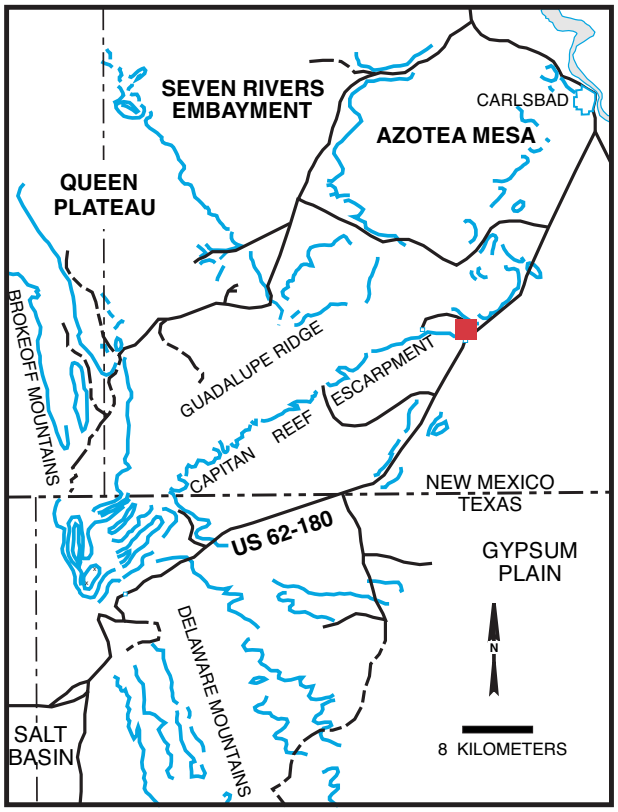

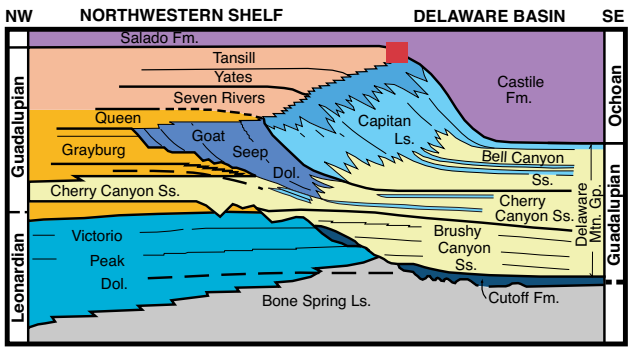

Cross (carefully!) on foot to south side of road, cross the dry channel of Walnut Creek and examine the spur of rock east of the National Park boundary fence. Then cross the spur and walk up the next draw to the south (Bat Cave Canyon or draw).

This locality, at the entrance to Walnut Canyon, provides excellent exposures of the reef and near-back-reef facies of the upper Capitan Limestone and Tansill and Yates Formations. In this area, the fore-reef facies and part of the reef have been buried beneath the thick Ochoan (and some thin Tertiary-Quaternary) filling of the Delaware Basin. The Castile Formation, although completely or partially removed in areas to the southwest, has been preserved in this area because of the northeastward tilting of this region. Thus, only a small exposure of the reef-crest and its transition to the near-back-reef are exposed. Because an outstanding guidebook is available for the entire Walnut Canyon route (Pray and Esteban, 1977), only brief descriptions will be given for these localities (this site corresponds to Locality guide I, stops I and II of Pray and Esteban, 1977).

We will examine the rock spur between Walnut and Bat Cave Canyons. We will pay particular attention to several fresh outcrops in Bat Cave Canyon, because these expose the reef fabric in an unweathered and more readily visible state. Babcock (1974a) noted a distinct faunal zonation within the reef (Fig. 33). He recognized an *Archaeolithoporella*-nodular boundstone, a phylloid algal boundstone and a *Tubiphytes*-sponge boundstone/packstone as well as some transitional zones (Figs. 96, 97). In all these facies, there are four salient elements: 1) an in-situ framework of oriented organisms; 2) encrusting and binding organisms that added stability to the framework; 3) internal sediment of skeletal fragments, pellets, or other grains that lodged in open pores in the framework; and 4) submarine cement crusts filling almost all remnant porosity.

The dominant framework organisms in this complex are the calcareous sponges (Figs. 32, 35, 98). Many different types existed here, including members of the genera *Guadalupia*,

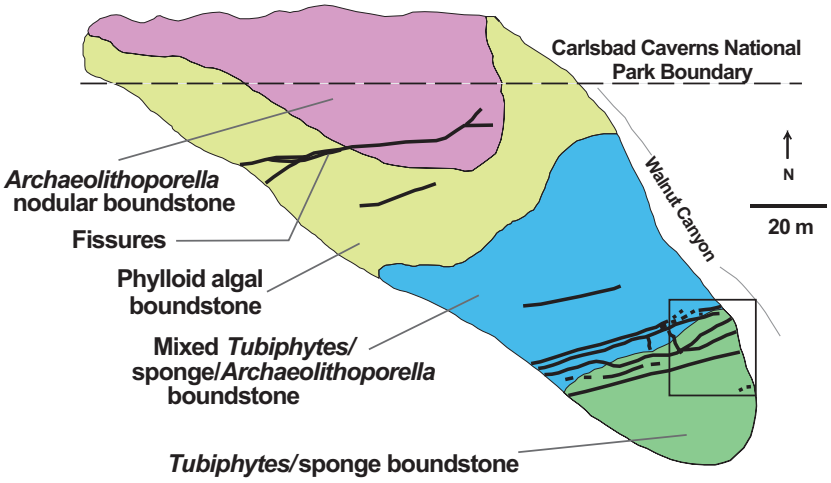

Figure 96. Map of microfacies distribution in the Capitan Limestone at the mouth of Walnut Canyon, Eddy Co., New Mexico. Rectangle shows area of detailed mapping (next figure). Adapted from J. Babcock (1974a).

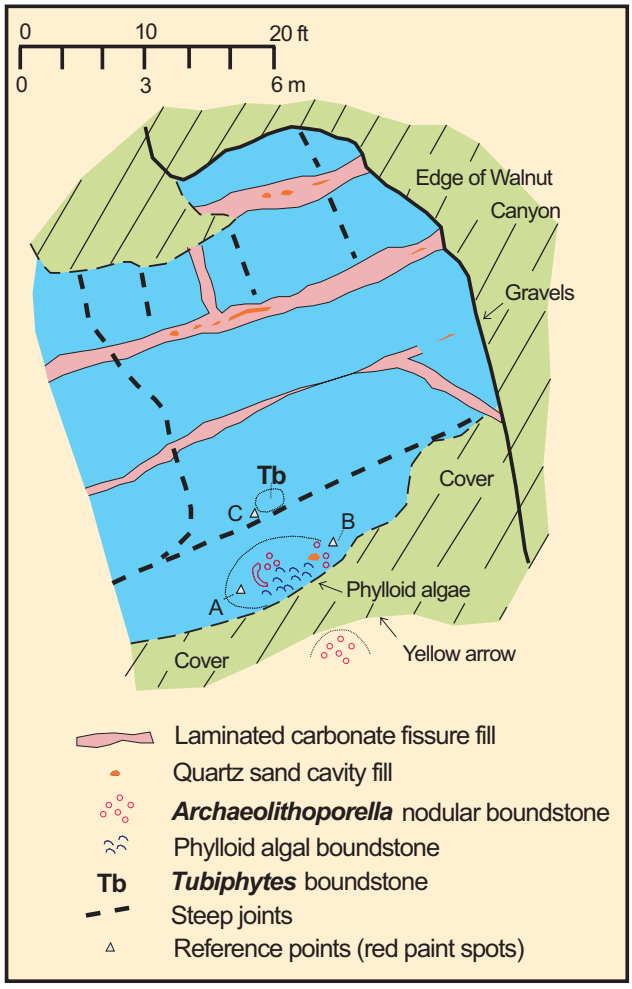

Figure 97. Detailed map of microfacies distribution in the Capitan Limestone at the mouth of Walnut Canyon, Eddy Co., New Mexico. Rectangle in previous figure shows area of detailed mapping relative to larger reef outcrop. Adapted from J. Babcock (1974a).

Amblysyphonella, *Cystaulete*, *Cystothalamia, Gigantospongia and Cystothalamia*. Some of the sponges grew as upright, solitary organisms; others branched; and still others were platy, with other species of sponges growing in shelter cavities, especially beneath platy sponges (Figs. 99, 100; Wood, 1999a, 1999b).

Other organisms such as *Tubiphytes* (Fig. 101), microbial crusts, phylloid algae (Fig. 102) and bryozoans (Fig. 99 bottom) can form significant framework elements. Solitary rugose corals are present locally, although they do not form a volumetrically important part of the reef framework.

Encrustation and stabilization of this skeletal framework was accomplished by *Archaeolithoporella* (a calcimicrobe), *Tubiphytes* (found as both framework and encrusting forms), *Solenopora* (a probable red alga), *Collenella* (a problematic algal form) and other, less common, organisms. Such encrustation, seen also in modern reefs, probably contributed greatly to the strengthening of the reef framework.

Internal sediment, although not a significant factor in the lithification of the reef, did play an important role in infilling and occluding the primary reef porosity. Internal sediments generally are found as massive to clotted (possibly microbial) fabrics, sometimes with interlayered submarine cements. The internal sediments commonly contain a diverse fauna including foraminifers, ostracods, echinoids,

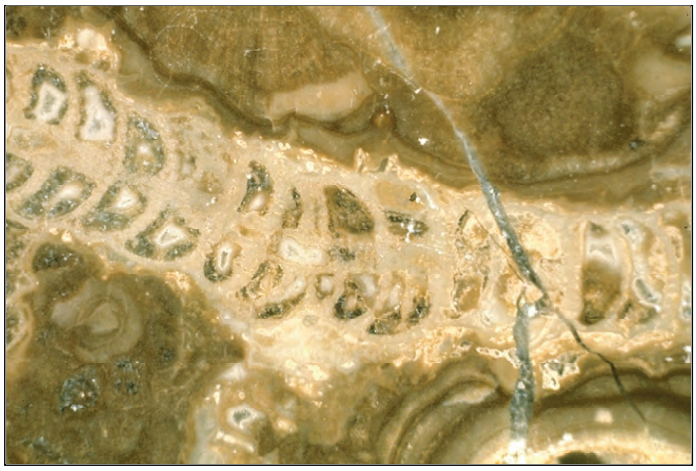

Figure 98. Polished slab of reef facies from the Capitan Formation showing a chambered calcareous sponge (center) as the main framework organism, encrusted by *Archaeolithoporella* (upper surface), *Tubiphytes* (lower right) and marine cements. Sample from Permian Reef Trail, McKittrick Canyon, Guadalupe Mountains National Park, Culberson Co., Texas. Long axis of photo = ca. 6 cm.

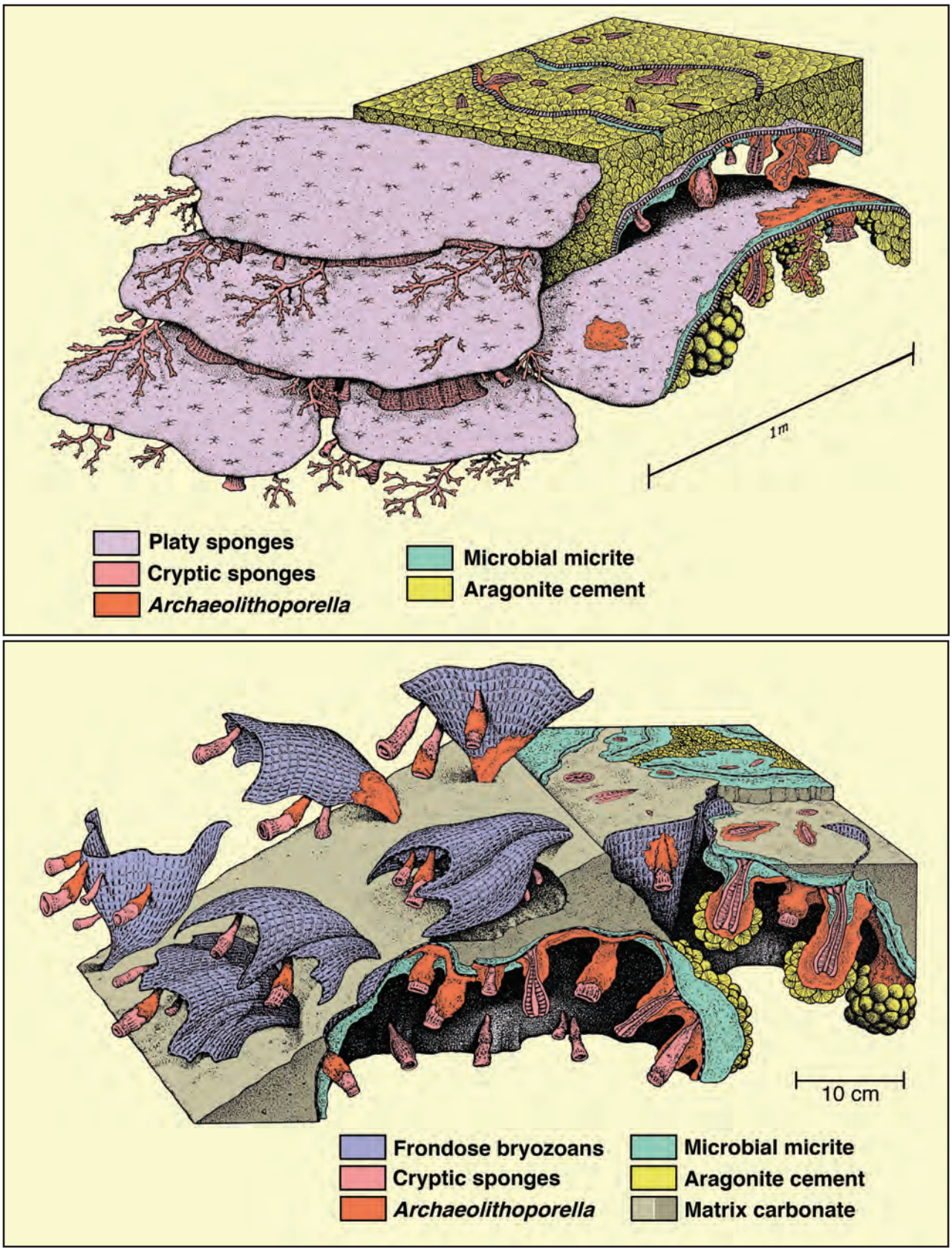

Figure 99. Reconstructions of the platy sponge community (top) and frondose bryozoan community (bottom) of the Capitan reef complex at Walnut Canyon and other localities. Note the abundance of cryptic (cavity-dwelling) fauna, microbial precipitates and synsedimentary marine cements. Modified from Wood (1999 a and b).

Figure 100. A platy sponge (black arrow) with smaller, finger-like, cryptic sponges (red arrow) growing downward into a shelter cavity beneath by the platy sponge.

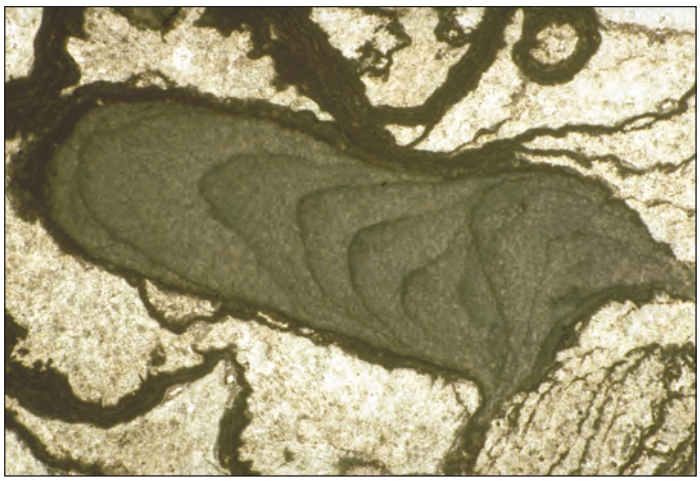

Figure 101. A photomicrograph (plane-polarized light) of a *Tubiphytes* encrustation (in oblique longitudinal section) —here associated with *Archaeolithoporella* and marine cement in a sponge-cement reef. *Tubiphytes* grew extensively on seafloor surfaces, but it may also have been a contributor to the cryptic reef communities, growing in dimly lit recesses and cavities. Photo long axis = 1.7 mm.

Figure 102. Phylloid algal-*Archaeolithoporella*-marine cement facies in Capitan reef. White, curved strips are oriented phylloid algae; white-gray patches are trapped micrite and darker encrustations consist mainly of *Archaeolithoporella* and marine cement.

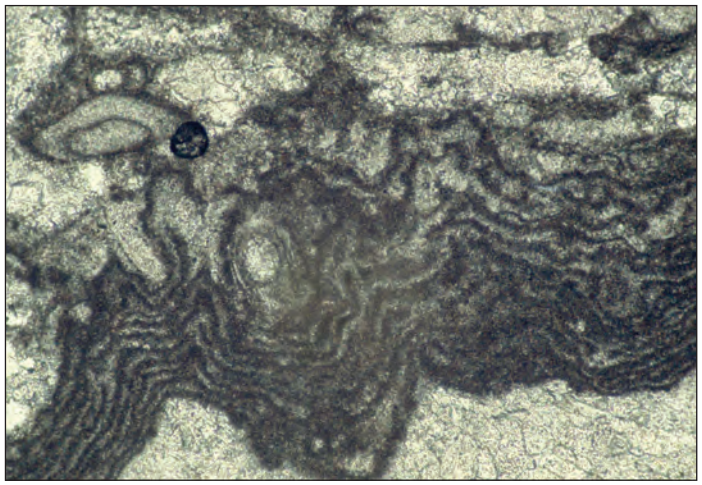

Figure 103. A photomicrograph (plane-polarized light) of *Archaeolithoporella*, a widespread, probably microbial encruster in the Permian reef. Sample from Capitan "massive" facies of Rattlesnake Canyon, Carlsbad Caverns National Park, Eddy Co., NM. Photo long axis = 1.7 mm.

pelecypods and other organisms that presumably lived within interstices in the reef framework. In areas dominated by phylloid algae, internal muddy sediment shows a strongly preferred fabric on the lee side of upright, curved algal blades (Fig. 102).

Submarine cements are a very important component of the Permian Reef. Coarse fans of radial-fibrous crystals fill much of the primary porosity in the reef and make up more than half the total volume of rock in many locations (as much as 70 percent in some areas; Mazzullo and Cys, 1977). The cement fans commonly are interlayered with *Archaeolithoporella* or other encrusting organisms (Figs. 103, 104, 105). The submarine cements are restricted to a relatively narrow zone that extends from one to two hundred meters (300-600 ft) down

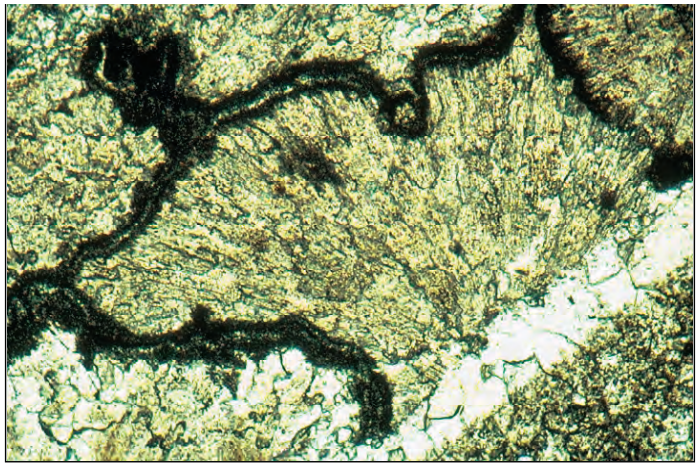

Figure 104. Thin-section photomicrograph (plane-polarized light) of marine cements in upper Capitan reef. Entire area represents an original void in the reef fabric; then filled with synsedimentary, fibrous to bladed, cloudy botryoids that were interlaminated with darker, micritic encrustations. Clear, blocky calcite filling of a later fracture can also be seen. Photo long axis = 3 mm.

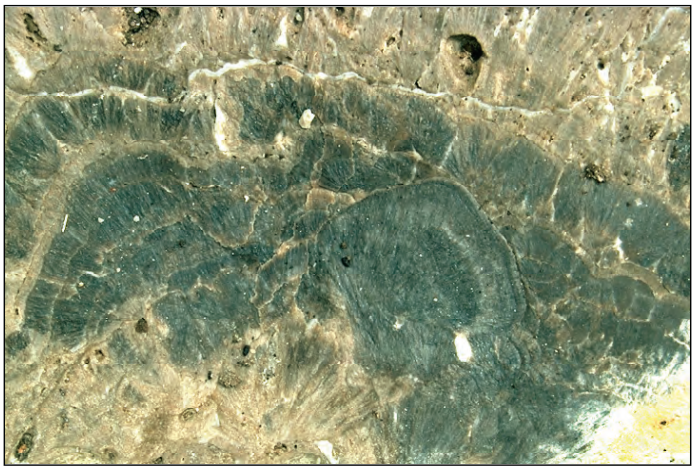

Figure 105. Acid-etched rock surface showing details of radial fibrous cement filling a large primary cavity in the upper Capitan reef framework. Originally, these cements were mainly aragonite with some high-Mg calcite and formed botryoidal crusts lining small as well as large pores. Virtually the entire field of view is marine cement that may form as much as 80 percent of the total rock volume.

the fore-reef slope to perhaps 0.8-1.5 km (0.5-1 mi) shelfward of the reef crest. Very similar relations have been seen in modern reefs such as in Belize, Florida and the Bahamas. In these areas, as in the Permian, submarine cementation, largely in the form of aragonitic and high-Mg calcite fans and crusts, is restricted to the reef face, upper fore-reef and near-back-reef zones (James and Ginsburg, 1979; Macintyre, 1977, 1985). Petrographic evidence has indicated the former existence of cements with both primary aragonite and high-Mg calcite fabrics although both have subsequently been altered to low-Mg calcite (Lohmann and Meyers, 1977; Loucks and Folk, 1976).

Submarine cements are seen filling synsedimentary fractures (Fig. 36) as well as large and small primary cavities in the reef (Fig. 105). The fractures are shelf-margin-parallel features that probably formed due to compaction of underlying reef rubble below a rigid slab of cemented reef. The fractures must have been contemporaneous with sedimentation since they are locally lined with sessile organisms. Extensive banded marine cements in the fractures, local silt infiltration into the fractures and dolomitization of fracture margins also support a synsedimentary to very early diagenetic origin of both the fractures and their fills. The down-to-the-basin movements of these faults probably play a significant role in the "rollover bedding" seen at the shelf edge in many areas and in allowing large-scale slumping of reef material onto the fore-reef slope (Saller, 1996; Hunt et al., 2002). Several such fractures are well exposed at this locality.

After seeing these major fabric elements where they are unweathered and well exposed in Bat Cave Canyon, we will cross the spur to Walnut Canyon. Examine the strata on this traverse and try to recognize the same reef fauna and cement fabrics where they are more intensely weathered. Also examine the fracture fillings along the margins of Walnut Canyon.

We will now walk up Walnut Canyon examining the transition from reef to near-back-reef areas, eventually crossing from the south to the north side of Walnut Canyon. On this traverse, be sure to note changes in bedding character as well as sediment composition. You should see reef rubble and/or patch reefs. Also note the remarkably rapidity of the lateral lithologic changes. The most obvious change is from a boundstone fabric to one of grainstones and packstones containing

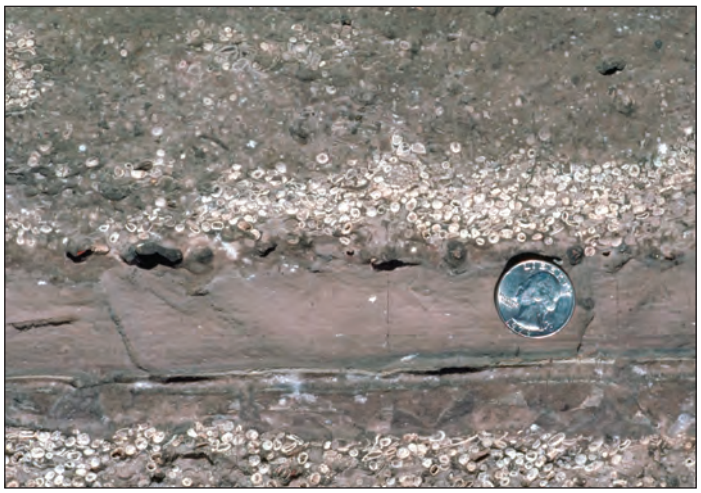

Figure 106. Oolitically coated fusulinid and algal grains in the near-back reef strata. Ooids are not common in the Capitan complex, but when they are found, they are most commonly in this setting associated with tidal channels and small islands or bars. Outcrop on northeast side of Walnut Canyon. The coin is 2.4 cm in diameter.

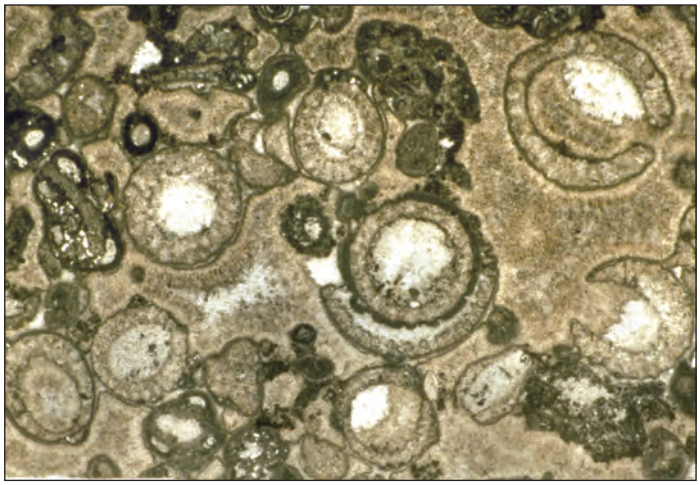

Figure 107. Thin section photomicrograph (plane-polarized light) of near-backreef grainstone containing dominantly coated green algal (*Mizzia*) grains. Note abundance of cloudy, bladed, probably originally aragonitic marine cement. Although hard to see without a microscope, synsedimentary marine cement is as widespread in this facies as it is in the reef. Photo long axis = 10 mm.

Figure 108. An erosional exposure surface between the underlying carbonate and one of the Triplet sandstones at the top of the Yates Formation (essentially the Yates-Tansill contact). Note the carbonate clasts in both the uppermost part of the lower carbonate unit and in the lower part of the sandstone. Outcrop on northeast side of Walnut Canyon.

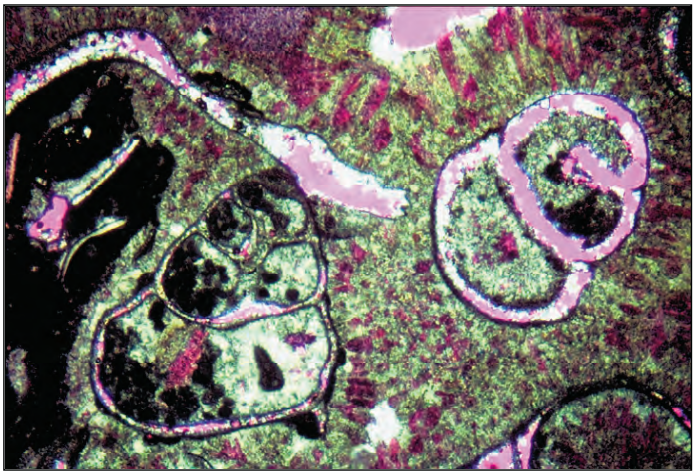

Figure 109. Thin-section photomicrograph (cross-polarized light with gypsum plate) of near-back-reef grainstone in the Tansill Formation. Predominant grains are gastropods that were encrusted penecontemporaneously with marine cement (cloudy, fibrous to bladed crusts). The sample subsequently was subjected to leaching of the aragonitic molluscan grains, presumably due to local meteoric exposure. Sample from south side of Walnut Canyon. Photo long axis = 6 mm.

ooids (Fig. 106) and skeletal grains. Cephalopods, foraminifers, pelecypods, gastropods and, most importantly, dasycladacean green algae, particularly *Mizzia* (Figs. 28, 107) and *Macroporella*, supplant sponges and bryozoans as the major skeletal components. Bedding in these well-sorted grainstones is massive and indistinct, but still is far better defined than in the reef facies. Grain size in these near-back reef deposits ranges from coarse silt to coarse sand; sorting is moderately good to excellent, and coated grains and ooids form a large percentage of the total sediment.

Strata farther up-canyon (farther back-reef) show increasing amounts of well-sorted, marine cemented, green algal grainstone (Fig. 107). Thin beds of coarser-grained, oolitically coated materials also occur (Fig. 106). Yet other beds, especially farther up-section or up-canyon, have substantial dolomite, fenestral fabrics, pisolitic grains, blue-green algal/microbial lamination, carbonate breccias, "tepee structures" and thin, clastic terrigenous sandstone-siltstone units with large carbonate rip-up clasts that mark the Tansill-Yates contact (Fig. 108). These strata also are characterized by repeated, stacked, small-scale cycles marking shifts from shallow marine to subaerial conditions (see Rush, 2001).

The abrupt lateral and vertical facies transitions from reef to back-reef are similar to those seen in many modern settings. In the Florida reef tract and on the western side of Andros Island in the Bahamas, for example, the change from reefal boundstones to skeletal, back-reef grainstones takes place over distances of just a few tens to hundreds of meters. The near-back-reef areas in Florida and the Bahamas generally consist of complex, small-scale microfacies of green-algal (*Halimeda*) grainstones, grapestones (coated and coalesced grains), ooids, skeletal fragments and other lithologies. In areas such as the Joulter's Cay region of the Bahamas, one can see these grainstone types closely intermingled as a series of submarine sand waves, islands, tidal channels and beaches. Associated with these grainstones are mudstone-wackestone microfacies in sheltered areas behind tidal flats and islands. The extremely varied lithologies in the Permian near-back-reef setting presumably reflect similarly complex microfacies patterns.

This is also evident in the intimate mixture of diagenetic patterns in the Permian near-back-reef sediments. Submarine as well as vadose and phreatic nonmarine cements (Figs. 28, 109) are all present in local zones in this area, probably as a result of local (island facies) recharge of nonmarine fluids. Selective leaching of originally aragonitic skeletal fragments, probably in a subaerial setting, led to development of substantial, if localized, secondary porosity (Fig. 109).

A major question in recent years has concerned the nature of the reef margin. Did the reef occupy a position as a topographic high point along the shelf margin or did it form in a slightly deeper water setting on the upper slope (with the ooid-*Mizzia* grainstones as the shelf edge "high"). Your observations on this traverse should focus, at least in part, on resolving this question.

Return to vehicle(s) and proceed up-canyon.

0.2	0.7	Near-back-reef *Mizzia*-dominated grainstones on right, which we have examined in our previous traverse.
0.2	0.9	Cross wash in Walnut Canyon.
0.2	1.1	Pisolite-bearing dolomites and faulted upper Yates sandstones in roadcut.
0.1	1.2	Upper Yates and lower Tansill sediments in canyon walls. This locality exposes mainly pisolitic dolomites and sandstones and is an excellent area of examining tepee structures.
1.0	2.2	Exhibit area on right.
0.3	2.5	Yates Formation dolomite and sandstone exposed in roadcuts on right.
1.0	3.5	Parking area on left with exposures of pisolitic dolomites, tepee structures and sandstones of Yates Formation.
0.5	4.0	Exhibit area (showing botanical diversity of the area) on the left. Canyon wall on left has exposures of Yates Formation, including the large, sand-filled cavern described by Dunham (1972, Stop II-5).
1.25	5.25	Sharp bend in road; entrance to primitive road on right can be used as parking area to view exposures of Yates Formation just ahead (but be sure not to block access as this is the exit for a back-reef scenic loop drive).

0.05 5.3 **STOP I-4. Hairpin Turn pisolite locality.**

Please remember that you are in the National Park and that collecting is not permitted.

Outstanding exposures of pisolitic dolomites of the upper Yates Formation (see Pray and Esteban, 1977; Dunham, 1972; Esteban and Pray, 1977). This locality illustrates numerous cycles of pisolitic, tepee-bearing sediments (termed "Walnutite cycles" by Pray and Esteban, 1977; Fig. 110). Tepee structures are visible in this outcrop and in the distant canyon wall to the north (Fig. 25). The main small-scale features to be seen at this outcrop are the abundant pisoliths that range from B-B-size to golf ball-size. They have concentric laminations of thin carbonate coatings around nuclei of fractured pisoliths or, rarely, marine fossils (Fig. 111). The pisoliths, which have been completely replaced by aphanocrystalline dolomite, occur in cyclic beds, commonly with reverse grading (Fig. 112). In some (but not most) cases, pisoliths have intergrown or interlocking textures (Figs. 24, 26).

There is considerable evidence to show that these pisoliths had original aragonite composition, now replaced by dolomite (Fig. 113). They are associated with sheet cracks —broad bands of displacive, fibrous carbonate, presumably also originally aragonite (Loucks and Folk, 1976) but now dolomite or calcite (Fig. 26). These displacive crusts are most likely closely related to the origin of the tepee structures of this area. The tepees clearly are expansion polygons formed by a volume increase of the associated sediments. This was most likely accomplished by in-situ, near surface, displacive growth of aragonite crusts and (or) evaporite minerals.

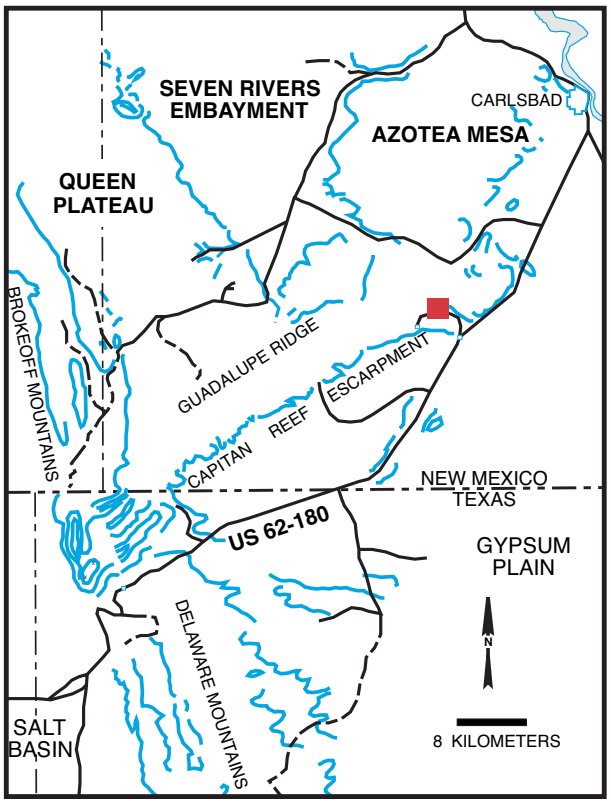

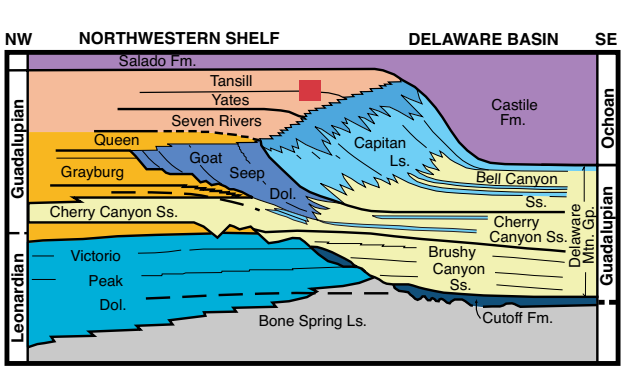

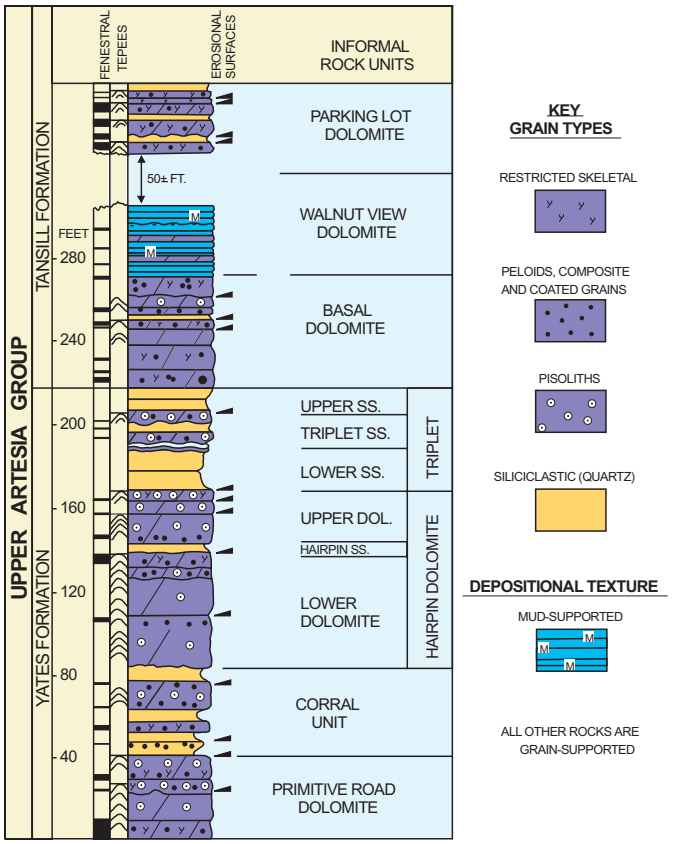

Figure 110. Stratigraphic section of the uppermost Yates Formation at the Hairpin Bend pisolite locality in Walnut Canyon, Carlsbad Caverns National Park, Eddy Co., New Mexico (modified from Pray and Esteban, 1977).

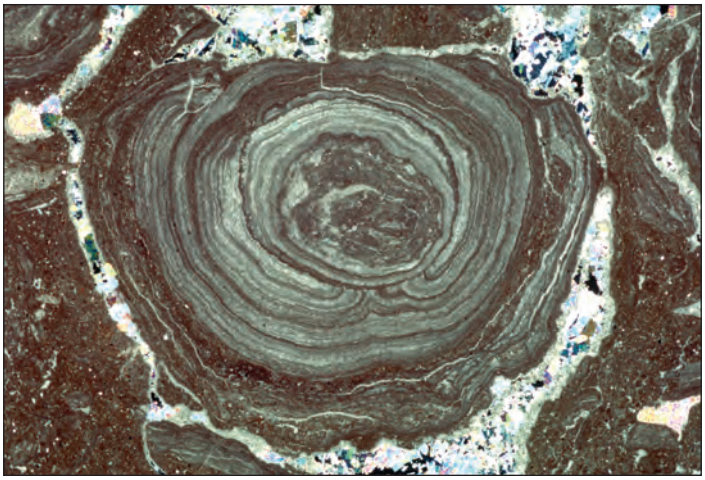

Figure 111. Thin-section photomicrograph (cross-polarized light) of a pisoid from the Yates Formation. Note irregular, lumpy, partially concentric coatings; fracturing ("autobrecciation") of micritic-peloidal matrix; and evaporite plugging of remnant intergranular porosity. Sample is from 1,708 ft (521 m) depth in the Gulf/Chevron PDB-04 well on Northwestern Shelf of Delaware basin, 30 km ENE of Carlsbad, Eddy Co., NM. Photo long axis = 14.5 mm.

Figure 112. Typical lenticular deposit of pisolitic dolomite from the uppermost Yates Formation. Note reverse grading of coated grains. Pisoids have been attributed to algal growth, caliche formation, marine spray-zone precipitation and seepage-spring development. Coin is 2.4 cm in diameter.

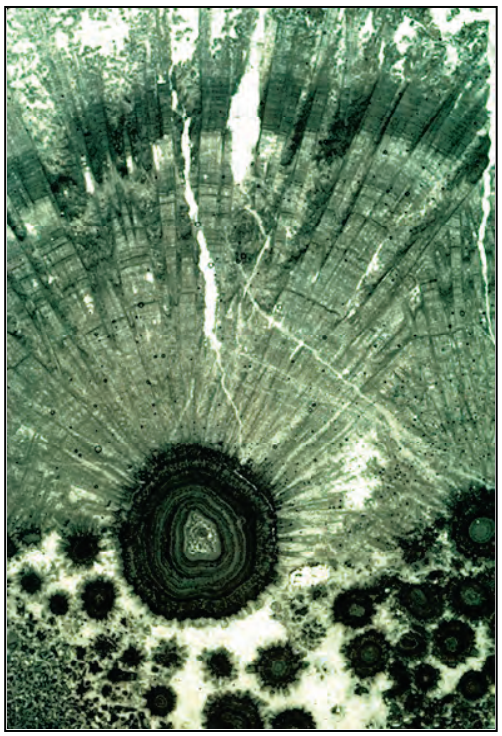

Figure 113. Thin-section photomicrograph (plane-polarized light) of a marine-cemented pisolitic dolomite showing transition from pisoid to botryoidal cement crust. The elongate rays of cement that extend from upper surface of pisoid show squared crystal terminations, evidence of an originally aragonitic composition for the cement (Loucks and Folk, 1976). Sample from 1739.3 ft (530 m) depth in the Gulf/Chevron PDB-04 well on Northwestern Shelf of Delaware Basin, Eddy Co., NM. Photo long axis = 16 mm.

The origin of pisoliths and tepee structures in these sediments has been the subject of numerous studies and considerable controversy. Basically there are three hypotheses: 1) the "all wet" model, that proposes that the pisoliths were formed by organic (algal) or inorganic coating of grains in a shallow-water shelf setting with each grain acting as a free, clastic particle (Esteban and Pray, 1977; Pray and Esteban, 1977); 2) the "caliche" hypothesis, that suggests that pisoliths formed in-situ as part of cyclic, reverse-graded, caliche profiles produced by alteration of carbonate sediment brought into the area by storms or other episodic processes (Dunham, 1972); and 3) the salina "seepage" model, that proposes that ocean water seepage through permeable barriers into sub-sealevel salinas can produce tepees and pisoliths by evaporation and precipitation (Handford et al., 1984; see Fig. 27). Advocates of any of these models can point to modern analogs (mainly from Persian Gulf, Red Sea or Australian areas) with scattered, small-scale accumulations of aragonitic pisoliths in marginal marine, hypersaline settings. Yet nowhere have we discovered an analog that comes close to modeling the abundance of pisoliths that one sees in the Permian.

The differences of interpretation of these deposits, although important to fully understand the rocks, are not of great significance to the explorationist. There can be little argument that this facies must have been close to a paleotopographic high-point in Guadalupian time. The persistence of this facies in space and time (it is present in Grayburg, Queen, Seven Rivers, Yates and Tansill strata), its consistent geometry (an elongate facies, parallel to the reef trend) and its equally consistent juxtaposition between open marine (grainstones with a high faunal diversity) and restricted (hypersaline mudstones and evaporites) environments indicate that the pisolite facies must either itself have been a major hydrographic barrier or it must have formed just landward of such a barrier. Nowhere in the world today are evaporitic mudstones and open marine, faunally diverse sediments in such close proximity without having an intervening barrier. It seems likely that to act as such a barrier, at least a narrow strip of land would have had to be subaerially exposed (except for tidal channels). This scenario would favor either the caliche or salina seep interpretations. Further support for the salina model may come from isopach studies of the thin sandstone/siltstone beds that are interspersed with the tepee-pisolith beds. Candelaria (1989) showed that these beds did not thin over the pisolite facies but did thin rapidly over the marine grainstones that lay just seaward of the pisolite facies. Although such a relationship may be due to reworking of shelf-margin sands by transgressive seas, it may also indicate depositional thinning over a topographic high in that area.

In summary, it seems most likely that the facies just seaward of the pisolites consisted of an elongate, irregular ridge of low-relief islands, tidal flats and dunes (Fig. 18) that allowed marine water seepage into the back barrier lagoon. Such seepage zones saw massive precipitation of aragonite cements and formation of pisoliths (comparable to that seen in modern Lake McLeod and Yorke Peninsula examples; Handford et al., 1984; Lock and Burne, 1986; Logan, 1987).

Figure 114. Map of Carlsbad Caverns showing the walking trail route. Adapted from Hill (1993).

Finally, it is possible that a combination of processes could have been involved in the formation of pisoliths. A number of different types of pisoliths can be seen in the Permian strata. These range from the small, irregularly coated grains seen at Stop III-2 (and which almost certainly formed in a marine setting) to the larger, smoother, and more extensively encrusted grains present at this locality. Thus, a number of different origins can be envisioned for the various pisolith types.

The tepee structures and sheet cracks found in association with pisolitic sediments can also be interpreted as either marine or nonmarine. Displacive aragonite crusts and tepees have been noted in submarine cemented areas within the Persian Gulf itself as well as in coastal caliches and sabkha surfaces of the surrounding, subaerially-exposed coastlines (Kendall, 1969; Shinn, 1969; Warren, 1983).

0.3 5.6 Exhibit area on left; the thin sandstone-siltstone unit that marks the Tansill-Yates contact is exposed on the left. The road ascends into Tansill Formation dolomites.

1.9 7.5 **STOP I-3. Carlsbad Caverns entrance parking lot.**

Please remember that you are in the National Park and sample collecting is not permitted.

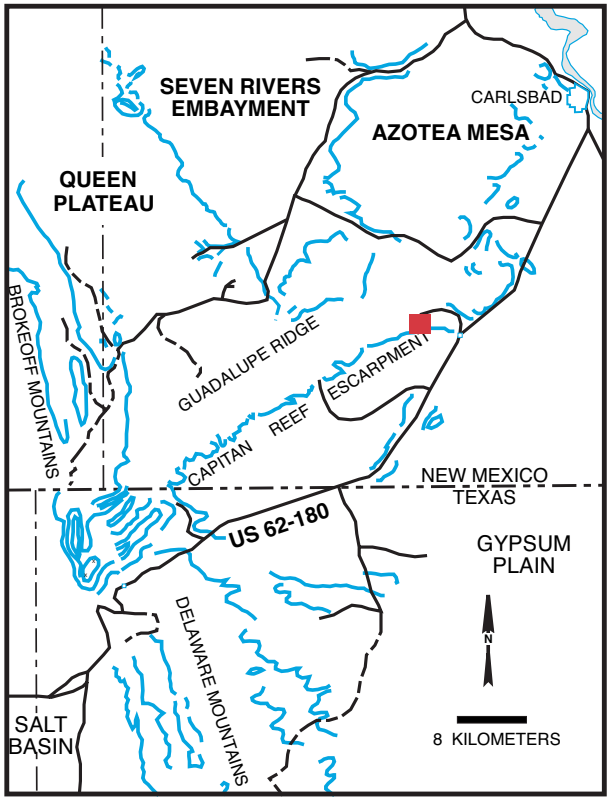

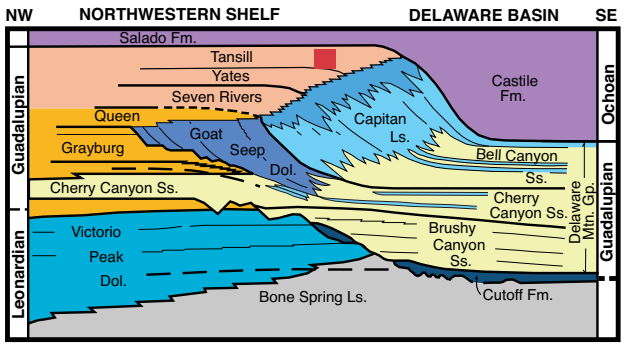

Cave entrance parking lot. We will do the complete walking tour of Carlsbad Caverns (Fig. 114) — the Roswell Geological Society 1964 field trip guidebook provides a trail log of the caverns (Sanchez, 1964) as does the 2006 New Mexico Geological Society Cave and Karst volume (Land et al., 2006). This cave is the largest (but by no means the longest) cavern system in the world and has spectacular speleothems (Fig. 115). The cave is developed primarily in the fractured reef and forereef Capitan Limestone, but the entrance (Fig. 116) and all of the upper level are in the back-reef dolomites of the Tansill and Yates Formations. The lowest parts of the cave extend down to a level approximately 260 m (850 ft) below the entrance. These deep parts of the cave are cut in the lower part of the reef as well as steeply-dipping fore-reef talus of the Capitan Formation. You should be able to see this fore-reef bedding on your circuit of the Big Room near the "Bottomless Pit" (or look back down the trail when you see the sign for "Bat Guano"). This deep level of dissolution is presumably related to the regional groundwater discharge surface in the Pecos valley to the northeast.

The history of cave development is extensively described by Jagnow (1979), Hill (1987, 1990, 1993), DuChene and McLean (1989), and Land et al. (2006). The location and orientation of the Capitan reef and its early fracture system have controlled, to a large degree, the geometry of the local cave systems. Pliocene-Pleistocene and earlier uplift allowed percolation of phreatic groundwater through the joint system and eventual excavation of the caverns. H_2S, from bacterial reduction of Permian sulfates in the presence of hydrocarbons rising from nearby oil fields, is common in groundwaters of the area and may also have played an important role in cave formation. The hydrocarbon leakage likely led to formation of sulfuric acid, which may have dissolved many of the caves in this region (Hill, 1987, 1990). Such speleogenesis, associated with rising rather than descending fluids, may have important

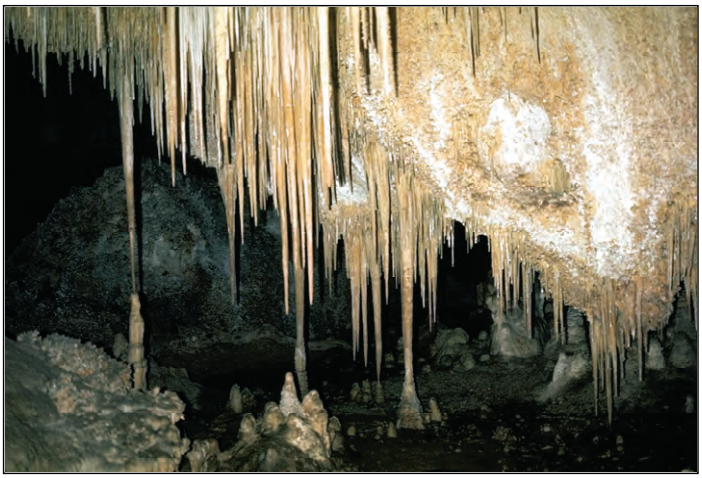

Figure 115. Carlsbad Caverns drapery with small stalactites and stalagmites.

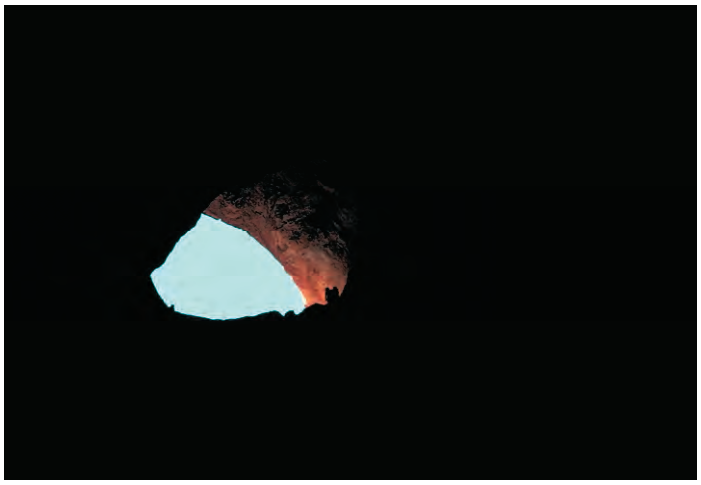

Figure 116. Carlsbad Caverns entrance looking out. Now that's porosity!

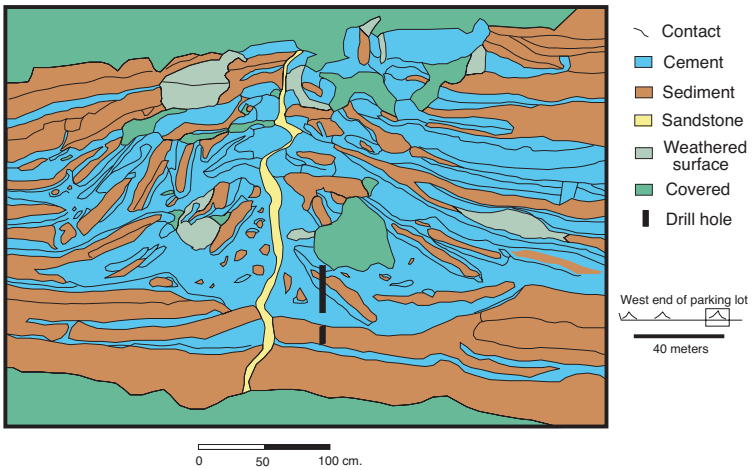

Figure 117. A diagrammatic representation of the tepee structure in Tansill Formation at the parking lot of Carlsbad Caverns.

implications for the origin of subsurface karstic oil resevoirs, such as the Yates field (K. Stafford, pers. comm., 2007).

The later-stage history of the cave involved the introduction (and later partial removal) of clay, silt, sand, and gypsum fills as well as calcitic (and even dolomitic) speleothems. Convective air circulation (Queen, 1981; Hill, 1987) may be responsible for much of the irregular distribution of precipitated calcite "popcorn" on the walls and formations of the cave (such as the Lion's Tail). With the exception of air circulation, the cave is largely inactive today except for some areas in the lowest cave levels.

The outcrops at the southwest end of the parking lot provide excellent exposures of tepee structures, sheet cracks, and pisolitic sediments of the Tansill Formation that we will visit if time permits. Use the description from Stop I-4 and the tepee diagram (Fig. 117) to guide your observations.

Return down Walnut Canyon.

DARK CANYON-SITTING BULL FALLS-ROCKY ARROYO GEOLOGIC ROAD LOG

Cumul. Mileage	Clockwise Loop Mileage	Counter-clockwise Loop Mileage	Location Description
0.0	0.0	80.1	Head west on paved road to Dark Canyon off US 62-180 at mileage 151.3 (reverse mileage 8.1) on El Paso-Carlsbad road log. (Alternatively, you can take a shortcut by heading west and southwest on a road that takes off on the right, just before Happy's Restaurant on the south side of Carlsbad.
0.4	0.4	79.7	The Hanson and Yates, King No. 1 well on the right is the entire Dark Canyon oil field. Numerous offset wells were dry holes. Many additional wells in this area are producing largely from Pennsylvanian reservoirs.
0.8	1.2	78.9	Rustler Formation dolomite, sandstone and gypsum make up the low Frontier Hills ahead.
1.5	2.7	77.4	Rustler Formation outcrops in hills on both sides of road.
1.2	3.9	76.2	Mouth of Dark Canyon. We have left the Delaware Basin and are now on the Northwest Shelf in the northeastern part of the Guadalupe Mountains. Bedded limestone outcrops representing the transition zone from Capitan reef to Tansill near-backreef facies are present on both sides of the canyon.
0.15	4.05	76.05	Road intersection; take sharp right.
0.2	4.25	75.85	**STOP III-1. Capitan reef to back-reef facies at north side of mouth of Dark Canyon.**

We will examine the reef to near-back-reef transition in the uppermost part of the Capitan and lower Tansill Formations. These strata have been mapped as reefal Capitan limestones by Motts (1962a) and as back-reef limestones of the Tansill Formation by Kelley (1971). Tyrrell (1969) and Toomey and Cys (1977) presented extensive evidence to show that this locality provides an exposure of the transition beds between the Capitan and Tansill carbonates. The major part of the reef front is buried beneath basinal sediments in this area (Fig. 118), but some reefal or patch reef deposits are still visible. You should be able to see a wide variety of fossils, or you could before the outcrop was vandalized by crazed geologists (with portable rock saws) who were dedicated to collecting the best fossil specimens. Among the fossils still present are calcareous sponges, *Archaeolithoporella* (an algal-microbial encruster), *Tubiphyte*s shrubs and encrustations, *Collenella* (stromatoporoid?) mounds or clusters, and crinoids (many still with intact stems and/or calyxes). Marine cements and marine-cemented fractures are very prominent in the reef zone and extend well back into shelf facies where they are harder to recognize in hand sample.

More shelfal or intermound deposits are also exposed, and you should be able to see near-back-reef skeletal grainstones containing ooids and algally coated grains, dasycladacean green algae (particularly *Mizzia* and *Macroporella*), articulate crinoids (including stems, holdfasts, calyxes and cirri; Fig. 119), calcitic bellerophontid gastropods (Fig. 120), aragonitic (moldic) gastropods and pelecypods, fusulinid Foraminifera, localized *Tubiphytes-Archaeolithoporella* colonies and sponges (see generalized microfacies reconstruction in Fig. 121). These rocks are similar in many ways to the sediments seen at the up-canyon end of the first stop in Walnut Canyon (Stop I-2). That would indicate that we are probably at, or only a short distance

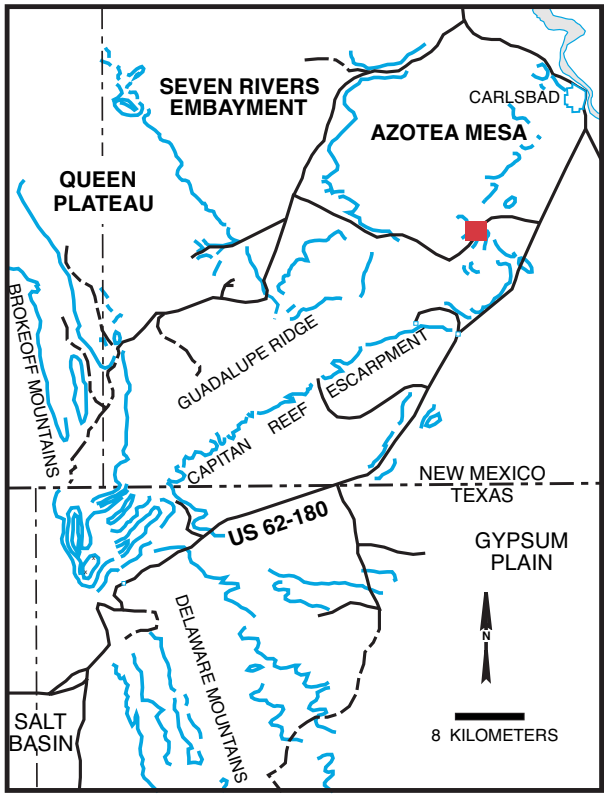

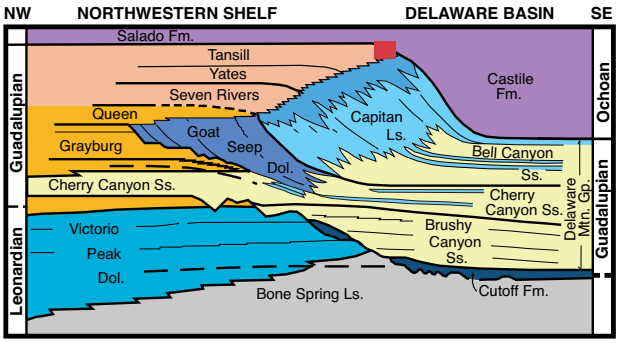

Index map for Stop III-1

shelfward of the main reef facies. Note the consistent change in bedding character as we walk either in a shelfward direction or up-section.

The abruptness of the facies transition seen here and in Walnut Canyon in the near-back-reef setting is very similar to modern facies transitions in areas such as Florida or the Bahamas. There, as here, reefal debris tends to move primarily into fore-reef talus; back-reef sands are dominated by green algal grains (*Halimeda* in modern sediments; *Mizzia* in the Permian), ooids or coated grains, and other particles of shelf origin. Submarine shoals, channels, islands and patch reefs have localized distribution and complex geometries. Such modern settings appear to be excellent analogs for these older environments.

We will not be able to stay within the Tansill Formation in our entire traverse through the Capitan-equivalent shelf strata because erosion has removed much of the far-back-reef Tansill (Fig. 118). We will see those farther-back-reef facies in older (but still Capitan-equivalent) strata of the Yates and Seven Rivers Formations. Evidence from remaining outcrops and subsurface data indicates that similar shelfward facies transitions occurred in all three back-reef units (Fig. 122). The general sequence of facies from the shelf-edge landward (Fig. 18) tends to be reef; massive skeletal (mainly green algal) grainstones; bedded and cross-bedded oolitic grainstones; dolomitized, fenestral grainstones and pisolitic mudstones; coarse, pisolitic, dolomitized grainstones with tepee structures; stromatolitic or peloidal dolomitized mudstones; pure, calcisphere-bearing, dolomitic mudstones with evaporite crystal casts and (or) collapse breccias; nodular gypsum or anhydrite units; and finally red siltstones.

Throughout this facies suite, thin but laterally persistent, fine-grained sandstone and siltstone beds are found. These sandstone-siltstone units, especially common in the Yates and Seven Rivers Formations, generally pinch out before reaching the reef facies (Candellaria, 1989); in several areas, these sandstones extend to within a few hundred meters of the reef. In the Yates (and the older Queen) strata, these terrigenous beds make up at least 1/3 of the formation thickness, are excellent regional correlation markers and can act as reservoir units.

Because there was extensive (3-5 km; 2-3 mi) basinward progradation of facies during the Capitan deposition, the facies previously described as being lateral equivalents can also be seen to some degree in vertical sequence, a fact which has significant influence on the early diagenetic history of much of the sediment package. The progressive basinward shift of the evaporite-carbonate transition zones in successively younger, Capitan-equivalent, back-reef units is clear from the diagram shown earlier (Fig. 122). Thus, the progradation of subaerial or restricted environments over more normal marine sections allowed very early input of meteoric fluids as well as meso- or hypersaline brines into unconsolidated and geochemically unstable sediments. Indeed, sediments from the shelfward edge of this outcrop to the platform interior show extensive signs of vadose as well as phreatic leaching and cementation combined with virtually complete, very finely crystalline dolomite replacement.

The approximate thickness of back reef units of the Artesia Group in this region are (in ascending order): Grayburg Formation, 120-150 m (400-500 ft); Queen For-

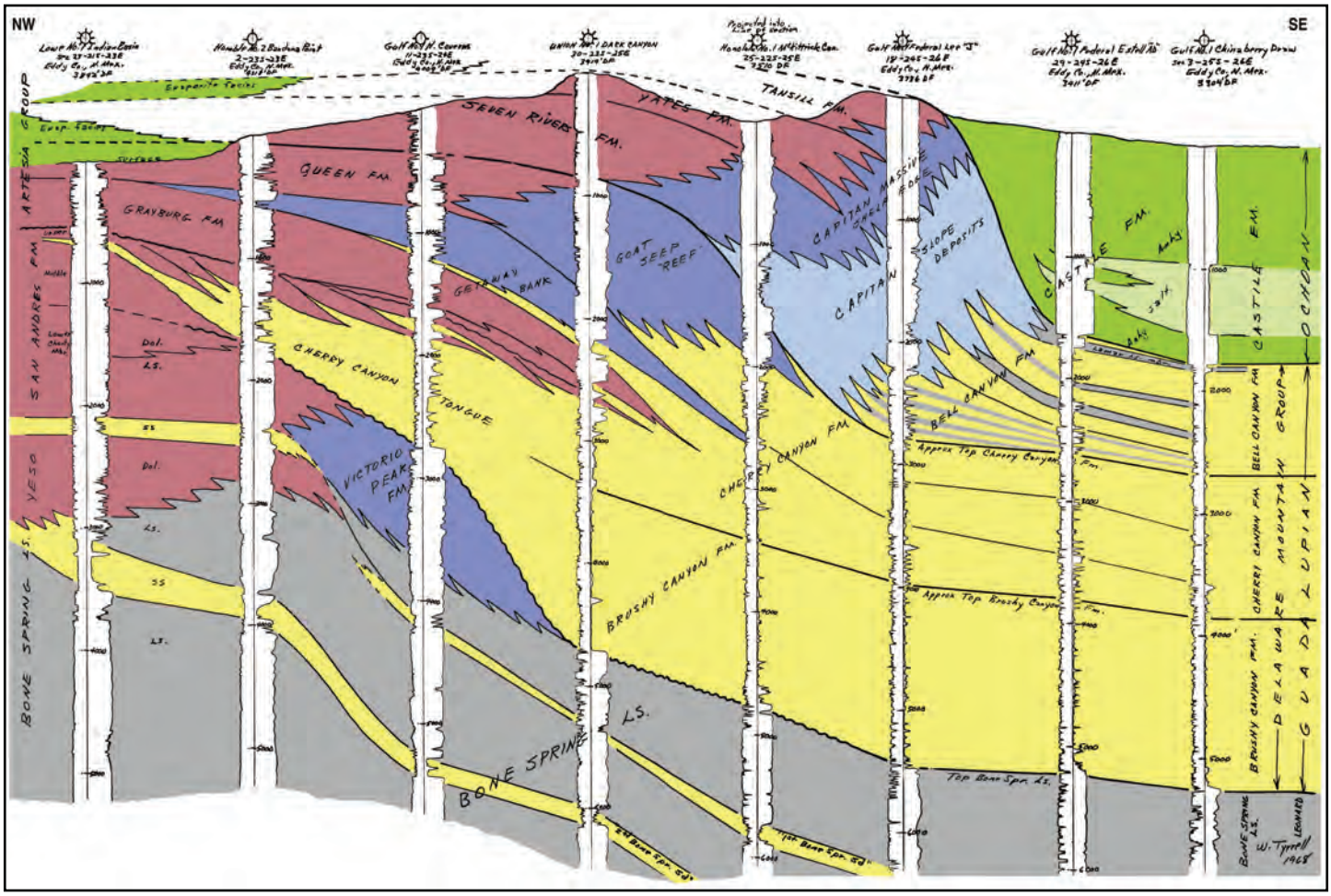

Figure 118. Interpreted well log-based NW-SE cross section of the Dark Canyon area. Note Ochoan evaporite fill lapping onto reef and stratigraphic downstepping of backreef outcrops to the NW. Courtesy of Willis Tyrrell (ca. 1980).

Figure 119. Articulate crinoid stem and calyx set in a marine-cemented grainstone from the very near-back-reef Capitan-Tansill Formation transition. Presence of such intact fossils indicates at least local pockets of low energy and/or high rates of marine cementation of sediment. The coin at top is 1.9 cm in diameter

Figure 120. Grainstone deposit from the very near-back-reef part of the Tansill Formation. Coated grains, green algae, fusulinids, molluscan fragments and other grains are present. Note also the large bellerophont gastropods that that were common sediment grazers in this environment. Outcrop on north side of mouth of Dark Canyon. The coin is 1.8 cm in diameter.

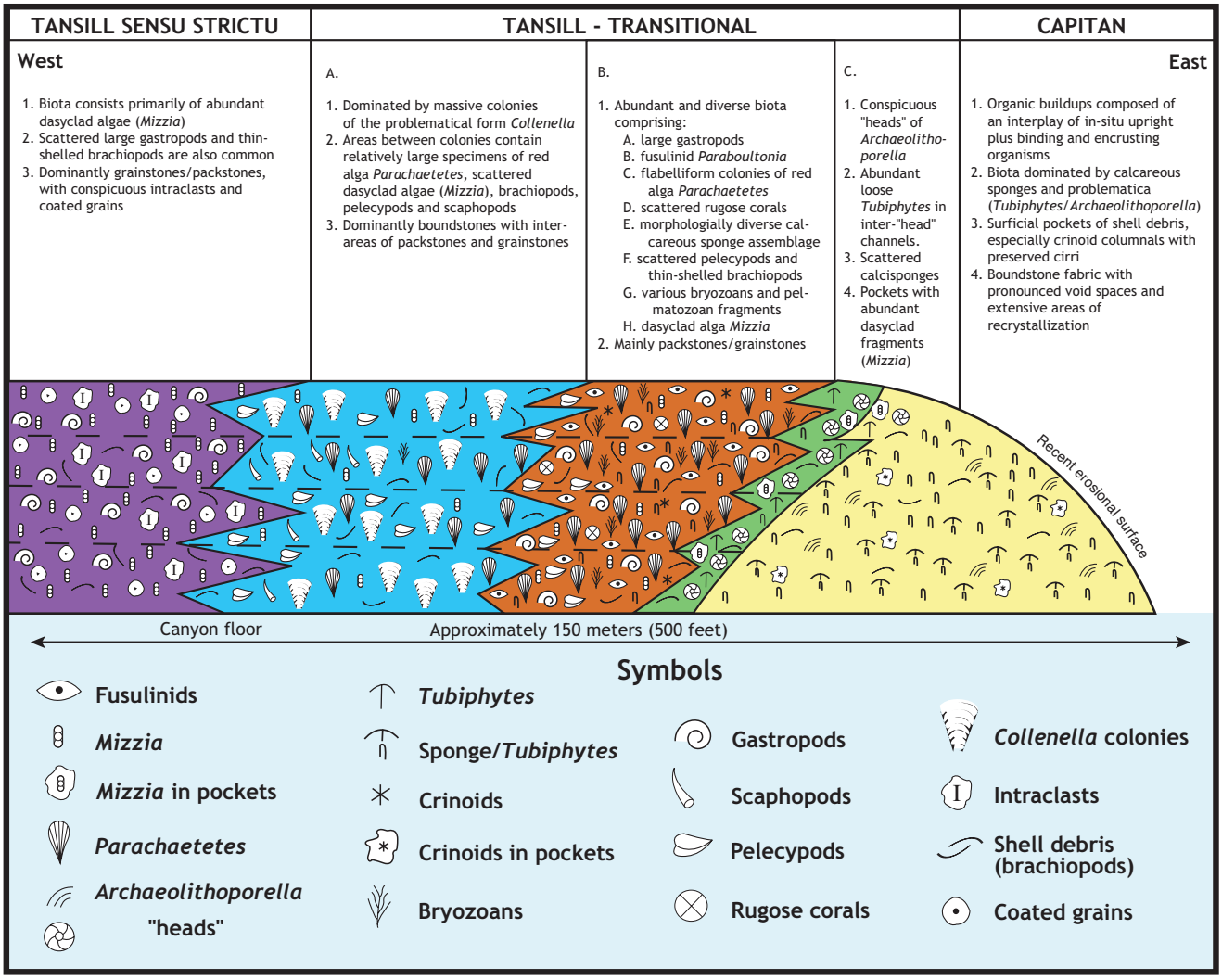

Figure 121. Diagrammatic representation of microfacies exposed at the mouth of Dark Canyon. Adapted from Toomey and Cys (1977).

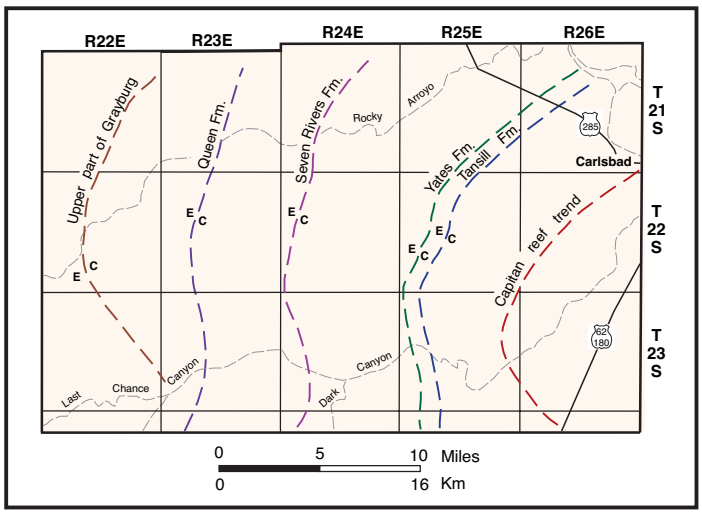

Figure 122. Map showing the approximate geographic position of the back-reef evaporite (E) to carbonate (C) transition in various Guadalupian shelf units in the Guadalupe Mountains. The progressive eastward shift of the transition zone through time reflects basin filling and eastward progradation of the shelf edge through this time period. This geographic shift, coupled with the eastward structural tilt of the Guadalupe Mountains, explains why one has to travel so far west on field trips to find evaporite facies—evaporitic strata in younger units have simply been eroded away. Adapted from Bjorklund and Motts (1959) and Motts (1968).

mation, 60-150 m (200-400 ft); Seven Rivers Formation, 135-180 m (450-600 ft); Yates Formation, 90-150 m (300-400 ft); and Tansill Formation, 30-100 m (100-325 ft)(all data from Kelley, 1971). The transitions from carbonate to evaporite facies generally occur within 8-24 km (5 to 15 mi) shelfward of the bank margin or reef throughout the history of the Artesia Group.

In an aside from the geological discussion, numerous grinding holes (metates) of the Mescalero Apache are found at this site (and several others in this area), indicating that this was a region populated long before historical times.

Turn around and return to the main road.

0.2 4.45 75.65 Intersection with main Dark Canyon road; turn right.

0.55 5.0 75.1 **STOP III-2. Tansill near-back-reef strata.** Turn at junction with small dirt road on left. Park and walk down road to cliff outcrop on south side of canyon.

This locality exposes limestones and dolomites of the near-back-reef Tansill Formation. A wide variety of sediment types are present here, typical of the complex, small-scale microfacies patterns in this paleogeographic zone. We can see pisolitic packstones, bird's-eye (fenestral) dolomites, cross-bedded to massive, marine-cemented green-algal grainstones (some of which look deceptively like mudstones), fenestral dolomites with tepee structures, and other lithologies intimately intermingled at this site. Fusulinid Foraminifera, bellerophontid gastropods, pelecypods, green algae and probable cyanobacteria or blue-green algae are particularly abundant in these strata.

These beds apparently represent subtidal sand flats with a series of migrating islands or banks; the strata are also characterized by a series of shallowing upward sequences (Maz-

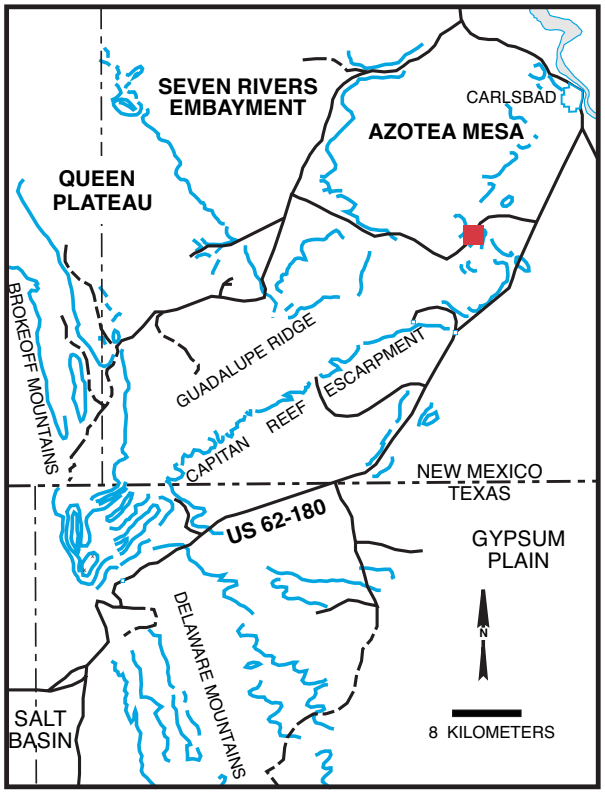

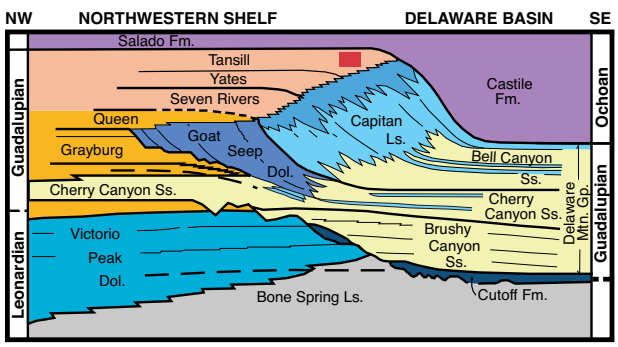

Figure 123. Peloidal and skeletal grainstones with fenestral fabric in the near-back-reef Tansill Formation. These strata were probably deposited on a relatively high-energy tidal flat. The coin is 2.4 cm in diameter.

Figure 124. Outcrop photograph of dolomitized shelfal grainstone/packstone with large, compound, calcite-lined vugs. The vugs are interpreted as leached anhydrite nodules and, along with the aphanocrystalline dolomite replacement, indicate very early influx of evaporitic pore fluids. Leaching probably occurred in association with Tertiary uplift and associated meteoric water input. Dark color in late-stage calcite vug linings is due to hydrocarbon inclusions. The coin is 1.9 cm in diameter.

Figure 125. Core photograph of oil-stained, dolomitized, shelfal packstone/wackestone with leached fossil fragments. Unplugged fossil molds and intercrystalline porosity are main contributors to the hydrocarbon productivity of this reservoir rock. Gulf Oil Co. N14N well, 4,413 ft (1,345 m) depth, Central Basin Platform northwest of Odessa, west Texas. Large scale divisions are centimeters.

zullo et al., 1989; Parsley and Warren, 1989; Scholle, 1980). The cross-bedded grainstones (Fig. 29) represent beach deposits on the seaward sides of islands; the fenestral (birdseye) dolomites (Fig. 123) represent leeward subaerial and intertidal flats, the pisolitic packstones to wackestones likely reflect subtidal restricted or sheltered sediment accumulation sites; the massive fossiliferous packstones and grainstones may have formed in intervening tidal channels and unrestricted subtidal areas; and the tepee dolomites found near the top of the section may represent exposure surfaces that cap the sequence. These facies patterns are quite similar to ones found in the Bahamas in regions such as Joulter's Cay or in the barrier-lagoon complexes of the Persian Gulf.

Diagenetically, these Permian units are equally complex. Aphanocrystalline dolomitization is patchy but extensive, especially in the peritidal and supratidal facies. Associated lobate and partitioned vugs (Fig. 124) clearly represent leached and/or calcitized early-diagenetic nodular evaporites. Note the close association between the areas of such evaporite vugs and dolomitization — both probably result from early reflux of evaporitic brines from more shelfward hypersaline lagoons.

In addition, one can find (most easily using a microscope) examples of aragonitic submarine cement as well as vadose and phreatic meteoric calcite cements (Fig. 28). Selective leaching of bioclasts is common in this setting, producing moldic fabrics (Fig. 109). Porosities in this zone are variable but include some of the highest values found anywhere in these strata. Subsurface equivalents of this facies host large volumes of oil, especially where dolomitization was followed by leaching of fossil fragments to form dolomoldic porosity (Fig. 125).

More recent diagenesis is also apparent at this outcrop. The cave system in

the center of the outcrop, and the solution-enlarged, calcite-filled fracture systems associated with it, were probably produced by the same Tertiary hydrologic system that formed Carlsbad Caverns. This late-stage meteoric water flow was also responsible for leaching or calcitization of precursor evaporites, which can be seen with increasing frequency from this locality landward.

0.3 5.3 74.8 **STOP III-3. Tansill-Yates contact.** Cross stream wash and examine two outcrops on north side of valley.

The Tansill-Yates contact is exposed in the western part of the outcrop, marked by a thin sandstone-siltstone unit. We can see microbially laminated dolomites, fusulinid grainstones, pisolitic beds, probable Permian breccia pipes, as well as infiltrated, red, lateritic soils in solution-enlarged fractures and voids (Fig. 126). The pisolitic microfacies was postulated by Dunham (1972) to be one of the highest paleotopographic zones in the Capitan complex. Pisolitic "caliche" zones and solution features would thus be a probable result of even minor relative sea-level drops during deposition. The red void-fillings consist calcium carbonate along with substantial kaolinite, hematite, quartz, goethite, illite, and amorphous iron oxide, a reasonable composition for a solution residue in this area.

Some arguments can be presented against this scenario, however. The associated sandstone-siltstone beds show no thinning over this zone, as one might expect if this were a topographic "high." Furthermore, topographic highs are rarely sites of significant accretionary sedimentation and, in fact, caliches are typically dissolution facies not accretionary ones. Scholle and Kinsman (1974) described some accretionary coastal caliche from the Persian (Arabian) Gulf, but the salina seep hypothesis of Handford et al. (1984) appears to account for the observed relationships better than any of the other models.

The thin sandstone-siltstone bed at the Yates-Tansill contact is typical of such terrigenous units in this area. They are generally 0.3-2.5 m (1-8 ft) thick, well-sorted, very fine sandstone or coarse siltstone, and have subarkosic or arkosic composition. Dunham (1972) showed that a progressive decrease

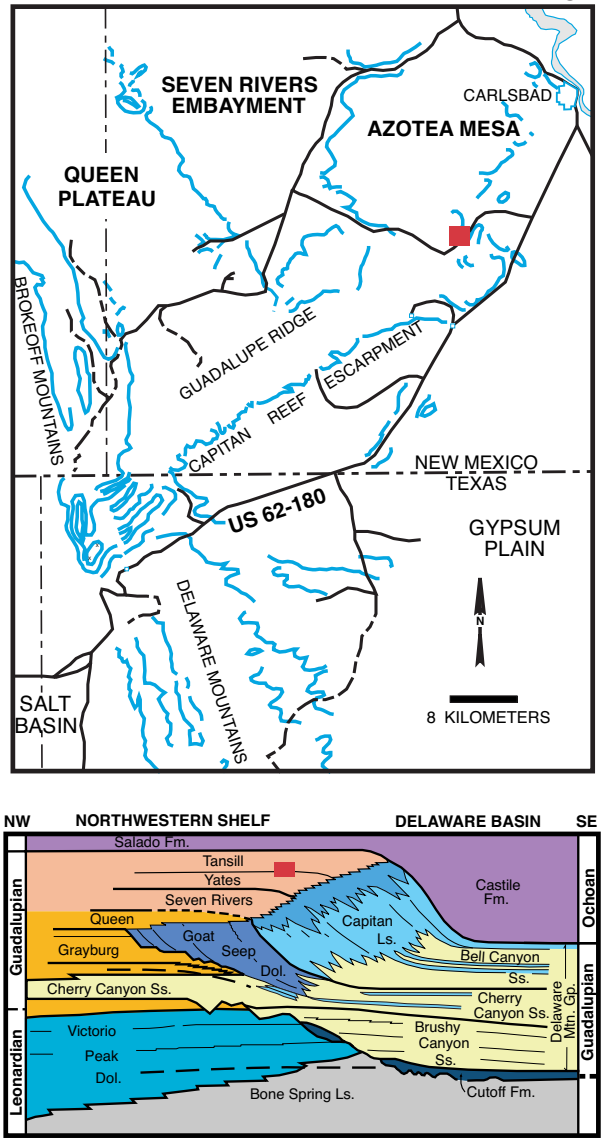

Figure 126. Reddish internal sediment in a solution-enlarged cavity in skeletal-pisolitic strata of the basal Tansill Formation. Concentration of such red sediments in the near-back reef facies may indicate that this zone was topographically higher than adjacent zones. The coin is 2.4 cm in diameter.

in feldspar content of these units from the shelf interior to the Capitan shelf margin is directly matched by a progressive increase in kaolinite content. Thus, these clastic terrigenous beds were probably uniformly arkosic but the near-reef sections underwent more intense post-depositional alteration.

In spite of their relative thinness, some these sandstone-siltstone beds have great lateral extent (more than 60,000 mi^2), particularly parallel to the reef trend, and serve as excellent stratigraphic marker beds (DeFord and Riggs, 1941). Some low-angle channel structures and vague adhesion ripples can be seen, locally, in these units, but generally these sediments are weakly horizontally laminated or structureless. They presumably represent largely wind-transported material; the horizontal lamination may have resulted from dune migration over an equilibrium deflation surface on a coastal sabkha as in the modern Persian Gulf (Kendall, 1969). Fuller discussion of these relationships may be found in the introduction and the description for Stop I-4.

0.4 5.7 74.4 OPTIONAL STOP III-3a. Pisolitic dolomites with "tepee" structures well exposed (Fig. 127) on south side of valley. Note the upward propagation of tepees through a thick stack of carbonate layers as well as the laminated sandstone-siltstone unit interrupting and truncating some "tepees." The sandstone-siltstone is the uppermost part of the Yates Formation; overlying dolomites are in the Tansill Formation.

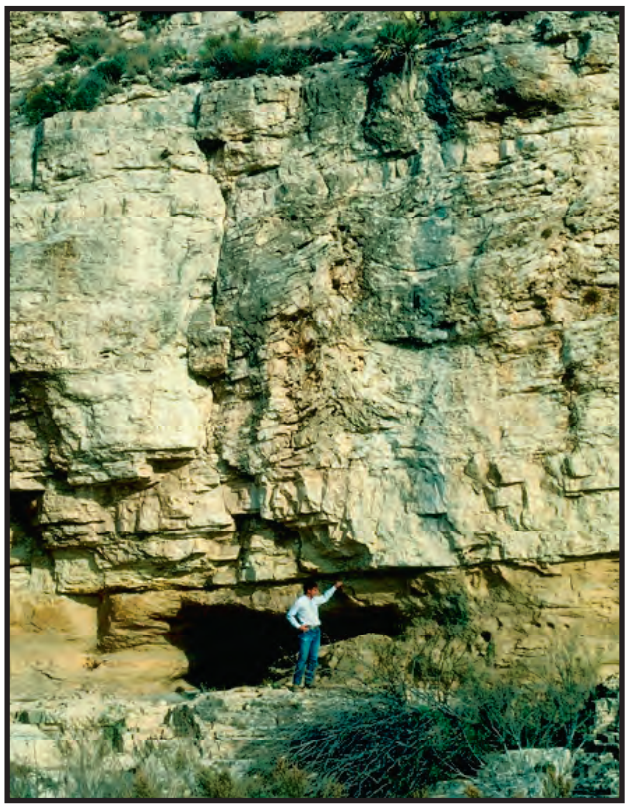

Figure 127. Stacked sequence of tepees in the basal part of the Tansill Formation. A 1.8 m thick sandstone at the base of the exposure (at level of man) has truncated tepee stacks in the underlying Yates Formation. These tepees are associated with fenestral and pisolitic dolomites. The sandstone sheets, which thin to a feather edge toward the shelf margin, have been interpreted as sabkha deposits formed by eolian processes during sea-level lowstands. Outcrop on south side of Dark Canyon road, approximately 2 km west of the canyon mouth.

Figure 128. Polished slab of aphanocrystalline dolomicrite from the upper part of the Seven Rivers Formation. Wispy remnants of lamination are an indication of extensive bioturbation but calcified skeletal fragments are extremely scarce in these strata. Dolomite here, as in most of the Permian shelf deposits of this region, appear to be a very early diagenetic replacement resulting from the reflux of hypersaline to mesosaline lagoonal brines. Slab from roadside outcrop along New Mexico Highway 137 in western Rocky Arroyo.

1.1	6.8	73.3	Yates outcrop on left contains pisolitic dolomite and sandstone.
0.3	7.1	73.0	Yates Formation pisolitic dolomite with evaporite crystal casts on right.
0.6	7.7	72.4	Yates Formation outcrop of thick-bedded, dolomitic mudstones with sparse evaporite crystal casts.
0.5	8.2	71.9	Mudstone, peloidal grainstone, and pisolites in Yates dolomite on right.
0.4	8.6	71.5	Yates Formation(?) dolomitized peloidal grainstones on left.
1.2	9.8	70.3	Road junction; continue straight ahead on Eddy Co. 408 toward Sitting Bull Falls.
0.2	10.0	70.1	**STOP III-4. Yates Formation lagoonal deposits.**

Walk down the stream bed to outcrops on north-northwest side of valley. Notice the clasts in the stream; occasionally, pyritized halite hoppers can be found. Exposure of thin-bedded, aphanocrystalline to very finely crystalline dolomitic mudstone (Fig. 128) with some zones containing contorted, fenestral mudstone (Fig. 23) representing stromatolitic deposits. In the subsurface much of the fenestral porosity is plugged with anhydrite or gypsum (Fig. 129) and that was true in these beds prior to uplift and dissolution — indeed, many beds exhibit abundant evaporite crystal casts (Fig. 130). Also common, in some zones, are nodular pyritic burrows (largely altered to hematite/limonite). A few beds within these penecontemporaneously dolomitized mudstones contain pellets, peloids (including coated, probably oncolitic grains), gastropods, scarce encrusting foraminifers, and, more commonly, calcispheres. These deposits, with their sparse assemblage of salinity-tolerant organisms and evaporite minerals, apparently represent a shallow, hypersaline lagoon similar to those found today in many areas of the Persian Gulf.

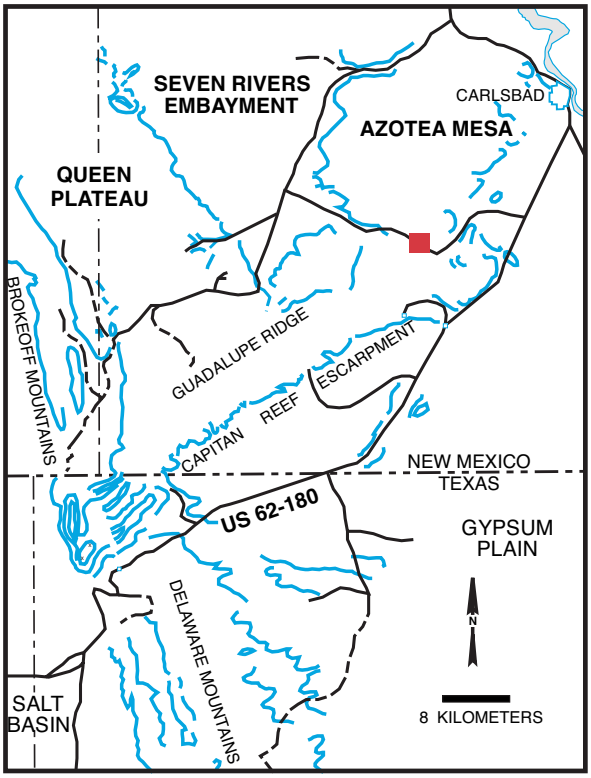

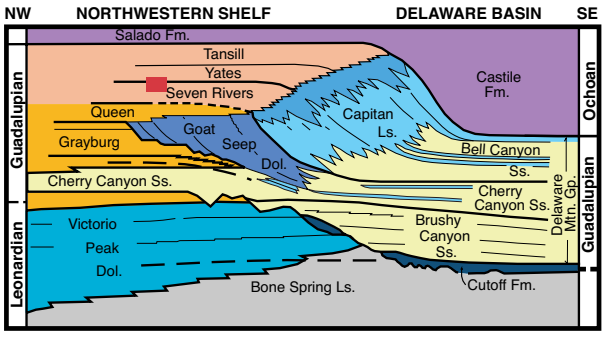

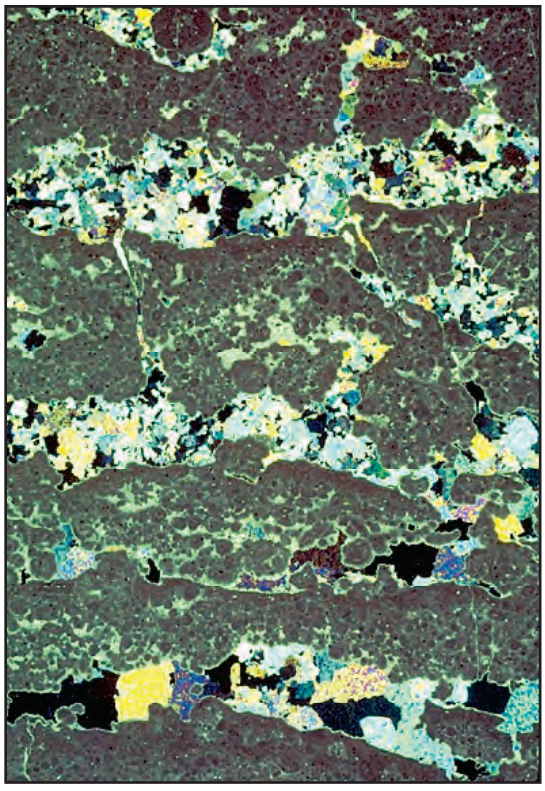

Figure 129. Thin-section photomicrograph (cross-polarized light) of anhydrite-filled porosity in a stromatolitic (fenestral boundstone) dolomite in the Yates Formation. Allochems trapped or formed within the stromatolite are mainly pellets (peloids) or pisoids. Sample from 1,658 ft (505 m) depth in Gulf/Chevron PDB-04 well on Northwestern Shelf of Delaware Basin, 30 km ENE of Carlsbad, Eddy Co., NM.

Figure 130. Evaporite crystal molds in dolomicrites from the basal Seven Rivers Formation. Loss of evaporites (dissolution and/or calcitization) is probably related to modern-cycle weathering. View is from outcrops near Stop III-9 along New Mexico Highway 137 in western Rocky Arroyo.

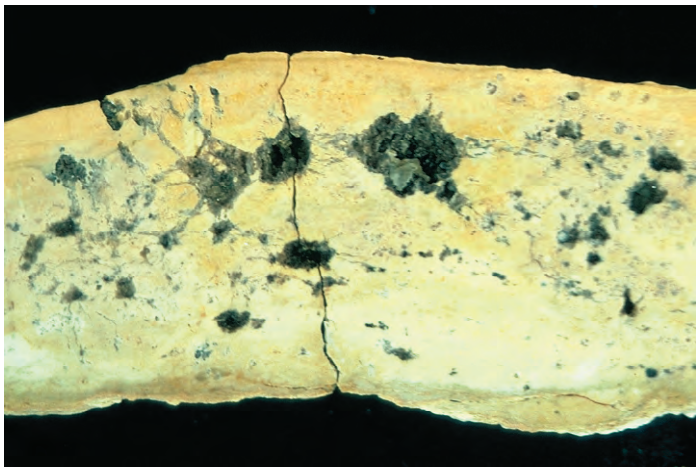

Figure 131. Polished rock slab showing quartz- and calcite-replaced evaporites in lagoonal, stromatolitic mudstones. Dark color of quartz crystals, in particular, reflects the abundance of hydrocarbon inclusions. Sample is from far back-reef facies of Yates Formation at Stop III-4. Length of slab = 12 cm.

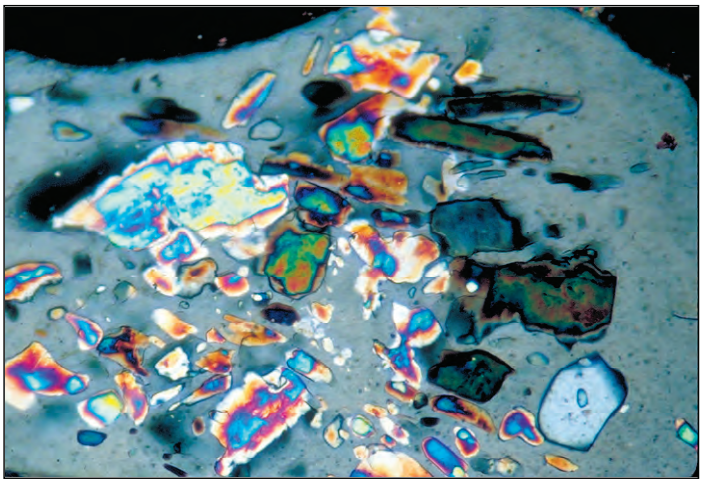

Figure 132. Thin section photomicrograph (cross-polarized light) of anhydrite inclusions in megaquartz replacement of precursor evaporite nodule in Yates Formation. Silicification preceded calcitization of evaporites and apparently occurred at or near maximum burial of these units. Thus, the silicified nodule rinds preserve both solid inclusions of evaporites and fluid inclusions of high-salinity brines and hydrocarbons. Long axis of photo = 0.51 mm.

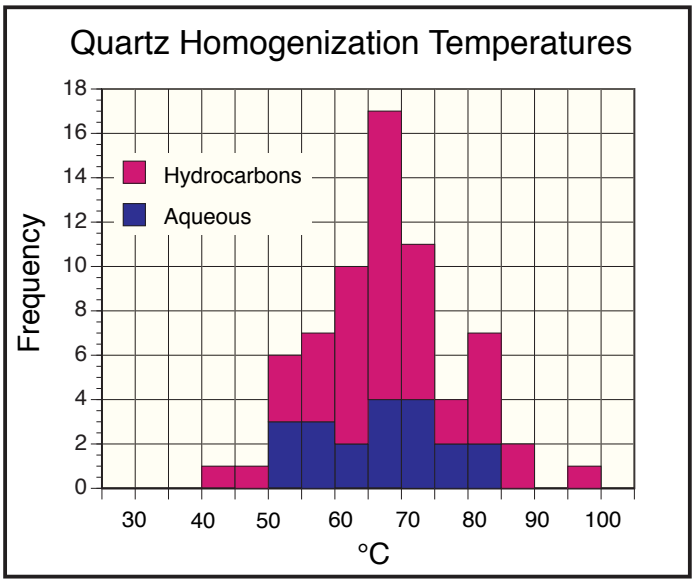

Figure 133. Homogenization temperatures for the aqueous and hydrocarbon inclusions in the replacement megaquartz (Ulmer-Scholle et al., 1993).

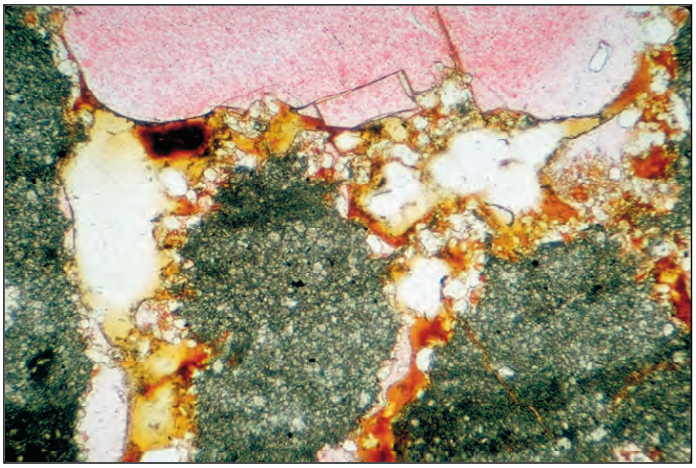

Figure 134. Thin section photomicrograph (plane-polarized light) of calcite (stained pink with Alizarin Red S) after an evaporite nodule in the Yates Formation. Evaporites were completely leached, oil (brown) entered secondary pores, and calcite precipitated in contact with oil (note curve meniscus surfaces on crystals). This calcite precipitation is considered to have occurred during late-stage uplift. Long axis of photo = 2.4 mm.

The coarser beds, which also contain rip-up clasts, may reflect discrete storm events that washed material in from more seaward parts of the lagoon and barrier complex.

You should be able to find abundant examples of dissolved, "calcitized" and silicified evaporites at this outcrop. Examine the units above the thick stromatolitic layer with pyritized burrows. Some of these thinner bedded stromatolitic horizons contain abundant black vugs (Fig. 131). The evaporites that once filled the vugs were first partially replaced by euhedral megaquartz (occasionally doubly terminated crystals — Herkimer Diamonds — can be found; Ulmer-Scholle et al., 1993). The megaquartz crystals are black, line the vugs and contain abundant evaporite inclusions (Fig. 132). The black coloration within the crystals is due to abundant, large hydrocarbon inclusions. In fact, the outcrop represents an exhumed oilfield as shown by the presence of residual oil in the pore spaces. Fluid inclusion analyses of both hydrocarbon- and brine-filled inclusions give average temperatures of formation of approximately 67.7°C and 61.7°C, respectively, well above normal diagenetic temperatures in this shallowly buried shelf setting (Fig. 133; Ulmer-Scholle et al., 1993).

The source of the silica likely was the dissolution of detrital feldspars within the back-reef strata. Organic acids associated with the basin-derived hydrocarbon-bearing fluids increased the silica solubility (Bennett and Siegel, 1987; Bennett et al., 1988). As the hotter hydrocarbon-bearing fluids displaced the cooler, shelf-derived groundwaters, the organic acids broke down, releasing the silica. Quartz precipitated, trapping hydrocarbons inclusions.

Late-stage meteoric water flow associated with Tertiary block faulting was probably responsible for the leaching of the remaining evaporites. Later calcite precipitation resulted in the partial filling of the vugs by late, blocky calcites that overlie residual hydrocarbons in the pores (Fig. 134).

0.5	10.5	69.6	Road junction; bear right.
2.1	12.6	67.5	Start former gravel road (now paved); continue straight ahead.
0.9	13.5	66.6	W. G. Smith ranch road on right; continue straight ahead. Road is on Seven Rivers Formation.
0.3	13.8	66.3	Road intersection on right; continue straight ahead on main road.
0.5	14.3	65.8	OPTIONAL STOP III-5. Interbedded thin-bedded, dolomitized mudstones and red siltstones of the Seven Rivers Formation on left. The Seven Rivers is the oldest Capitan-equivalent unit in the Artesia Group. These outcrops have been mapped as basal Yates Formation by Motts (1962b) but are considered to belong to the Seven Rivers by most other workers. Note the uniformity of the aphanocrystalline to very-finely-crystalline replacement dolomite. The depositional environment presumably represents a shallow lagoonal or coastal sabkha environment. Such finely-crystalline dolomitization is thought to represent the same processes seen on modern sabkhas (e.g., Patterson and Kinsman, 1982; McKenzie, 1981). In this model, the precipitation of calcium sulfates (gypsum or anhydrite) from sabkha brines leads to depletion of Ca^{+2} and relative enrichment of Mg^{+2} in pore waters. With calcium to magnesium ratios in excess of 60, the pore fluids react with very small aragonite needles to produce penecontemporaneous replacement dolomite.

The redbeds in this section show few sedimentary structures. Indistinct horizontal lamination, minor adhesion ripples, evaporite crystal casts, and the general absence of trace fossils all point toward deposition in an arid, dominantly nonmarine setting. Although no dune structures are found, most recent workers consider that these are eolian sediments deposited mainly in interdune flats.

0.3	14.6	65.5	Medium-scale contortions visible in Seven Rivers Formation. These were probably caused by near-surface dissolution of interbedded gypsum and anhydrite, although the Seven Rivers consists mainly of dolomites and siltstones in this area.
0.4	15.0	65.1	Road intersection on left; continue straight ahead.
0.9	15.9	64.2	Road intersection on left; bear right on main road.
1.2	17.1	63.0	Varicolored sediments on right are interbedded massive gypsum, dolomite, and red beds of Seven Rivers Formation.
0.2	17.3	62.8	Ranch road on left; continue straight ahead.
1.7	19.0	61.1	**STOP III-6. Borrow pit in gypsum of Seven Rivers Formation.**

Borrow pit in gypsum of Seven Rivers Formation. Surface weathering makes viewing of gypsum outcrops a frustrating exercise; most are altered to a very great degree with a solution residue covering most fabric elements. This borrow pit exposes the freshest samples easily accessible to a field trip group. Gray-white gypsum with a nodular, enterolithic texture (Fig. 1135) can be seen in isolated blocks scattered around the pit. This "chicken-wire" fabric may be related to a sabkha origin of the evaporite, but may also be a consequence of dehydration-rehydration reactions during burial and uplift (although the unit is gypsum on outcrop, it is generally anhydrite at greater than 600-900 m (2,000-3,000 ft) depth in the subsurface). The "chicken-wire" texture, with thin clay films between gypsum nodules, has been interpreted as the product of displacive growth of subaqueous gypsum in silty-clayey sediments in a shallow-water lagoon

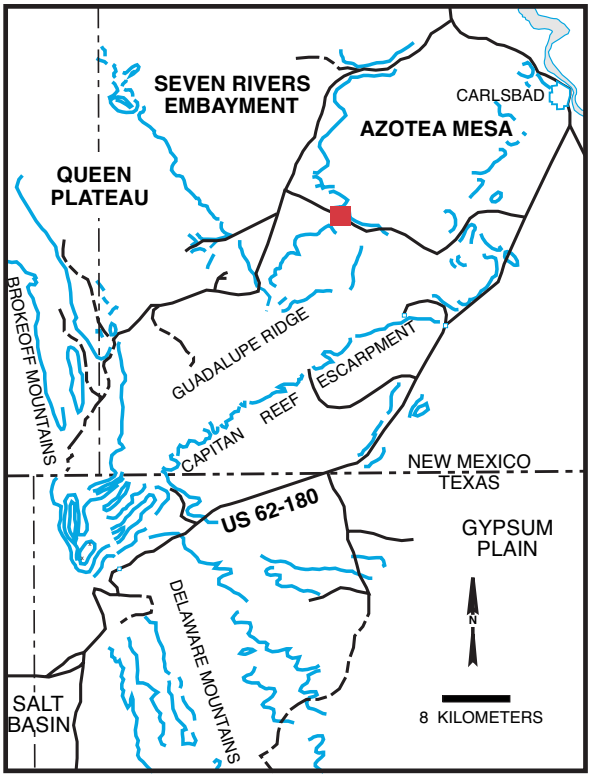

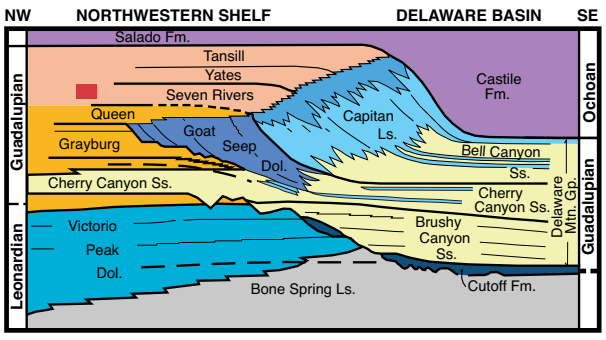

Figure 135. Massive nodular gypsum in the Seven Rivers Formation. Although nodular fabrics usually are interpreted as indicative of formation in coastal sabkha settings, such nodular structures can also be produced diagenetically in evaporites of other origins. These evaporites probably have been converted from anhydrite to gypsum during Tertiary/Quaternary uplift.

Figure 136. Gypsum rosette fabrics from evaporites facies of the Seven Rivers Formation. These are bottom-nucleated crystals that grew into shallow, standing water bodies (salinas). Coin is 1.9 cm in diameter.

(Sarg, in Pray and Esteban, 1977). Other blocks show fine examples of gypsum rosettes (Fig. 136). These clusters of crystals characterize bottom-nucleated gypsum growth from standing brine bodies in shallow salina settings.

On the left, is a reentrant of the Seven Rivers Embayment, an extensive planar topographic feature developed by dissolution of the massive evaporite deposits of the Seven Rivers Formation in this area. The reddish hillslopes consist of silty redbeds with bedded or nodular gypsum (Fig. 20) although these are very difficult to examine because the slopes typically are covered with a thick residue of evaporite dissolution.

0.3	19.3	60.8	Road junction to right; continue straight ahead.
1.2	20.5	59.6	Road on left; continue straight ahead on main road.
0.8	21.3	58.8	Ranch house on right. Well drilled to left (Humble's Bandanna Point Unit No. 1 gas well) was completed as a gas producer from Morrowan (Pennsylvanian) sandstone. It encountered the following units: San Andres Formation (top at 229 m; 750 ft depth); Bone Spring Ls. (858 m; 2,815 ft); Wolfcamp limestone (2,179 m; 7,150 ft); Pennsylvanian (2,301 m; 7,550 ft); Mississippian (Chester) (3,119 m; 10,234 ft); Woodford Shale (3,313 m; 10,868 ft); Devonian (3,332 m; 10,932 ft); Montoya Group (3,542 m; 11,622 ft); Simpson Group (3,656 m; 11,995 ft); and Ellenburger Group (3,673 m; 12,050 ft) (data from Anonymous, 1962, p. 18).
1.2	22.5	57.6	Azotea Mesa on right is composed of Seven Rivers Formation gypsum capped by a prominent dolomitic ledge. The ridge ahead in the distance consists of Queen and Grayburg beds downwarped along the Huapache Monocline. We are now entering the main part of the Seven Rivers Embayment with the road on thin alluvium over Queen Formation.
1.0	23.5	56.6	Intersection with New Mexico Highway 137 (a paved road from El Paso Gap to the Brantley Dam area north of Carlsbad). TURN LEFT toward El Paso Gap. Guadalupe Mountains ahead in distance; road traverses the Seven Rivers Embayment atop the Queen Formation.
2.6	26.1	54.0	Junction with road to Sitting Bull Falls on right; TURN RIGHT. Ahead lies the main western prong of the Guadalupe Mountains underlain by lower Guadalupian strata (San Andres, Queen, and Grayburg Formations) uplifted across the Huapache monocline.
3.2	29.3	50.8	Queen Formation(?) redbeds, dolomites, and evaporites on right.
1.0	30.3	49.8	Road crosses approximate Queen-Grayburg contact and passes onto Grayburg .
0.2	30.5	49.6	Entering Lincoln National Forest.
0.2	30.7	49.4	Road crosses first wash and traverses Huapache monocline ahead. Although the feature had precursors in the Pennsylvanian, the present flexure is a Tertiary feature (Hayes, 1964).
0.6	31.3	49.1	Road crosses onto San Andres Limestone.
0.1	31.4	49.0	Steel gate. About 30 m (100 ft) east of the gate is the site of the Humble Huapache Unit No. 1, a 3,850 m (12,631 ft) dry hole drilled in 1955. The well encountered a repeated section of Siluro-Devonian at about 3 km (10,000 ft) depth; a thrust fault, presumably associated with the Huapache flexure has been inferred for this structure. Throw on the fault exceeds 1,200 m (4,000 ft) in this area and 1,920 m

(6,300 ft) farther northeast (Reid et al, 1988).

0.2 31.6 48.5 Lenticular, partly silicified, skeletal grainstones of the San Andres, probably filling channels, on right at base of slope near stream crossing. Brown, thin-bedded Cherry Canyon sandstone beds can be seen in cliffs on right. This tongue of the generally basinal Cherry Canyon Formation extends many miles into the shelf environment in this area. The Cherry Canyon sandstone tongue is 50 m (164 ft) thick near the mouth of Sitting Bull Canyon.

0.7 32.3 47.8 A massive upper San Andres buildup, overlain by Grayburg Formation is visible ahead on right. Note lenticular bedding to the left of the "bioherm" (originally described as such but now thought of as a skeletal bank).

0.6 32.9 47.2 **STOP III-7. Junction of Sitting Bull Canyon and Last Chance Canyon.**

Cliff on north side of Last Chance Canyon (on right) has exposures of lower San Andres Ls. (at very base) overlain by the thick sandstone tongue of the Cherry Canyon Formation with large clinoforms. Upper San Andres carbonate and Grayburg Formation sandstones and carbonates form the top of the section. A major angular discordance is visible between the downlapping beds of the Cherry Canyon sandstone tongue and the lower San Andres Formation. A thin, recessive, condensed, black shale section can be seen on the downlap surface just above the lower San Andres carbonates. A more subtle discordance is also present between the upper San Andres and Grayburg Formations, marked by a prominent but thin white sandstone ledge (equivalent to the Premier Sandstone in the subsurface). Also note silica-replaced evaporite nodules in these slope to base of slope sands good evidence for refluxing of shelf-derived brines (Fig. 137).

Mescalero Apache petroglyphs (and more recent markings) can be seen on the Cherry Canyon Sandstone Tongue cliffs. The Mescalero Apaches (from the Zuni word "Apachu" meaning

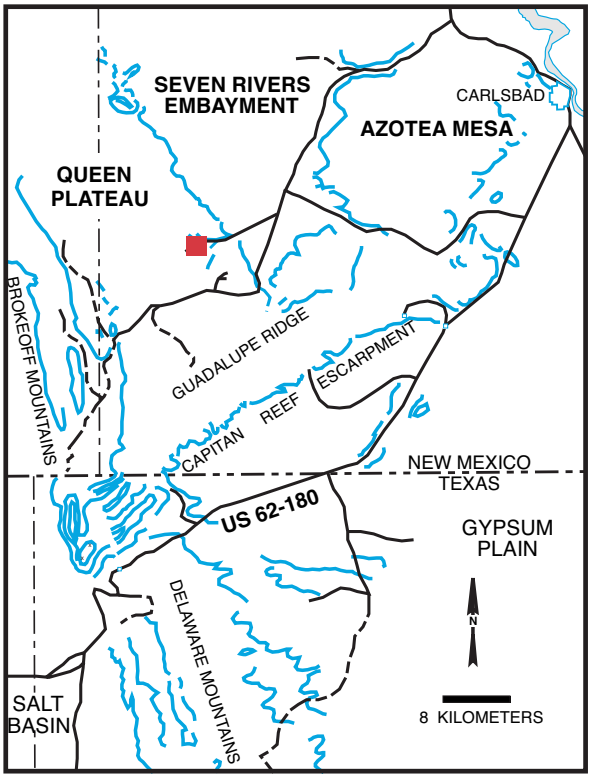

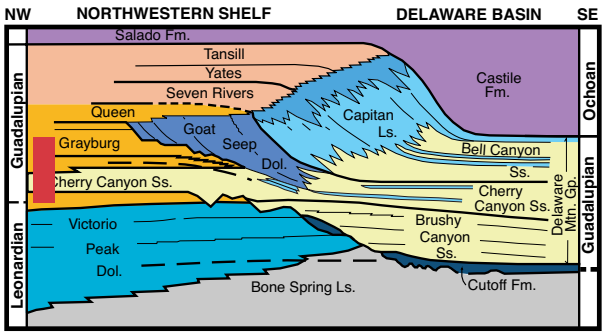

Figure 137. Silica-lined nodular vugs at base of Cherry Canyon Sandstone downlap onto the Lower San Andres Formation. These are leached and/or replaced former anhydrite nodules that formed where refluxing brines reached an impermeable horizon.

Figure 138. Hummocky top of a debris flow on a pre-Capitan Delaware basin margin (Cutoff or Lower San Andres Formation). Subsequent slope deposits onlap onto the mounded topography of the debris flow.

Figure 139. Sharp, truncational contact at base of a debris flow on a pre-Capitan Delaware Basin margin (Cutoff or Lower San Andres Formation.). Clasts are dominantly fragments of bioturbated, fine-grained, slope limestones and shaly limestones.

"enemy") are believed to have entered this area from the north in about 1300 AD. These hunter-gatherers built wooden lean-tos or lived in caves and under rock overhangs like this one.

Excellent, if extensively dolomitized, exposures of the lower San Andres Formation, as well as outstanding debris flows of the Cutoff Shale, can be examined by walking up Last Chance Canyon for a few hundred meters. Recent field descriptions based on seismic and sequence stratigraphic studies (Sarg, 1986; Sarg and Lehmann, 1986a, 1986b; Wilkinson et al., 1991; Gardner, 1991; Sonnenfeld, 1991, 1993, 2000; Sonnenfeld and Cross, 1993; Adams, 1993) are especially useful for those who wish to explore these outcrops more fully. A walk up-canyon to view the outcrops of Lower San Andres and/or Cutoff Formation slope facies carbonates is well worth the effort of battling through the thorn brush. Thin bedded, dark colored, heavily bioturbated limestones with stylonodular fabrics represent typical Late Paleozoic slope-facies deposits. Interspersed with these more or less in-situ materials are numerous slide and debris flow deposits. Superb exposures of the scoured bases and hummocky tops of multiple debris flows with onlapping slope sediments are to be found there and are well worth the short if painful, hike (Fig. 120).

Return to paved road and continue toward Sitting Bull Falls parking area. You are entering a U.S. Forest Service park area and sample collecting is illegal unless you have a research permit.

0.2	33.1	47.0	The Cherry Canyon-San Andres unconformity is well exposed on both sides of the road.
0.3	33.4	46.7	Cherry Canyon sandstone outcrops with well developed cross-bedding are visible on right.

0.5 33.9 46.2 **STOP III-8. Sitting Bull Falls.** When finished at this stop, return down-canyon to the El Paso Gap-Carlsbad road.

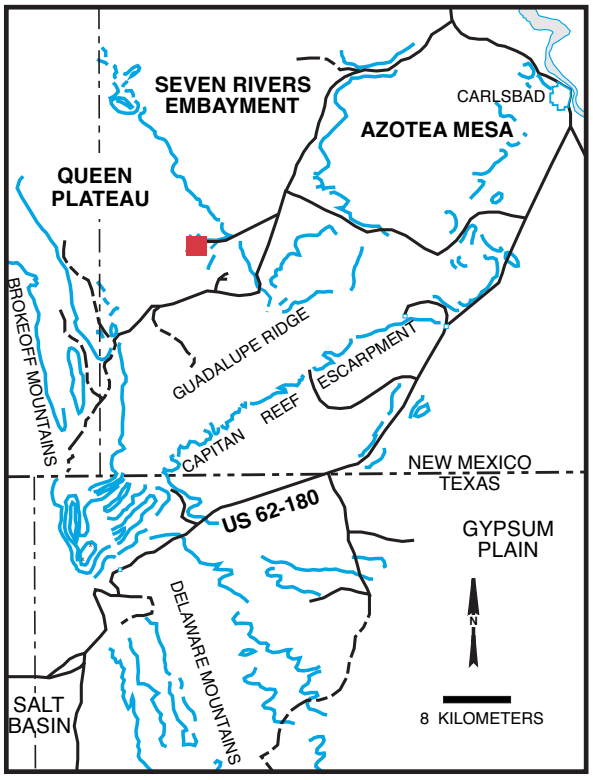

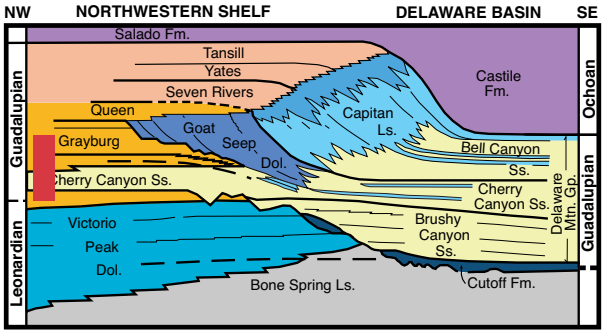

Lunch stop at picnic benches. The entire cliff on the northwest side of the picnic area is formed of modern travertine that can be examined in numerous fallen blocks (for general information on travertines see Chafetz and Folk, 1984 and Ford and Pedley, 1996). A short walk to the active waterfall area shows travertine in the process of formation (Fig. 121). Calcium bicarbonate and carbon dioxide saturated waters emerge from springs in the Grayburg and San Andres units a short distance (about 0.6 km; 1 mi) upstream from the falls. Warming of the waters, combined with release of CO_2 from waters plunging over the falls, induces precipitation of calcium carbonate. The withdrawal of CO_2 from the water by the numerous algae and higher plants that abound at the falls also contributes to the calcite precipitation. These plants are then incorporated within the calcite, later to rot away. This accounts for the unusual, porous fabric with abundant impressions of leaves and stems seen in the travertine blocks.

If you climb up or under the waterfalls, please take great care as the rocks here are very slippery. The other walls of the canyon in this area expose the Cherry Canyon sandstone tongue in their lower part, the upper San Andres Limestone in the middle part, and Grayburg Formation in the upper part. Note apparent bioherm or reef structures in the San Andres; they are fusulinid grainstone banks rather than reefs. If you climb to the top of the waterfalls you will be able to see that what look like isolated bioherms are really part of a shelf margin bank that is rolling over the prograding shelf-slope break and that has been irregularly dissected by the canyon. If you climb still farther up you will be able to see some large-scale channels in the Cherry Canyon slope facies as well as the tidal (herring-bone) cross-bedding and shallowing upward sequences of the topset beds of the San Andres Formation. For more detailed descriptions of this area see Harrison (1966), Naiman (1982), McDermott (1983) or Sarg and Lehmann (1986a).

Return down-canyon to the El Paso Gap-Carlsbad road.

7.7 41.6 38.5 Junction with New Mexico Highway 137 (El Paso Gap-Carlsbad road). Note West Hess Hills at 2:00 to 3:00 o'clock and Azotea Mesa at 10:00 to 11:00 o'clock - both are composed of gypsum, red siltstones, and dolomites of the Seven Rivers Formation. Turn left toward Carlsbad.

2.6 44.2 35.9 Unpaved Dark Canyon road on right; continue straight ahead. Road is on Queen Formation.

3.2 47.4 32.7 Road now crossing the approximate contact between the Queen and Seven Rivers Formations. The road is located almost directly on this contact for the next few miles, with Queen strata on the left and Seven Rivers deposits on the right.

1.2 48.6 31.5 Hills ahead and to the right are composed of Seven Rivers evaporites and red siltstones. The strongly developed vertical gullying is characteristic of the evaporite facies of the Guadalupian far-back-reef units and contrasts sharply with the horizontal bedding that dominates in areas of carbonate facies within these same units. Most of these hills are capped by the resistant "Azotea Tongue" (usage of Sarg,

			1976), a dolomite unit in the Seven Rivers Formation.
4.4	53.0	27.1	Road passes from Seven Rivers Embayment into Rocky Arroyo.
0.6	53.6	26.5	Road is at the level of the contact of the Queen Formation (Shattuck Sandstone unit of Sarg, 1976) and Seven Rivers Formation. We are nearly 1.6 km (1 mi) shelfward (northwest) of the carbonate-evaporite transition of the Seven Rivers Formation (Sarg, 1976, 1981). This transition is remarkably abrupt (within about 150 m/500 ft) and remains in approximately the same location for nearly 200 ft of section (Bates, 1942; Pray and Esteban, 1977). This Seven Rivers facies transition has been shown by Sarg (1976, 1981) to be related to a depositional ridge in the underlying Shattuck Sandstone of the Queen Formation. The gullied hillside on the southeast side of the road has good exposures of the Seven Rivers evaporite facies (see Pray and Esteban, 1977, Stop VII). The section is dominated by bedded, nodular, mosaic gypsum with thin, pelletal or grapestone-bearing dolomites and red, gypsum-cemented, sandy siltstones. Note invigorating, heady aroma of hydrocarbons in the air; it emanates from the Indian Basin field about 0.3 miles ahead. The main production is from extremely permeable Upper Pennsylvanian (Canyon and Cisco) dolomites at 2,130-2,440 m (7,000-8,000 ft); further production comes from Morrowan sandstones at 2,740-3,000 m (9,000-10,000 ft) (Frenzel, 1988). The field had cummulative production of 26.7 million barrels of oil and condensate along with more than 2 TCF of gas from Upper Pennsylvanian (Canyon; Missourian) shelf carbonate reservoirs from discovery in 1963 to the end of 2003. An additional 50 BCF of gas had been produced from underlying Morrow strata and 2 BCF from the Strawn through the end of 2000. The high H_2S content of the hydrocarbons is a continuing problem in the operation of this field, as are the enormous volumes of produced waters, most of that must currently be reinjected into Devonian strata at roughly 12,000 ft depth. The northward extension of this reservoir, the separately named Dagger Draw North and South fields, has been one of the larger hydrocarbon developments in New Mexico over the past two decades.
0.1	53.7	26.4	Low road cuts on right are Queen Formation (Shattuck Sandstone). Conical hill visible to the north of the road is "The Tepee" and is capped by the resistant "Azotea Tongue" a massive dolomite of the Seven Rivers Formation. Underlying Seven Rivers evaporites, the Shattuck Sandstone and dolomites of the Queen Formation are also exposed.
2.3	56.0	24.1	Intersection with road on left leading to Marathon Oil Co. Indian Basin oil and gas field and plant. Continue on main road.
0.1	56.1	24.0	OPTIONAL VIEW STOP III-8a. Excellent view of the carbonate-evaporite facies transition in the Seven Rivers Formation (see description of Stop VI in Pray and Esteban, 1977) on north wall of Rocky Arroyo. This extremely rapid transition can be seen in a narrow, nearly vertical, band in the upper half to two-thirds of the far wall of the valley. The transition is visible because of the radically different weathering patterns of the evaporite (vertical gullying) and carbonate (horizontal bedding) facies. The transition was first described by Bates (1942) and has been recently examined by Sarg (1976, 1981). Also exposed in the lower part of the cliff is the upper dolomite and the overlying Shattuck Sandstone unit of the Queen Formation. The Shattuck, generally about 27 m (90 ft) thick in this region, thickens to about 43 m (140 ft) beneath the carbonate-evaporite transition and may have been partly responsible for the generation of restricted, evaporitic conditions shelfward of this point during Seven Rivers deposition (Sarg, in Pray and Esteban, 1977).

0.75 6.8 23.3 **STOP III-9. Shattuck Sandstone (Queen Formation) and Seven Rivers Formation collapse breccia.**

Excellent exposures of Shattuck Sandstone (Queen Formation) on the right (see Dunham, 1972, Stop I-5; Pray and Esteban, 1977, southwest end of Stop VIII; Mazzullo et al., 1991). The sandstone has broad, channel-like structures with northwest-southeast axes. Note bimodal eolian lag(?) deposits at some horizons and small adhesion ripples, suggesting that much of the sand may have been deposited on sabkhas or interdune flats. Other sedimentary structures, in lower horizons, indicate sheet-flood or ephemeral stream sedimentation; marine trace fossils are also present in basal exposures of the sandstone. Thus, there may be an upward progression of depositional environments from marine to fluvial to eolian.

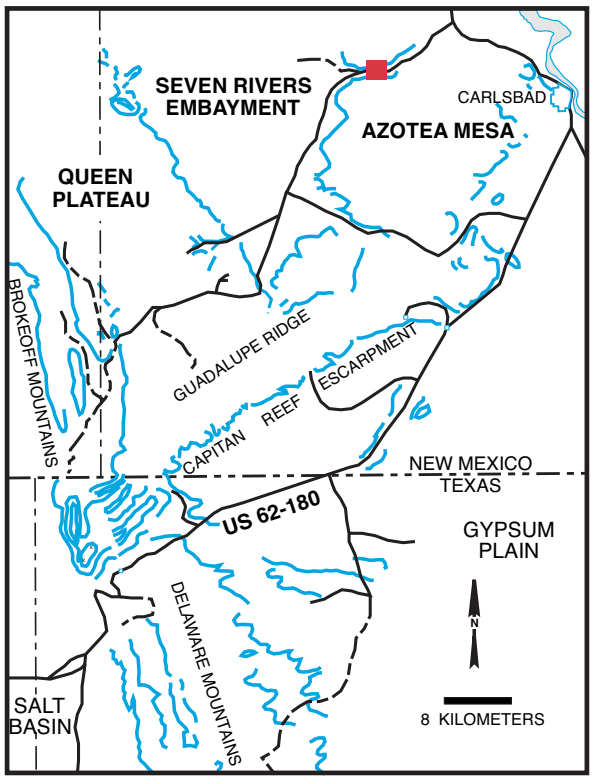

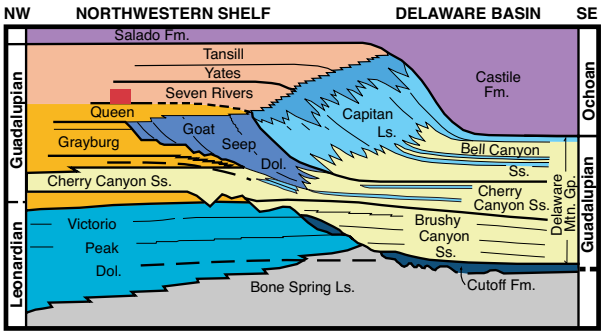

Walk uphill along the continuation of the outcrop. These medium-to thin-bedded dolomites, about 19 km (12 mi) shelfward of the Capitan scarp, are generally placed in the Seven Rivers Formation; Sarg (1976), however, included them in the Queen Formation. Some interesting collapse breccias occur in these strata (Fig. 22), which were included by Dunham (1972) in his "calcisphere dolomite wackestone" facies. The largest breccia occurs as an isolated pocket in a thick, light-tan dolomite bed. The breccia has large, angular clasts of dolomite with corroded and altered borders (Fig. 140). The clasts are held in a partial matrix of microcrystalline calcite, internal sediment (green illite-kaolinite clay and quartz silt), and coarsely crystalline, blocky, late, sparry calcite cement. Considerable remnant porosity also is present in the breccia zones. The presence of the greenish clays and abundant evaporite crystal molds (Fig. 130) indicate that these breccias are probably the result of interstratal evaporite dissolution. The presence of some zones with calcitic nodules with geopetal collapse features associated with evaporite removal (Fig. 141) and other zones with gypsum pseudomorphs (Fig. 142) reinforces that interpretation.

Pray and Esteban (1977) argued for a modern karstic origin for these features; Dunham (1972) postulated a Permian origin, presumably related to weathering and dissolution of evaporite min-

Figure 140. Polished rock slab showing an evaporite solution-collapse breccia in the basal part of the Seven Rivers Formation. The clasts are dolomite and residual clays, calcite cements, and epoxy fills the interstices. Dissolution and collapse probably took place during Tertiary uplift, but some dissolution may also have taken place during latest Permian time.

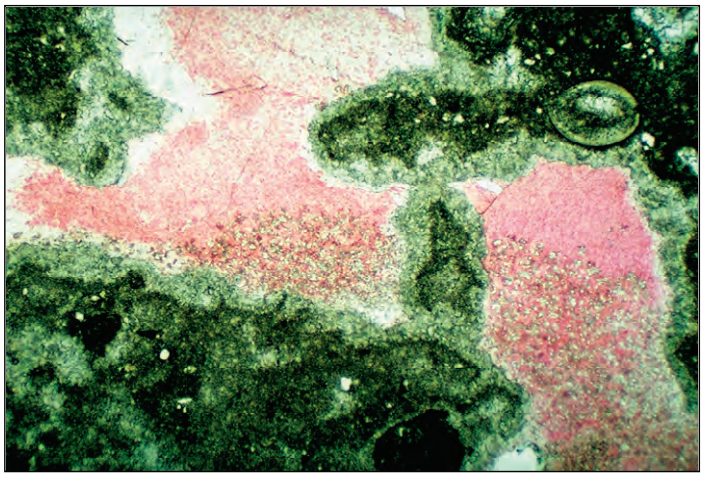

Figure 141. Thin section photomicrograph (plane-polarized light) of calcite (stained pink with Alizarin Red S) filling irregular vugs inferred to be former evaporite nodules in the basal Seven Rivers Formation. Note the cloudy, geopetal fabric within the calcite — the "cloudy" material consists of kaolinite booklets that have fallen to the bottom of the vugs when the evaporites were leached. Photo Long Axis = 13.5 cm.

Figure 142. Calcitized evaporite rosettes in sandy dolomite of the Seven Rivers Formation. Replacement by calcite is interpreted to have occurred relatively recently, in association with Late Tertiary uplift and ground water circulation. The coin is 1.8 cm in diameter.

			erals during pluvial intervals. Note the abundant evidence of associated evaporite (mainly gypsum) crystal casts in these dolomites and see if you can find convincing evidence as to the timing of dissolution.
0.4	57.2	22.9	Cyclic deposits of dolomite and red, silty shales. Generally grouped in the Seven Rivers Formation, these sediments were included in the uppermost part of the Shattuck Sandstone (Queen Formation) by Sarg (1976) and Pray and Esteban (1977; see description for Stop VIII). These strata have been interpreted as "dolocalcrete cycles" with evidence of repeated deposition, exposure, weathering, and calichification (Pray and Esteban, 1977). Note also the abundant crystal- and nodule-casts of former gypsum (some voids now partly filled with calcite; see Fig. 130).
0.8	58.0	22.1	A thick section of Seven Rivers dolomitic packstones and mudstones of probable lagoonal origin exposed on left. Note absence of evaporites and red beds.
0.3	58.3	21.8	Strata exposed behind Shafer Ranch are fossiliferous, dolomitic, pelletal packstones.
0.2	58.5	21.6	Dry wash across Rocky Arroyo with massive travertine deposits exposed on left.
0.5	59.0	21.1	Small cemetery on right. Cliffs to the southeast expose Seven Rivers Formation fossiliferous, dolomitic, pelletal packstones containing ostracods, calcispheres, and some small foraminifers. Queen Formation (Shattuck Sandstone) is exposed at the cliff base.
0.3	59.3	20.8	On the south side of the arroyo are cliffs exposing thin-bedded dolomite of the Seven Rivers Formation dominated by pelletal wackestone and mudstone. Stromatolitic(?) units have been described from this locality (Sarg, 1976). Other, similar outcrops are along road on left.
0.5	59.8	20.3	OPTIONAL STOP III-9a. Road cuts to left are Seven Rivers dolomite (Dunham's (1972) Stop I-6). This section, 18.8 km (11.7 mi) shelfward of the Capitan escarpment, consists of thin-bedded, stromatolitic(?), dolomitic wackestone with pellets, ostracods and calcispheres. In and along the stream valley, travertine is abundant along with travertine-cemented gravels. The deposits are characterized by repeated meter-scale shallowing-upward cycles. These progress from subtidal wackestones and mudstones to intertidal stromatolitic sediments, with occasional supratidal caps.

			The dolomite in these sediments, as in most of the back-reef areas, is very finely crystalline to aphanocrystalline and appears to be of very early diagenetic origin. Formation of early dolomite is probably related to restricted circulation in these back-reef lagoonal areas, precipitation of $CaSO_4$ minerals, and consequent increase in Mg/Ca ratios of lagoonal and interstitial fluids. Contact of Mg-rich surface and interstitial waters with unstable aragonitic muds has led to partial dolomitization of modern carbonate muds in the Persian Gulf and this most likely took place in the Permian back-reef areas as well. The exact mechanisms of this dolomitization (reflux brine movement, evaporative pumping, and other models) are debated even in modern setting and are even more disputed for the Permian examples.
0.9	60.7	19.4	Leaving Rocky Arroyo. Outcrops to the south are upper Seven Rivers Formation. Yates Formation is present on the crest and eastern side of the hills to the south.
4.4	65.1	15.0	Junction with U. S. Highway 285; straight ahead and to the north are Brantley dam and Brantley lake on the Pecos River. Turn right toward Carlsbad. The road here is on Quaternary alluvium overlying Yates Formation. The Seven Rivers Hills, to the northwest, are the type section of the Seven Rivers Formation (Meinzer et al., 1926).
0.8	65.9	14.2	Bridge crossing over Rocky Arroyo.
0.9	66.8	13.3	Interbedded dolomites and red-brown sandstone of the Yates Formation on both left and right.
0.6	67.5	12.7	Yates Formation exposed in road cut.
0.3	67.8	12.4	Yates Formation exposed in road cut.
1.5	69.2	10.9	Intersection of U. S. Highway 285 with U. S. 285 (Truck Rte.) on right. Continue left on main U. S. Highway 285.
0.3	69.5	10.6	Basal Tansill Formation is exposed in low cuts on both sides of road. Thin-bedded to laminated dolomitic mudstones with evaporite (anhydrite?) crystal casts can be found just below road level to the west. All back-reef units dip gently basinward in this area.
0.4	69.9	10.2	The Ocotillo Hills at 1:00 o'clock and Avalon Hills at 11:00 to 12:00 o'clock are composed of back-reef Tansill and Yates evaporitic dolomites. The hills are the topographic expression of an anticlinal structure over the buried Capitan reef, one of many such structures in the shelf area to the north and west of Carlsbad.
1.9	71.8	8.3	Thin-bedded Tansill dolomites with evaporite crystal casts present in roadcut. The type locality of the Tansill Formation, as described by DeFord and Riggs (1941), is located nearby in the Ocotillo Hills.
0.4	72.2	7.9	Gently dipping Tansill and Yates strata in canyon to right are on eastern flank of the Tracy Dome.
1.1	73.3	6.8	Tansill dolomite overlying Yates sandstone is exposed in canyon on right.
0.7	74.0	6.1	Pecos River on left. Tansill Formation in road cuts on right.
0.8	74.8	5.3	Living Desert State Park turn-off on right.
3.1	77.9	2.2	Carlsbad city center (junction of U. S. Highways 62-180 (from north) and 285. Continue straight ahead.
2.2	80.1	0.0	Intersection of U. S. Highways 62-180 (from south) and 285 (from southeast).

Road log ends.

BIBLIOGRAPHY

ACHAUER, C.W., 1969, Origin of Capitan formation, Guadalupe Mountains, New Mexico and Texas: AAPG Bull., v. 53, p. 2314-2323.

ADAMS, J.E., and FRENZEL, H.N., 1950, Capitan barrier reef, Texas and New Mexico: Jour. of Geology, v. 58, p. 289-312.

ADAMS, J.W., 1988, Historic Guadalupe Pass*, in* Reid, S.T., Bass, R.O., and Welch, P., eds., Guadalupe Mountains Revisited, Texas and New Mexico: Mildand, TX, West Texas Geol. Soc. Pub. 88-84, p. 191-196.

ADAMS, J.W., LOVE, D.W., and HAWLEY, J.W., 1993, Third-day road log, from Carlsbad to Dark Canyon, Last Chance Canyon, Sitting Bull Falls, Rocky Arroyo and return to Carlsbad*, in* Love, D.W., Hawley, J.W., Kues, B.S., Adams, J.W., Austin, G.S., and Barker, J.M., eds., Carlsbad Region, New Mexico and West Texas, New Mexico Geol. Soc., 44th Annual Field Conf. Guidebook, p. 69-86.

AÏSSAOUI, D.M., 1985, Botryoidal aragonite and its diagenesis: Sedimentology, v. 32, p. 345-361.

ALEXANDER, J.I.D., and WATKINSON, A.J., 1989, Microfolding in the Permian Castile Formation: an example of geometric systems in multilayer folding, Texas and New Mexico: GSA Bull., v. 101, p. 742-750.

ANDERSON, R.Y., 1982, A long geoclimatic record from the Permian: Jour. of Geophys. Res., v. 87, p. 7285-7294.

ANDERSON, R.Y., 1984, Orbital forcing of evaporite sedimentation*, in* Berger, A., Imbrie, J., Hays, J., Kukla, G., and Saltzman, B., eds., Milankovitch and Climate, Part 1: NATO ASI Series C, Vol. 126: Dordrecht (Netherlands), D. Reidel Publishing Co., p. 147-162.

ANDERSON, R.Y., 1991, Solar variability captured in climatic and high-resolution paleoclimatic records: a geologic perspective*, in* Sonett, C.P., Giampapa, M.S., and Mathews, M.S., eds., The Sun in Time: Tucson, AZ, University of Arizona Press, p. 543-561.

ANDERSON, R.Y., 2006, Pangean monsoon and climatic cycles in NM-Texas state-line outcrop, in Land, L., Lueth, V.W., Raatz, W., Boston, P., and Love, D.L., eds., Caves and Karst of Southeastern New Mexico, New Mexico Geol. Soc., 57th Annual Field Conf. Guidebook, p. 75-77.

ANDERSON, R.Y., and DEAN, W.E., 1995, Filling the — hydrologic and climatic controls on the Upper Permian Castile Formation varved evaporite*, in* Scholle, P.A., Peryt, T.M., and Ulmer-Scholle, D.S., eds., The Permian of North Pangea: Springer-Verlag, Sedimentary basins and economic resources, p. 61-78.

ANDERSON, R.Y., DEAN, W.E., KIRKLAND, D.W., and SNIDER, H.I., 1972, Permian Castile varved evaporite sequence, west Texas and New Mexico: GSA Bull., v. 83, p. 59-86.

ANDERSON, R.Y., and KIRKLAND, D.W., 1988, Banded Castile evaporites, Delaware Basin, New Mexico*, in* Reid, S.T., Bass, R.O., and Welch, P., eds., Guadalupe Mountains Revisited, Texas and New Mexico: Midland, West Texas Geol. Soc. Pub. 88-84, p. 187-190.

ANONYMOUS, 1960, Geology of the Delaware basin and field trip guidebook (1960 Field Trip Guidebook): Midland, West Texas Geol. Soc., 97 p.

ANONYMOUS, 1962, Permian of the central Guadalupe Mountains, Eddy County, New Mexico: Midland, Hobbs, Roswell, and West Texas Geol. Socs. Field Trip Guidebook and Geological Discussions, Pub. No. 62-48, 115 p.

ANONYMOUS, 1964, Geology of the Capitan reef complex of the Guadalupe Mountains, Culberson County, Texas and Eddy County, New Mexico (1964 Field Trip Guidebook): Roswell, Roswell Geol. Soc., 124 p.

ANONYMOUS, 1969, Delaware Basin Exploration: Midland, West Texas Geol. Soc. Pub. 68-55a, 170 p.

ANONYMOUS, 1982, Selected Oil and Gas Fields in West Texas (a reprint of Symposium Volumes I, II and III): Midland, West Texas Geol. Soc. Pub. 82-75, 689 p.

BABCOCK, J.A., 1974a, The role of algae in the formation of the Capitan Limestone (Permian, Guadalupian), Guadalupe Mountains, west Texas and New Mexico [unpublished Ph.D. thesis]: University of Wisconsin—Madison, Madison, WI, 241 p.

BABCOCK, J.A., 1977a, Calcareous algae, organic boundstones, and the genesis of the upper Capitan Limestone (Permian, Guadalupian), Guadalupe Mountains, west Texas and New Mexico*, in* Hileman, M.E., and Mazzullo, S.J., eds., Upper Guadalupian facies, Permian reef complex, Guadalupe Mountains, New Mexico and west Texas: Midland, Permian Basin Section-SEPM Pub. 77-16, p. 3-44.

BABCOCK, J.A., 1979, Calcareous algae and algal problematica of the Capitan Reef (Permian), Guadalupe Mountains, west Texas and New Mexico, U.S.A.: Bull. des Centres de Recherches Exploration-Production Elf-Aquitaine, v. 3, p. 419-428.

BABCOCK, J.A., and YUREWICZ, D.A., 1989, The massive facies of the Capitan Limestone, Guadalupe Mountains, Texas and New Mexico*, in* Harris, P.M., and Grover, G.A., eds., Subsurface and Outcrop Examination of the Capitan Shelf Margin, Northern Delaware Basin: Tulsa, SEPM Core Workshop No. 13, p. 365-371.

BABCOCK, L.C., 1974b, Conodont paleoecology of a Guadalupian (Permian) shelf to basin sequence, Permian reef complex, west Texas and New Mexico [abs.]: GSA, Abstracts with Programs, v. 6, p. 489.

BABCOCK, L.C., 1977b, Life in the Delaware basin — the paleoecology of the Lamar Limestone*, in* Hileman, M.E., and Mazzullo, S.J., eds., Upper Guadalupian facies, Permian reef complex, Guadalupe Mountains, New Mexico and west Texas: Midland, Permian Basin Section-SEPM Pub. 77-16, p. 357-390.

BALL, M.M., 1967, Tectonic control of the configuration of the Bahama Banks: Trans. Coast Assoc. Geol. Socs., v. 17, p. 265-267.

BALL, M.M., HARRISON, C.G.A., HURLEY, R.J., and LEIST, C.E., 1969, Bathymetry in the vicinity of the northeastern scarp of the Great Bahama Bank and Exuma Sound: Bull. Marine Science, v. 19, p. 243-252.

BARKER, C.E., and PAWLEWICZ, M.J., 1987, The effects of igneous intrusions and higher heat flow on the thermal maturity of Leonardian and younger rocks, western Delaware Basin, Texas*, in* Cromwell, D.W., and Mazzullo, L., eds., The Leonardian Facies in W. Texas and S. E. New Mexico and Guidebook to the Glass Mountains, West Texas: Midland, Permian Basin Section-SEPM Pub. 87-27, p. 69-83.

BARNES, V.E., 1968, Geologic atlas of Texas, Van Horn-El Paso sheet (1:250,000 scale map): Univ. Texas, Bur. Econ. Geol..

BASHMAN, W.L., 1996, Delaware Mountain Group sandstone channel orientations: implications for sediment sources and deposition*, in* DeMis, W.D., and Cole, A.G., eds., The Brushy Canyon Play in Outcrop and Subsurface: Concepts and Examples: Midland, Permian Basin Section-SEPM Pub. 96-38, p. 91-102.

BATES, R.L., 1942, Lateral gradation in the Seven Rivers Formation, Rocky Arroyo, Eddy County, New Mexico: AAPG Bull., v. 26, p. 80-99.

BEAUBOUEF, R.T., ROSSEN, C., ZELT, F.B., SULLIVAN, M.D., MOHRIG, D.C., and JENNETTE, D.C., 1999, Deep-Water Sandstones: Brushy Canyon Formation, west Texas: Tulsa, AAPG Course Note Series #40, 48 p.

BEBOUT, D.G., and HARRIS, P.M., 1986, Hydrocarbon Reservoir Studies, San Andres/Grayburg Formations, Permian Basin: Midland, Permian Basin Section-SEPM Pub. 86-26, 143 p.

BEBOUT, D.G., and KERANS, C., eds., 1993, Guide to the Permian Reef Geology Trail, McKittrick Canyon, Guadalupe Mountains National Park, west Texas: Austin, TX, Texas Bur. Econ. Geol., Guidebook 26, 48 p.

BENNETT, P., and SIEGEL, D.I., 1987, Increased solubility of quartz in water due to complexing by organic compounds: Nature, v. 326, p. 684-686.

BENNETT, P.C., MELCER, M.E., SIEGEL, D.I., and HASSETT, J.P., 1988, The dissolution of quartz in dilute aqueous solutions of organic acids at 25°C: Geochim. Cosmochim. Acta, v. 52, p. 1521-1530.

BENSON, L., and THOMPSON, R.S., 1987, The physical record of lakes in the Great Basin*, in* Ruddiman, W.F., and Wright, H.E., Jr., eds., The Geology of North America, Volume K-3, North America and Adjacent Oceans During the Last Deglaciation: Boulder, CO, GSA, p. 241-260.

BERG, R.R., 1979, Reservoir sandstones of the Delaware Mountain Group, southeast New Mexico, in Sullivan, N.M., ed., Guadalupian Delaware Mountain Group of West Texas and Southeast New Mexico: Midland, Permian Basin Section-SEPM Pub. 79-18, p. 75-95.

BJORKLUND, L.J., and MOTTS, W.S., 1959, Geology and groundwater resources of the Carlsbad area, New Mexico: U. S. Geol. Surv. Open-file Report 322, Section A7, 322 p.

BLANCHARD, W.G., JR., and DAVIS, M.J., 1929, Permian stratigraphy and structure of parts of southeastern New Mexico and southwestern Texas: AAPG Bull., v. 13, p. 957-995.

BORER, J.M., and HARRIS, P.M., 1991, Lithofacies and cyclicity of the Yates Formation, Permian Basin: implications for reservoir heterogeneity: AAPG Bull., v. 75, p. 726-779.

BOYD, D.W., 1958, Permian sedimentary facies, central Guadalupe Mountains, New Mexico: Socorro, NM Bur. Mines & Min. Resour. Bull. 49, 100 p.

BOZANICH, R.G., 1979, The Bell Canyon and Cherry Canyon Formations, eastern Delaware Basin, Texas: Lithology, environments and mechanisms of deposition, *in* Sullivan, N.M., ed., Guadalupian Delaware Mountain Group of West Texas and Southeast New Mexico: Midland, Permian Basin Section-SEPM Pub. 79-18, p. 121-141.

BROWN, A., 2006, Delaware (Lamar) Limestone roadcut, in Land, L., Lueth, V.W., Raatz, W., Boston, P., and Love, D.L., eds., Caves and Karst of Southeastern New Mexico, New Mexico Geol. Soc., 57th Annual Field Conf. Guidebook, p. 73-74.

BROWN, A.A., and LOUCKS, R.G., 1988a, Comments on Lamar Limestone road cuts, *in* Reid, S.T., Bass, R.O., and Welch, P., eds., Guadalupe Mountains Revisited, Texas and New Mexico: Midland, West Texas Geol. Soc. Pub. 88-84, p. 9-10.

BROWN, A.A., and LOUCKS, R.G., 1988b, Castiles in the Castile Formation, in Reid, S.T., Bass, R.O., and Welch, P., eds., Guadalupe Mountains Revisited, Texas and New Mexico: Midland, West Texas Geol. Soc. Publication 88-84, p. 114-116.

BROWN, A.A., and LOUCKS, R.G., 1993a, Influence of sediment type and depositional processes on stratal patterns in the Permian Basin-margin Lamar Limestone, McKittrick Canyon, Texas, *in* Loucks, R.G., and Sarg, J.F., eds., Carbonate Sequence Stratigraphy: Recent Developments and Applications: Tulsa, AAPG Memoir 57, p. 133-156.

BROWN, A.A., and LOUCKS, R.G., 1993b, Toe of slope, *in* Bebout, D.G., and Kerans, C., eds., Guide to the Permian Reef Geology Trail, McKittrick Canyon, Guadalupe Mountains National Park, West Texas: Austin, TX, University of Texas, Bur. Econ. Geol. Guidebook 26, p. 5-13.

BURKE, W.H., DENISON, R.E., HETHERINGTON, E.A., KOEPNICK, R.B., NELSON, H.F., and OTTO, J.B., 1982, Variation of seawater $^{87}Sr/^{86}Sr$ throughout Phanerozoic time: Geology, v. 10, p. 516-519.

CANDELARIA, M.P., 1982, Sedimentology and depositional environment of upper Yates Formation siliciclastics (Permian, Guadalupian), Guadalupe Mountains, southeast New Mexico [unpublished Master's thesis]: University of Wisconsin - Madison, Madison, WI, 267 p.

CANDELARIA, M.P., 1988, Synopsis of the Late Paleozoic depositional history of the Orogrande basin, New Mexico and Texas, *in* Robichaud, S.R., and Gallick, C.M., eds., Basin to Shelf Facies Transition of the Wolfcampian Stratigraphy of the Orogrande Basin: Midland, Permian Basin Section-SEPM Pub. No. 88-28, p. 1-4.

CANDELARIA, M.P., 1989, Shallow marine sheet sandstones, upper Yates Formation, Northwest Shelf, Delaware Basin, New Mexico, *in* Harris, P.M., and Grover, G.A., eds., Subsurface and Outcrop Examination of the Capitan Shelf Margin, Northern Delaware Basin: Tulsa, SEPM Core Workshop No. 13, p. 319-324.

CAPUTO, M.V., and CROWELL, J.C., 1985, Migration of glacial centers across Gondwana during Paleozoic Era: GSA Bull., v. 96, p. 1020-1036.

CARR, M., and GARDNER, M.H., 2000, Portrait of a basin-floor fan for sandy deepwater systems, Permian lower Brushy Canyon Formation, west Texas, *in* Bouma, A.H., and Stone, C.G., eds., Fine-Grained Turbidite Systems: Tulsa, SEPM Special Pub. No. 68/AAPG Memoir 72, p. 215-231.

CHAFETZ, H.S., and FOLK, R.L., 1984, Travertines: depositional morphology and the bacterially constructed constituents: Jour. Sediment. Petrol., v. 54, p. 289-316.

COLGAN, R.E., 1990, Depositional facies, diagenesis, and isotope stratigraphy of the San Andres Formation (Lower Guadalupian), northern Algerita escarpment, New Mexico [unpublished Master's thesis]: Southern Methodist University, Dallas, TX, 163 p.

COOPER, G.A., and GRANT, R.E., 1972, Permian brachiopods of west Texas, Pt. I: Smithsonian Contributions to Paleobiology No. 14, p. 231.

COOPER, G.A., and GRANT, R.E., 1974, Permian brachiopods of west Texas, Pt. II: Washington, D.C., Smithsonian Contributions to Paleobiology No. 15, p. 233-793.

COOPER, G.A., and GRANT, R.E., 1975, Permian brachiopods of west Texas, Pt. III: Washington, D.C., Smithsonian Contributions to Paleobiology No. 19, p. 795-1921.

COOPER, G.A., and GRANT, R.E., 1976a, Permian brachiopods of west Texas, Pt. IV: Smithsonian Contributions to Paleobiology No. 21, p. 503-662.

COOPER, G.A., and GRANT, R.E., 1976b, Permian brachiopods of west Texas, Pt. V: Smithsonian Contributions to Paleobiology No. 24, p. 2609-3159.

COOPER, G.A., and GRANT, R.E., 1977, Permian brachiopods of west Texas, Pt. VI: Smithsonian Contributions to Paleobiology No. 32, p. 3161-3370.

CRANDALL, K.H., 1929, Permian stratigraphy of southeastern New Mexico and adjacent parts of western Texas: AAPG Bull., v. 13, p. 927-944.

CRAWFORD, G.A., 1981, Depositional history and diagenesis of the Goat Seep Dolomite (Permian, Guadalupian), Guadalupe Mountains, west Texas-New Mexico [unpublished Ph.D. thesis]: University of Wisconsin-Madison, Madison, WI, 300 p.

CRAWFORD, G.A., 1988, Toe-of-slope sedimentation, Goat Seep and Getaway carbonates, Western Escarpment, Guadalupe Mountains, west Texas, *in* Reid, S.T., Bass, R.O., and Welch, P., eds., Guadalupe Mountains Revisited, Texas and New Mexico: Midland, West Texas Geol. Soc. Pub. 88-84, p. 163-168.

CRAWFORD, G.A., 1989, Goat Seep — precursor to the Capitan, *in* Harris, P.M., and Grover, G.A., eds., Subsurface and Outcrop Examination of the Capitan Shelf Margin, Northern Delaware Basin: Tulsa, SEPM Core Workshop No. 13, p. 373-378.

CROWELL, J.C., 1978, Gondwana glaciation, cyclothems, continental positioning, and climate changes: American Jour. of Science, v. 278, p. 1345-1372.

CROWELL, J.C., 1982, Continental glaciation through geologic times, Climate in Earth History: National Academy of Sciences, Studies in Geophysics: Washington, D.C., National Academy Press, p. 77-82.

CUNNINGHAM, B.K., and CROMWELL, D.W., 1989, The Lower Paleozoic of west Texas and southern New Mexico — Modern Exploration Concepts: Midland, Permian Basin Section-SEPM Pub. No. 89-31, 223 p.

CYS, J.M., TOOMEY, D.F., BREZINA, J.L., GREENWOOD, E., GROVES, D.B., KLEMENT, K.W., KULLMANN, J.D., McMILLAN, T.L., SCHMIDT, V., SNEED, E.D., and WAGNER, L.H., 1977, Capitan Reef — evolution of a concept, *in* Hileman, M.E., and Mazzullo, S.J., eds., Upper Guadalupian Facies, Permian Reef Complex, Guadalupe Mountains, New Mexico and West Texas: Midland, Permian Basin Section-SEPM Pub. 77-16, p. 201-322.

DAVIES, G.R., 1977, Former magnesian calcite and aragonite submarine cements in Upper Paleozoic reefs of the Canadian Arctic: a summary: Geology, v. 5, p. 11-15.

DAVIES, G.R., and KROUSE, H.R., 1975, Carbon and oxygen isotopic composition of Late Paleozoic calcite cements, Canadian Arctic Archipelago — preliminary results and interpretation: Ottawa, ON, Geol. Surv. of Canada Paper 75-1, part B, p. 215-220.

DEAN, W.E., and ANDERSON, R.Y., 1978, Salinity cycles — evidence for deepwater deposition of the Castile and lower Salado Formations, Delaware basin, Texas and New Mexico, *in* Austin, G.S., ed., Geology and Mineral Deposits of Ochoan Rocks in Delaware Basin and Adjacent Areas: Socorro, NM, NM Bur. Mines & Min. Resour. Circular 159, p. 15-20.

DeFORD, R.K., and RIGGS, G.D., 1941, Tansill Formation, west Texas and southeastern New Mexico: AAPG Bull., v. 25, p. 1713-1728.

DOLTON, G.L., COURY, A.B., FREZON, S.E., ROBINSON, K., VARNES, K.L., WUNDER, J.M., and ALLEN, R.W., 1979, Estimates of undiscovered oil and gas, Permian Basin, west Texas and southeast New Mexico: U. S. Geol. Surv. Open-file Report 79-838, p. 1-118.

DUCHENE, H.R., and McLEAN, J.S., 1989, The role of hydrogen sulfide in the evolution of caves in the Guadalupe Mountains of southeastern New Mexico, *in* Harris, P.M., and Grover, G.A., eds., Subsurface and Outcrop Examination of the Capitan Shelf Margin, Northern Delaware Basin: Tulsa, SEPM Core Workshop No. 13, p. 475-481.

DUNHAM, R.J., 1969, Vadose pisolite in the Capitan reef (Permian), New Mexico and Texas, *in* Friedman, G.M., ed., Depositional Environments in Carbonate Rocks: Tulsa, SEPM Special Pub. 14, p. 182-191.

DUNHAM, R.J., 1970, Stratigraphic reefs versus ecologic reefs: AAPG Bull., v. 54, p. 1931-1932.

DUNHAM, R.J., 1972, Capitan Reef, New Mexico and Texas: Facts and questions to aid interpretation and group discussion: Midland, Permian Basin Section-SEPM Pub. 72-141, 272 p.

DUTTON, S.P., KIM, E.M., BROADHEAD, R.F., BRETON, C.L., RAATZ, W.D., RUPPEL, S.C., and KERANS, C., 2004, Play Analysis and Digital Portfolio of Major Oil Reservoirs in the Permian Basin: Application and transfer of advanced geological and engineering technologies for incremental production opportunities: Austin, TX, Bur. Econ. Geol. and New Mexico Bureau of Geology & Mineral Resources, 104 p.

ESTEBAN, M., and PRAY, L.C., 1977, Origin of the pisolite facies of the shelf crest, *in* Hileman, M.E., and Mazzullo, S.J., eds., Upper Guadalupian Facies, Permian Reef Complex, Guadalupe Mountains, New Mexico and west Texas

(1977 Field Conf. Guidebook): Midland, Permian Basin Section-SEPM Pub. 77-16, p. 479-486.

FIELDING, C.R., FRANK, T.D.B.L.P., THOMAS, S.G.R.M.C., and JONES, A.T., 2005, Revised Permian glacial record of eastern Australia [abs.]: Geol. Soc. Amer., Abstracts with Programs , 2005 annual meeting, v. 37, p. 256.

FISCHER, A.G., and SARNTHEIN, M., 1988, Airborne silts and dune-derived sands in the Permian of the Delaware Basin: Jour. Sediment. Petrol., v. 58, p. 637-643.

FORD, T.D., and PEDLEY, H.M., 1996, A review of tufa and travertine deposits of the world: Earth-Science Reviews, v. 41, p. 117-175.

FRAKES, L.A., and FRANCIS, J.E., 1988, A guide to Phanerozoic cold polar climates from high-latitude ice-rafting in the Cretaceous: Nature, v. 333, p. 547-549.

FRANSEEN, E.K., 1985, Sedimentology of the Grayburg and Queen Formations (Guadalupian) and the shelf margin erosion surface, western escarpment, Guadalupe Mountains, west Texas [unpublished Master's thesis]: University of Wisconsin-Madison, Madison, WI, 188 p.

FRANSEEN, E.K., 1988, The Grayburg and Queen Formations (Permian) and the associated erosion surface at the shelf margin, Western Escarpment, Guadalupe Mountains, west Texas*, in* Reid, S.T., Bass, R.O., and Welch, P., eds., Guadalupe Mountains Revisited, Texas and New Mexico: Midland, West Texas Geol. Soc. Pub. 88-84, p. 155-162.

FRANSEEN, E.K., 1989, Depositional sequences and correlation of Middle to Upper Miocene carbonate complexes, Las Negras area, southeastern Spain [unpublished Ph.D. thesis]: University of Wisconsin-Madison, Madison, WI, 374 p.

FRANSEEN, E.K., FEKETE, T.E., and PRAY, L.C., 1989, Evolution and destruction of a carbonate bank at the shelf margin: Grayburg Formation (Permian), western escarpment, Guadalupe Mountains, Texas*, in* Crevello, P.D., Wilson, J.L., Sarg, J.F., and Read, J.F., eds., Controls on Carbonate Platform and Basin Development: Tulsa, SEPM Special Pub. No. 44, p. 289-304.

FRENZEL, H.N., 1988, The Indian Basin Upper Pennsylvanian gas field, Eddy County, New Mexico*, in* Reid, S.T., Bass, R.O., and Welch, P., eds., Guadalupe Mountains Revisited, Texas and New Mexico [1988 Field Seminar]: Midland, West Texas Geol. Soc. Pub. 88-84, p. 169-170.

FRIEDMAN, G.M., 1966, Occurrence and origin of Quaternary dolomite of Salt Flat, west Texas: Jour. Sediment. Petrol., v. 36, p. 263-267.

GALLOWAY, W.E., EWING, T.E., GARRETT, C.M., TYLER, N., and BEBOUT, D.G., 1983, Atlas of Major Texas Oil Reservoirs: Austin, TX, University of Texas, Bur. Econ. Geol., 139 p.

GARBER, R.A., GROVER, G.A., and HARRIS, P.M., 1989, Geology of the Capitan shelf margin — subsurface data from the northern Delaware Basin*, in* Harris, P.M., and Grover, G.A., eds., Subsurface and Outcrop Examination of the Capitan Shelf Margin, Northern Delaware Basin: Tulsa, SEPM Core Workshop No. 13, p. 3-269.

GARDNER, M.H., 1991, High-frequency cyclicity within shelf-margin and slope strata of the Upper San Andres sequence, Last Chance Canyon*, in* Meader-Roberts, S., Candelaria, M.P., and Moore, G., eds., Sequence Stratigraphy, Facies and Reservoir Geometries of the San Andres, Grayburg, and Queen Formations, Guadalupe Mountains, New Mexico and Texas: Midland, Permian Basin Section-SEPM Pub. 91-32, p. 11-51.

GARDNER, M.H., and BORER, J.M., 2000, Submarine channel architecture along a slope to basin profile, Brushy Canyon Formation, West Texas*, in* Bouma, A.H., and Stone, C.G., eds., Fine-Grained Turbidite Systems: Tulsa, SEPM Special Pub. No. 68/AAPG Memoir 72, p. 195-213.

GAWLOSKI, T.F., 1987, Nature, distribution, and petroleum potential of Bone Spring detrital sediments along the Northwest Shelf of the Delaware Basin*, in* Cromwell, D.W., and Mazzullo, L., eds., The Leonardian Facies in W. Texas and S. E. New Mexico and Guidebook to the Glass Mountains, West Texas: Midland, Permian Basin Section-SEPM Pub. 87-27, p. 85-106.

GEISEN, J.H., and SCHOLLE, P.A., 1990, Regional basinal sandstone depositional patterns during the Guadalupian (Late Permian), Delaware basin, west Texas-New Mexico [abs.]: AAPG Bull., v. 74, p. 660-661.

GINSBURG, R.N., 1964, South Florida carbonate sediments: Boulder, CO, GSA, Guidebook for Field Trip No. 1 (Miami Beach Meeting), 72 p.

GINSBURG, R.N., and JAMES, N.P., 1976, Submarine botryoidal aragonite in Holocene reef limestones, Belize: Geology, v. 4, p. 431-436.

GIVEN, R.K., and LOHMANN, K.C., 1986, Isotopic evidence for the early meteoric diagenesis of the reef facies, Permian reef complex of west Texas and New Mexico: Jour. Sediment. Petrol., v. 56, p. 183-193.

GLENNIE, K.W., 1970, Desert Sedimentary Environments: New York, Elsevier, 222 p.

GOETZ, L.K., and DICKERSON, P.W., 1985, A Paleozoic transform margin in Arizona, New Mexico, west Texas and northern Mexico*, in* Dickerson, P.W., and Muehlberger, W.R., eds., Structure and Tectonics of Trans-Pecos Texas: Midland, West Texas Geol. Soc. Pub. 85-81, p. 173-184.

GRADSTEIN, F.M., OGG, J.G., and SMITH, A.G., 2004, A Geologic Time Scale 2004: Cambridge, U.K., Cambridge University Press, 589 p.

GRAUTEN, W.F., 1965, Fluid relationships in Delaware Mountain sandstone*, in* Young, A., and Galley, J.E., eds., Fluids in Subsurface Environments: Tulsa, AAPG Memoir 4, p. 294-307.

GROSSMAN, E.L., 1994, The carbon and oxygen isotope record during the evolution of Pangea: Carboniferous to Triassic*, in* Klein, G.D., ed., Pangea: Paleoclimate, Tectonics, and Sedimentation During Accretion, Zenith, and Breakup of a Supercontinent: Boulder, CO, GSA Special Paper 288, p. 207-228.

GROTZINGER, J.P., and KNOLL, A.H., 1995, Anomalous carbonate precipitates: is the Precambrian the key to the Permian?: Palaios, v. 10, p. 578-596.

HALLEY, R.B., and SCHOLLE, P.A., 1985, Radiaxial fibrous calcite as early-burial, open-system cement: isotopic evidence from Permian of China [abs.]: AAPG Bull., v. 69, p. 261.

HANDFORD, C.R., KENDALL, A.C., PREZBINDOWSKI, D.R., DUNHAM, J.B., and LOGAN, B.W., 1984, Salina-margin tepees, pisoliths, and aragonite cements, Lake MacLeod, Western Australia: their significance in interpreting ancient analogs: Geology, v. 12, p. 523-527.

HARMS, J.C., 1974, Brushy Canyon Formation, Texas: A deep-water density current deposit: GSA Bull., v. 85, p. 1763-1784.

HARMS, J.C., and WILLIAMSON, C.R., 1988, Deep-water density current deposits of Delaware Mountain Group (Permian), Delaware Basin, Texas and New Mexico: AAPG Bull., v. 72, p. 299-317.

HARRIS, P.M., KERANS, C., and BEBOUT, D.G., 1993, Ancient outcrop and modern examples of platform carbonate cycles — implications for subsurface correlation and understanding reservoir heterogeneity*, in* Loucks, R.G., and Sarg, J.F., eds., Carbonate Sequence Stratigraphy: Recent Developments and Applications: Tulsa, AAPG Memoir 57, p. 475-492.

HARRIS, P.M., and SIMO, J.A., 2000, Permian Platforms and Reefs in the Guadalupe and Hueco Mountains: Tulsa, SEPM-IAS Research and Field Conf. Guidebook (17-19 May 2000), 82+ p.

HARRIS, P.M., and WIGGINS, W.D., 1985, Allochthonous carbonates of the Getaway Limestone*, in* Crevello, P.D., and Harris, P.M., eds., Deep-water Carbonates — a core workshop (New Orleans, March 23-24, 1985): Tulsa, SEPM Core Workshop No. 6, p. 174-211.

HARRISON, S.C., 1966, Depositional mechanics of Cherry Canyon sandstone tongue [unpublished Master's thesis]: Texas Tech College, Lubbock, TX, 114 p.

HARWOOD, G.M., 1989, Large-scale channel development within the Capitan reef complex — evidence from Carlsbad Caverns*, in* Harris, P.M., and Grover, G.A., eds., Subsurface and Outcrop Examination of the Capitan Shelf Margin, Northern Delaware Basin: Tulsa, SEPM Core Workshop No. 13, p. 379-386.

HAYES, P.T., 1964, Geology of the Guadalupe Mountains, New Mexico: U. S. Geol. Surv. Prof. Pap. 446, 69 p.

HAYES, P.T., and GALE, B.T., 1957, Geology of the Carlsbad Caverns East quadrangle, New Mexico: U. S. Geol. Surv. Geologic Quadrangle Map GQ-98.

HEEZEN, B.C., and DRAKE, C.L., 1964, Grand Banks slump: AAPG Bull., v. 48, p. 221-225.

HENDERSON, C.M., 2005, International correlation of the marine Permian time scale, in Lucas, S.G., and Ziegler, K.E., eds., The Nonmarine Permian: Albuquerque, NM, New Mexico Museum of Natural History and Science Bull. 30, p. 104-105.

HILL, C.A., 1987, Geology of Carlsbad Cavern and other caves in the Guadalupe Mountains, New Mexico and Texas, NM Bur. Mines & Min. Resour. Bull. 117, 150 p.

HILL, C.A., 1990, Sulfuric acid speleogenesis of Carlsbad Cavern and its relationship to hydrocarbons, Delaware Basin, New Mexico and Texas: AAPG Bull., v. 74, p. 1685-1694.

HILL, C.A., 1993, Geologic walking tour of Carlsbad Cavern*, in* Love, D.W., Hawley, J.W., Kues, B.S., Adams, J.W., Austin, G.S., and Barker, J.M., eds., Carlsbad Region, New Mexico and West Texas, New Mexico Geol. Soc., 44th Annual Field Conf. Guidebook, p. 117-128.

HILLS, J.M., 1984, Sedimentation, tectonism, and hydrocarbon generation in Delaware Basin, west Texas and southeastern New Mexico: AAPG Bull., v. 68, p. 250-267.

HILLS, J.M., 1985, Structural evolution of the Permian Basin of west Texas and New Mexico, *in* Dickerson, P.W., and Muehlberger, W.R., eds., Structure and tectonics of Trans-Pecos Texas: Midland, West Texas Geol. Soc. Pub. 85-81, p. 89-99.

HISS, W.L., 1980, Movement of ground water in Permian Guadalupian aquifer systems, southeastern New Mexico and western Texas, in Dickerson, P.W., and Hoffer, J.M., eds., Trans-Pecos Region, Southeastern New Mexico and West Texas: 31st Field Conf. Guidebook: Albuquerque, NM, New Mexico Geol. Soc., p. 289-294.

HOBSON, J.P., JR., CALDWELL, C.D., and TOOMEY, D.F., 1985, Early Permian deep-water allochthonous limestone facies and reservoir, west Texas: AAPG Bull., v. 69, p. 2130-2147.

HOLT, R.M., POWERS, D.W., and LOWENSTEIN, T.K., 2006, Halite depositional cycles in the Upper Permian Salado Formation, in Land, L., Lueth, V.W., Raatz, W., Boston, P., and Love, D.L., eds., Caves and Karst of Southeastern New Mexico, New Mexico Geol. Soc., 57th Annual Field Conf. Guidebook, p. 75-77.

HULL, J.P.D., JR, 1957, Petrogenesis of Permian Delaware Mountain sandstone, Texas and New Mexico: AAPG Bull., v. 41, p. 278-307.

HUNT, D., FITCHEN, W.M., and KOSAA, E., 2002, Syndepositional deformation of the Permian Capitan reef carbonate platform, Guadalupe Mountains, New Mexico, USA: Sed. Geology, v. 154, p. 89-126.

HURLEY, N.F., 1979, Seaward primary dip of fall-in beds, lower Seven Rivers Formation, Permian Guadalupe Mountains [abs.]: AAPG Bull., v. 63, p. 471.

HURST, J.M., SCHOLLE, P.A., and STEMMERIK, L., 1988, Submarine cemented bryozoan mounds, Upper Permian, Devondal, East Greenland, *in* Geldsetzer, H.J., James, N.P., and Tebbutt, G.E., eds., Reefs, Canada and Adjacent Areas: Calgary, Canada, Can. Soc. Petrol. Geol. Memoir 13, p. 672-676.

HUSSAIN, M., ROHR, D.M., and WARREN, J.K., 1988, Depositional environments and facies in a Quaternary continental sabkha, *in* Reid, S.T., Bass, R.O., and Welch, P., eds., Guadalupe Mountains Revisited, Texas and New Mexico: Midland, West Texas Geol. Soc. Pub. 88-84, p. 177-186.

HUSSAIN, M., and WARREN, J.K., 1985, Origin of laminae in Holocene-Pleistocene evaporite sequence of Salt Flat playas, west Texas and New Mexico [abs.]: AAPG Bull., v. 69, p. 268.

HUSSAIN, M., and WARREN, J.K., 1988, Dolomitization in a sulfate-rich environment: modern example from Salt Flat sabkha (dried playa lake) in west Texas-New Mexico: Carbonates and Evaporites, v. 3, p. 165-273.

IRVING, E., and IRVING, G.A., 1982, Apparent polar wander paths Carboniferous through Cenozoic and the assembly of Gondwana: Geophysical Surveys, v. 5, p. 141-188.

JACKA, A.D., BECK, R.H., ST. GERMAIN, L.C., and HARRISON, S.C., 1968, Permian deep-sea fans of the Delaware Mountain Group (Guadalupian), Delaware basin, Guadalupian Facies, Apache Mountains Area, West Texas: Midland, Permian Basin Section-SEPM Pub., p. 49-90.

JAGNOW, D.H., 1979, Cavern development in the Guadalupe Mountains: Columbus, OH, Cave Research Foundation, 55 p.

JAMES, N.P., and GINSBURG, R.N., 1979, The seaward margin of Belize barrier and atoll reefs: Oxford, Internat. Assoc. Sedimentol. Special Pub. No. 3, 191 p.

KELLEY, V.C., 1971, Geology of the Pecos country, southeastern New Mexico: Socorro, NM, NM Bur. Mines & Min. Resour. Memoir 24, 75 p.

KELLEY, V.C., 1972, Geometry and correlation along Permian Capitan escarpment, New Mexico and Texas: AAPG Bull., v. 56, p. 2192-2211.

KENDALL, A.C., and HARWOOD, G.M., 1989, Shallow-water gypsum in the Castile Formation — significance and implications, *in* Harris, P.M., and Grover, G.A., eds., Subsurface and Outcrop Examination of the Capitan Shelf Margin, Northern Delaware Basin: Tulsa, SEPM Core Workshop No. 13, p. 451-457.

KENDALL, C.G.St.C., 1969, An environmental re-interpretation of the Permian evaporite-carbonate shelf sediments of the Guadalupe Mountains: GSA Bull., v. 80, p. 2503-2526.

KENDALL, C.G.St.C., and WARREN, J., 1987, A review of the origin and setting of tepees and their associated fabrics: Sedimentology, v. 34, p. 1007-1028.

KERANS, C., and FITCHEN, W.M., 1995, Sequence hierarchy and facies architectures of a carbonate-ramp system: San Andres Formation of Algerita Escarpment and western Guadalupe Mountains, west Texas and New Mexico: Austin, TX, University of Texas, Bur. Econ. Geol. Report of Investigations No. 235, 86 p.

KERANS, C. and FITCHEN, W. M., 1997, Stratigraphic constraints on the origin of Brushy Canyon sandstones: West Texas Geol. Soc. Bull., v. 36 (5), p. 5-10.

KERANS, C., and KEMPTER, K., 2002, Hierarchical Stratigraphic Analysis of a Carbonate Platform, Permian of the Guadalupe Mountains: Tulsa, AAPG Discovery Series, No. 5 (CD-ROM).

KERANS, C., LUCIA, F. J. and SENGER, R. K., 1994, Integrated characterization of carbonate ramp reservoirs using Permian San Andres Formation outcrop analogs: AAPG Bull., v. 78, p. 181-216.

KERANS, C., and NANCE, H.S., 1991, High frequency cyclicity and regional depositional patterns of the Grayburg Formation, Guadalupe Mountains, New Mexico, *in* Meader-Roberts, S., Candelaria, M.P., and Moore, G.E., eds., Sequence Stratigraphy, Facies, and Reservoir Geometries of the San Andres, Grayburg, and Queen Formations, Guadalupe Mountains, New Mexico and Texas: Midland, Permian Basin Section-SEPM Pub. 91-32, p. 53-69.

KESSLER, J.L.P., SOREGHAN, G.S., and WACKER, H.J., 2001, Equatorial aridity in western Pangea: Lower Permian loessite and dolomitic paleosols in northeastern New Mexico, U.S.A: Jour. Sed. Res., Section A: Sedimentary Petrology and Processes, v. 71, p. 817-832.

KING, P.B., 1948, Geology of the southern Guadalupe Mountains, Texas: U. S. Geol. Surv. Prof. Pap. 215, 183 p.

KING, P.B., 1967, Reef and associated deposits in the Permian of west Texas, in McKee, E.D., ed., Paleotectonic Maps of the Permian System: U. S. Geol. Survey Misc, Invest. Map I-450 (with text), p. 36-44.

KIRKLAND, B.L., BANNER, J.L., LYNCH, F.L., and WARD, W.B., 1999a, A dynamic model for formation of the tepee-pisoid facies in the Permian reef complex Guadalupe Mountains, New Mexico: AAPG, Official Program 1999 Annual Convention, v. 8, p. A73.

KIRKLAND, B.L., LONGACRE, S.A., and STOUDT, E.L., 1999b, The dynamic Capitan Reef: An image of an ancient reef and suggestions for future research, *in* Saller, A.H., Harris, P.M., Kirkland, B.L., and Mazzullo, S.J., eds., Geologic Framework of the Capitan Reef: Tulsa, SEPM Special Pub. No. 65, p. 161-173.

KIRKLAND, B.L., and MOORE, C.H., Jr., 1990, New evidence for the barrier reef model, Permian Capitan reef complex, New Mexico [abs.]: AAPG Bull., v. 74, p. 696.

KIRKLAND, B.L., and MOORE, C.H., 1996, Microfacies analysis of the Tansill outer shelf, Permian Reef Complex, *in* Martin, R.L., ed., Permian Basin Oil and Gas Fields: Keys to Success that Unlock Future Reserves: Midland, West Texas Geol. Soc. Pub. 96-101, p. 99-106.

KIRKLAND, D.W., 2003, An explanation for the varves of the Castile evaporites (Upper Permian), Texas and New Mexico, U.S.A.: Sedimentology, v. 50, p. 899-920.

KIRKLAND, D.W., DENISON, R.E., and DEAN, W.E., 2000, Parent brine of the Castile evaporites (Upper Permian), Texas and New Mexico: Jour. Sed. Res., Section A: Sedimentary Petrology and Processes, v. 70, p. 749-761.

KLUTH, C.F., and CONEY, P.J., 1981, Plate tectonics of the ancestral Rocky Mountains: Geology, v. 9, p. 10-15.

LAND, L., LUETH, V.W., RAATZ, W., BOSTON, P., and LOVE, D.L., 2006, Caves and Karst of Southeastern New Mexico, New Mexico Geol. Soc., 57th Annual Field Conf. Guidebook, 344 p.

LANG, W.B., 1937, The Permian formations of the Pecos Valley of New Mexico and Texas: AAPG Bull., v. 21, p. 833-898.

LAWSON, E.C., 1989a, Subaqueous gravity flows in the Rader Member, Capitan reef complex (Permian), Delaware Mountains, west Texas, *in* Harris, P.M., and Grover, G.A., eds., Subsurface and Outcrop Examination of the Capitan Shelf Margin, Northern Delaware Basin: Tulsa, SEPM Core Workshop No. 13, p. 427-430.

LAWSON, E.G., 1989b, Subaqueous gravity flows and associated deposits in the Rader Member, Capitan reef complex (Permian), Delaware Mountains, west Texas [unpublished Master's thesis]: University of Wisconsin-Madison, Madison, WI, 160 p.

LEMONE, D.V., 1988, Precambrian and Paleozoic stratigraphy; Franklin Mountains, west Texas, *in* Hayward, O.T., ed., South-Central Section of the GSA: Boulder, CO, GSA Centennial Field Guide Volume 4, p. 387-394.

LEMONE, D.V., and LOVEJOY, E.M.P., 1976, Symposium on the Franklin

Mountains: El Paso, TX, El Paso Geol. Soc. Field Trip Guidebook, 250 p.
LESLIE, A., KENDALL, A., and HARWOOD, G., 1993, The Castile Formation: a continuing paradox, *in* Love, D.W., Hawley, J.W., Kues, B.S., Adams, J.W., Austin, G.S., and Barker, J.M., eds., Carlsbad Region, New Mexico and West Texas, New Mexico Geol. Soc. 44th Annual Field Conf. Guidebook, p. 13-14.
LINDSAY, R.F., and REED, C.L., 1992, Sequence Stratigraphy Applied to Permian Basin Reservoirs: Outcrop Analogs in the Caballo and Sacramento Mountains of New Mexico: Midland, West Texas Geol. Soc. Pub. No. 92-92, 131 p.
LLOYD, E.R., 1929, Capitan Limestone and associated formations of New Mexico and Texas: AAPG Bull., v. 13, p. 645-658.
LOCK, D.E., and BURNE, R.V., 1986, Modern carbonate sedimentation in the coastal regions of the Coorong, Yorke Peninsula and Spencer Gulf, South Australia, including Lake Eliza and Fisherman Bay, 12th International Sedimentological Congress, Sediments Down-under, *in* Post-Congress Field Tour 19B, Guidebook: Canberra, Bureau of Mineral Resources, Geology and Geophysics, p. 1-59.
LOFTIN, T.R., Jr., 1996, Depositional stacking patterns within the Cherry Canyon Formation, Delaware Basin, west Texas, *in* DeMis, W.D., and Cole, A.G., eds., The Brushy Canyon Play in Outcrop and Subsurface: Concepts and Examples: Midland, Permian Basin Section - SEPM Pub. 96-38, p. 137-145.
LOGAN, B.W., 1987, The MacLeod Evaporite Basin, Western Australia: Tulsa, AAPG Memoir 44, 140 p.
LOHMANN, K.C., and MEYERS, W.J., 1977, Microdolomite inclusions in cloudy prismatic calcites: a proposed criterion for former high magnesium calcites: Jour. Sediment. Petrol., v. 47, p. 1075-1088.
LONGLEY, A.J., 1999, Differential compaction and its effects on the outer shelf of the Permian Capitan reef complex, Guadalupe Mountains, New Mexico, *in* Saller, A.H., Harris, P.M., Kirkland, B.L., and Mazzullo, S.J., eds., Geologic Framework of the Capitan Reef: Tulsa, SEPM Special Pub. No. 65, p. 85-105.
LOUCKS, R.G., and FOLK, R.L., 1976, Fanlike rays of former aragonite in Permian Capitan reef pisolite: Jour. Sediment. Petrol., v. 46, p. 483-485.
LOWENSTEIN, T., 1983, Deposition and alteration of an ancient potash evaporite: the Permian Salado Formation of New Mexico and west Texas [unpublished Ph.D. thesis]: John Hopkins University, Baltimore, MD, 410 p.
LOWENSTEIN, T.K., 1988, Origin of depositional cycles in a Permian "saline giant": the Salado (McNutt zone) evaporites of New Mexico and Texas: GSA Bull., v. 100, p. 592-608.
MACINTYRE, I.G., 1977, Distribution of submarine cements in a modern Caribbean fringing reef, Galeta Point, Panama: Jour. Sediment. Petrol., v. 47, p. 503-516.
MACINTYRE, I.G., 1985, Submarine cements — the peloidal question, *in* Schneidermann, N., and Harris, P.M., eds., Carbonate Cements: Tulsa, SEPM Special Pub. No. 36, p. 109-116.
MAGARITZ, M., ANDERSON, R.Y., HOLSER, W.T., SALTZMAN, E.S., and GARBER, J., 1983, Isotope shifts in the Late Permian of the Delaware Basin, Texas, precisely timed by varved sediments: Earth and Planetary Science Letters, v. 66, p. 111-124.
MATTICK, R.E., 1967, A seismic and gravity profile across the Hueco bolson, Texas: U. S. Geol. Surv. Prof. Pap. 575-D, p. 85-91.
MAZZULLO, L.J., and REID, A.M., II, 1987, Stratigraphy of the Bone Spring Formation (Leonardian) and depositional setting in the Scharb Field, Lea County, New Mexico, *in* Cromwell, D., and Mazzullo, L.J., eds., The Leonardian Facies in W. Texas and S. E. New Mexico and Guidebook to the Glass Mountains, West Texas: Midland, Permian Basin Section-SEPM Pub. 87-27, p. 107-111.
MAZZULLO, S.J., BISCHOFF, W.D., and HEDRICK, C.L., 1989, Stacked island facies in Tansill outer-shelf platform, Dark Canyon, Guadalupe Mountains, New Mexico, *in* Harris, P.M., and Grover, G.A., eds., Subsurface and Outcrop Examination of the Capitan Shelf Margin, Northern Delaware Basin: Tulsa, SEPM Core Workshop No. 13, p. 287-293.
MAZZULLO, S.J., and CYS, J.M., 1977, Submarine cements in Permian boundstones and reef-associated rocks, Guadalupe Mountains, west Texas and southeastern New Mexico, *in* Hileman, M.E., and Mazzullo, S.J., eds., Upper Guadalupian Facies, Permian Reef Complex, Guadalupe Mountains, New Mexico and West Texas: Midland, Permian Basin Section-SEPM Pub. 77-16, p. 151-200.
MAZZULLO, J., MALICSE, A., and SIEGEL, J., 1991, Facies and depositional environments of the Shattuck Sandstone on the Northwest Shelf of the Permian Basin: Journal of Sedimentary Petrology, v. 61, p. 940-958.
McDANIEL, P.N., and PRAY, L.C., 1967, Bank to basin transition in Permian (Leonardian) carbonates, Guadalupe Mountains [abs.]: AAPG Bull., v. 51, p. 474.
McDERMOTT, R.W., 1983, Depositional processes and environments of the Permian Sandstone Tongue of the Cherry Canyon Formation and the upper San Andres Formation, Last Chance Canyon, southeastern New Mexico [unpublished Master's thesis]: University of Texas-Austin, Austin, TX, 179 p.
McGLASSON, E.H., and SEEWALD, K.O., 1968, Second day — El Paso to Hueco Mountains, *in* Stewart, W.J., ed., Delaware Basin Exploration [1968 Guidebook]: Midland, West Texas Geol. Soc. Pub. 68-55a, p. 24-34.
McKEE, E.D., ORIEL, S.S., and OTHERS, 1967a, Paleotectonic investigations of the Permian System in the United States: U. S. Geol. Surv. Prof. Pap. 515, 271 p.
McKEE, E.D., ORIEL, S.S., and OTHERS, 1967b, Paleotectonic maps of the Permian System: U. S. Geol. Surv. Miscellaneous Geological Investigations Map I-450, 164 p.
MCKENZIE, J.A., 1981, Holocene dolomitization of calcium carbonate sediments from the coastal sabkhas of Abu Dhabi, U.A.E.: a stable isotope study: Jour. Geology, v. 89, p. 185-198.
McNEAL, R.P., 1965, Hydrodynamics of the Permian basin, in Young, A., and Galley, J.E., eds., Fluids in Subsurface Environments: Tulsa, AAPG Memoir 4, p. 308-326.
MEADER-ROBERTS, S.J., 1983, Geology of the Sierra Diablo and southern Hueco Mountains, west Texas: Midland, Permian Basin Section-SEPM Pub. 83-22, 178 p.
MEADER-ROBERTS, S.J, CANDELARIA, M.P., and MOORE, G.E., 1991, Sequence Stratigraphy, Facies, and Reservoir Geometries of the San Andres, Grayburg, and Queen Formations, Guadalupe Mountains, New Mexico and Texas [Annual Field Trip Guidebook]: Midland, Permian Basin Section-SEPM Pub. 91-32, 141 p.
MEINZER, O.E., RENICK, B.C., and BRYAN, K., 1926, Geology of No. 3 Reservoir Site of the Carlsbad Irrigations Project, New Mexico, with reference to water-tightness: U. S. Geol. Surv. Water-Supply Paper 580-A, 39 p.
MEISSNER, F.F., 1972, Cyclic sedimentation in middle Permian strata of the Permian basin, *in* Elam, J.G., and Chuber, S., eds., Cyclic Sedimentation in the Permian Basin, second edition: Midland, West Texas Geol. Soc. Pub. 72-60, p. 203-232.
MELIM, L.A., 1991, The origin of dolomite in the Permian (Guadalupian) Capitan Formation, Delaware Basin, west Texas and New Mexico: implications for dolomitization models [unpublished Ph.D. thesis]: Southern Methodist University, Dallas, TX, 200 p.
MELIM, L.A., and SCHOLLE, P.A., 1989a, Dolomitization model for the forereef facies of the Permian Capitan Formation, Guadalupe Mountains, Texas-New Mexico, *in* Harris, P.M., and Grover, G.A., eds., Subsurface and Outcrop Examination of the Capitan Shelf Margin, Northern Delaware Basin: Tulsa, SEPM Core Workshop No. 13, p. 407-413.
MELIM, L.A., and SCHOLLE, P.A., 1989b, Subaerial exposure and erosion in the Capitan reef (Permian), Guadalupe Mountains, New Mexico [abs.]: AAPG Bull., v. 73, p. 390.
MELIM, L.A., and SCHOLLE, P.A., 1999, Diagenesis of the Capitan Formation forereef facies (Permian, west Texas and New Mexico), *in* Saller, A.H., Harris, P.M., Kirkland, B.L., and Mazzullo, S.J., eds., Geologic Framework of the Capitan Reef: Tulsa, SEPM Special Pub. No. 65, p. 193-210.
MELIM, L.A., and SCHOLLE, P.A., 2002, Dolomitization of the Capitan Formation forereef facies (Permian, west Texas and New Mexico): seepage reflux revisited: Sedimentology, v. 49, p. 1207-1227.
MENNING, M., and 19 others, 2006, Global time scale and regional stratigraphic reference scale of Central and West Europe, East Europe, Tethys, South China, and North America as used in the Devonian-Carboniferous-Permian Correlation Chart 2003 (DCP 2003): Palaeogeography, Palaeoclimatology, Palaeoecology, v. 240, p. 318-372.
MOTTS, W.S., 1962a, Generalized geology of part of the Guadalupe Mountains and vicinity, Permian of the Central Guadalupe Mountains, Eddy County, New Mexico (Guidebook): Midland, Hobbs, Roswell, and West Texas Geol. Socs. Pub. 62-48, p. 99-100.
MOTTS, W.S., 1962b, Geology of the West Carlsbad quadrangle, New Mexico: U. S. Geol. Surv. Geologic Quadrangle Map GQ-167.

MOTTS, W.S., 1968, The control of ground-water occurrence by lithofacies in the Guadalupian reef complex near Carlsbad, New Mexico: GSA Bull., v. 79, p. 283-298.

MRUK, D.H., 1985, Cementation and dolomitization of the Capitan Limestone (Permian), McKittrick Canyon, west Texas [unpublished Master's thesis]: University of Colorado, Boulder, CO, 153 p.

MRUK, D.H., 1989, Diagenesis of the Capitan Limestone, Upper Permian, McKittrick Canyon, west Texas, *in* Harris, P.M., and Grover, G.A., eds., Subsurface and Outcrop Examination of the Capitan Shelf Margin, Northern Delaware Basin: Tulsa, SEPM Core Workshop No. 13, p. 387-406.

MULLINS, H.T., NEWTON, C.R., HEATH, K., and VAN BUREN, H.M., 1981, Modern deep-water coral mounds north of Little Bahama Bank: criteria for the recognition of deep-water coral bioherms in the rock record: Jour. Sediment. Petrol., v. 51, p. 999-1013.

MULTER, H.G., 1969, Field Guide to Some Carbonate Rock Environments: Florida Keys and Western Bahamas: Miami, FL, Miami Geol. Soc., 159 p.

MUTTI, M., and SIMO, J.A., 1993, Stratigraphic patterns and cycle-related diagenesis of upper Yates Formation, Permian, Guadalupe Mountains, *in* Loucks, R.G., and Sarg, J.F., eds., Carbonate Sequence Stratigraphy: Recent Developments and Applications: Tulsa, AAPG Memoir 57, p. 515-534.

NAIMAN, E.R., 1982, Sedimentation and diagenesis of a shallow-marine carbonate and siliciclastic shelf sequence: the Permian (Guadalupian) Grayburg Formation, southeastern New Mexico [unpublished Master's thesis]: University of Texas - Austin, Austin, TX, 197 p.

NELSON, L.A., and HAIGH, B.R., 1958, Franklin and Hueco Mountains, Texas: Midland, West Texas Geol. Soc. 1958 Field Trip Guidebook, 91 p.

NESTELL, M.K., NESTELL, G.P., WARDLAW, B.R., and SWEATT, M.J., 2006, Integrated biostratigraphy of foraminifers, radiolarians and conodonts in shallow and deep water Middle Permian (Capitanian) deposits of the "Rader slide", Guadalupe Mountains, west Texas: Stratigraphy, v. 3, p. 161-194.

NEUMANN, A.C., and BALL, M.M., 1970, Submersible observations in the Straits of Florida: geology and bottom currents: GSA Bull., v. 81, p. 2861-2874.

NEUMANN, A.C., KOFOED, J.W., and KELLER, G.H., 1977, Lithoherms in the Straits of Florida: Geology, v. 5, p. 4-10.

NEWELL, N.D., RIGBY, J.K., FISCHER, A.G., WHITEMAN, A.J., HICKOX, J.E., and BRADLEY, J.S., 1953, The Permian Reef Complex of the Guadalupe Mountains Region, Texas and New Mexico: San Francisco, CA, W.H. Freeman and Co., 236 p.

NOE, S.U., and MAZZULLO, S.J., 1992, Upper Tansill patch reef facies, Sheep Draw Canyon, Guadalupe Mountains, Eddy County, New Mexico: West Texas Geol. Soc. Bull., v. 32, p. 5-11.

NIELSON, P.D., and SHARP, J.M., JR., 1985, Tectonic controls on the hydrology of the Salt Basin, Trans-Pecos Texas, *in* Dickerson, P.W., and Muehlberger, W.R., eds., Structure and Tectonics of Trans-Pecos Texas: Midland, West Texas Geol. Soc. Pub. 85-81, p. 231-234.

ORIEL, S.S., MYERS, D.A., and CROSBY, E.J., 1967, West Texas Permian Basin region, Paleotectonic Investigations of the Permian System in the United States, U. S. Geol. Surv. Prof. Pap. 515-C, p. C17-C60.

OSLEGER, D.A., 1998, Sequence architecture and sea-level dynamics of Upper Permian shelfal facies, Guadalupe Mountains, southern New Mexico: Jour. Sed. Res., Section B: Stratigraphy and Global Studies, v. 68, p. 327-346.

PALMER, A.R., 1983, The Decade of North American Geology 1983 geologic time scale: Geology, v. 11, p. 503-504.

PARSLEY, M.J., and WARREN, J.K., 1989, Characterization of an Upper Guadalupian barrier-island complex from the middle and upper Tansill Formation (Permian), east Dark Canyon, Guadalupe Mountains, New Mexico, *in* Harris, P.M., and Grover, G.A., eds., Subsurface and Outcrop Examination of the Capitan Shelf Margin, Northern Delaware Basin: Tulsa, SEPM Core Workshop No. 13, p. 279-285.

PATTERSON, R.J., and KINSMAN, D.J.J., 1982, Formation of diagenetic dolomite in coastal sabkha along Arabian (Persian) Gulf: AAPG Bull., v. 66, p. 28-43.

PAYNE, M.W., 1979, Submarine-fan channel depositional processes in the Permian Bell Canyon Formation, west Texas and southeast New Mexico, *in* Sullivan, N.M., ed., Guadalupian Delaware Mountain Group of West Texas and Southeast New Mexico: Midland, Permian Basin Section-SEPM Pub. 79-18, p. 96-103.

POL, J.C., 1982, Sedimentation and diagenesis of an Upper Pennsylvanian (Virgilian) mixed carbonate-clastic sequence, Hueco Mountains, El Paso County, Texas [unpublished Master's thesis]: University of Texas at Austin, Austin, TX, 212 p.

POL, J.C., 1988a, Depositional environments of Lower Permian (Wolfcamp) marginal marine mixed carbonate-clastic system, Hueco Mountains, Texas, *in* Robichaud, S.R., and Gallick, C.M., eds., Basin to Shelf Facies Transition of the Wolfcampian Stratigraphy of the Orogrande Basin: Midland, Permian Basin Section-SEPM Pub. No. 88-28, p. 57-64.

POL, J.C., 1988b, Depositional history of Virgilian phylloid algal mound complex, Hueco Mountains, El Paso County, Texas, *in* Robichaud, S.R., and Gallick, C.M., eds., Basin to Shelf Facies Transition of the Wolfcampian Stratigraphy of the Orogrande Basin: Midland, Permian Basin Section-SEPM Pub. No. 88-28, p. 65-66.

PRAY, L.C., 1975, Basin facies carbonates and associated features of the Guadalupe Mountain escarpment, Texas: Tulsa, SEPM Preliminary guidebook for Field Trip No. 2 (Dallas, Texas, AAPG-SEPM Annual Meeting), 16 p.

PRAY, L.C., 1977, The all wet constant sea level hypothesis of Upper Guadalupian shelf and shelf edge strata, Guadalupe Mountains, New Mexico and Texas, *in* Hileman, M.E., and Mazzullo, S.J., eds., Upper Guadalupian Facies, Permian Reef Complex, Guadalupe Mountains, New Mexico and West Texas: Midland, Permian Basin Section-SEPM Pub. 77-16, p. 433-436.

PRAY, L.C., 1985, The Capitan-massive and its proximal carbonate and minor siliciclastics of the Capitan back-reef Walnut Canyon area, Carlsbad Caverns National Park, New Mexico, *in* Cunningham, B.K., and Hedrick, C.L., eds., Permian Carbonate/ Clastic Sedimentology, Guadalupe Mountains: Analogs for Shelf and Basin Reservoirs: Midland, Permian Basin Section-SEPM Pub. 85-24, p. 25-41.

PRAY, L.C., 1988a, Geology of the western escarpment, Guadalupe Mountains, Texas, *in* Sarg, J.F., Rossen, C., Lehmann, P.J., and Pray, L.C., eds., Geologic Guide to the Western Escarpment, Guadalupe Mountains, Texas: Midland, Permian Basin Section-SEPM Pub. 88-30, p. 1-8.

PRAY, L.C., 1988b, Trail Guide: Day One, Bone and Shumard Canyon area, *in* Reid, S.T., Bass, R.O., and Welch, P., eds., Guadalupe Mountains Revisited, Texas and New Mexico: Midland, West Texas Geol. Soc. Pub. 88-84, p. 40-60.

PRAY, L.C., and ESTEBAN, M., 1977, Upper Guadalupian Facies, Permian Reef Complex, Guadalupe Mountains, New Mexico and West Texas — Road logs and locality guides: Midland, Permian Basin Section-SEPM Pub. 77-16, 194 p.

PURDY, E.G., 1963, Recent calcium carbonate facies of the Great Bahama Bank. 2. Sedimentary facies: Jour. of Geology, v. 71, p. 472-497.

QUEEN, J.M., 1981, A discussion and field guide to the geology of Carlsbad Caverns: Carlsbad, NM, Unpublished Report to Carlsbad Caverns National Park, 64 p.

RASMUSSEN, J.A., PIASECKI, S., STEMMERIK, L., and STOUGE, S., 1990, Late Permian conodonts from central East Greenland: Neues Jahrbuch für Geologie und Paläontologie, Abhandlungen, v. 178, p. 309-324.

REICHE, P., 1938, An analysis of cross-lamination in the Coconino Sandstone: Journal of Geology, v. 46, p. 905-932.

REID, S.T., BASS, R.O., and WELCH, P., 1988, Guadalupe Mountains Revisited, Texas and New Mexico: Midland, West Texas Geol. Soc. Pub. 88-84, 200 p.

RIGBY, J.K., 1957, Some submarine mass movements: GSA Bull., v. 68, p. 1872.

ROBICHAUD, S.R., and GALLICK, C.M., 1988, Basin to shelf facies transition of the Wolfcampian stratigraphy of the Orogrande Basin: Midland, Permian Basin Section-SEPM Pub. No. 88-28, 114 p.

ROSS, C.A., 1979, Late Paleozoic collision of North and South America: Geology, v. 7, p. 41-44.

ROSS, C.A., 1986, Paleozoic evolution of southern margin of Permian basin: GSA Bull., v. 97, p. 536-554.

ROSS, C.A., and ROSS, J.R.P., 1985a, Carboniferous and Early Permian biogeography: Geology, v. 13, p. 27-30.

ROSS, C.A., and ROSS, J.R.P., 1985b, Late Paleozoic depositional sequences are synchronous and worldwide: Geology, v. 13, p. 194-197.

ROSS, C.A., and ROSS, J. R. P., 1987a, Biostratigraphic zonation of Late Paleozoic depositional sequences, *in* Ross, C.A., and Haman, D., ed., Timing and Depositional History of Eustatic Sequences: Constraints on Seismic Stratigraphy: Washington, D.C., Cushman Foundation for Foraminiferal Research, Special Pub. No. 24, p. 151-168.

ROSS, C.A., and ROSS, J.R.P., 1987b, Late Paleozoic sea levels and depositional sequences, *in* Ross, C.A., and Haman, D., eds., Timing and Depositional

History of Eustatic Sequences: Constraints on Seismic Stratigraphy: Washington, D.C., Cushman Foundation for Foraminiferal Research, Special Pub. No. 24, p. 137-149.

ROSS, C.A., and ROSS, J.R.P., 1988, Late Paleozoic transgressive-regressive deposition, *in* Wilgus, C.K., Hastings, B.S., Kendall, C.G.St.C., Posamentier, H.W., Ross, C.A., and Van Wagoner, J.C., eds., Sea-Level Changes: An Integrated Approach: Tulsa, SEPM Special Pub. No. 42, p. 227-248.

ROSSEN, C., 1985, Sedimentology of the Brushy Canyon Formation (Permian, Early Guadalupian) in the onlap area, Guadalupe Mountains, west Texas [unpublished Master's thesis]: University of Wisconsin-Madison, Madison, WI, 314 p.

ROSSEN, C., and SARG, J.F., 1988, Sedimentology and regional correlation of a basinally restricted deep-water siliciclastic wedge: Brushy Canyon Formation-Cherry Canyon tongue (Lower Guadalupian), Delaware Basin, *in* Reid, S.T., Bass, R.O., and Welch, P., eds., Guadalupe Mountains Revisited, Texas and New Mexico [1988 Field Seminar]: Midland, West Texas Geol. Soc. Pub. 88-84, p. 127-132.

RUSH, J.W., 2001, Sequence architecture of a late Guadalupian carbonate rimmed shelf, Walnut Canyon, New Mexico: Masters thesis, University of Texas at Austin, Austin, TX, 77 p.

SALLER, A.H., 1996, Differential compaction and basinward tilting of the prograding Capitan reef complex, Permian, west Texas and southeast New Mexico, U.S.A.: Sedimentary Geology, v. 101, p. 21-30.

SANCHEZ, P.G., 1964, Trail log of Carlsbad Caverns, Geology of the Capitan Reef Complex of the Guadalupe Mountains: Roswell, NM, Roswell Geol. Soc. Field Trip Guidebook, p. 47-65.

SARG, J.F., 1976, Sedimentology of the carbonate-evaporite facies transition of the Seven Rivers Formation (Guadalupian, Permian) in southeast New Mexico [unpublished Ph.D. thesis]: University of Wisconsin - Madison, Madison, WI, 313 p.

SARG, J.F., 1981, Petrology of the carbonate-evaporite facies transition of the Seven Rivers Formation (Guadalupian, Permian), southeast New Mexico: Jour. Sediment. Petrol., v. 51, p. 73-95.

SARG, J.F., 1985, Unconformities and depositional sequences of seismic stratigraphic scale (Permian) of western Guadalupe Mountains, Texas-New Mexico: West Texas Geol. Soc. Bull., v. 24, p. 17.

SARG, J.F., 1986, Facies and stratigraphy of upper San Andres basin margin and lower Grayburg inner shelf, *in* Moore, G.E., and Wilde, G.L., eds., Lower and Middle Guadalupian Facies, Stratigraphy, and Reservoir Geometries, San Andres/Grayburg Formations, New Mexico and Texas: Midland, Permian Basin Section-SEPM Pub. 86-25, p. 83-93.

SARG, J.F., 1989a, Middle-Late Permian depositional sequences, Permian Basin, west Texas-New Mexico, *in* Bally, A.W., ed., Atlas of Seismic Stratigraphy: Tulsa, AAPG Studies in Geology No. 27, p. 140-157.

SARG, J.F., 1989b, Stratigraphy and sedimentology of the back-reef upper Queen-lower Seven Rivers strata, Goat Seep-Capitan reef complexes (middle-late Guadalupian, Permian), southeast New Mexico, *in* Harris, P.M., and Grover, G.A., eds., Subsurface and Outcrop Examination of the Capitan Shelf Margin, Northern Delaware Basin: Tulsa, SEPM Core Workshop No. 13, p. 347-352.

SARG, J.F., and LEHMANN, P.J., 1986a, Facies and stratigraphy of lower-upper San Andres shelf crest and outer shelf and lower Grayburg inner shelf, *in* Moore, G.E., and Wilde, G.L., eds., Lower and Middle Guadalupian Facies, Stratigraphy, and Reservoir Geometries, San Andres/Grayburg Formations, New Mexico and Texas: Midland, Permian Basin Section-SEPM Pub. 86-25, p. 9-35.

SARG, J.F., and LEHMANN, P.J., 1986b, Lower-Middle Guadalupian facies and stratigraphy, San Andres/Grayburg formations, Permian basin, Guadalupe Mountains, New Mexico, *in* Moore, G.E., and Wilde, G.L., eds., Lower and Middle Guadalupian Facies, Stratigraphy, and Reservoir Geometries, San Andres/Grayburg Formations, New Mexico and Texas: Midland, Permian Basin Section-SEPM Pub. 86-25, p. 1-8.

SARNTHEIN, M., and DIESTER-HAASS, L., 1977, Eolian-sand turbidites: Jour. Sediment. Petrol., v. 47, p. 868-890.

SCHMIDT, V., 1977, Inorganic and organic reef growth and subsequent diagenesis in the Permian Capitan reef complex, Guadalupe Mountains, Texas, New Mexico, *in* Hileman, M.E., and Mazzullo, S.J., eds., Upper Guadalupian Facies, Permian Reef Complex, Guadalupe Mountains, New Mexico and West Texas: Midland, Permian Basin Section-SEPM Pub. 77-16, p. 93-132.

SCHMIDT, V., and KLEMENT, K.W., 1971, Early diagenetic origin of reef framework in the Permian reef complex, Guadalupe Mountains, Texas and New Mexico [abs.]: Heidelberg, 8th International Sedimentology Congress, Program with Abstracts, p. 89.

SCHOLLE, P.A., 1980, A field guide to the geology of the Permian bank-to-basin section of the Guadalupe Mountains area, west Texas, and New Mexico, *in* Scholle, P.A., and Halley, R.B., eds., Upper Paleozoic Depositional and Diagenetic Facies in a Mature Petroleum Province: U. S. Geol. Surv. Open-File Report 80-383, p. 1-139.

SCHOLLE, P.A., 1995, Carbon and sulfur isotope stratigraphy of the Permian and adjacent intervals, *in* Scholle, P.A., Peryt, T.M., and Ulmer-Scholle, D.S., eds., The Permian of Northern Pangea, Vol. 1, Paleogeography, Paleoclimates, Stratigraphy: New York, Springer-Verlag, p. 133-149.

SCHOLLE, P.A., and KINSMAN, D.J.J., 1974, Aragonitic and high-Mg calcite caliche from the Persian Gulf — a modern analog for the Permian of Texas and New Mexico: Jour. Sediment. Petrol., v. 44, p. 904-916.

SCHOLLE, P.A., ULMER, D.S., and MELIM, L.A., 1992, Late-stage calcites in the Permian Capitan Formation and its equivalents, Delaware Basin margin, west Texas and New Mexico: evidence for replacement of precursor evaporites: Sedimentology, v. 39, p. 207-234.

SCHROEDER, J.H., 1972, Fabrics and sequences of submarine carbonate cements in Holocene Bermuda cup reefs: Geologische Rundschau, v. 61, p. 708-730.

SCOTESE, C.R., BAMBACH, R.K., BARTON, C., VAN DER VOO, R., and ZIEGLER, A.M., 1979, Paleozoic base maps: Jour. of Geology, v. 87, p. 217-235.

SCOTESE, C.R., and LANGFORD, R.P., 1995, Pangea and the paleogeography of the Permian, *in* Scholle, P.A., Peryt, T.M., and Ulmer-Scholle, D.S., eds., The Permian of Northern Pangea, Vol. 1, Paleogeography, Paleoclimates, Stratigraphy: New York, Springer-Verlag, p. 3-19.

SCOTESE, C.R., and McKERROW, W.S., 1990, Revised world maps and introduction, *in* McKerrow, W.S., and Scotese, C.R., eds., Palaeozoic Palaeogeography and Biogeography: London, Geol. Soc. (London) Memoir No. 12, p. 1-21.

SHINN, E.A., 1969, Submarine lithification of Holocene carbonate sediments in the Persian Gulf: Sedimentology, v. 12, p. 109-144.

SHINN, E.A., 1983, Tidal flat environment, *in* Scholle, P.A., Bebout, D.G., and Moore, C.H., eds., Carbonate Depositional Environments: Tulsa, AAPG Memoir 33, p. 171-210.

SILVER, B.A., and TODD, R.G., 1969, Permian cyclic strata, northern Midland and Delaware Basins, west Texas and southeastern New Mexico: AAPG Bull., v. 53, p. 2223-2251.

SMITH, A.G., BRIDEN, J.C., and DREWRY, G.E., 1973, Phanerozoic world maps, *in* Hughes, N.F., ed., Organisms and Continents Through Time: Palaeontological Association (London) Special Paper No. 12: Oxford, Blackwell Scientific Pub.s, p. 1-42.

SONNENFELD, M.D., 1991, High-frequency cyclicity within shelf-margin and slope strata of the upper San Andres sequence, Last Chance Canyon, *in* Meader-Roberts, S., Candelaria, M.P., and Moore, G.E., eds., Sequence Stratigraphy, Facies, and Reservoir Geometries of the San Andres, Grayburg, and Queen Formations, Guadalupe Mountains, New Mexico and Texas: Midland, Permian Basin Section-SEPM Pub. 91-32, p. 11-51.

SONNENFELD, M.D., 1993, Anatomy of offlap: upper San Andres Formation (Permian, Guadalupian), Last Chance Canyon, Guadalupe Mountains, New Mexico, *in* Love, D.W., Hawley, J.W., Kues, B.S., Adams, J.W., Austin, G.S., and Barker, J.M., eds., Carlsbad Region, New Mexico and West Texas, New Mexico Geol. Soc. 44th Annual Field Conf. Guidebook, p. 195-203.

SONNENFELD, M.D., 2000, Stratal geometry, cycle hierarchy, and dynamic facies associations within shelf-margin and slope strata of upper San Andres high-frequency sequences G12 and G13: Last Chance Canyon, New Mexico, *in* Classic Permian Geology of West Texas and Southeastern New Mexico: 75 years of Permian Basin oil & gas exploration & development: Midland, West Texas Geol. Soc. Publ. 00-108, p. 179-197.

SONNENFELD, M.D., and CROSS, T.A., 1993, Volumetric partitioning and facies differentiation within the Permian upper San Andres Formation of Last Chance Canyon, Guadalupe Mountains, New Mexico, *in* Loucks, R.G., and Sarg, J.F., eds., Carbonate Sequence Stratigraphy: Recent Developments and Applications: Tulsa, AAPG Memoir 57, p. 435-474.

STANLEY, S.M., 1966, Paleoecology and diagenesis of Key Largo Limestone, Florida: AAPG Bull., v. 50, p. 1927-1947.

STRAIN, W.S., 1969, Cenozoic rocks in the Mesilla and Hueco Bolsons, Dela-

ware Basin Exploration (Guidebook): Midland, West Texas Geol. Soc. Pub. No. 68-55a, p. 83-84.

TINKER, S., 1998, Shelf-to-basin facies distributions and sequence stratigraphy of a steep-rimmed carbonate margin: Capitan depositional system, McKittrick Canyon, New Mexico and Texas: Jour. Sed. Res., Section B: Stratigraphy and Global Studies, v. 68, p. 1146-1174.

TOOMEY, D.F., and BABCOCK, J.A., 1983, Precambrian and Paleozoic algal carbonates, west Texas-southern New Mexico: Golden, Colorado School of Mines Professional Contributions, v. 11, p. 345.

TOOMEY, D.F., and CYS, J.M., 1977, Rock/biotic relationships of the Permian Tansill-Capitan facies exposed on the north side of the entrance to Dark Canyon, Guadalupe Mountains, southeastern New Mexico, *in* Hileman, M.E., and Mazzullo, S.J., eds., Upper Guadalupian Facies, Permian Reef Complex, Guadalupe Mountains, New Mexico and West Texas: Midland, Permian Basin Section-SEPM Pub. 77-16, p. 133-150.

TYRRELL, W.W., JR., 1969, Criteria useful in interpreting environments of unlike but time-equivalent carbonate units (Tansill-Capitan-Lamar), Capitan reef complex, west Texas and New Mexico, *in* Friedman, G.M., ed., Depositional Environments in Carbonate Rocks: Tulsa, SEPM Special Pub. No. 14, p. 80-97.

UDDEN, J.A., 1924, Laminated anhydrite in Texas: GSA Bull., v. 35, p. 347-354.

ULMER-SCHOLLE, D.S., SCHOLLE, P.A., and BRADY, P.V., 1993, Silicification of evaporites in Permian (Guadalupian) back-reef carbonates of the Delaware Basin, west Texas and New Mexico: Jour. Sediment. Petrol., v. 63, p. 955-965.

VEEVERS, J.J., and POWELL, C.M., 1987, Late Paleozoic glacial episodes in Gondwanaland reflected in transgressive-regressive depositional sequences in Euramerica: GSA Bull., v. 98, p. 475-487.

WARD, R.F., KENDALL, C.G.St.C., and HARRIS, P.M., 1986, Upper Permian (Guadalupian) facies and their association with hydrocarbons — Permian basin, west Texas and New Mexico: AAPG Bull., v. 70, p. 239-262.

WARDLAW, B.R., 1987, Leonardian-Wordian (Permian) conodont biostratigraphy of the Del Norte and Glass Mountains, West Texas [abs.]: GSA, Abstracts with Programs, v. 19, p. 180.

WARREN, J.K., 1982, The hydrological significance of Holocene tepees, stromatolites and boxwork limestones in coastal salinas in South Australia: Jour. Sediment. Petrol., v. 52, p. 1171-1201.

WARREN, J.K., 1983, Tepees, modern (South Australia) and ancient (Permian —Texas and New Mexico)—a comparison: Sedimentary Geology, v. 34, p. 1-19.

WARREN, J.K., 1985, Tepees: an environmental clue in ancient carbonates, *in* Cunningham, B.K., and Hedrick, C.L., eds., Permian Carbonate/Clastic Sedimentology, Guadalupe Mountains — Analogs for Shelf-Basin Reservoirs: Midland, Permian Basin Section SEPM, Pub. 85-24, p. 69-70.

WATKINSON, A.J., and ALEXANDER, J.I.D., 1993, Castile microfolding, *in* Love, D.W., Hawley, J.W., Kues, B.S., Adams, J.W., Austin, G.S., and Barker, J.M., eds., Carlsbad Region, New Mexico and West Texas, New Mexico Geol. Soc., 44th Annual Field Conf. Guidebook, p. 14-16.

WATSON, W.G., 1979, Inhomogeneities of the Ramsey Member of the Permian Bell Canyon Formation, Geraldine Ford Field, Culberson and Reeves Counties, Texas, *in* Sullivan, N.M., ed., Guadalupian Delaware Mountain Group of West Texas and Southeast New Mexico: Midland, Permian Basin Section-SEPM Pub. 79-18, p. 2-38.

WENDT, J., 1977, Aragonite in Permian reefs: Nature, v. 267, p. 335-337.

WIGGINS, W.D., and HARRIS, P.M., 1985, Burial diagenetic sequence in deep-water allochthonous dolomites, Permian Bone Spring Formation, southeast New Mexico, *in* Crevello, P.D., and Harris, P.M., eds., Deep-water Carbonates — A Core Workshop (New Orleans, March 23-24, 1985): Tulsa, SEPM Core Workshop No. 6, p. 140-173.

WIGGINS, W.D., HARRIS, P.M., and BURRUSS, R.C., 1993, Geochemistry of post-uplift calcite in the Permian Basin of Texas and New Mexico, USA: GSA Bull., v. 105, p. 779-790.

WILDE, G.L., 1975, Fusulinid-defined Permian stages, *in* Cys, J.M., and Toomey, D.F., eds., Permian Exploration, Boundaries, and Stratigraphy: Midland, West Texas Geol. Soc. Pub. 75-65, p. 67-83.

WILDE, G.L., 1988, Fusulinids of the Roadian Stage, *in* Reid, S.T., Bass, R.O., and Welch, P., eds., Guadalupe Mountains Revisited, Texas and New Mexico: Midland, West Texas Geol. Soc. Pub. 88-84, p. 143-148.

WILDE, G.L., and RUDINE, S.F., 1996, Lamar-Post Lamar equivalent fusulinacean sequences (Guadalupe, Apache, and Glass mountains, west Texas) and their relationship to a Guadalupian-Dzhulfian boundary solution [abs.], *in* Wardlaw, B.R., and Rohr, D.M., eds., Guadalupian II, Second International Guadalupian Symposium and Guidebook: Alpine, TX, Sul Ross State University, p. 22-23.

WILDE, G.L., RUDINE, S.F., and LAMBERT, L.L., 1999, Formal designation: Reef Trail Member, Bell Canyon Formation, and Its significance for recognition of the Guadalupian-Lopingian boundary, *in* Saller, A.H., Harris, P.M., Kirkland, B.L., and Mazzullo, S.J., eds., Geologic Framework of the Capitan Reef: Tulsa, SEPM Special Pub. No. 65, p. 63-83.

WILKINSON, C.E., JR., RITTER, S.M., LAMBERT, L.L., and WILDE, G.L., 1991, Stratigraphy and biostratigraphy of the lower and middle San Andres Formation in Last Chance Canyon, Guadalupe Mountains, New Mexico, *in* Meader-Roberts, S., Candelaria, M.P., and Moore, G.E., eds., Sequence Stratigraphy, Facies, and Reservoir Geometries of the San Andres, Grayburg, and Queen Formations, Guadalupe Mountains, New Mexico and Texas: Midland, Permian Basin Section-SEPM Pub. 91-32, p. 99-110.

WILLIAMSON, C.R., 1977, Deep-sea channels of the Bell Canyon Formation (Guadalupian), Delaware Basin, Texas-New Mexico, *in* Hileman, M.E., and Mazzullo, S.J., eds., Upper Guadalupian Facies, Permian Reef Complex, Guadalupe Mountains, New Mexico and West Texas: Midland, Permian Basin Section-SEPM Pub. 77-16, p. 409-432.

WILLIAMSON, C.R., 1979, Deep-sea sedimentation and stratigraphic traps, Bell Canyon Formation (Permian), Delaware Basin, *in* Sullivan, N.M., ed., Guadalupian Delaware Mountain Group of West Texas and Southeast New Mexico: Midland, Permian Basin Section-SEPM Pub. 79-18, p. 39-74.

WILSON, J.L., 1972, Cyclic and reciprocal sedimentation in Virgilian strata of southern New Mexico, *in* Elam, J.G., and Chuber, S., eds., Cyclic Sedimentation in the Permian Basin (2nd edition): Midland, West Texas Geol. Soc. Pub. 72-60, p. 82-99.

WILSON, J.L., 1975, Carbonate Facies in Geologic History: New York, Springer Verlag, 471 p.

WOOD, R., 1999a, Reef Evolution: Oxford, Oxford University Press, 410 p.

WOOD, R., 1999b, Paleoecology of the Capitan Reef, *in* Saller, A.H., Harris, P.M., Kirkland, B.L., and Mazzullo, S.J., eds., Geologic Framework of the Capitan Reef: Tulsa, SEPM Special Pub. No. 65, p. 129-137.

WOOD, R., DICKSON, J.A.D., and KIRKLAND-GEORGE, B., 1994, Turning the Capitan Reef upside down: a new appraisal of the ecology of the Permian Capitan reef, Guadalupe Mountains, Texas and New Mexico: Palaios, v. 9, p. 422-427.

WOOD, R.A., DICKSON, J.A.D., and KIRKLAND, B.L., 1996, New observations on the ecology of the Permian Capitan reef, Guadalupe Mountains, Texas and New Mexico: Palaeontology, v. 39, p. 733-762.

WUELLNER, D.E., LEHTONEN, L.R., and JAMES, W.C., 1986, Sedimentary-tectonic development of the Marathon and Val Verde basins, West Texas, U.S.A.: a Permo-Carboniferous migrating foredeep, *in* Allen, P., and Homewood, P., eds., Foreland Basins: Oxford, Internat. Assoc. Sedimentol. Special Pub. No. 8, p. 15-39.

YANG, K.-M., and DOROBEK, S.L., 1993, Late Paleozoic synorogenic stratigraphy and tectonic evolution of the Permian Basin, west Texas and New Mexico, *in* Gibbs, J., and Cromwell, D., eds., New Dimensions in the Permian Basin: Midland, West Texas Geol. Soc. Pub. 93-93, p. 8-18.

YANG, K.-M., and DOROBEK, S.L., 1994, The Permian Basin of west Texas and New Mexico: Tectonic history of a "composite" foreland basin and its effects on stratigraphic development, *in* Dorobek, S.L., and Ross, G.M., eds., Stratigraphic Evolution of Foreland Basins: Tulsa, SEPM Special Pub. No. 52, p. 147-172.

YE, H., ROYDEN, L., BURCHFIEL, C., and SCHUEPBACH, M., 1996, Late Paleozoic deformation of interior North America: the greater Ancestral Rocky Mountains: AAPG Bull., v. 80, p. 1397-1432.

YUREWICZ, D.A., 1976, Sedimentology, paleoecology, and diagenesis of the massive facies of the lower and middle Capitan Limestone (Permian), Guadalupe Mountains, New Mexico and west Texas [unpublished Ph.D. thesis]: University of Wisconsin-Madison, Madison, WI, 278 p.

YUREWICZ, D.A., 1977, The origin of the massive facies of the lower and middle Capitan Limestone (Permian), Guadalupe Mountains, New Mexico and west Texas, *in* Hileman, M.E., and Mazzullo, S.J., eds., Upper Guadalupian Facies, Permian Reef Complex, Guadalupe Mountains, New Mexico and West Texas: Midland, Permian Basin Section-SEPM Pub. 77-16, p. 45-92.

PART II

UPPER PALEOZOIC BIOHERMS IN THE NORTHERN SACRAMENTO MOUNTAINS

ROBERT H. GOLDSTEIN, PETER A. SCHOLLE, and ROBERT B. HALLEY

INTRODUCTION TO THE GEOLOGY OF THE SACRAMENTO MOUNTAINS

Exposures of Upper Paleozoic strata in the northern Sacramento Mountains offer a superb opportunity to view varied carbonate lithologies, local facies changes, and the products of diagenesis within a variety of shelf and slope carbonate buildups. Similar buildups occur in the subsurface in nearby basins in New Mexico, Texas and Utah and are known to be excellent hydrocarbon reservoirs. They have been targets of exploration in the area for the last 40 years.

We will visit three types of mounds and discuss their similarities and differences in the field. We will study phylloid algal mounds, structures which are widespread throughout the United States (Wray 1968). We will compare a Virgilian mound (Pennsylvanian), which is largely a carbonate mud accumulation, with a Wolfcampian mound (Permian) that contains copious amounts of submarine cement. We will visit an Osagean (Mississippian) buildup composed of a carbonate mud-fenestrate bryozoan-marine cement core facies and crinoidal sand flank beds. This mound is similar to Lower Carboniferous mounds of Europe, known as Waulsortian mounds and named from occurrences near Waulsort, Belgium (Bolton et al. 1982; Lees 1964; Lees 1982; Lees et al. 1985; Lees and Miller 1985). Comparable mounds are also found in Pennsylvanian and even Permian carbonates in many areas of the world (Davies et al. 1988a; Davies et al. 1988b; Füchtbauer 1980; Hurst et al. 1988; Smith 1981).

The exposures in the Sacramento Mountains provide a cross-sectional view of the rocks, but it is not possible to develop a regional picture of facies relationships in a few days as can be done for the Permian basin. The Guadalupe Mountains part of this field course visits an area where erosion and evaporite dissolution produced outcrops that may be relatively easily related to a paleogeographic framework. In contrast, strata in the northern Sacramento Mountains dip into the subsurface a few miles to the east of the outcrops, and they are downfaulted below the Tularosa Valley to the west.

The northern Sacramento Mountains area was closer to sources of terrigenous clastic sediments than the Carlsbad area during the Late Paleozoic. The Pedernal land mass repeatedly shed material south and west to the Alamogordo area (Carr 1985). Some of the tectonism which occurred during this time is evidenced in the Sacramento Mountains by Late Paleozoic faulting. Some tectonism may also be reflected in the sediments themselves, which show evidence of repeated relative sea level changes, probably of both tectonic and eustatic origin.

In the northern Sacramento Mountains we will continue to investigate many of the themes developed in the Carlsbad area, but now in a considerably different setting. These themes include facies relationships, faunal and lithologic variation, reef models, marine cementation, subaerial exposure, porosity and permeability development and preservation. They are themes that are increasingly incorporated into modern exploration scenarios and are well illustrated by the outcrops we will visit.

SUMMARY OF SIGNIFICANCE TO PETROLEUM EXPLORATION

The general geology of the northern Sacramento Mountains has been worked out by Pray (1952; 1961) and Otte (1959b), providing the framework for many later, more detailed studies. Pray (1959) summarizes work in the area before 1950. Excellent general field guides to the area have been published by Pray (1959), Butler (1977) and Fly and Speer (1988). Pray (1975a) edited a field guide to shelf-edge and basin facies limestones in the Sacramento Mountains. Several additional guides to the Late Paleozoic stratigraphy of the area have been published more recently (Bachtel et al. 1998; Stanton 2000). Figure 1 indicates the position of

our field stops on a generalized stratigraphic section for the northern Sacramento Mountains.

Several processes discussed and developed at outcrops in the Permian Reef complex will again be evoked to explain observations on these older bioherms. The significance of these processes varies from buildup to buildup, and the internal structure and composition of the bioherms reflect these differences. Some buildups are cement-rich, some mud-rich, some contain shallow-water fossils, some deep-water fossils. We will try to extract as much interpretive data as possible from bioherm outcrops. Such observations will help to interpret similar rocks in the subsurface.

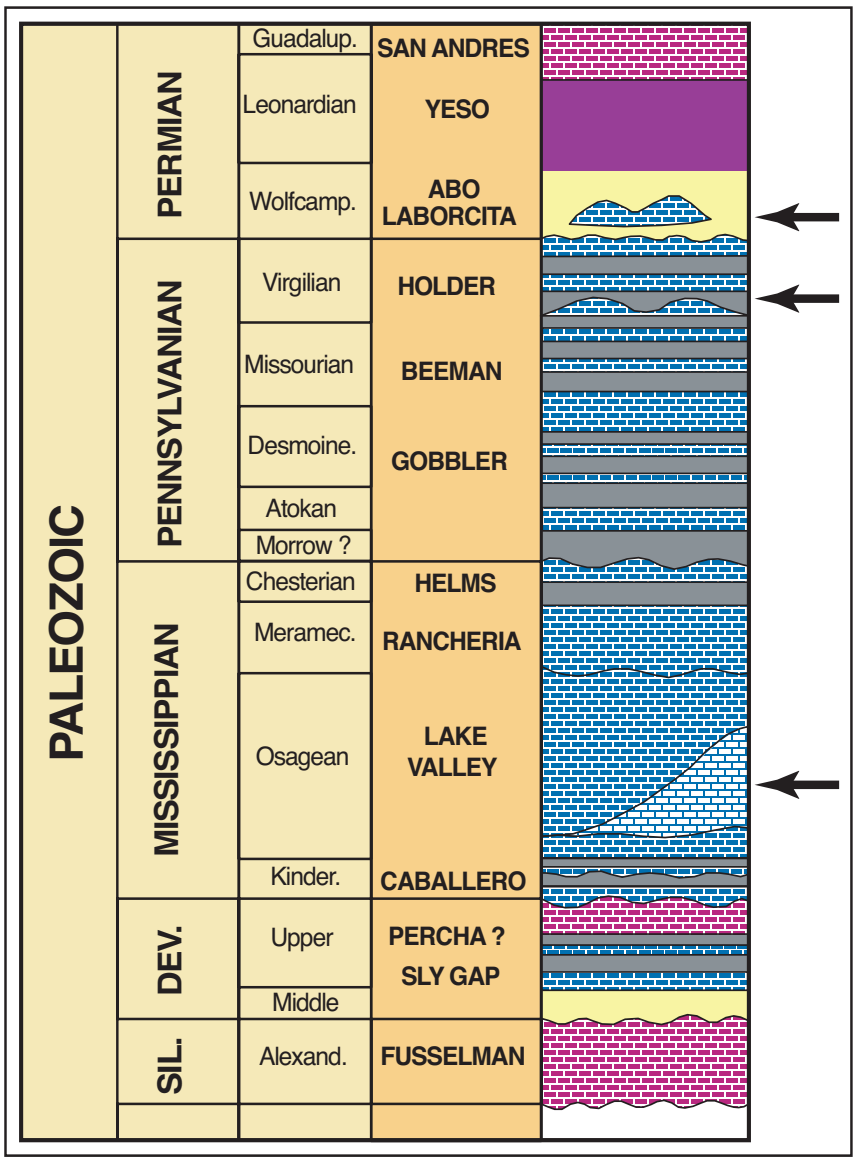

Figure 1. Partial stratigraphic column of the northern Sacramento Mountains. Section is generalized after Pray (1961) and AAPG Geologic Road Map of Eastern Colorado and New Mexico. Arrows indicate major units covered on this trip.

In contrast to the Capitan reef facies, which (unlike its back-reef and basinal equivalents) does not produce significant oil in the subsurface, bioherms similar to those we visit in the Sacramento Mountains do form excellent reservoirs. Phylloid algal limestones, like those at the Yucca mound, act as reservoir rocks in Aneth Field (Elias 1963; Irwin 1963; Peterson and Ohlen 1963), Ismay Field (Choquette 1983; Choquette and Traut 1963), New Lucia Field (Toomey and Winland 1973), Lusk Field (Thornton and Gaston 1968), several fields in the "Horseshoe Atoll" (Schatzinger 1983; Vest 1970), and Saunders and Conley fields (Kerr 1969). These studies show, in some cases, direct association of subsurface porosity with the presence of phylloid algae. Porosity takes the form of shelter pores beneath algal blades in mudstones and wackestones, intergranular porosity in algal plate grainstones, and secondary porosity in leached algal plate mudstones. In some cases, additional porosity and permeability are provided by fracturing or dolomitization in this facies. Several of the associated lithologies also provide excellent reservoir rock, some of which are oolitic, crinoidal and fusulinid grainstones. It is significant that production from many fields appears to be from the shelf-edge buildups themselves and not from fore-reef or back-reef facies. Fields along the Abo Trend (LeMay 1972; Mack and James 1986; Wright 1962) and the Kemnitz-Townsend Trend (Malek-Aslani 1970) occur at the shelf edge, a position occupied by the tight Capitan Limestone in younger units to the south. Early submarine cementation is a major factor in the lack of oil production from the Capitan reef. In addition, many of the clastic terrigenous units interspersed with the carbonate buildups act as reservoir rocks (e.g., Broadhead 1984).

The retention of porosity in the subsurface is still a topic of considerable study. We see little matrix porosity in outcrops of Late Paleozoic mounds (although vugs are characteristic of the lower Virgil mound). The original porosity in these carbonate sediments was very high (40-85%), and the processes involved in such great porosity loss have not been well delineated. One of the best-documented cases of porosity loss in carbonate sands comes from studies of the crinoidal facies of the Lake Valley Formation (Meyers 1974; Meyers 1978; Meyers 1988; Meyers et al. 1982; Meyers and Lohmann 1985).

Hydrocarbon reservoirs in rocks similar to those that occur in the Lake Valley appear to be rare but not non-existent. Pray (1958a) reported that cores from the La Pan Field of Clay County, Texas, are similar to lithologies associated with Muleshoe bioherm. La Pan field may therefore be a buildup similar to Muleshoe bioherm. Other production has come from numerous small fields in the Chappel Limestone (Ahr and Ross 1982) and from the European mid- to Late Permian Zechstein Fm. (Peryt 1986); porous zones in Permian bioherms have also been reported from unexplored strata in Greenland (Scholle et al. 1991; Stemmerik et al. 1993).

Meyers (1974) showed that cementation and porosity loss in Lake Valley non-biohermal sediments are linked to periods of subaerial exposure. As much as 60% of the original porosity was lost within about five million years of sediment deposition. Almost all the rest was lost within 20-30 million years of continued burial. Cementation took place primarily during two episodes of subaerial exposure (Meyers 1978). It is interesting to note, however, that early subaerial exposure is credited with producing leached porosity in many phylloid algal and bryozoan-cement mounds (Stemmerik et al. 1993; Surlyk et al. 1986; Wilson 1975a). Apparently, exposure and fresh-water diagenesis act as a double-edged sword (i.e., under some circumstances exposure helps produce reservoir rocks); in other cases, exposure destroys reservoir properties. The particular circumstances which control the products of exposure are not well understood. Factors that probably exert considerable influence on the diagenetic history of these rocks include rate of transgression or regression, duration of exposure, climate, original sediment mineralogy and local paleohydrology.

Even less well understood are later diagenetic processes which affected these limestones in the subsurface. The Holder and Laborcita mounds were buried to at least 750 m (2,500 ft) and the Lake Valley bioherms as deeply as 2,000 m (6,500 ft) by the end of the Paleozoic. Processes, such as compaction, pressure-solution cementation, fracturing,

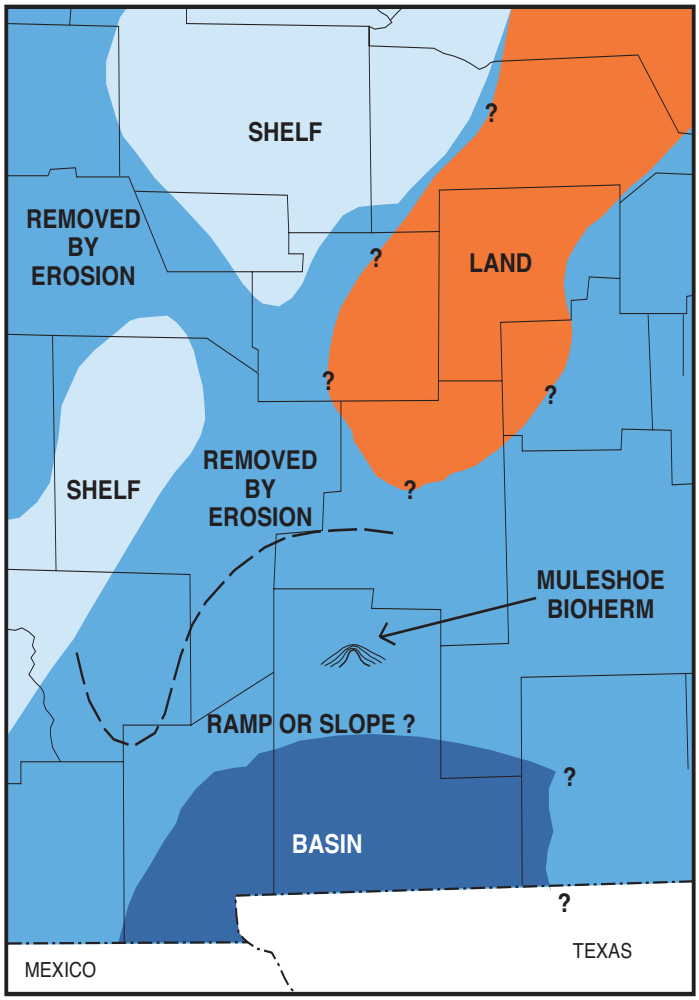

Figure 2. Generalized paleogeography of southeastern New Mexico during Late Osagean time. After Armstrong (1962; 1967) and Wilson (1975b).

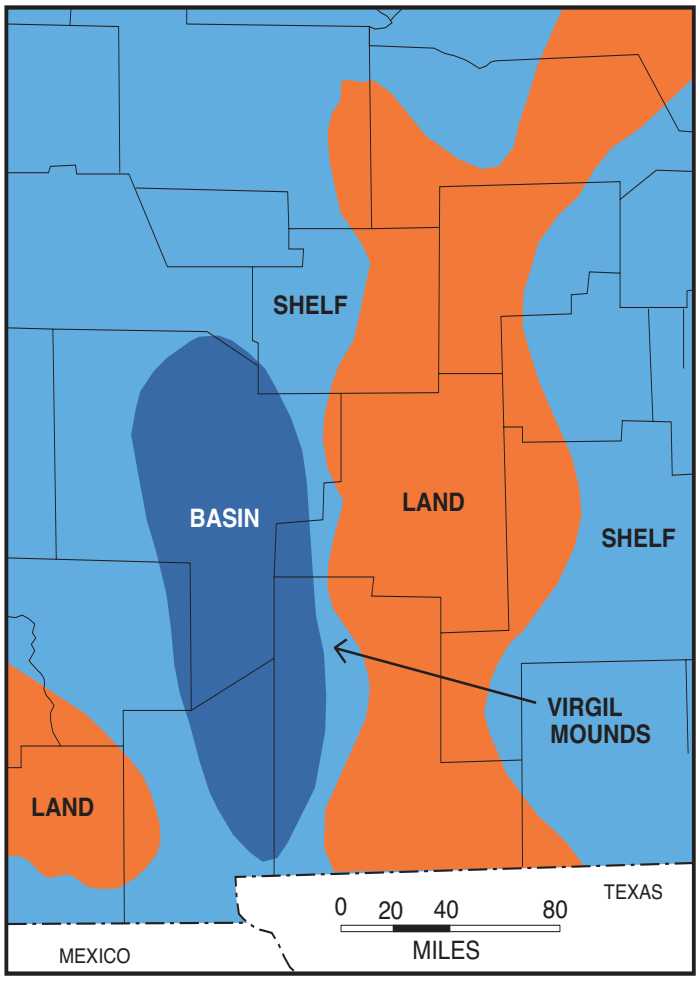

Figure 3. Generalized paleogeography of southeastern New Mexico during Virgilian time. After Bachman (1975) and Meyer (1966).

cementation by dolomite and anhydrite, are known to occur at depth but are undocumented in these rocks.

Finally, one wonders what the effect has been of uplift and the current episode of exposure on these rocks. Might some of the differences between the rocks we see in outcrop and their subsurface counterparts be due to their Cenozoic uncovering? Or was the character of these rocks essentially fixed during their burial?

Again, it should be emphasized that we will not develop a regional picture of sedimentary facies in the Sacramento Mountains as we do in the Guadalupe Mountains. Generalized paleogeographic maps for the Osagian and Virgilian Stages of the area are outlined in Figures 2 and 3. We will review principles of carbonate deposition as they apply to late Paleozoic bioherms and formulate new questions that have particular significance to petroleum exploration.

STRUCTURE AND STRATIGRAPHY OF THE SACRAMENTO MOUNTAINS ESCARPMENT

Holocene Geography

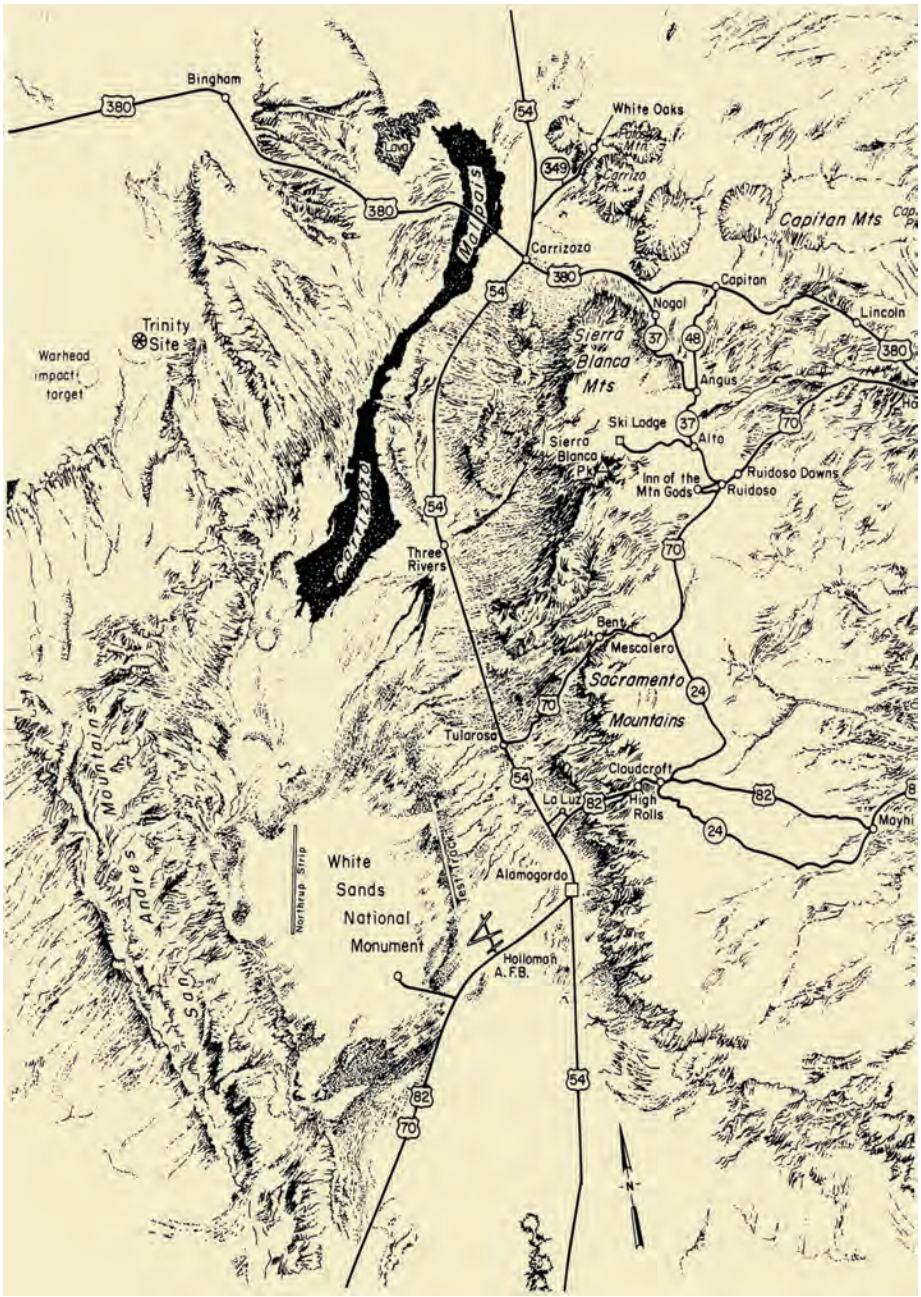

Figure 4 - Location map and topographic elements of the Sacramento Mountains escarpment, southern New Mexico (after Ahlen and Hanson.M.E. 1986).

The geology of the Sacramento Mountains was first mapped as a dissertation project by Lloyd C. Pray. This summary is based on Pray's publications (1959; 1961). The Sacramento Mountains are the mountain range that comprises the easternmost element of the Basin and Range Province. This part of the Basin and Range is known as the Rio Grande Rift. The Sacramento Mountains are a northwest-southeast trending, fault bounded uplift that is bounded to the west by the broad graben-like feature called the Tularosa Basin (Fig. 4). The Northern part of the range is called the Sierra Blanca Mountains. It consists of Tertiary intrusives and extrusives and Cretaceous strata. Its peak reaches 12,000 feet and has been described as the southernmost point of Pleistocene Mountain glaciation in the United States.

The southern part of the Sacramento Mountains consists of Precambrian through Cretaceous strata, but is dominated by Paleozoic sedimentary rocks. This part of the range reaches an elevation of 9,700 feet. There is about a mile of vertical relief across the frontal escarpment. West of the uplift is the Tularosa Basin that lies at an elevation of about 4,000 feet (Fig. 5). Its topography is characterized by Holocene alluvial fans, lava flows, sand dunes, arroyos, and playa lake deposits. West of the Tularosa Basin rises the next Basin and Range uplift to the west, the San Andres Mountains. East of the Sacramento Mountains, the Great Plains Province begins. To the southeast, the Sacramento Moun-

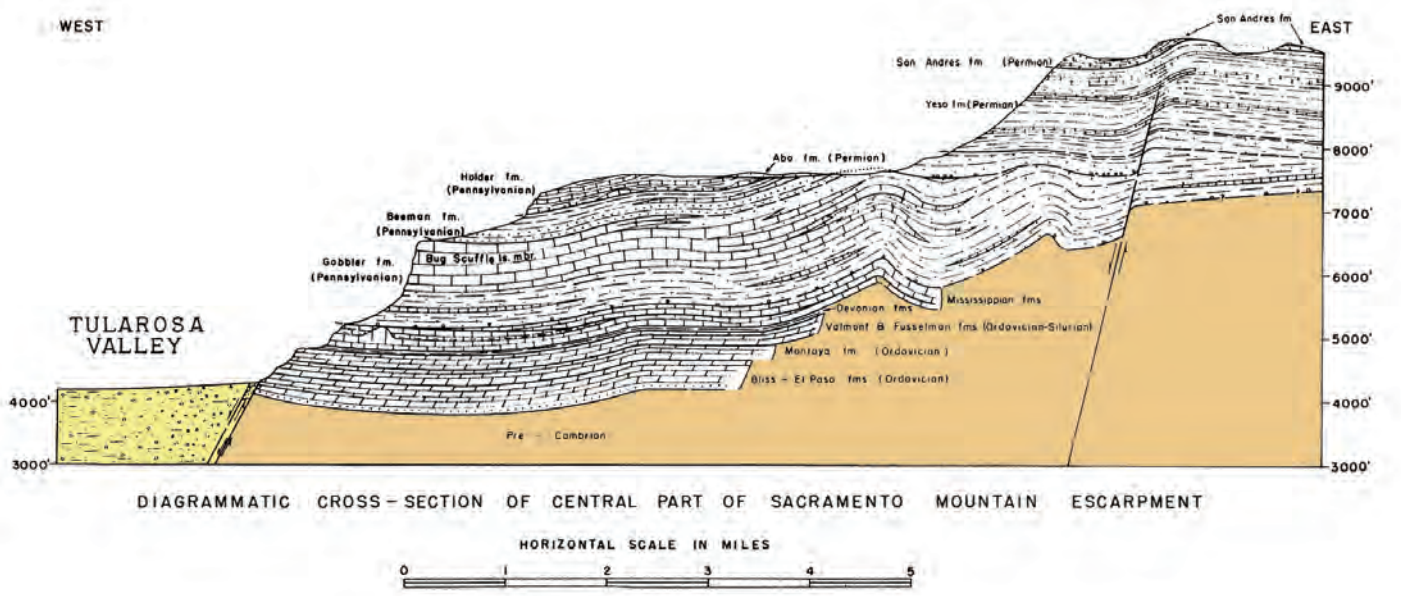

Figure 5 - West to east cross section through the Sacramento Mountains escarpment (after Pray 1959).

tains escarpment loses relief and passes into the Guadalupe Mountains escarpment.

STRATIGRAPHY OF THE SACRAMENTO MOUNTAINS ESCARPMENT

The major Paleozoic units that crop out in the Sacramento Mountains are summarized in the stratigraphic section of Figure 6.

Bliss Formation - This unit is Cambro-Ordovician in age. It consists of reddish sandstone some of which is glauconitic. Parts of this unit are well-burrowed and contain lingulid brachiopods. This unit is the basal sandstone overlying the Precambrian unconformity.

El Paso Formation - This stratigraphic unit is Early Ordovician in age. It consists of medium - light gray and olive gray dolomite with minor chert. Bedding is generally several feet thick.

Montoya Formation - This unit is Middle Ordovician in age. At its base is a thin sandstone that is probably equivalent to the St. Peter sandstone. Above this are dark, massive cliffs of dolomite, overlain by lighter colored slopes of cherty dolomite. The top of the unit is marked by a 1-3 foot thick bed of massive chert,

Valmont Dolomite - The Valmont is Late Ordovician in age. It consists of light gray, finely crystalline dolomite.

Fusselman Formation - The Fusselman is Silurian in age. It is a dark, massive dolomite that commonly forms low cliffs. It is commonly cherty and in some areas contains well developed stromatoporoid-coral mounds.

Oñate Formation - The Oñate is Mid-Late Devonian in age. It consists of silty dolomite and dolomitic siltstone.

Sly Gap Formation - The Sly Gap is Late Devonian in age. It consists of interbedded gray calcareous shale, thin-bedded gray limestone and black shale.

Percha Shale - The Percha is Late Devonian in age. It consists of black shale containing abundant phosphate nodules. It is essentially equivalent to the Chattanooga Shale of the Midcontinent.

Caballero Formation - This Mississippian unit consists of black shale, nodular phosphorite, and crinoidal mudstone and wackestone. It is interpreted to have been deposited at a slow rate of sedimentation in deep marine waters.

Lake Valley Formation - Carbonate buildups are common in the Lake Valley Formation. Biota in the buildups are dominated by fenestrate bryozoans, crinoids, and brachiopods. Conspicuously lacking in the mounds are any algae. In general, the fenestrate bryozoans display relatively undisturbed textures and other fossil debris is largely unreworked and unabraded. Common fabrics in the mounds are wackestone and mudstone. Framestones

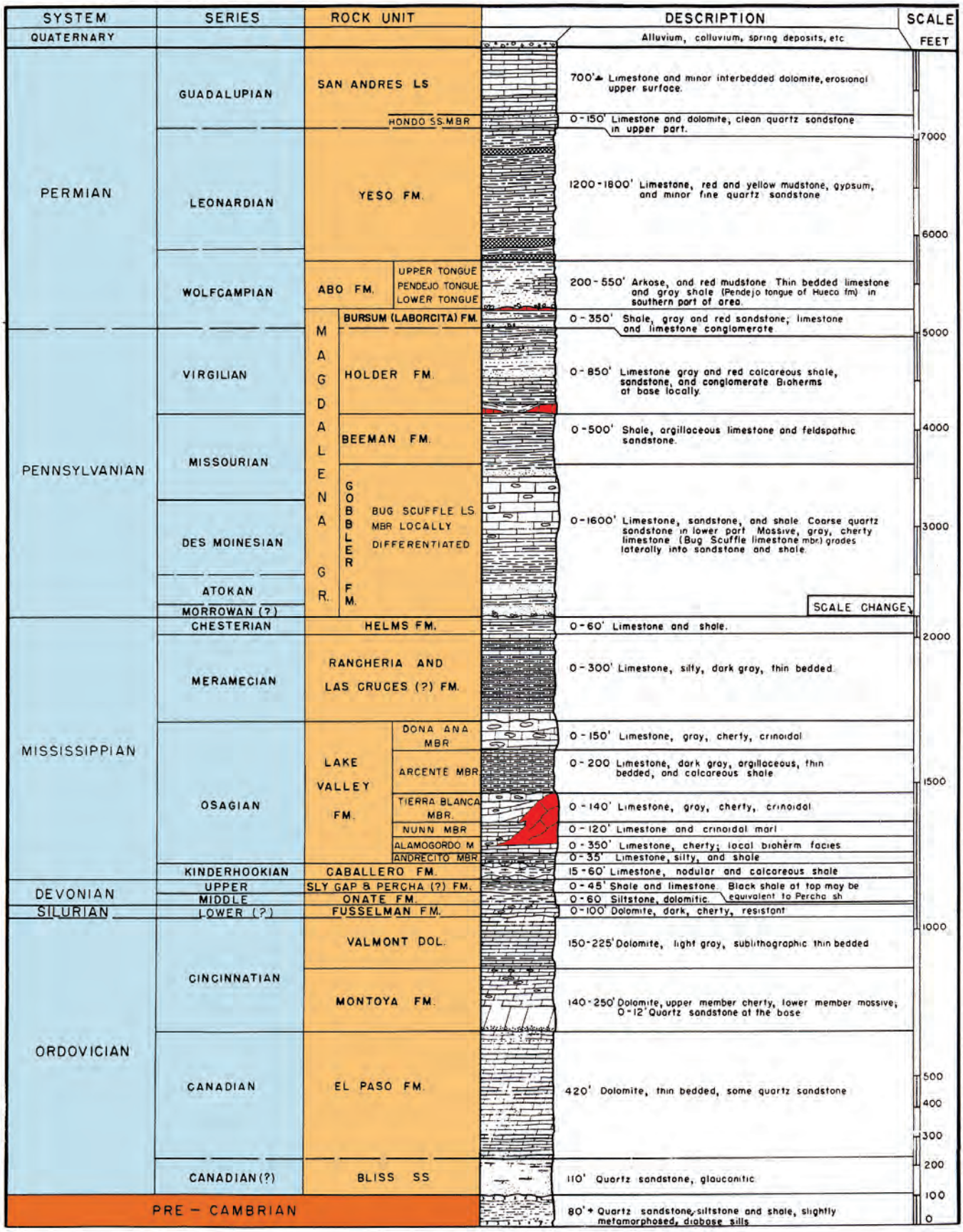

Figure 6 - Composite stratigraphic section of Paleozoic strata of the Sacramento Mountains (after Pray 1959). Units marked in red contain bioherms visited on this trip..

are absent and grain supported fabrics are unusual. Most mounds are relatively massive and structureless, although vague bedding can be discerned in a few mounds.. Dips on the order of 20-30 degrees can be observed on the mound flanks. Common features in mound lithologies are stromatactis cavities, irregular cavities containing marine cement and multiple generations of internal sediment. Many neptunian dikes are known to cut across the mound lithologies and megabreccias are developed on the flanks as the deposits of debris flows. Both features indicate the mound sediment was well cemented very early in its history. Carbonate mounds with these characteristics are commonly referred to as Waulsortian facies, named after exposures in Waulsort, Belgium. In general, the Waulsortian mounds of the Sacramento Mountains are large and hemispherical to the south and become smaller and more tabular to the north. Many sedimentologists believe that the Waulsortian facies forms on relatively deep shelf settings.

Andrecito Member - This Mississippian unit consists of interbedded lime mudstone, gray calcareous shale and crinoidal wackestone. *Zoophycos* is a common association of trace fossils. The unit is interpreted to have been deposited under moderate depths of marine water.

Alamogordo Member - This Mississippian unit consists of dark gray lime mudstone, crinoidal wackestone and black nodular chert. It is interpreted to have been deposited at the same water depth as the Andrecito or perhaps under more shallow water with moderate influence of carbonate mounds.

Nunn Member - This Mississippian unit is light in color and consists of argillaceous crinoidal lime packstone and grainstone. It contains carbonate mounds and is interpreted to have been deposited in shallower water than the units below.

Tierra Blanca Member - This Mississippian unit consists of crinoidal wackestones, packstones, and grainstones. In the northern part of the Sacramento Mountains , it builds up to form a shelf. Carbonate mounds are present on the shelf and in more basinal positions. Water depth is interpreted as moderate on the shelf, with strata, affected by wave base. Water depth becomes much greater to the south.

Arcente Member - This Mississippian unit consists of dark gray shales, and evenly bedded dark argillaceous lime mudstones. It laps out against the topography of the Tierra Blanca shelf and topography of the mounds. Water depth has been interpreted as relatively deep, but others have suggested a shallower origin in settings with restricted circulation.

Doña Ana Member - This Mississippian unit laps out against the topography of the mounds and the topography of the Tierra Blanca shelf. It consists of cherty fossiliferous wackestones and packstones. Most workers believe it was deposited in shallower, or at least more normal marine conditions than the underlying Arcente.

Rancheria Formation - The Rancheria is a Mississippian unit that is underlain by a surface of erosional truncation that many workers interpret to have formed from a relative fall in sea level. The unit contains abundant fine-grained, cross-bedded grainstones.

Pre-Pennsylvanian Unconformity - Before deposition of Pennsylvanian strata, significant subaerial exposure resulted in regional karsting of Mississippian strata and significant erosion of pre-Pennsylvanian strata.

Gobbler Formation - The Gobbler Formation is Pennsylvanian in age (probably Morrowan, Atokan, and Desmoinesian) and consists of a suite of mixed carbonates and siliciclastics. The carbonate-rich facies are designated as the Bug Scuffle Limestone Member. The appearance of the Gobbler's shales, siltstones, and sandstones in the Pennsylvanian mark the appearance of a new nearby source area (the Pedernal Uplift) that tends to rearrange the north-south shelf to basin transition of the Mississippian to an east-west shelf to basin transition for the Pennsylvanian. Regionally, the siliciclastics appear to fill a northwest trending' depression that was parallel to the Pedernal uplift. Strata of the Gobbler Formation show a striking cyclicity at a relatively small scale. There are three types of cyclic sequences, a carbonate dominated one, a mixed carbonate-siliciclastic cycle, and a siliciclastic dominated cycle.

The carbonate dominated cycle is essentially a shoaling upward sequence. The basal component is spiculitic mudstone and wackestone or bioclastic wackestone. This is overlain by bioclastic wackestone and packstone or phylloid algal wackestone and packstone. The whole sequence is capped by bioclastic grainstone.

The carbonate- siliciclastic cycle has spiculitic mudstone and wackestone or bioclastic wackestone at its base. It is overlain by bioclastic wackestone and packstone or phylloid algal wackestone. This is capped by siliciclastics that are overlain by bioclastic packstone and phylloid algal wackestones or packstone.

The siliciclastic parts of the cycle described above are cycles in their own right. These units are dominated by rippled siltstone with plant fragments at the base which pass upward into fine sandstone. These are overlain by lenticular bodies of medium sandstone that are up to 5 meters thick and contain abundant marine fossils. This unit is overlain

by rippled siltstone, sandstone and some coal which passes upward to a coarse sandstone. The cycle is capped by a fossiliferous, fine-grained sandstone which passes upward into carbonate rocks.

Beeman Formation - The Beeman is Pennsylvanian (Missourian) in age. To the west, it is dominated by thin-bedded argillaceous limestone and dark gray shales. Some dark-colored grainstones are also present in this somewhat offshore position. To the east, the unit is dominated by massive pure limestones that are interbedded with gray and red marls. The lithologic alternations are very cyclic in nature. The east to west facies shift reflects an east to west shelf to basin transition.

Holder Formation - The Holder is Pennsylvanian (Virgilian) in age. It was deposited as about 20 carbonate- siliciclastic cycles. The ideal shelf cycle reflects an event of relative sea level rise and fall. Carbonate buildups are conspicuous. The distribution of facies apparently is controlled by active tectonism in Pennsylvanian time.

Laborcita Formation - The Laborcita Formation is Permian (Wolfcampian) in age. It is similar to the Holder in that it consists of carbonate- siliciclastic cycles and contains carbonate buildups.

Abo Formation - The Abo is Permian (Wolfcampian) in age and was deposited above a major angular unconformity. It is dominated by red-colored fluvial sandstone, shale and conglomerate.

Yeso Formation - The Yeso is Permian (Leonardian) in age. It consists of multicolored shales, gypsum, sandstone and shallow shelf carbonates that are rich in foraminifera and ostracodes.

San Andres Formation - The San Andres is Permian (Guadalupian) in age. It consists of marine and restricted marine carbonates.

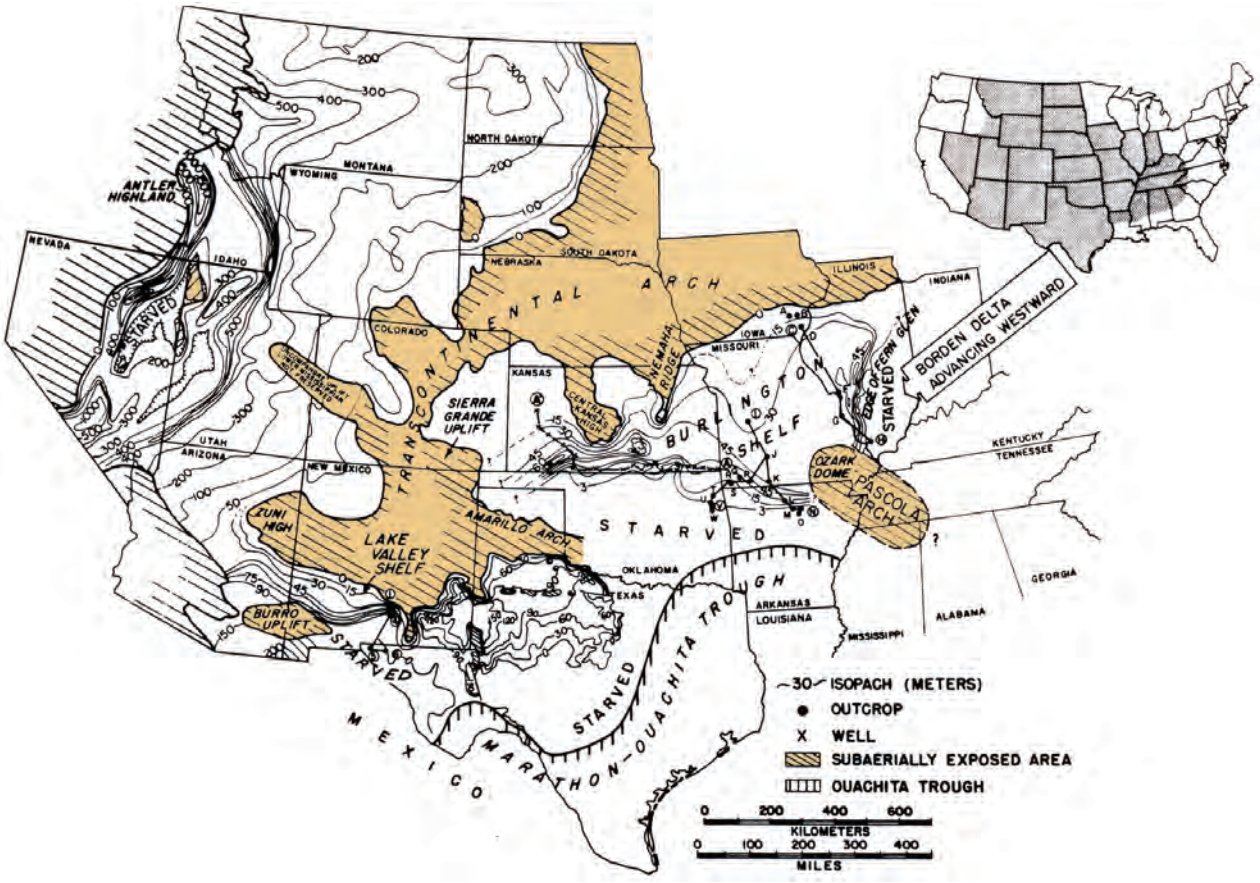

Figure 7 - Isopach map of early Middle Mississippian rocks of the United States. Note position of the Lake Valley Shelf in relation to the Transcontinental Arch (after Lane 1982).

MISSISSIPPIAN, PENNSYLVANIAN AND EARLY PERMIAN PALEOGEOGRAPHY

Mississippian Deposition - Mississippian limestones and shales of the Midcontinent show, a clear relationship of thickness and facies distribution to the Transcontinental arch. The southern tip of the Transcontinental arch extended southward into New Mexico and terminated north of the Mississippian outcrops of the Sacramento mountains escarpment (Figs. 7, 8). In general, Mississippian strata thickened to the south and west in response to this paleogeographic element. Until just before deposition of the Tierra Blanca Member, Mississippian strata showed little lateral thickness change, and broad facies belts indicating deeper water to the south. Largely, the Mississippian has been interpreted as a ramp during this time. Rapid deposition of carbonates in the central and northern Sacramento Mountains created a flat shelf that maintained a steep dropoff into a more basinal setting to the south (Fig. 9). Much of the Tierra Blanca shelf relief was reduced by deposition of onlapping Mississippian carbonates of the Arcente and Doña Ana Members in the intervening low areas (Fig. 10). So, to summarize Mississippian paleogeography one would note that there was shallow to deep transition from north to south because of the position of the southern tip of the Transcontinental arch. A Mississippian ramp developed on this margin and eventually changed to a shelf with a north to south shelf to basin transition cropping out in the central Sacramento Mountains. Later much of the shelf-to basin topography was reduced through deposition in the low areas.

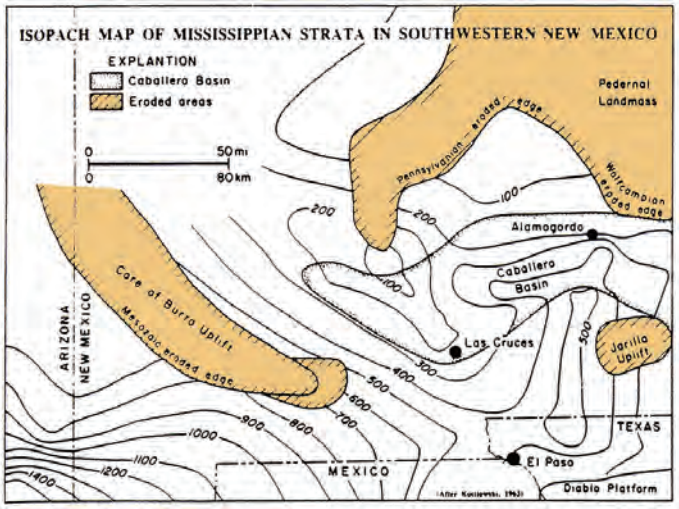

Figure 8 - Isopach map of the Mississippian strata of southwestern New Mexico. (after Ahr 1989; modified from Kottlowski 1960). Contours are in feet.

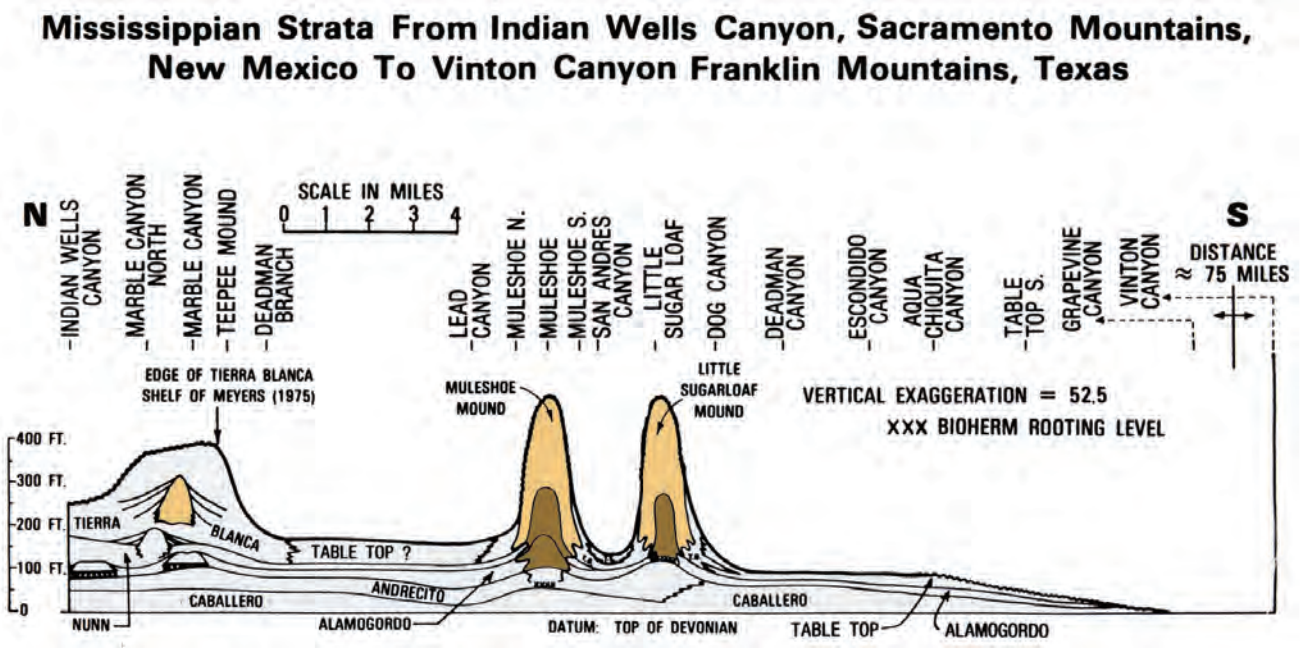

Figure 9 - North-south cross section of pre-Arcente Mississippian strata of the Sacramento Mountains. Notice the buildup of the Tierra Blanca Shelf to the north (after Lane 1982).

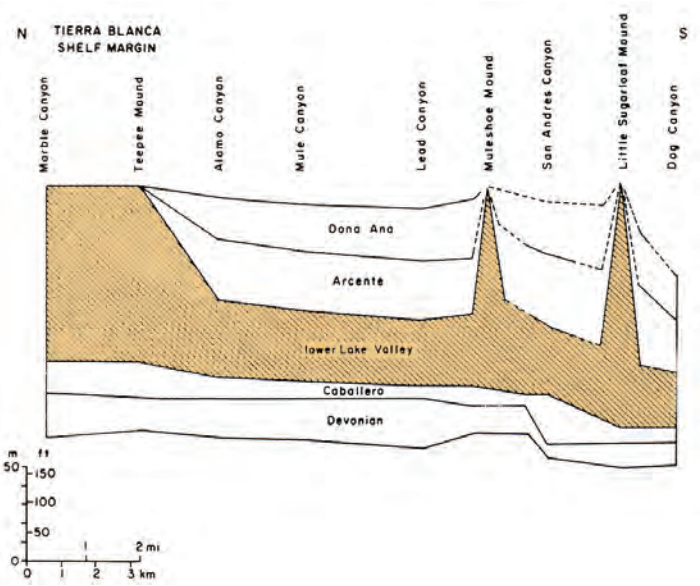

Figure 10 - North-south cross section of Mississippian strata of Sacramento Mountains escarpment. Notice that the Arcente and Doña Ana members reduce the topography of the shelf and basinal buildups (after Ahr 1989).

PENNSYLVANIAN TO EARLY PERMIAN PALEOGEOGRAPHY

The north to south slope of Mississippian time radically changed in Pennsylvanian time. The Sacramento Mountains outcrops mark the transition between a new uplift with a north-south orientation (the Pedernal Uplift) and a basin to the west called the Orogrande Basin. Most Pennsylvanian and early Permian units in the Sacramento Mountains were deposited on a north-south shoulder between the Pedernal uplift and the Orogrande Basin (Figure 11). Most Pennsylvanian units show evidence of a siliciclastic source from the east. Facies and preserved paleotopography indicate deepening into the Orogrande basin to the west.

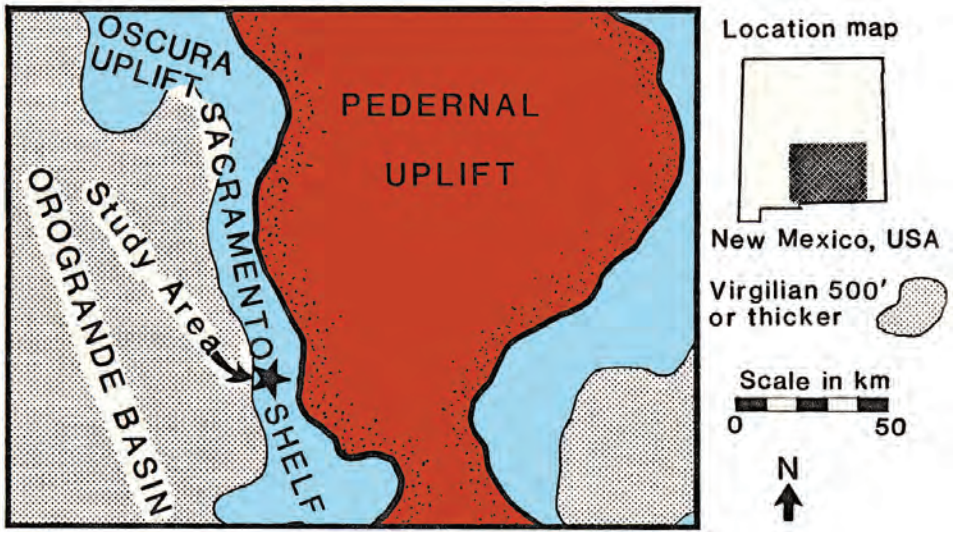

Figure 11 - Virgilian (Upper Pennsylvanian) paleogeography of southern New Mexico (after Meyer 1966).

STRUCTURAL AND TECTONIC EVOLUTION OF THE SACRAMENTO MOUNTAINS

Tectonically, the story for the Sacramento Mountains began in the Mississippian. Minor changes in thickness and facies of Mississippian strata have been related to subtle structures that apparently developed during the Mississippian. The erosional unconformity at the base of the Rancheria is slightly angular in some places. In several places, the Pre-Pennsylvanian unconformity is slightly angular. Outcrops along the front of the range show synclines and anticlines that trend north-south, at an angle to the northwest trend of the frontal escarpment.

Most of these folds do not involve Abo strata and thus must predate deposition of much of the Abo (Fig. 5, 12). Many of the folds exert a control on Pennsylvanian facies. There are also north-south trending faults, many of which are normal, with up to 1500 feet of displacement. These faults are either erosionally truncated at the base of the Laborcita or truncated at the base of Abo. Thus, development of the faults and folds are Pennsylvanian to early Permian in age. Overall, the Mississippian to early Permian structure reflects uplift of the Pedernal landmass, a component of the ancestral Rocky Mountains.

Thrust faults are observable along the frontal escarpment of the Sacramento Mountains. The faults indicate eastward thrusting and probably formed as a result of Laramide uplift and deformation in the earliest Tertiary. Common intrusives of Eocene to Oligocene age cut across the thrust faults but probably result from a later Laramide event.

The present Basin and Range uplift probably became active in the Miocene and normal faulting and intrusion still continues. Along the frontal escarpment of the range, modern fault scarps cut through some of the alluvial fans. Basaltic volcanism only 1,500 years ago was responsible for a large flow in the Tularosa Basin (the Carrizozo Malpais, shown in Fig. 4).

In summary, the Sacramento Mountains are a unique place to

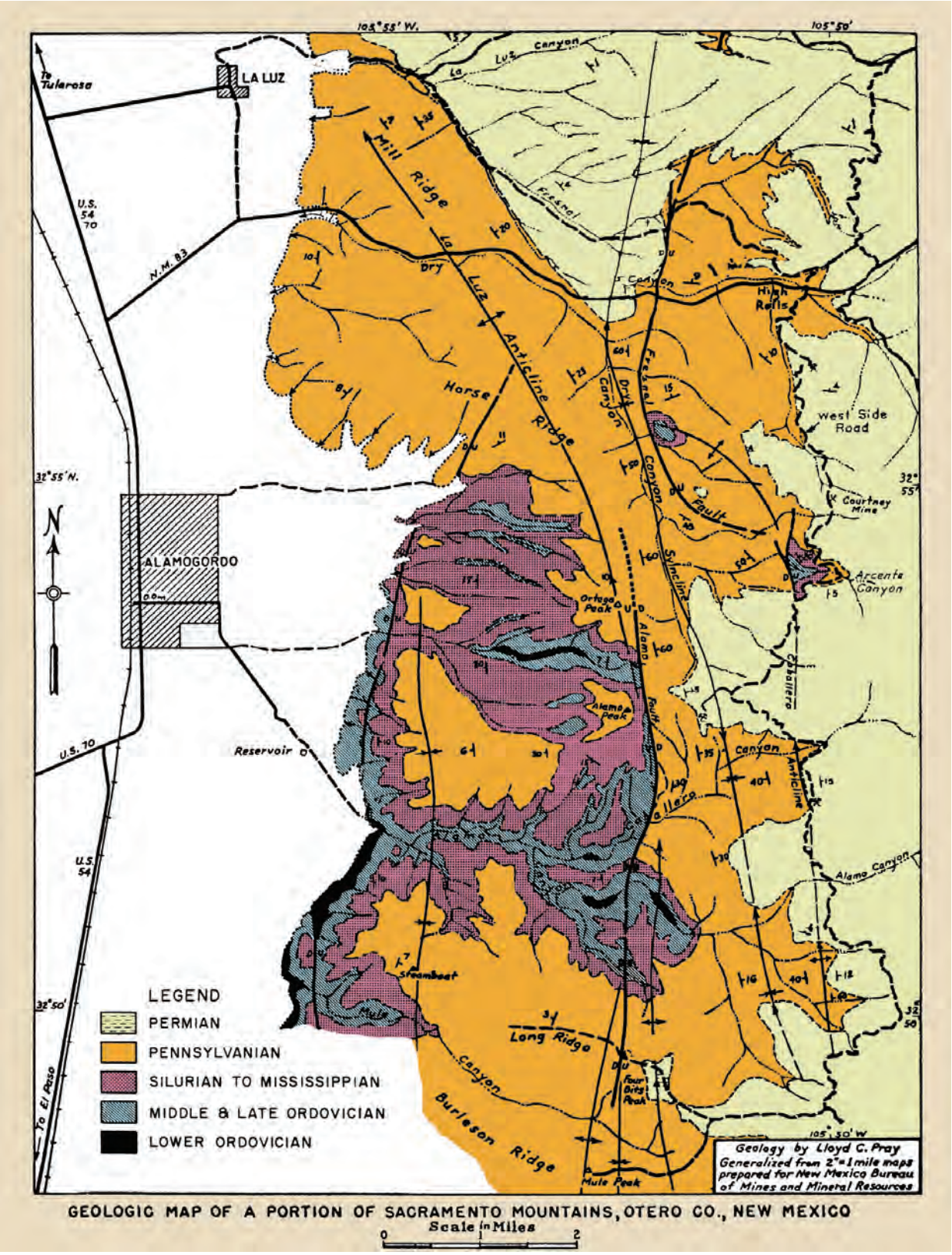

Figure 12 - Geologic map of the Sacramento Mountains escarpment (after Pray 1959).

observe multiple episodes of tectonism. The superposition of Ancestral Rockies, Laramide, and Basin and Range events is striking along the frontal part of the Sacramento Mountains.

GENERAL SUMMARY OF PENNSYLVANIAN AND EARLY PERMIAN CARBONATES

Age

The carbonate rocks of Pennsylvanian and Early Permian (Wolfcampian) age are well known in North America and maintain a consistency in character much different from Mississippian and later Permian rocks. Much of our field trip through the Sacramento Mountains will deal with rocks of this age, so it is useful to summarize some of the general aspects of their deposition and paleogeography. This paper concerns rocks from about 310 to 275 million years of age. North American stage subdivisions are as follows:

PERMIAN	Wolfcampian
PENNSYLVANIAN	Virgilian
	Missourian
	Desmoinesian
	Atokan
	Morrowan

This interval, including Morrowan through Wolfcampian time, will be referred to as Penn-Perm in the rest of the paper.

Location

Penn-Perm carbonates are well known across much of North America, including Alaska. They are also known from rocks of Northern Gondwana and scattered occurrences in the Tethyan realm. Much of the North American Midcontinent was in a clearly equatorial region. Although there is some controversy concerning exact locations, most workers believe the US Midcontinent was within 15 degrees north or south of the Pennsylvanian equator (Fig. 13). This would put much of the North American Midcontinent and New Mexico in an area under the influence of trade winds. On North America, carbonate abundance tends to vary laterally with tremendous rapidity. Carbonate sections pass laterally into siliciclastic dominated facies (Fig. 14). The dominant clastic sources appear to be the Appalachian margin, the Ouachita-Marathon Belt and other isolated sources within the craton. Carbonates become dominant with increasing distance away deltaic sources. Apparently detritus from these source areas suppressed carbonate production (Fig. 15).

Tectonic Setting

The Penn-Perm tectonic environment of North America has had an important effect on sedimentation patterns on the North American Craton. Eastern North America was the site of continental-continental collision in the form of the Appalachian or Alleghenian Orogeny. The south coast of the craton became another collision orogen with the onset of the Ouachita-Marathon Event. Both eastern and southern mountains shed huge clastic wedges into foreland basins. With all the collision to east and south, it is not surprising that the craton was relatively active tectonically during this time. Many small uplifts and basins formed within the craton (Fig. 16). In the southwestern and western states, these uplifts have been called the "Ancestral Rocky Mountains" because of their location near the present Rocky Mountains. Many of the boundary faults to the uplifts and basins are reactivated older structures. An example of a cratonal structure reactivated in Pennsylvanian time is the Arbuckle Mountain region of Southern Oklahoma, located along the margin of the early Paleozoic "Southern Oklahoma aulocogen". In Southern New Mexico, the Pedernal Uplift and Orogrande basins are large structural elements mobilized during the Pennsylvanian and Early Permian.

Penn-Perm stratigraphy directly reflects the location of the uplifts and basins. Unconformities coalesce on the crests of the uplifts; other stratigraphic units onlap the paleo-highs (Fig. 17). Some of the uplifts form localized sources of clastic sediments that interfinger with carbonates and deepen outward away from the uplifts. Carbonate strata reflect this topography. Mounds tend to form on the shoulders of the uplifts in localized shallow water environments.

The most important tectonic controls on Penn-Perm carbonate sedimentation were the localized and important sources of siliciclastic debris. Because of this, most Penn-Perm carbonates are intimately interbedded with siliciclastics. Carbonates can be thought of as the "clear water facies" of Penn-Perm sedimentation.

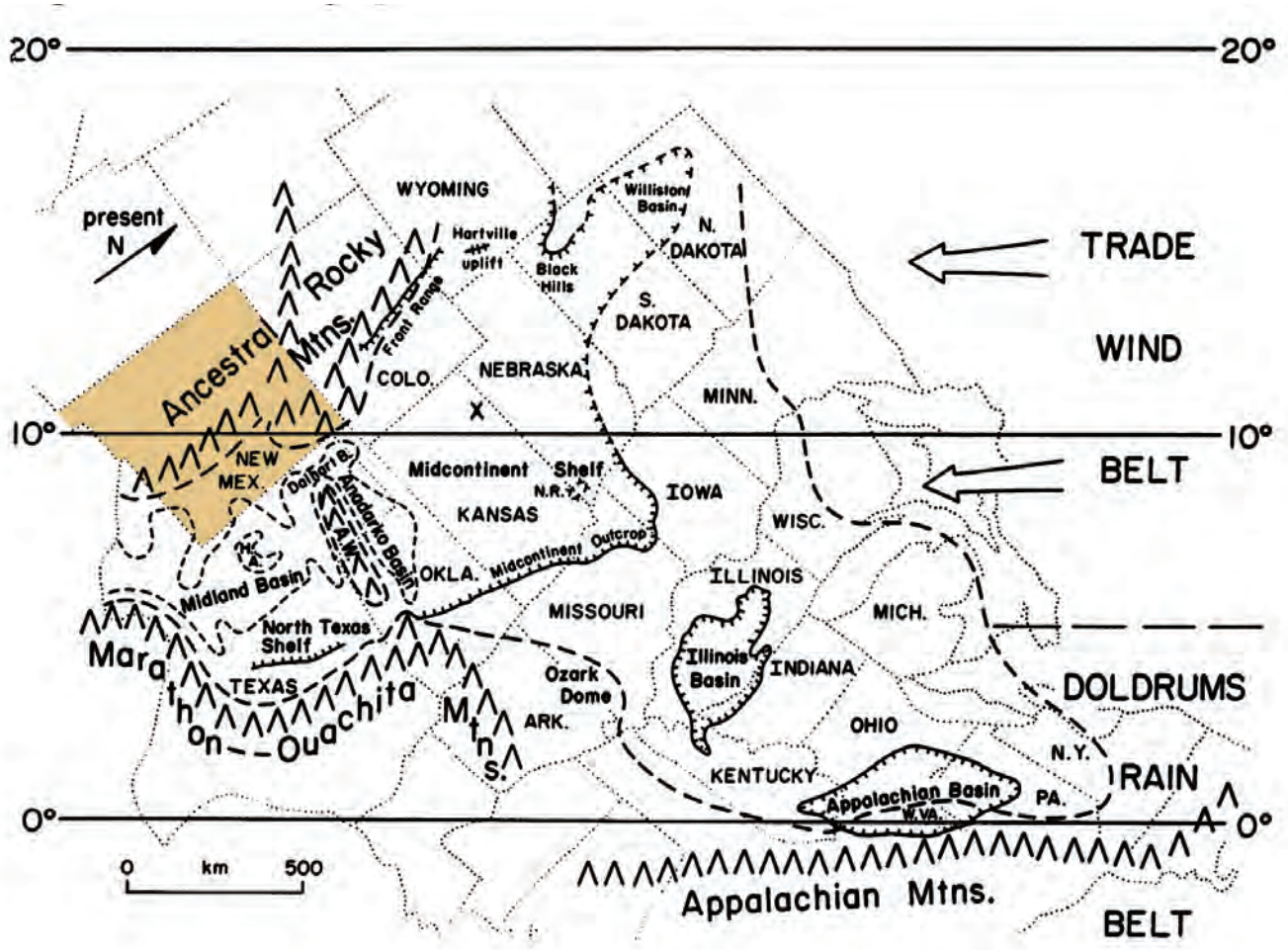

Figure. 13 - Paleogeographic reconstruction for Late Pennsylvanian for central United States (after Heckel 1980). Notice that most of the region is in tropical latitudes. Note position of New Mexico in trade wind belt.

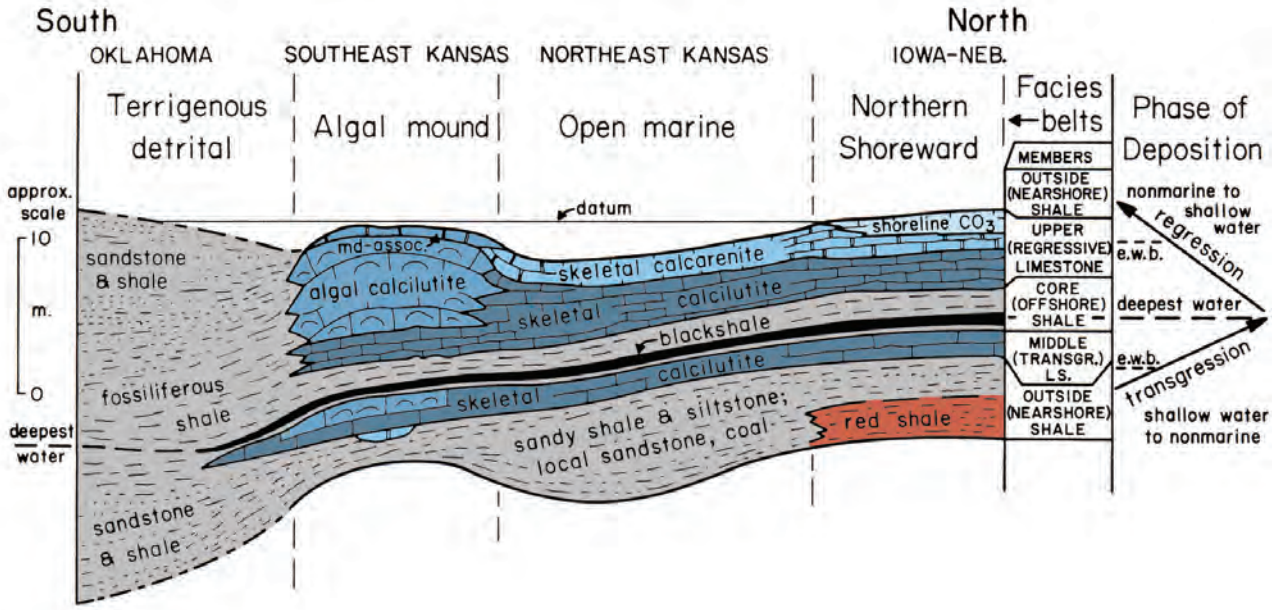

Figure 14 - Cross-section illustrating Upper Pennsylvanian cyclothems as they pass laterally from carbonate-rich to siliciclastic-rich facies near source regions in Oklahoma (after Heckel 1980).

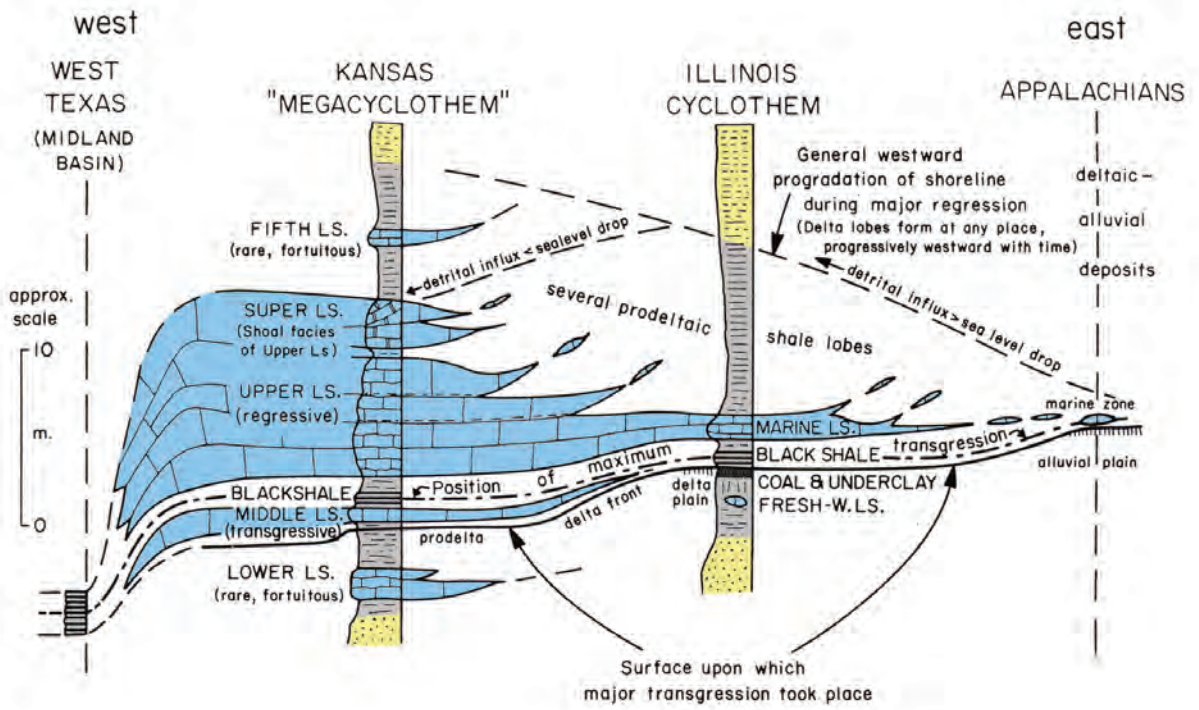

Figure 15 - Cross-section of an Upper Pennsylvanian cyclothem passing westward into a basinal environment and passing eastward into the influence of deltaic influx from source areas to the east.

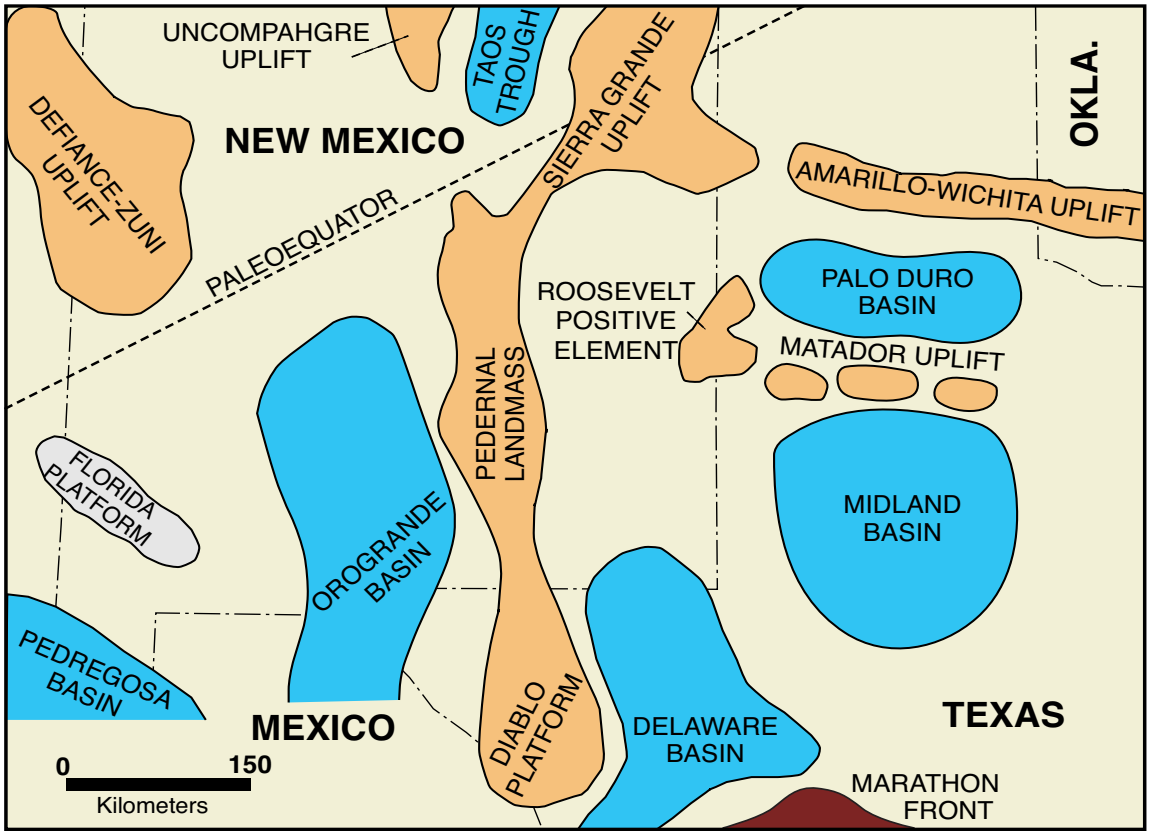

Figure 16 - Map illustrating the major Late Paleozoic structural elements of the southwestern United States during prominence of the Ancestral Rocky Mountains. 1 - Pedernal Uplift, 2 - Diablo Platform, 3 - Sierra Grande Uplift, 4 - Florida Platform, 5 - Defiance-Zuni Uplift, 6 - Uncompahgre Uplift, 7 - Roosevelt Positive Element, 8 - Amarillo-Wichita Uplift, 9 - Matador Uplift, and 10 - Marathon Salient of Ouachita fold belt (after Pol 1982; adapted from Toomey and Babcock 1983).

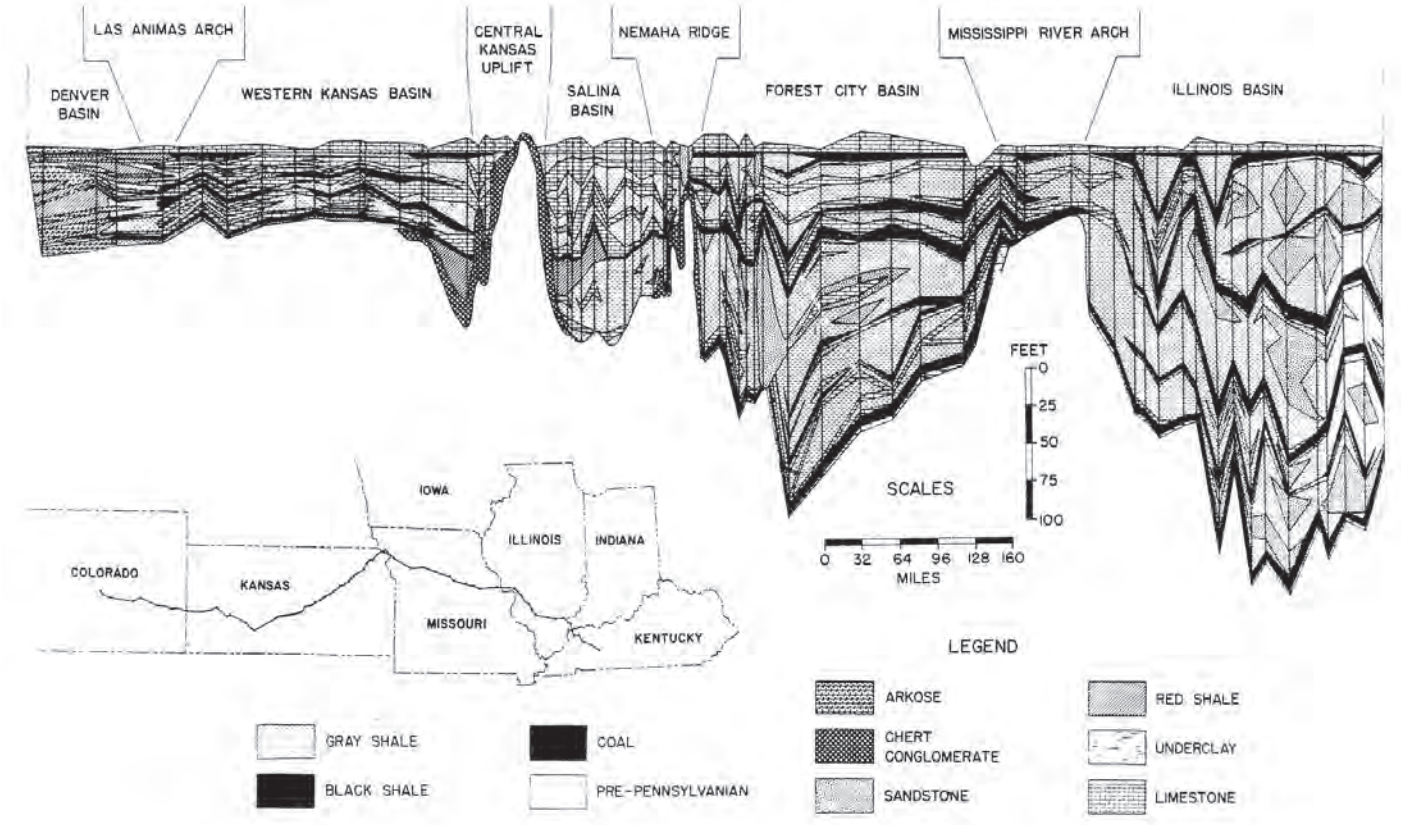

Figure 17 - Lithologic cross section across central United States illustrating the onlap of units against uplifts and coalescence of unconformities on crests of uplifts (after Wanless 1972).

Climate

Penn-Perm climates are easily reconstructed for North America. From Mississippian to Early Permian times, carbonate production was prevalent, thus indicating the tropical climes of the area. By studying diagenesis associated with subaerial exposure and certain climate-sensitive lithologies, a very generalized progression in Pennsylvanian climates can be identified.

The unconformity separating Mississippian from Pennsylvanian strata is readily recognized across most of North America. In many places, this is a strongly paleokarsted surface. This indication of intense limestone dissolution suggests a humid climate for Early Pennsylvanian time. In addition, Early and Middle Pennsylvanian sedimentary rocks contain abundant coals. These are further evidence of a humid climate during Pennsylvanian deposition (Parrish 1993; Schutter and Heckel 1983).

Many Mid-Late Pennsylvanian limestones were exposed subaerially during sea-level lowstands. The exposure resulted in development of paleosols. These old soils tend to be rich in calcareous crusts and "caliche" fabrics. When shales were exposed subaerially, soils developed with hydromorphic characteristics, such characteristics are caused by soaking followed by drying of the soil. These paleosols are well known to develop in strongly seasonal climates in which there is a marked wet and dry season.

Late Pennsylvanian and Early Permian rocks contain similar paleosols that must have formed in seasonally wet and dry climates. However, the strata differ from the older rocks in that the siliciclastics contain more red beds. These are especially common in the Early Permian strata. This suggests more intense oxidation resulting from a stronger dry season than existed for the older rocks. In addition, the coals have mostly disappeared by this time. Early Permian rocks contain more abundant gypsum evaporites than earlier deposits. Although Late Pennsylvanian to Early Permian climates were seasonally wet and dry, the evidence suggests a rather strong and increasing trend toward aridity.

In summary, the Penn-Perm sequence of North America is one of initially humid conditions, followed by seasonal wet and dry climates that progressed to increasingly dry climates into the Early Permian. Superimposed on these general climatic changes are probably a high degree of climatic variability. The cause for this variability is the areal

expanse of continent covered by epeiric seas. During times of high sea level, one might expect relatively humid climates on the continent. During times of low sea level, the continent could have been relatively dry.

The Pennsylvanian-Permian rocks of Gondwana are well known for laterally extensive diamictites and striated pavements. These deposits of continental glaciers represent multiple events of glaciation and deglaciation.

Some of these layers correlate with events of apparently glacioeustatic sea level change on other continents (Crowell, 1978).

Common Lithofacies - Environments

Penn-Perm lithofacies are best known for their variability in a vertical sense and their lateral variability related to uplifts and basins. These units are best known for the fact that limestones tend to be interbedded with shales and sandstones on the scale of several meters or several tens of meters.

Many of the limestones have muddy lithologies that are dominated by wackestone and packstone. These limestones are well bedded and nodularly bedded. Internally, beds typically are burrowed. Most beds are separated by shaly breaks modified by micro-stylolites. For the most part, these units contain a diverse marine flora and fauna that contains red and green algae dominated by free growing or encrusting phylloid (leaf-like) algal plates, brachiopods, corals, foraminifera (mostly fusulinids), crinoids, and mollusks. In many cases, fossils are in life position or near to it. Some grainy layers represent sporadic currents, and a few oncolites suggest rolling of grains. Overall, not much abrasion is suggested by preservation of dedicated fossils.

Other common facies of interest:

1. Ooid grainstone. Fossil fragments are well abraded and units are cross-bedded.
2. Fossil fragment grainstone, dominated by a diverse assemblage of foraminifers, dasycladacean algae, and other fossils.
3. Phylloid algal blade packstone with crinoids, brachiopods and fusulinids.
4. Unfossiliferous mudstone to muddy lithologies dominated by mollusks.
5. Crinoidal grainstones to mud-poor packstones in which little if any transport of grains is indicated.

Although many other varieties of lithofacies types are present. The above listing contains common ones that serve to illustrate many aspects of Pennsylvanian limestone sedimentation. In addition, "Pennsylvanian reefs" were rather unique.

Reefs

Penn-Perm "reefs" tend to be localized at breaks in slope. Most people feel more comfortable calling these features mounds (or bioherms and biostromes), rather than true reefs. Size and depositional topography on the mounds were variable but generally small, ranging from tens of centimeters to 20 meters. Most are several meters to 20 meters thick. Some are crudely bedded and many lack internal structure. Others consist of a series of dipping foresets.

The most common mound lithology is the phylloid algal bioherm. The most obvious structures in these mounds are corn flake to leaf-sized pieces of calcareous algal blades. Most of these were green algae, but some were probably reds. A few were encrusters or binders whereas most were simply free-standing leaves. Phylloid algal mounds generally have a wackestone or packstone lithology. Whereas some are massive, many consist of steeply dipping (25°) foresets. Commonly associated fauna include fusulinids, tubular foraminifera, brachiopods and crinoids, all indicative of a normal marine environment. For most phylloid algal mounds, no real frame-builder has been identified.

Careful observers have noted another fauna within some phylloid algal mounds and some mounds are dominated by this largely frame-building fauna. Some consist of knobby and digitate masses of brownish sparry material. These masses are thought to originate as intergrowths of encrusting foraminifera and algae (perhaps blue-greens) or bacteria. The knobby masses have the appearance of light and dark spots which gives the lithology the descriptive appearance of "leopard rock". Other encrusting and frame-building organisms are *Archaeolithophyllum* (a red alga), encrusting foraminifera, *Syringopora* (a tabulate coral), and sponges. These common associates, along with leopard rock, may construct a true framework mound and be common fauna in phylloid algal mounds. The other major mound type is dominated by massive heads and tabular masses of chaetitids. These uncommon organisms are thought to be calcareous sponges.

Most Penn-Perm mounds have a muddy matrix, algal flora, and normal marine association. Most are interpreted to have formed in normal marine waters deeper than those in which modern reefs are found, but still no deeper than several tens of meters.

Environment and Biota

Through comparison between lithology and included biota, various workers have constructed models of the relationship between biota, water depth, and degree of restriction (Fig. 18, 19). A restricted, possibly brackish,

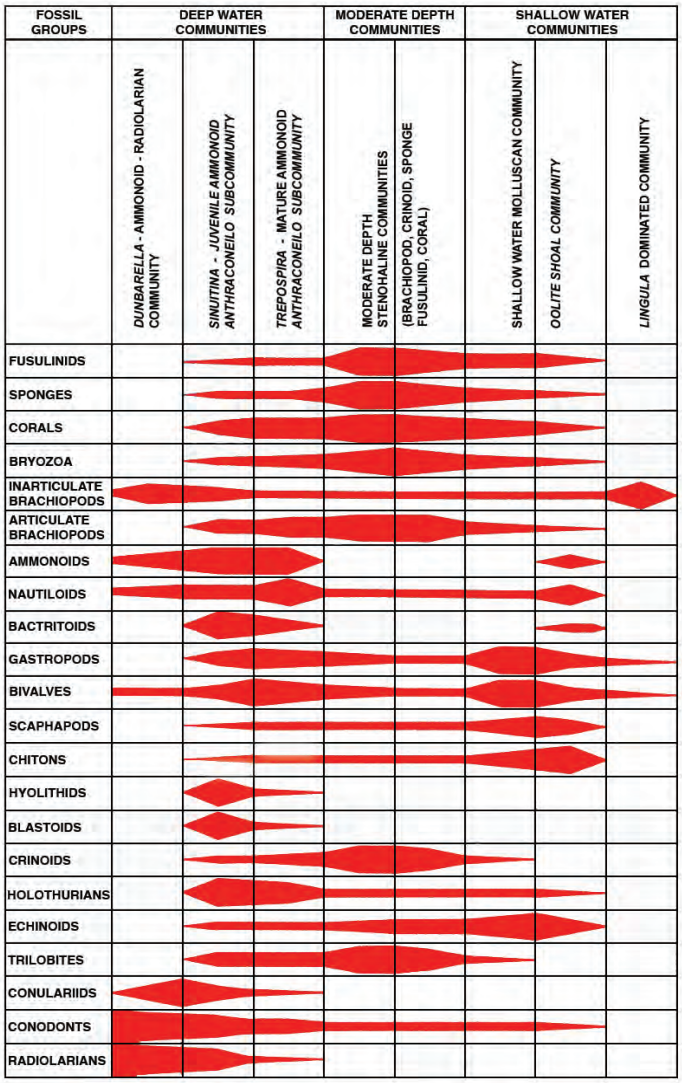

Figure 18 - Distribution of fossil organisms in Pennsylvanian rocks. Note depth controlled distribution of communities (after Boardman et al. 1984).

nearshore marine fauna is composed of *Lingula*, *Myalina*, *Dunbarella*, ornamented ostracodes, and arenaceous foraminifers. Another fauna is identified that is thought to have lived in shallow waters with restricted conditions, perhaps subject to non-normal salinities. This molluscan fauna is dominated by Bellerophontids and high spired gastropods and *Myalina* and other pelecypods; most normal marine fossils are missing here. Other normal marine assemblages are rich in brachiopods, bryozoans, sponges, corals, echinoderms and phylloid algae — this fauna was deposited at moderate depths. In even deeper water, other organisms dominate. Boardman et al. (1984) have summarized their models on depth and salinity control on these fossil assemblages.

Vertical Relationships

The most obvious aspect of Penn-Perm sedimentation is the dominantly cyclic nature of sedimentary units. These cycles are reflected in carbonate- siliciclastic alternation, as well as in apparent changes in water depth reflecting repeated alternation between marine and nonmarine or deeper marine and shallower marine. These "cyclothems" are on the scale of ten meters or so and seem to change lithologic character laterally. Two of the best known types of cyclothems are those described by Wilson (1967, 1972) for New Mexico (Fig. 20) and those of Heckel (1980) for the U.S. Midcontinent (Fig. 21). In both models, carbonates have been interpreted to show evidence of shoaling upward. The New Mexico example is asymmetric in that

Figure 19 - Cross-sectional model explaining depth related distribution of Pennsylvanian organisms (after Boardman et al. 1984).

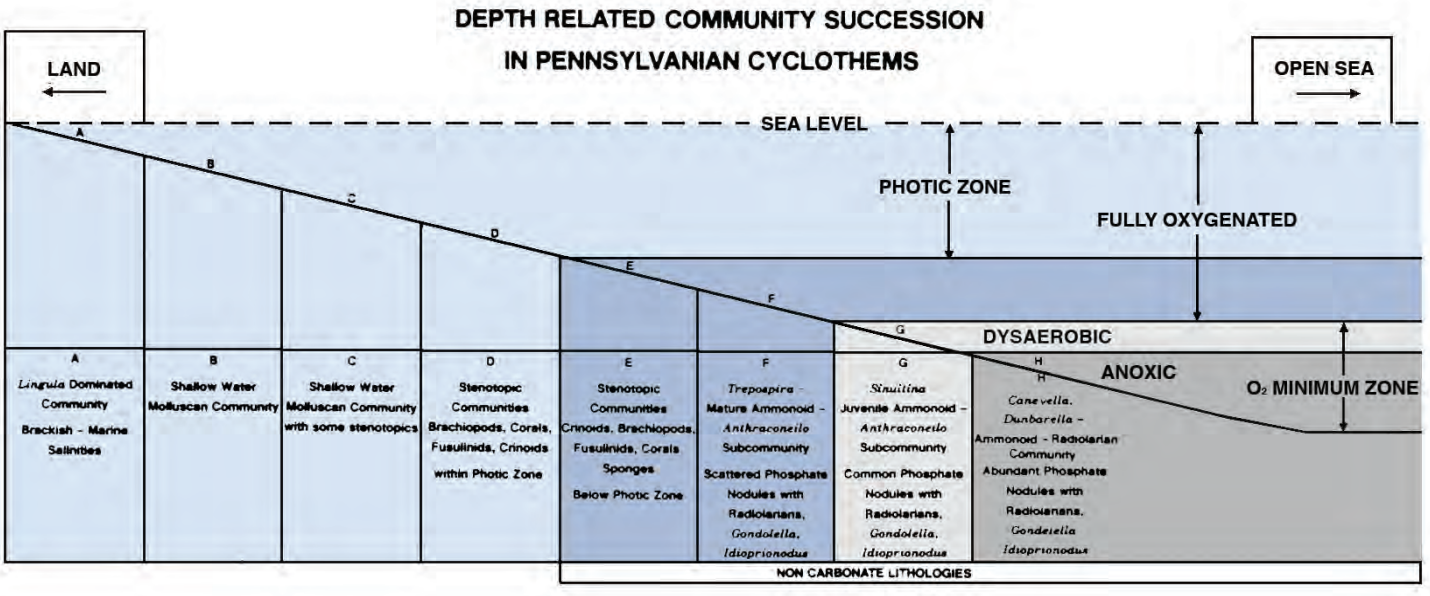

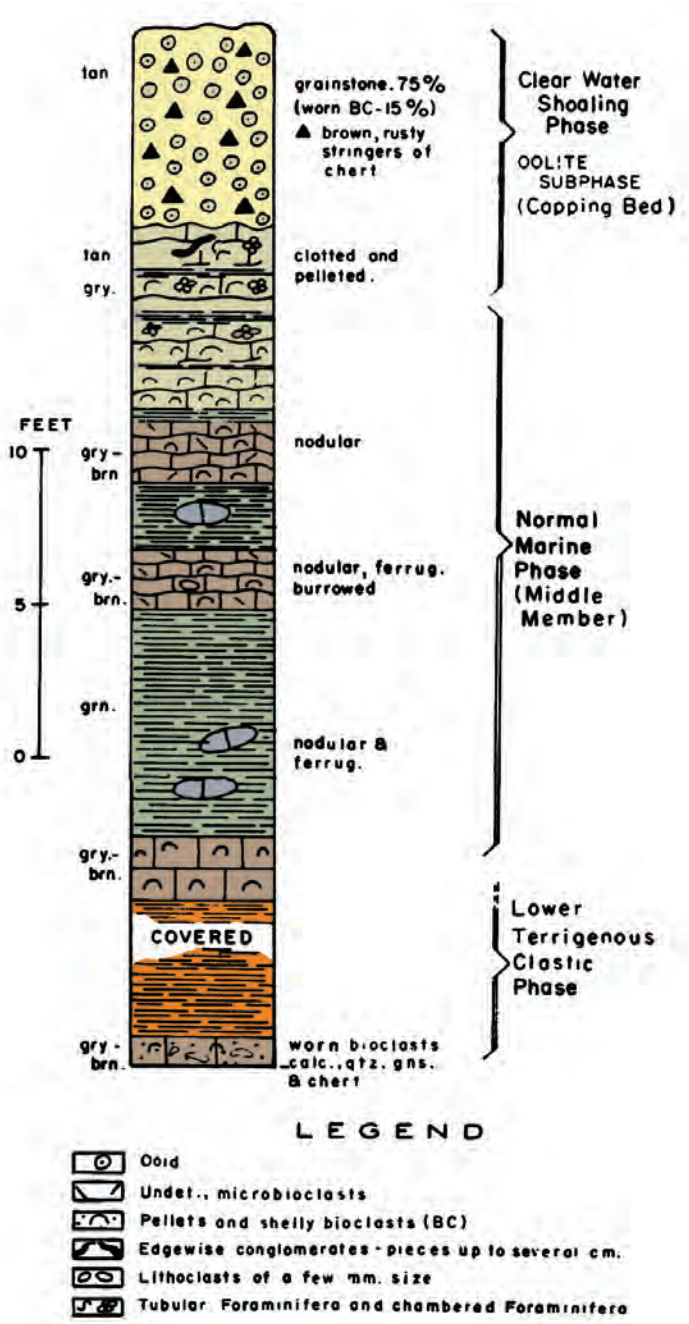

Figure 20 - Typical shelf cycle from Virgilian Holder Formation, Sacramento Mountains New Mexico (after Wilson 1967).

it reflects cyclic and reciprocal sedimentation in that little is deposited on the shelf during relative lowstands of sea level. The Kansas-Iowa cycle of Heckel is more symmetrical around a deep (anoxic) core shale. Suggestions for cyclicity have been switching of delta lobes, yo-yo tectonics, and eustatic changes in sea-level. Many cycles are laterally traceable for hundreds of miles. If total numbers of cycles are divided by the total amount of time, each cycle would occupy about 1 million to 250,000 yrs. Most workers believe that glacio-eustatic sea level change is the predominant driver for cyclothem development (Ross and Ross 1987; Watney et al. 1989).

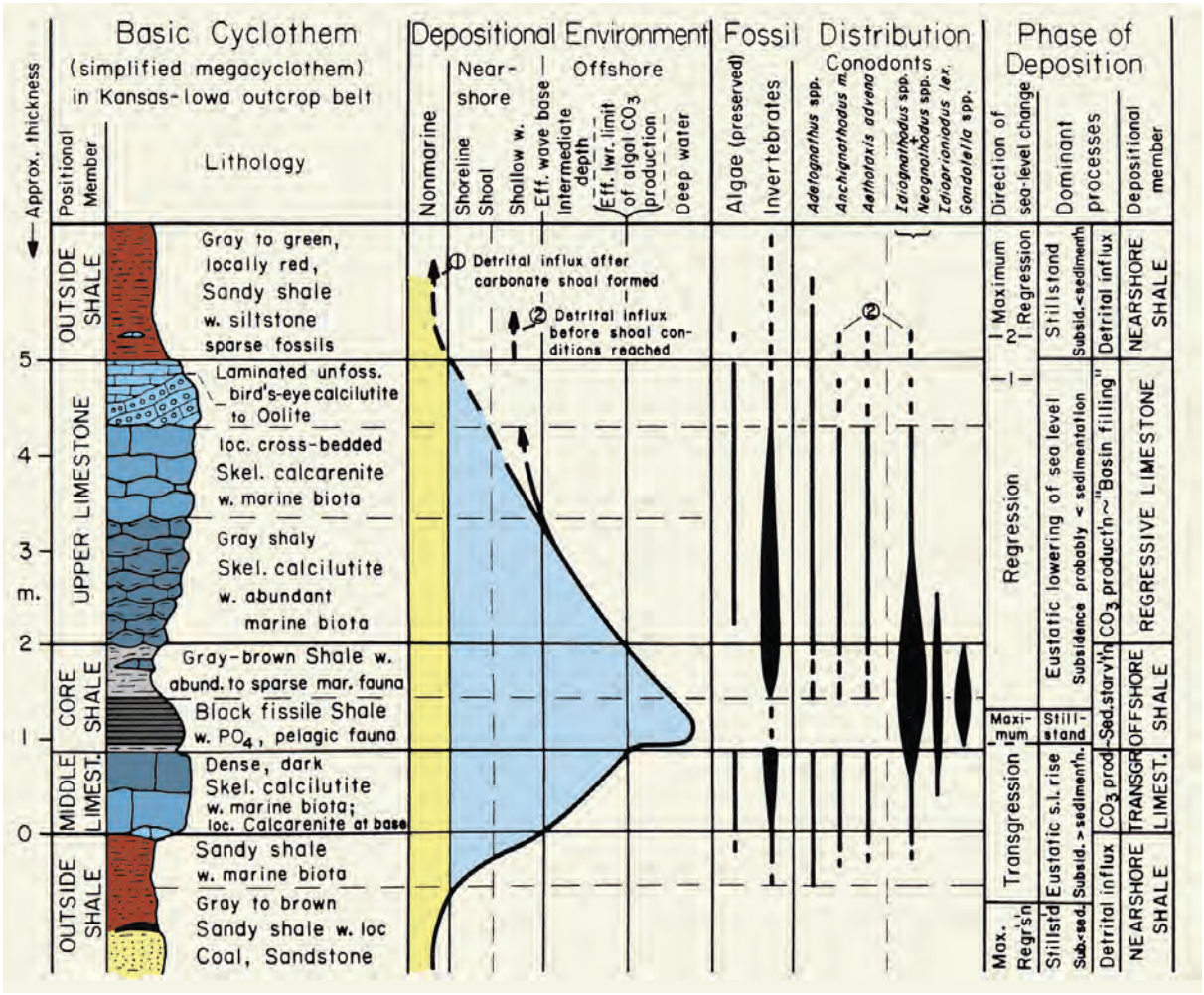

Figure 21 - Kansas Upper Pennsylvanian cyclothem model illustrating lithology, depositional environments conodont and algal distribution, and process (after Heckel 1980).

CARLSBAD TO ALAMOGORDO ROAD LOG

Cumul. Mileage	Mileage From Carlsbad	Description
0.0	0.0	Leave Carlsbad traveling north on U.S. 285 from its junction with U.S. 62-180 in downtown Carlsbad traveling toward Artesia, NM.
21.3	21.3	Junction with NM 137. Continue north on U.S. 285. As we travel northward, we cross several "reef" zones in the subsurface. Just a few miles north of here, our route crosses the trend of the San Andres reef zone (Miller 1969) and further to the north, we cross the Abo reef trend about 5 miles south of Artesia (LeMay 1972). In general, these trends parallel the Capitan Reef trend in the subsurface along the northern end of the Delaware basin.
0.8	22.1	Next 2 miles, low road cuts through thin-bedded dolomites (with evaporite crystal casts) and redbeds of the restricted lagoon facies of the Yates and Seven Rivers Fms., similar to outcrops visited in Dark Canyon and Rocky Arroyo on Day III.
5.6	29.7	Junction with NM 381. Hills visible 10 km (6 mi) to the east form the McMillan Escarpment and are composed of the Permian Artesia Group (undivided Tansill, Yates and Seven Rivers Fms.).
9.4	39.1	Junction with NM 335, continue north to U.S. 285 toward Artesia.
4.1	43.2	Entering Artesia, NM. This is the home of the Holly Corp.'s Navajo Refinery which is one of only three refineries in the state. It has a crude oil capacity of 75,000 BPD and the ability to process a variety of sour crude oils into high value light products (such as gasoline, diesel fuel and jet fuel). Artesia is also the home of Yates Petroleum Co. and several related companies.
1.5	44.7	Turn left at junction with U.S. 82 (U.S. 83 on maps published prior to 1968) traveling west toward Cloudcroft. Road traverses 32 km (20 mi) of Quaternary alluvium, good time for a nap or reading detailed descriptions of future stops.
21.3	66.0	Hope Village center.
6.9	72.9	Chaves County line.
5.7	78.6	Junction with NM 13, continue west on U.S. 82.
0.2	78.8	Roadcut in Quaternary alluvium.
0.3	79.1	Next 1 3 miles, scattered outcrops of dark grainstones of the San Andres Fm.
1.7	93.8	Junction with NM 24 on left. Continue on U.S. 82 west into foothills on the east side of the Sacramento Mountains. Hillsides and roadcuts for the next 45 miles are either limestones of the San Andres Fm. or red and yellow terrigenous clastics of the Yeso Fm. U.S. 82 slowly climbs the east side of the Sacramento Mts. (almost a dip slope), gradually cutting deeper into the San Andres limestones and into the Yeso below. As elevation increases, we will pass through several vegetation zones, from open desert scrub to alpine conifer forest.
12.4	106.2	Village of Elk, NM.
2.3	108.5	Mule Canyon Road on left.
0.8	109.3	Otero County line.
0.2	109.5	Enter Lincoln National Forest.
8.6	118.1	Mayhill town limit. For the next 16 km (10 mi), the valley is floored by the Yeso Fm., and the San Andres Fm. occurs on the surrounding higher areas.
0.4	118.5	Junction with NM 130 on left.
10.3	128.8	Junction with Springs Canyon Road on right.
1.1	129.9	Entering town of Winsatt, NM.
4.1	134.0	Cloudcroft Ski Area on left.
1.9	135.9	Junction with NM 24 on right.
1.3	137.2	Cloudcroft town center, elevation about 2,650 m (8,700 ft). Formerly a lumbering center, the area now survives mainly on tourism -- it has both a ski area and the "highest golf

		course in the United States. From here, U.S. 82 drops rapidly, some 1,200 m (4,000 ft) in the next 32 km (20 mi), down the west face of the Sacramento Mts.
0.2	137.4	Alluvium exposed in roadcut to left and right. On the left one can see remnants of the trestles and roadbed of a railway built from Alamogordo to Cloudcroft. The grade was so steep that the trains could not use a simple serpentine ascent but had a Y system in which the train pulled into one arm of the Y, decoupled its engine and had a new engine coupled at the rear in order to continue its journey. Originally built to supply lumber for the construction of the railroad from El Paso to Alamogordo, the line also proved popular for touristic outings around the turn of the century and ran open-air weekend trains from El Paso into the mountains. The railroad also built "The Lodge", a beautiful resort which still is operated on the south side of the town. The railroad line was dismantled in the late 1940's when U. S. Hwy. 82 was built, and today, the trestle is the only reminder of its existence. The area now also boasts one of the largest solar observatories, called "Sunspot", which has been constructed approximately 24 km (15 mi) south of this area. You will be able to see it clearly on the Sacramento Mountain skyline when we go to White Sands.
0.2	137.6	Lower San Andres Fm.
1.7	139.3	Yeso Fm. on right. U.S. 82 drops through over 370 m (1,200 ft) of Yeso Fm. in next 8 km (5 mi).
1.5	140.8	Lower Yeso redbeds typical of the next 5 km (3 mi).
3.2	144.0	Gradational contact of Yeso Fm. (marine) with underlying Abo Fm. (nonmarine) occurs in this general area.
0.6	144.6	Mountain Park, NM.
0.9	145.5	High Rolls, NM and junction with West Side Road. High Rolls is a lead and copper mining district with ores occurring in arkosic beds of the Abo Fm. (Jerome et al. 1965).
1.0	146.5	East side of tunnel and Fresnal Box Canyon — walls are composed of the Bug Scuffle Limestone Member of the Gobbler Fm. (Middle Pennsylvanian). On this side (east side) of the Fresnal Fault, the Laborcita, Holder and Beeman Fms. are missing, but they are present on the west side of the fault.
0.3	146.8	Fresnal Box Canyon vista on right. Effects of drag from the Fresnal Fault Zone on Bug Scuffle Ls. Member may be viewed to the west on the north side of the canyon. Fresnal fault in this area were active during the latest Pennsylvanian and earliest Permian. Delgado and Pray (1977) estimate as much as 490 m (1,600 ft) of displacement, down to the west, along the fault zone in this area. The widespread red coloration of the terrain on the downthrown side of the fault results from exposure of thick Lower Permian Abo (Laborcita) redbeds.
0.7	147.5	Dry Canyon ahead and to the left (south).
0.8	148.3	Tertiary dike and sill intruding Laborcita Fm. on right.
0.8	149.1	Covered, unconformable contact between Laborcita and Holder Fms. at approximately this point.
0.5	149.6	View ahead of flank beds dipping eastward off Virgil bioherms.
0.7	150.3	Virgil bioherm. Lincoln National Forest boundary sign and parking area on left. The west flank of the bioherm is strikingly exposed to the north of the road. Beds with apparent dips of almost 45° at the west end give way to less steeply dipping strata and massive units in the center of the bioherm outcrop. Faint bedding near the center suggests the escarpment does not expose core facies or that the bioherm core is very similar to flanking beds. The 18-25 m (60-80 ft) thick feature is typical of many such bioherms in the area and shares features in common with many late Paleozoic buildups.
0.3	150.6	Cattle guard.
0.3	150.9	Yucca mound Canyon on the right.
3.2	154.1	Junction of U.S. 82 with U.S. 54/70. Turn left (south) toward Alamogordo.
4.4	158.5	Turn left into hotel area of Alamogordo.

SACRAMENTO MOUNTAINS FIELD TRIP AND ROAD LOG

Cum. Mileage	Miles	
0.0	0.0	Leave hotel area, Alamogordo. Turn left (north) onto U.S. 70/54.
0.7	0.7	Turn right (east) onto First Street.
1.8	2.5	At the end of First Street, turn right (south) onto Scenic Drive.
1.0	3.5	At the end of the paved road, continue straight (south) onto gravel road.
0.15	3.65	Gravel Road curves to the right.
1.05	4.7	**STOP 1 - ALAMO CANYON TRAVERSE** - Park vehicles next to pump station and chlorination plant at mouth of Alamo Canyon. Traverse up through the Ordovician section that is on the north side of the mouth of Alamo Canyon. The best traverse is through the cleft made by the dike that is near the south side of the outcrop.

Proceed upward through the upper 80 feet of the Lower Ordovician El Paso Formation (Fig. 6). The section exposed here is the upper 80 feet of a section that is nearly 400 feet thick in the Sacramento Mountains. The entire 400 feet can be observed about a mile to the south where the lowest part of the section is exposed along the frontal escarpment. The El Paso Formation is equivalent to important units such as the Arbuckle Group and the Ellenburger Fm. Most of the El Paso is a light grey dolomite and much of it is muddy in texture. Some intervals contain abundant normal marine fauna. Other intervals are unfossiliferous and burrow mottled suggesting somewhat restricted marine conditions. The El Paso contains significant intervals with irregular blebs of replacive chert.

Climb up through the section and get to the base of the first cliffy exposure on the traverse. Here, there is about a meter and a half thick bed of carbonate rich granulestone to sandstone. The base of this granule rich facies represents the top of the El Paso and the base of the Montoya Dolomite. This sandstone is Middle Ordovician in age and correlates with other transgressive sandstones that are well known around North America. The best known transgressive sandstone of this age is the St. Peter Sandstone. It is possible that this sandstone also correlates with the Cable Canyon sandstone of the Montoya Group of the Caballo Mountains.

Continue traverse upwards through the Montoya Dolomite, middle Ordovician in age. Locally, the Montoya is about 210 feet thick and is extremely fossiliferous, especially in its lower and uppermost parts. In general, it contains a diverse marine assemblage of fossils. The uppermost part of the Montoya is marked by a one to three foot thickness of massive chert. Near the crest of the lower southern nose of the hill, about fifteen feet below the top, there is a one and a half foot thick bed of grey chert that has tan to light orange weathering. This marks the top of the Montoya and the base of the Valmont Dolomite.

The Valmont Dolomite here is about 175 feet thick. It is light grey, generally very fine-grained dolomite. Upper Ordovician fossils occur near the top of the lower part of it. Above us are the browner, dark, massive cliffs of the Silurian Fusselman Dolomite.

Walk to the eastern end of the lower nose to get a panoramic view of Alamo Canyon and the South Deadman branch of Alamo Canyon (to the south). We are at an important transition point in the Sacramento Mountains for Mississippian sedimentation, Pennsylvanian sedimentation and tectonics, Laramide tectonics, and Basin and Range tectonics.

The high limestone cliffs to the North are Mississippian units of the Lake Valley Formation (Fig. 22), mostly comprised of about (approaching) 220 feet of Tierra Blanca Member. These echinodermal calcarenites thin dramatically to about 60 feet (Lane and Ormiston 1982) as one looks southeast at the far wall of South Deadman Branch. In the southern Sacramento mountains, the Tierra Blanca is only about 5 feet thick and is dominated by cherty, spiculitic wackestones (Meyers et al. 1982). The buildup of the Tierra Blanca shelf is an example of rapid localized sedimentation forming on the updip portions of a south-

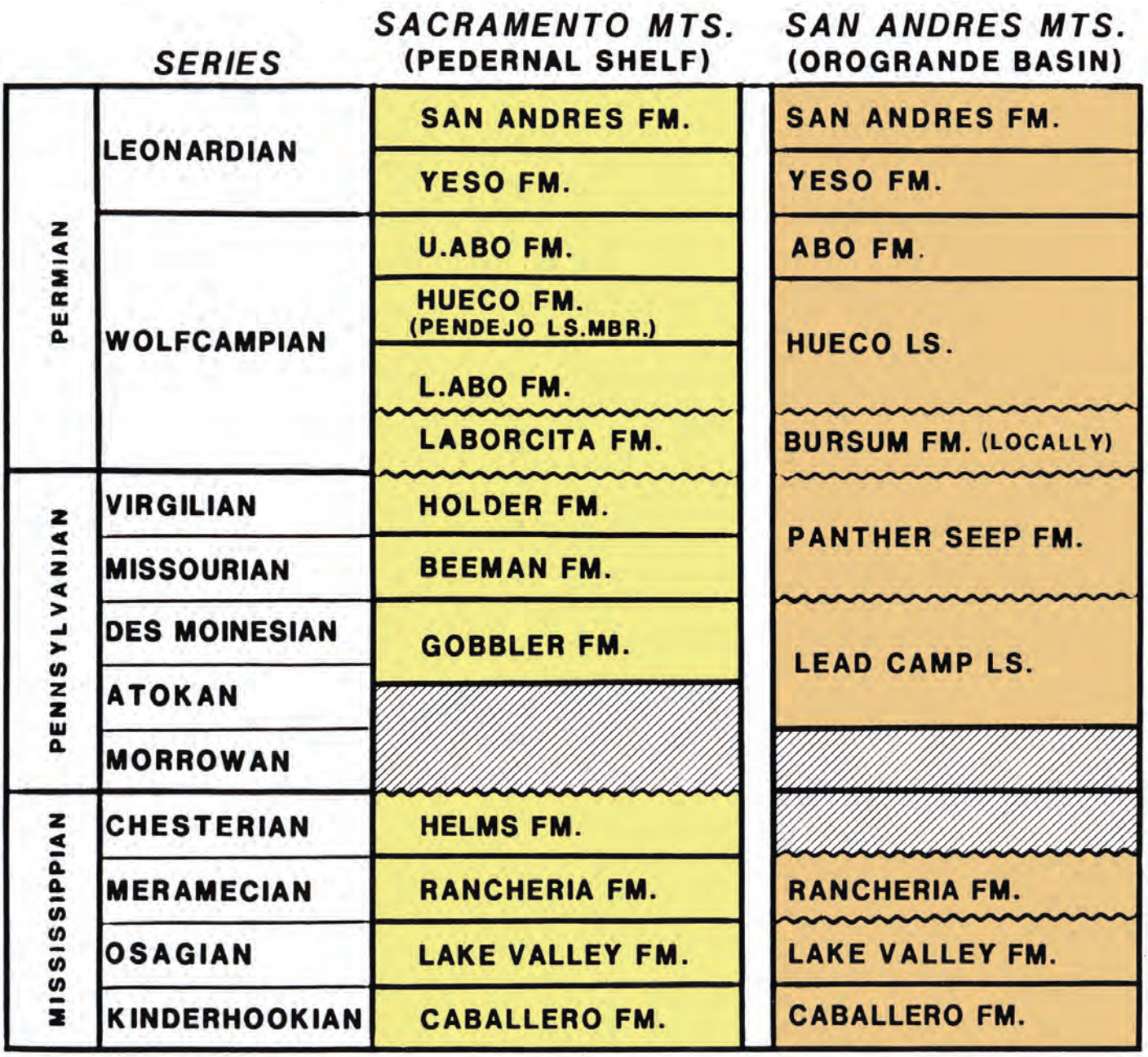

Figure 22 - Stratigraphic correlation chart summarizing the Mississippian, Pennsylvanian, and Permian stratigraphy of the Sacramento Mountains and Orogrande basin (from Candelaria, 1988; after Pray, 1959 and Bachman and Myers, 1975).

ward sloping ramp (Ahr 1989) to produce a carbonate shelf. In general, the north to south shelf edge exposed in Alamo Canyon reflects the north to south slope of the Mississippian basin that protrudes southward from the southern tip of the Transcontinental Arch (Figs. 7, 8, 23).

In South Deadman Branch and southward, much of the topography of the Tierra Blanca shelf edge is reduced by onlapping facies of the Arcente and Doña Ana Members (Fig. 10). From a sequence or seismic stratigraphy point of view, these units might be thought of as basinally-restricted onlapping wedges.

The Mississippian cliffs to the north and south of this vantage point contain some rather massive looking units. These units are generally crinoidal and bryozoan wackestones and

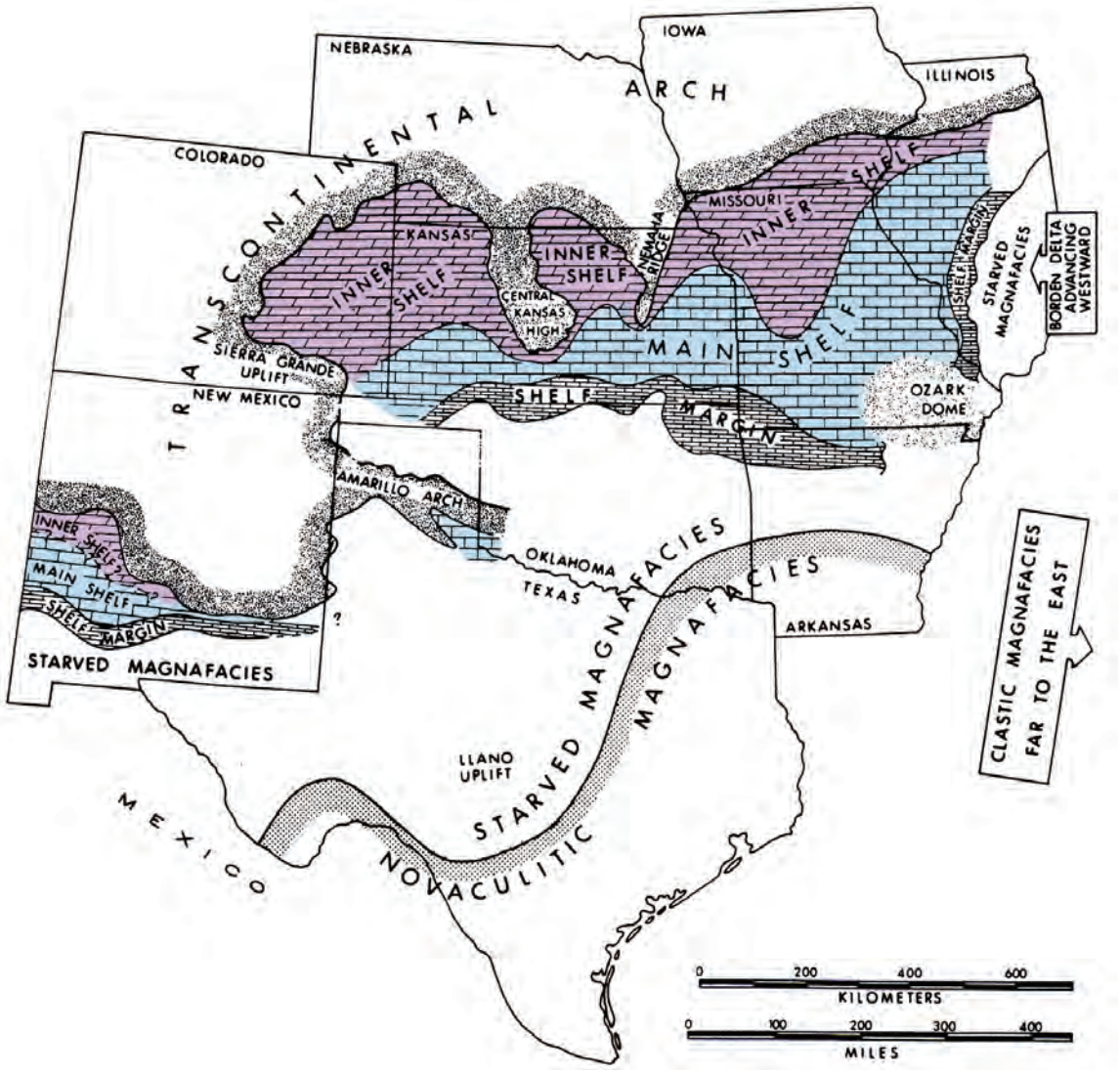

Figure 23 - Distribution of Mississippian facies (Tournasian) of the central United States. Note the reflection of the North to South shelf to basin transition in southern New Mexico (after Lane 1982).

packstones. Some of them contain large *stromatactis* cavities filled with internal sediment and submarine cement. Algae are lacking. The massive units pass laterally into well-bedded flanking crinoidal packstones and grainstones. Such massive units have the characteristics of Waulsortian facies (similar to those of Waulsort, Belgium). The massive units in this locality are carbonate buildups of mounds that have formed within the Alamogordo, Nunn, and Tierra Blanca members. Most of the mounds appear to be asymmetric and tabular. Similar mounds to the south are much larger and hemispherical in shape. Although the Waulsortian facies is generally thought to indicate formation in relatively deep shelf environments, the tabular or asymmetric character of the mounds of this area may indicate that they formed under the influence of currents above or just above wave base (Jackson and DeKeyser 1989).

If one looks to the south at the high ridge on the horizon (Steamboat) one can see exposure of the Pennsylvanian limestones of the Bug Scuffle member of the Gobbler Formation. Trace the exposure to the east and notice the increase in cover and slope formation that is coincident with an increase in predominance of siliciclastics in the unit. In a simpli-

		fied sense, the transition may be taken to indicate the influx of a new source of siliciclastics to the east. Thus, uplift of the Pedernal landmass (the siliciclastic source) is suggested in Pennsylvanian time. The transition from a north to south slope in Mississippian time, to an east to west slope in Pennsylvanian time is indicative of an important tectonic event concurrent with formation of the Ancestral Rocky Mountains.
		Look due south across the canyon at folded and faulted exposures of the Ordovician and Silurian units. Such eastward-directed thrust faults are suggestive of an event of uplift and deformation during the early Tertiary Laramide Orogeny.
		The modern scarp we have climbed is a product of recent events of Basin and Range faulting.
	4.7	Return to vehicles and reverse direction
1.2	5.9	Gravel road meets paved road. Continue north on paved road called Scenic Drive.
1.0	6.9	Turn left (west) on First Street
1.8	8.7	Turn left (south) on U.S. 54/70.
1.6	10.3	Turn left (south) onto U.S. 54 going towards El Paso.
4.95	15.25	Turn left (west) across railroad tracks.
2.0	17.25	Turn right (south) at T-intersection.
1.0	18.25	Turn left (east) towards mountain range. The turn is about half a mile past the large water tank and about a couple of tenths of a mile past the well head on the left.
0.35	18.6	Cross under power lines, continue straight
0.1	18.7	Well head, where buses could stop. Four-wheel drive vehicles are desirable after this point. There is a good turn around point for buses here. Continue on rough road all the way up to the mouth of San Andres Canyon.
1.0	19.7	At the mouth of San Andres Canyon, as far as one can go, there is finally a turn to the left. Turn left here and continue down the alluvial fan to the northwest.
0.3	20.0	Corral and water tank. Take road to the right that goes northwest towards Muleshoe Canyon.
0.65	20.65	**STOP 2 - MULESHOE MOUND** Arrive at the mouth of Muleshoe Canyon.
		From mouth of Muleshoe Canyon, walk up the Canyon staying to the south side. Walk up along the trail that traverses a low Valmont saddle. Continue up canyon until you reach the base of the Fusselman cliff. Look north at Muleshoe mound.
		From this vantage point, a good large-scale view of Muleshoe is possible.
		Muleshoe mound is Mississippian (Kinderhookian and Osagian) in age. It rises out of the Andrecito, Nunn, Alamogordo, and Tierra Blanca Members of the Lake Valley Formation (see Figs. 24, 25) (Lane and Ormiston 1982) . The mound can be divided into five deositional units separated by hiatal surfaces (Kirkby and Hunt, 1996; Figs. 26 and 27) Although the face exposed in Figs. 24 and 28 represent an off center cut, a cross-section more than 100 meters thick is observed. Steep dips are observable on the flanks of the mound. Whereas the mound core lithologies are muddy, the flank beds are crinoid-bryozoan packstone and grainstone. A large pod of megabreccia is observable on the east flank (Fig. 28). The Arcente and Doña Ana lap out against the mound. The Doña Ana is erosionally truncated at the base of the Rancheria. The Rancheria and the top of Muleshoe are truncated by the pre-Pennsylvanian unconformity and overlain by siliciclastics of the Gobbler Formation.
		Next, walk north into the ravine of Muleshoe Canyon. Walk up the small ravine that heads upward toward the Muleshoe megabreccia pod that is to the northeast. Continue heading upward through outcrop of Ordovician Valmont Dolomite. Continue and traverse through good outcrops of Silurian Fusselman Dolomite in which silicified globular stromatoporoids are exposed at the base and silicified laminar stromatoporoids are exposed at the top. The best exposures of Muleshoe's megabreccia are in large float blocks that occur within and above the ravine as it cuts though the Fusselman. Walk upward through cov-

Figure 24 - Photograph of Muleshoe Mound. Notice the overall domal internal geometry observable. Large pod of megabreccia is present on the far right. The flat top may have been caused by erosional truncation before deposition of overlying Pennsylvanian strata of the Gobbler Formation.

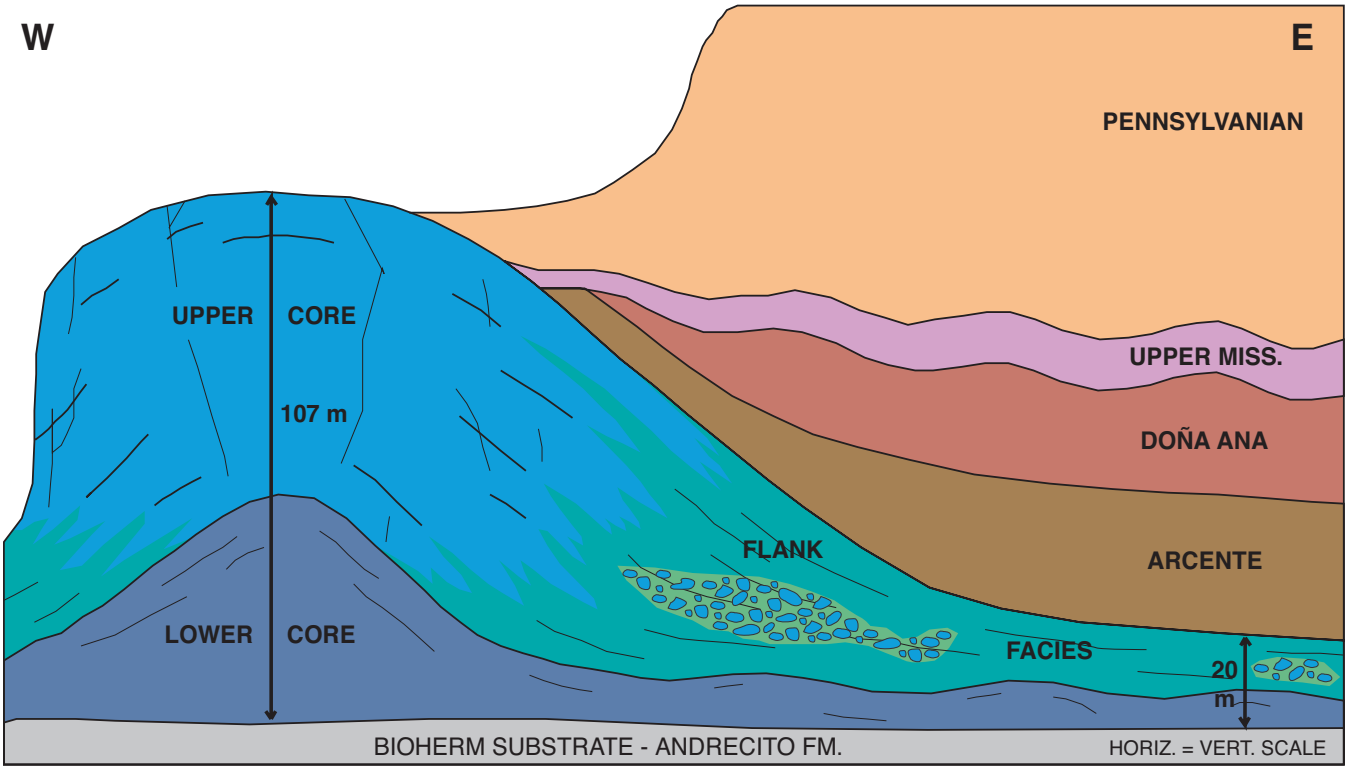

Figure 25 - Field sketch of Muleshoe Mound. Notice steeply dipping flank facies, differentiation between lower mound core and upper mound core, megabreccia pod, onlap of the Arcente and Doña Ana, and erosional surfaces below Rancheria (Upper Mississippian) and Pennsylvanian strata.

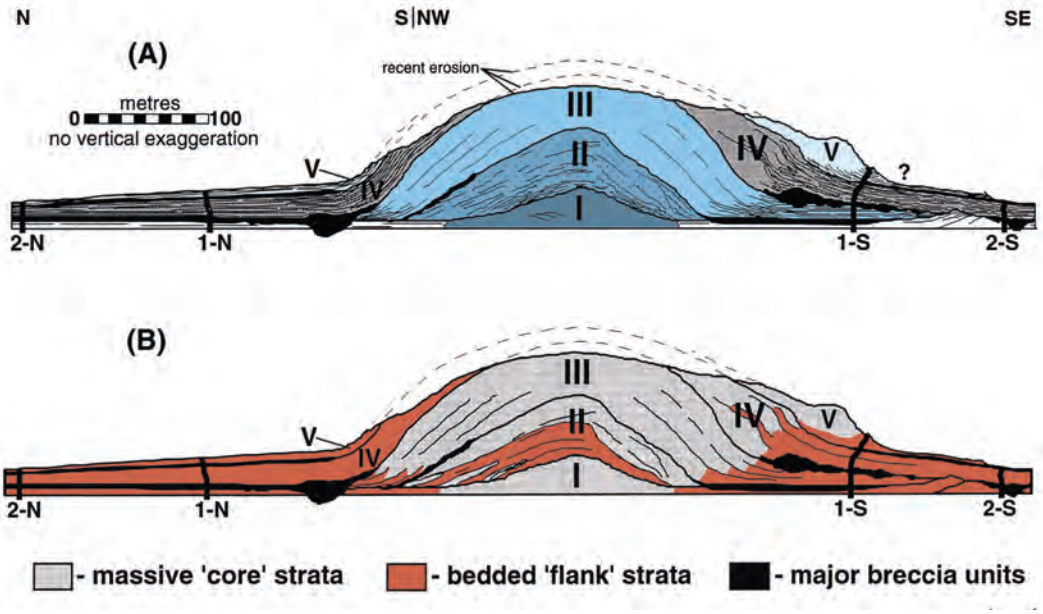

Figure 26 - (A) Five mapped component stratal units of Muleshoe Mound; (B) Distribution of massive Waulsortian "core" facies, bedded flank strata, and megabreccias in Muleshoe Mound. After Kirkby and Hunt (1996).

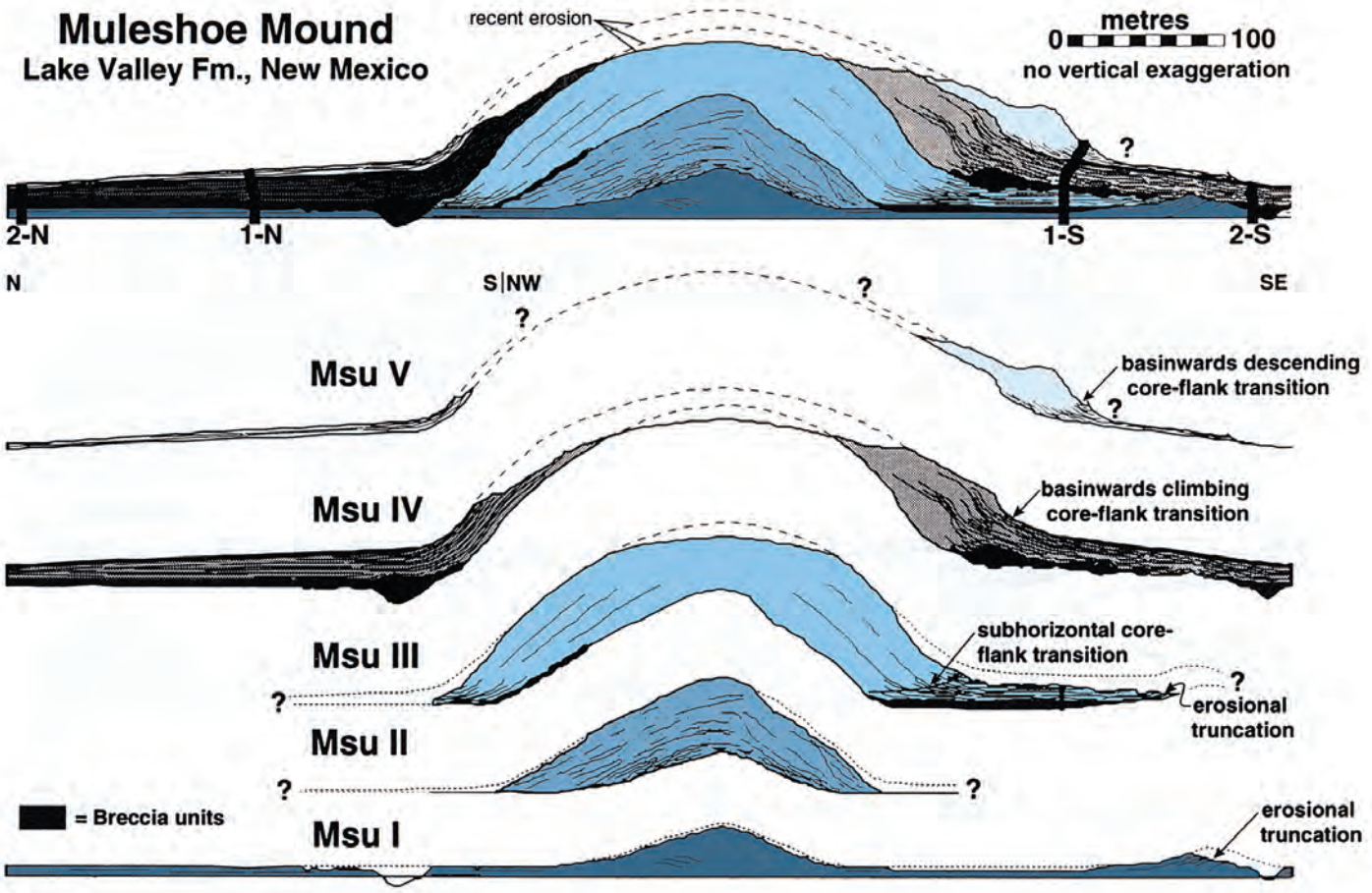

Figure 27 - Cross-section through Muleshoe Mound based on measured sections, field study, and photomosaics. Composite section (top) is broken down to show distribution and geometry of component stratal units. After Kirkby and Hunt (1996).

Figure 28 - Eastern flank of Muleshoe Mound. Notice pod of megabreccia (mb), steep, and well bedded flank beds that pass directly into massive units of the mound. Overlying covered slope is wedge of Arcente (A) that laps out against the mound. Cliff overlying the Arcente is Doña Ana (DA) at the base and is overlain by the Rancheria (R). Higher slopes are in the Pennsylvanian Gobbler Formation (P).

ered interval. There is an outcrop of the Devonian dark phosphatic shale above a small sill. Further climbing reveals interbedded nodular limestone and gray shale of the Caballero Formation. This is overlain by shales and more evenly-bedded limestones of the Andrecito Member. A massive cliff of limestones (with dark chert nodules) of the Alamogordo Member overlies this (nearby section in Fig. 29).

Climb to the top of the Alamogordo and continue toward the core of Muleshoe. You are walking along the base of Muleshoe's flanking beds. Notice the extremely grainy crinoidal lithology. Is any grading present that might indicate transport off of the mound? Or does it appear that the flank beds developed essentially in place? Look towards the mound proper to see that flank beds pass directly into the massive mound facies. They do not lap out against it. Continue walking along base of the bioherm. Study the upper and lower core facies. Notice the abundant crinoids, fenestrate bryozoans and other normal marine fossils. No algae have been found in the mound. Also notice gray sparry patches that contain internal sediment, fibrous marine cement and fenestrate bryozoans (Fig. 30). Also notice irregular pockets (several to tens of centimeters across) that are filled with laminated internal sediment. Continue westward traverse to far end of Muleshoe. Just around corner, see small (5-10 centimeters wide) neptunian dike with laminated internal fills. Traverse eastward back to other side of Muleshoe to large pod of megabreccia.

OPTIONAL CLIMB - The group may head down to the vehicles the way we came up, or we may climb up over the flank beds to the top of Muleshoe and then drop back down the other side. Continue under the large bed of megabreccia, and where it pinches

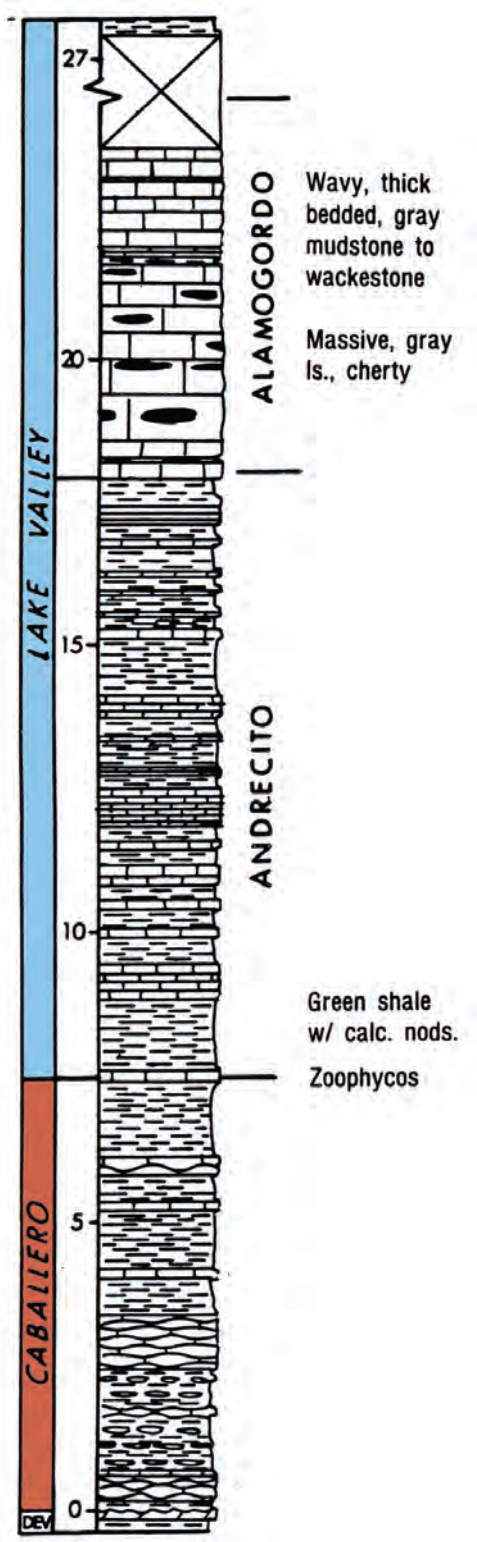

Figure 29 - Stratigraphic section that is nearby the traverse below Muleshoe Mound. This is the Muleshoe South locality of Lane and Ormiston (1982) (after Lane and Ormiston 1982).

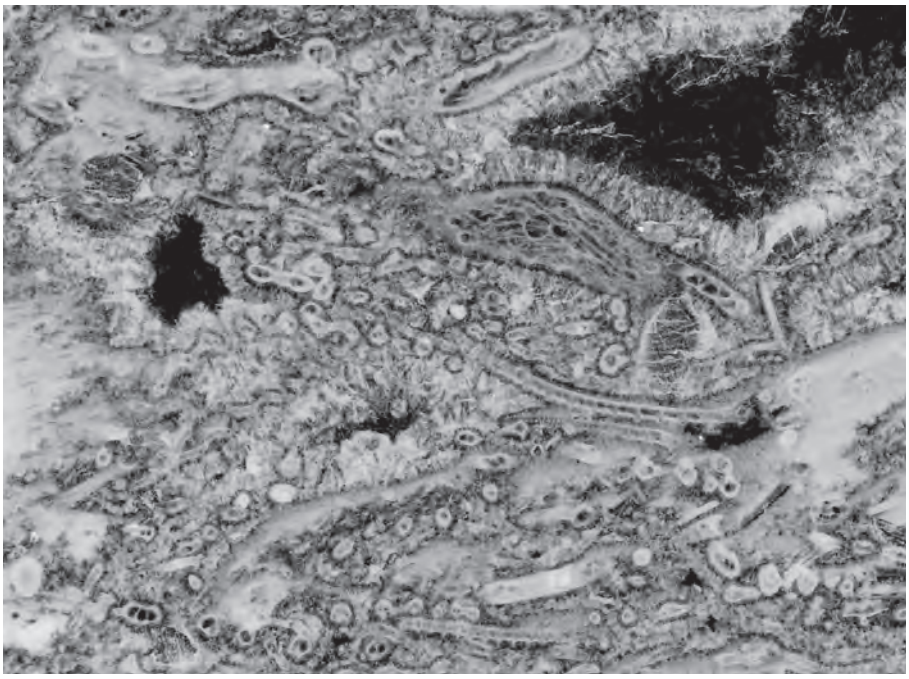

Figure 30 - Negative print of thin section of Muleshoe Mound core facies. Notice the abundant fenestrate bryozoans that are heavily encrusted with cloudy submarine cement. Scale is about one centimeter across.

out laterally to a very thin bed, climb over it to continue back towards the bioherm on the top of the megabreccia unit. Climb above the steeply dipping flank beds where you can (this is fairly close to the bioherm itself). Here it is easy to get a real feel for the steep dip on the flank beds. Notice the grainy nature of the flank beds as compared to the muddy bioherm. How is it possible for these two environments to have coexisted? Above the flank beds, notice the poor outcrop of the Arcente Member. For a sequence or seismic stratigrapher, this restricted wedge of sediment appears to onlap the mound and mound flanks. Higher, notice the erosional truncation on the top of the Doña Ana Member (overlain by Rancheria; Fig. 31). This is another important geometric component of sequence stratigraphy. Climb to the top of Muleshoe to observe mound core and neptunian dikes. Traverse down the northwest side of the mound. Notice the reworked clasts of chert in the Rancheria. This relationship clearly demonstrates an early, pre-Rancheria, origin for the chert. Continue down to vehicles.

Muleshoe has been studied in increasing detail for more than 65 years (Laudon and Bowsher, 1941; Bowsher, 1948; Laudon and Bowsher, 1949; Pray, 1958a; Pray, 1975b; Meyers, 1974; Lane, 1982; Lane and Ormiston, 1982; Shinn et al., 1983); Jackson, 1983; Jackson and DeKeyser, 1984a, 1984b; George and Ahr, 1986; Ahr, 1989; Jackson and DeKeyser, 1989; Hunt et al., 1995; Kirkby and Hunt, 1996; Hunt, 2000; Kirkby et al., 2000a, 2000b; Wu and Chafetz, 2002). General descriptions were first given by Laudon and Bowsher (1941, 1949), who subdivided the Lake Valley Formation into six members. Muleshoe bioherm occurs in the lower four members of the Lake Valley. It rises above the last two members of the Lake Valley, above the level of the overlying Rancheria Formation, and protrudes into the base of overlying Pennsylvanian deposits of the Gobbler Formation (Pray, 1958b;

Figure 31 - Field photograph east of Muleshoe Mound. White cliff at base is of the Doña Ana Member. Several dark beds above are of the Rancheria. Notice the erosional truncation on the top of the Doña Ana.

Pray 1961). Bioherms about 8 km (5 mi.) to the north are decidedly elongate in a north-south direction and are not as thick as Muleshoe bioherm. Muleshoe is estimated to have stood more than 100 m (300 ft.) above the sea floor and may have developed on a relatively deep portion of a shelf that became more shallow to the north. Armstrong (1962) has suggested that a starved basin lay to the south, and tidal flat deposits are found 260 km (160 mi.) to the north. Muleshoe bioherm appears almost circular in plan and may have formed in deeper water than the bioherms to the north. Wilson (1975a) stated that most geologists acquainted with Mississippian bioherms believe they accumulated below wave base and perhaps below the photic zone. It is tempting to make comparisons between these bioherms and the lithoherms of the Straits of Florida described by Neumann et al. (1977).

Ahr (1989) examined the regional setting of the Mississippian bioherms and concluded that they formed on a very gentle ramp. The bioherms were "preferentially sited on paleobathymetric highs of tectonic and depositional origin" (Ahr 1989, p. 211). These structural and depositional features were very subtle, however, with only minor topographic relief. Wu and Chafetz (2002) noted isotopic signatures in mound constituents indicative of methane seepage, so it is an interesting thought that the location of such seeps on the seafloor may have localized bioherm formation.

It is interesting to note that the faunal components of the bioherm did not require light for their survival. The common forms seen in both the core and flanking beds are crinoids, brachiopods, bryozoans, and solitary corals. In contrast to other bioherms observed on this trip, calcareous algae are absent. Other typically shallow-water forms, such as massive corals, clams and calcareous sponges, are rare or absent. The crinoidal grainstones of the flank beds are poorly sorted and contain articulated columnals several inches long, which suggest flanking crinoidal beds formed in close proximity to where the crinoids lived.

These biogenic sediments appear not to have been transported far from their source. The maximum slope of these flank beds approaches 40 degrees.

The core facies have been studied in great detail by Pray (1958a; 1965a; 1965b; 1969), Lohmann and Meyers (1977), Shinn et al. (1983), and Stanton et al. (2000a; 2000b). Approximately two-thirds of the core consists of mud; the major faunal component of the bioherm cores is fenestrate bryozoans. There is considerable question as to the origin of the carbonate mud in Muleshoe bioherm and other Paleozoic mud mounds. Are the muddy cores the result of currents piling up fine-grained sediment? The circular plan view of some mounds would make this possibility unlikely but some authors have proposed internal waves within the oxygen-minimum zone as a possible setting for these mounds (Stanton et al. 2000a). Some authors (Dix and James 1987; Tsien 1985; Tsien 1994) consider the mud to have been at least partly contributed through the activities of simple calcimicrobes (bacteria and/or algae, perhaps negating the arguments about water depth). Other authors (McKinney et al. 1987), have suggested that fenestrate bryozoan colonies may have produced strong cilia-generated currents which led to trapping and accumulation of mud produced from a variety of biogenic or abiogenic sources.

Throughout the core facies, the sediments contain bryozoan fragments coated with banded, isopachous cement, which is cloudy when viewed in thin section. This cement was interpreted as marine in origin by Pray (1965a; 1965b). The cloudy cements contain inclusions of microdolomite, as illustrated by Lohmann and Meyers (1977), and are believed to be diagenetically altered high-Mg calcite marine cement. The presence of this penecontemporaneous, generally stable cement has precluded substantial compaction in the bioherm core facies, unlike its flank equivalents (Shinn and Robbin 1983).

The details of the construction of Muleshoe bioherm and similar Lower Carboniferous mud mounds still hold many questions. What was the source of the mud? Why are the flank beds so distinct and sharply separate from the core facies? What role did submarine cement play in building these mounds? What localized the position of such mounds? Why are they so abundant in the Upper Paleozoic? Many of these questions cannot be answered very satisfactorily. Submarine cement by itself did not build Muleshoe bioherm, but it would take only a small amount to act as a binding agent to hold the core facies together. If this were the case, then the next question is why did the cement form here, localized in this mound? The sandy flank beds evoke clear visions of crinoidal meadows on the sides of the bioherm, but why not on top or in the center, where the core facies predominate? Was the central position of the bioherm dominated by some mud-producing organism that decayed so completely that no trace is left behind? Or, was the center isolated from nutrient-rich currents, which fed animals on the sides of the bioherm? Wilson (1975a, p. 165-167) suggests formation through a combination of hydrologic accumulation and baffling by crinoids and bryozoans to form the muddy core facies (see also McKinney et al. 1987). Gentle currents would have winnowed the sides of the bioherm.

It is interesting to draw comparisons between these mounds and modern lithoherms in the Straits of Florida (Neumann et al. 1977). The processes involved in their formation include: (1) hydrologic accumulation, (2) biogenic sediment contribution and biologic entrapment of sediment, and (3) subsea lithification by marine cement. An organic framework, typical in modern reefs, is absent in these Mississippian mounds and is not a requirement for mound growth. Although organisms and hydrologic regime are not directly comparable between modern lithoherms and Muleshoe bioherm, a combination of the three processes active in modern lithoherms could probably account for the features we see in these Mississippian buildups.

The diagenesis in non-biohermal Lake Valley sediments has been studied in considerable detail during the last 10 years. Using cathodoluminescent petrography, Meyers (1974) found five generations of cement in crinoidal grainstones like those we observe off

		the flanks of Muleshoe bioherm. Most of this cement occurs as syntaxial overgrowths on crinoidal sands. Marine cements like those in the bioherm core facies are rare in inter-bioherm areas. The syntaxial, clear overgrowths are interpreted to have formed in a fresh-water aquifer that occupied Lake Valley sediments during periods of sea level change and regional subaerial exposure. Careful examination of cements at post-Lake Valley unconformities revealed three cement zones to predate Gobbler deposition. These two periods of subaerial exposure led to a great porosity loss in these sediments and resulted in 90-95% of the total intergranular cement in Lake Valley grainstones (Meyers 1978).
	20.65	Leave Muleshoe Canyon
0.55	21.2	Turn left (southeast) at the corral.
0.3	21.5	At the mouth of San Andres Canyon, turn right, then right again to head west.
1.1	22.6	Arrive at well head.
0.4	23.0	Turn right (north) onto main gravel road.
0.4	23.4	Pass Donald Taylor ranch. Mr. Taylor has been kind to geologists and offered them access to Muleshoe mound and surrounding areas. His address is Box 3656, Boles Station, Alamogordo. Please check with Mr. Taylor before traveling ranch roads. His rifle range is active on the fourth Sunday of every month, a good time to avoid.
0.2	23.6	Turn left (west)
1.95	25.55	Turn right (north) on main highway.
5.05	30.6	Exit right onto U.S. 54/70 towards Alamogordo.
0.7	31.3	Pass hotel area and continue north on U.S. 54/70,
4.4	35.7	Turn right on New Mexico 82 (east).
2.0	37.7	Arrive at intersection of NM 82 and Florida Avenue. Note red flashing light and Conoco station.
0.3	38.0	Look east into Dry Canyon. The low covered hills are of the Pennsylvanian (Missourian) Beeman Formation. Notice the banded nature of the upper half of the hillside. This results from the interbedded limestones and siliciclastics of the Upper Pennsylvanian (Virgilian) Holder formation. Thickenings in the cliffy limestones are phylloid algal bioherms.
0.8	38.8	At mileage marker 3, look to the north to see basinal biohermal strata of the Holder Formation (about a third of the way up the hillside). These bioherms can be traced upslope to the east about halfway up the hillside. Notice the laterally continuous carbonate unit above that becomes stratigraphically closer to the bioherms toward the east. The intervening dominantly siliciclastic strata lap out against the basal biohermal strata to produce a basinally restricted wedge of siliciclastics.
0.15	38.95	Go through road cut of the Missourian Beeman Formation.
0.05	39.0	Look north, where the power lines are in Yucca Mound Canyon, to view phylloid algal mounds and the stacked nature of many of phylloid algal buildups built along the Virgilian shelf edge of the Holder Formation.
1.2	40.2	Outcrop of the Beeman Formation. Lowermost redbeds of the Beeman crop out here.
0.4	40.6	Basal Holder Formation
2.5	43.1	**STOP 3 - TUNNEL VISTA - FRESNAL BOX CANYON** - Turn left into the Tunnel Vista and turn around vehicles. This stop is in the box canyon of Fresnal Creek in which limestones of the Bugscuffle Limestone Member of the Gobbler Formation crops out along the canyon walls. Look down canyon to see that the cliffs are spectacularly truncated and that the limestones are folded. You are looking at a major fault, the Fresnal Fault, which is mostly a normal fault. The position of this stop is on the eastern upthrown block, and it is downthrown to the west. The overall vertical displacement on the Fresnal Fault is approximately 1,600 feet. Detailed mapping and stratigraphic studies by Pray (1959), Otte (1959b) and Delgado and Pray (1977) have documented the age in which the fault was active. To the south, the Fresnal Fault cuts across the late Wolfcampian (Permian) Abo Formation and displaces it by several hundred feet. Just about a mile to the north, the

Fresnal Fault is splayed into two normal faults. Along one of these faults, Holder Formation (Virgilian) strata have been cut, yet the fault is unconformably overlain by strata of the Laborcita Formation (lower Wolfcampian, Permian). At the other fault to the north, with a displacement of at least 400 feet, the Laborcita Formation is cut by the fault, yet the fault is unconformably overlain by the continuous strata of the basal Abo Formation (Fig. 5). Thus, from these relationships it is apparent that fault movement was occurring from Virgilian through Wolfcampian time. This fault can be thought of as one of the frontal structures associated with uplift of the Pedernal Landmass during formation of the Ancestral Rocky Mountains.

Look to the west in the distance through Dry Canyon, see the units of the Holder Formation and the large bioherm (Virgil Mound) that crops out along the cliff wall. This large bioherm forms along the crest of an anticline known as the La Luz anticline. The east limb of the anticline is dipping toward us. Apparently sedimentary patterns both in thickness and in facies tend to mimic this anticlinal structure (Wilson 1969). Thus, the anticline (and the Dry Canyon syncline to the east of it) was active in Virgilian time responding to the same tectonism that formed the Fresnal Fault

	43.1	Continue road log going west on NM 82.
0.3	43.4	Drive through fault zone
0.15	43.55	**STOP 4 - HOLDER FORMATION CYCLE** - Pull bus to the right and park. Note tank off to the right to help find the stop. Be extremely careful of dangerous traffic.

Viewing the Fresnal Fault from this locality. Note the drag of the Bugscuffle and the Holder Formation and the Laborcita Formation on the downthrown side of the fault (Fig.

Figure 32 - Field photograph of the Fresnal Fault. On the right are outcrops of the Middle Pennsylvanian Bugscuffle limestone Member, Notice the fault drag. On the left are folded strata of the Upper Pennsylvanian and Lower Permian Holder and Laborcita formations. This fault was active during the Late Paleozoic.

32).

The road cut is in strata of the Holder Formation. Here, we will investigate aspects of Pennsylvanian cyclicity that are so typical of Upper Pennsylvanian carbonates and siliciclastics. Being careful with the traffic here, walk down the hill on either side of the road, examining the stratigraphic section. Unlike many Pennsylvanian sedimentary cycles, this cycle has no discrete siliciclastic phase. In vertical stratigraphic section, the cycle (Fig. 33) passes upward from a paleosol unit at the base. The paleosol is partially silicified, contains root molds, microkarstic cavities, phosphatic and hematitic coatings on grains and ped surfaces, and is capped by a shaly residuum of soil material. It is overlain by a

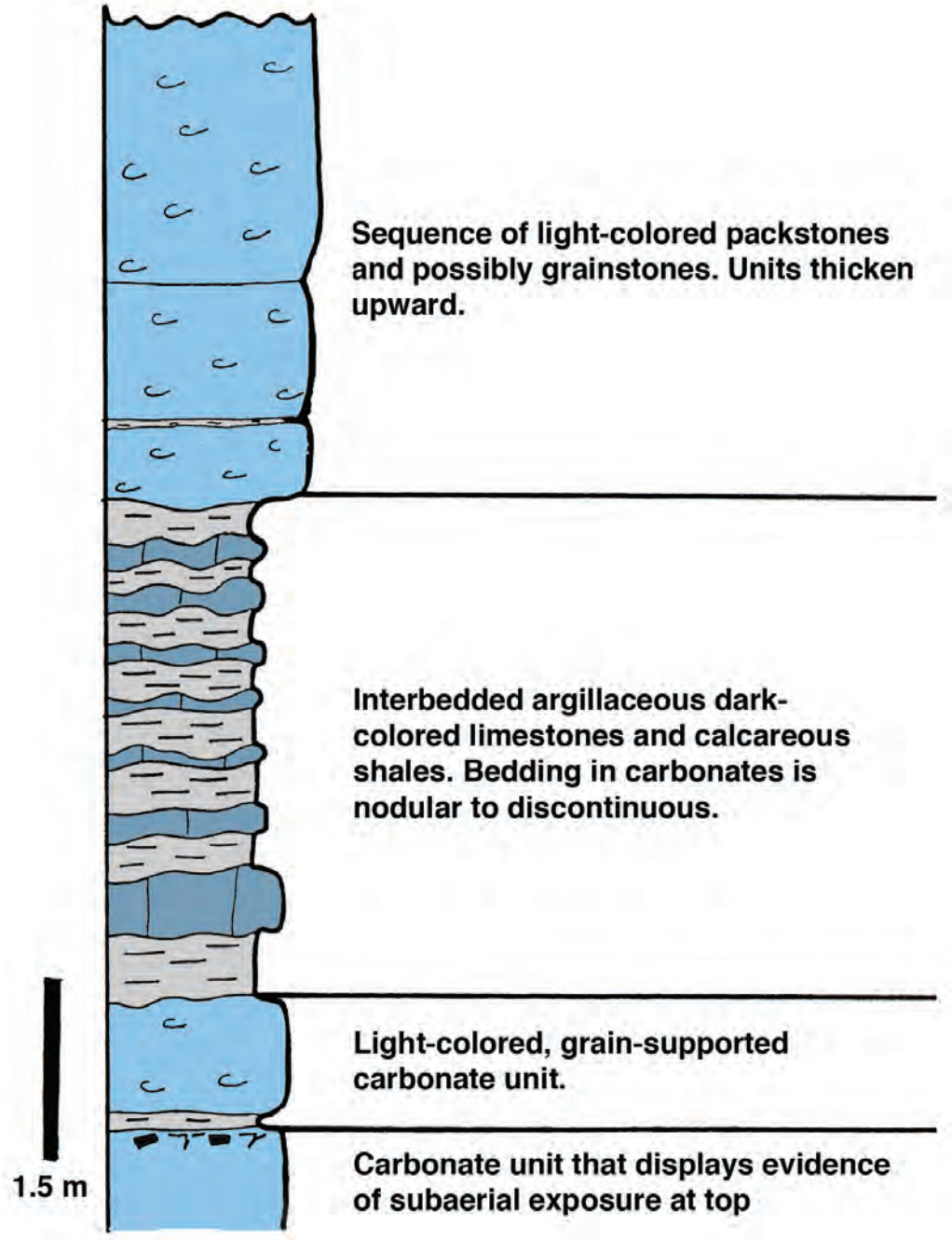

Figure 33 - Generalized stratigraphic column of sequence exposed in roadcut. Paleosol is at the base, and is overlain by a transgressive grain-supported carbonate. This is capped by a shoaling-upward sequence (after French 1987).

massive grain-supported carbonate bed. The overlying strata can be thought of as a shoaling-upward sequence that consists of interbedded calcareous shales and nodular fossil fragment packstone and wackestone that passes upward into more massively bedded fossil fragment packstones. There has always been controversy about the water depth required for the upward transition from nodular to massive limestones in carbonate cycles. This outcrop answers the question.

Climb to the top of the outcrop on the north side of the highway and look south. The sequence can be seen to have been caused by progradation of a bank of fossil fragment debris in which the nodular limestones represent the downslope end and the massive units represent the shoalwater end (Figs. 34, 35). Thus, the difference in water depth between the two facies appears to have been on the order of two to five meters (French, 1987). Further, the geometries observed here provide clues as to the internal geometries expected in cyclic units. Offlapping and progradational geometries should be expected and they

Figure 34 - Field photograph of outcrop at stop 4. Thick continuous limestone bed at the base of the photograph is high energy transgressive limestone. Overlying rocks are a shoaling upward, progradational sequence.

should play a significant role in the heterogeneity of carbonate reservoirs.

0.55	43.65	More strata of the Holder Formation on the limb of the Dry Canyon Syncline.
0.12	43.77	Intersect strata of the Permian Laborcita Formation (Wolfcampian).
0.22	43.9	**OPTIONAL STOP 5 - LABORCITA FORMATION CONGLOMERATE AND CALCRETE** - Pull bus to the right, just before the "Run-away Truck Ramp 1 Mile" sign The exposure is on the south side of the highway. Beware of traffic. **Warning**, relatively unstable outcrop.

There are two calcretized conglomerates. One at the top of the road cut and then the other

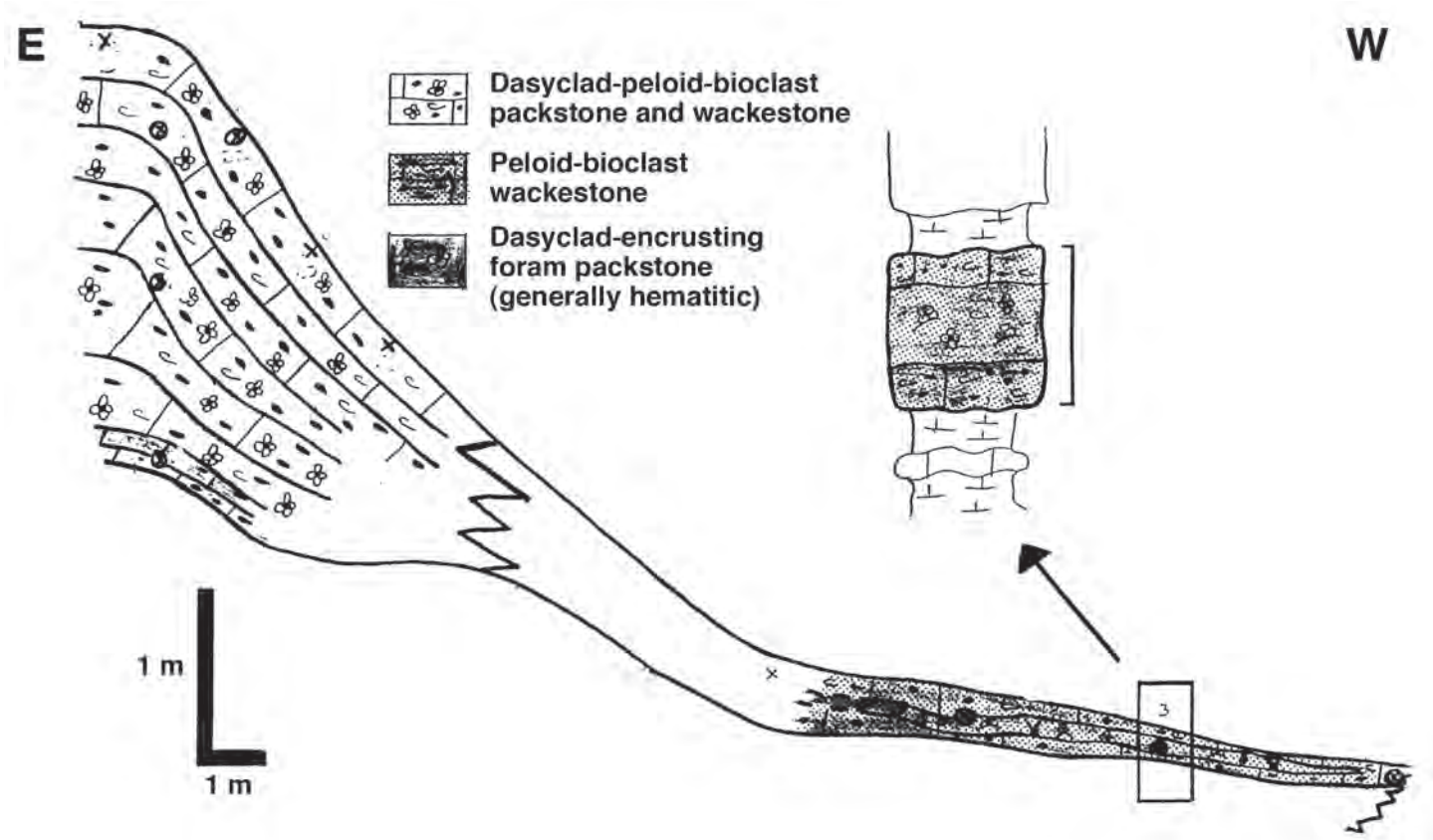

Figure 35 - Schematic diagram of progradational package of shoaling upward cycle, sketched from outcrop of Stop 4. Note, brick pattern is diagrammatic and does not indicate scale of bedding (after French 1987).

one that is stratigraphically above that at the west end of the outcrop (Delgado, 1977).

0.4	44.3	Beds are flat-lying now, we are in the core of the Dry Canyon syncline.
0.35	44.65	Dike cutting the Laborcita Formation. Now on the east limb of the La Luz anticline.
0.35	45.0	Inclined strata of the Pennsylvanian upper Holder Formation (Virgilian).
0.55	45.55	**STOP 6 - CYCLES OF THE HOLDER FORMATION** - Turn off to the left at the pull-over with the Prevent Forest Fire sign. Examine the road cut of the lower part of the Holder Formation that is on the north side of the highway. Beware of traffic.

Look down the hill to the west to see the large bioherm (Virgil mound) and see beds dipping towards us on the bioherm flank. Remember this bioherm is essentially on the crest of the La Luz anticline (which formed a topographic entity in Pennsylvanian time). Essentially, the beds at the basal part of this road cut are equivalent to the biohermal strata. Therefore, we are in a lagoonal setting compared to the shelf crest bioherm.

Cline (1959) emphasized the cyclic nature of Virgilian rocks in this area, and Wilson (1967) related these shelf cycles to basinal cycles in the Orogrande basin. Shelf cycles consist of a variable sandstone and shale lower member with local channel-fill conglomerates which grade upward into normal marine limestone and shale. These in turn pass upward into shallow-water limestones (grainstones and bioherms) that cap the shelf cycles. Wilson (1967) interpreted these cycles to be the result of repeated sea level fluctuations, which periodically exposed the shelf and bioherms to subaerial weathering and diagenesis (Figs. 20, 36).

Here, we will examine the muddy lagoonward cycles in the Holder Formation and compare them to later shelf crest and shelf edge facies that we will see at a later stop. The measured stratigraphic section is presented in Figure 37. Walk upward through three cycles in

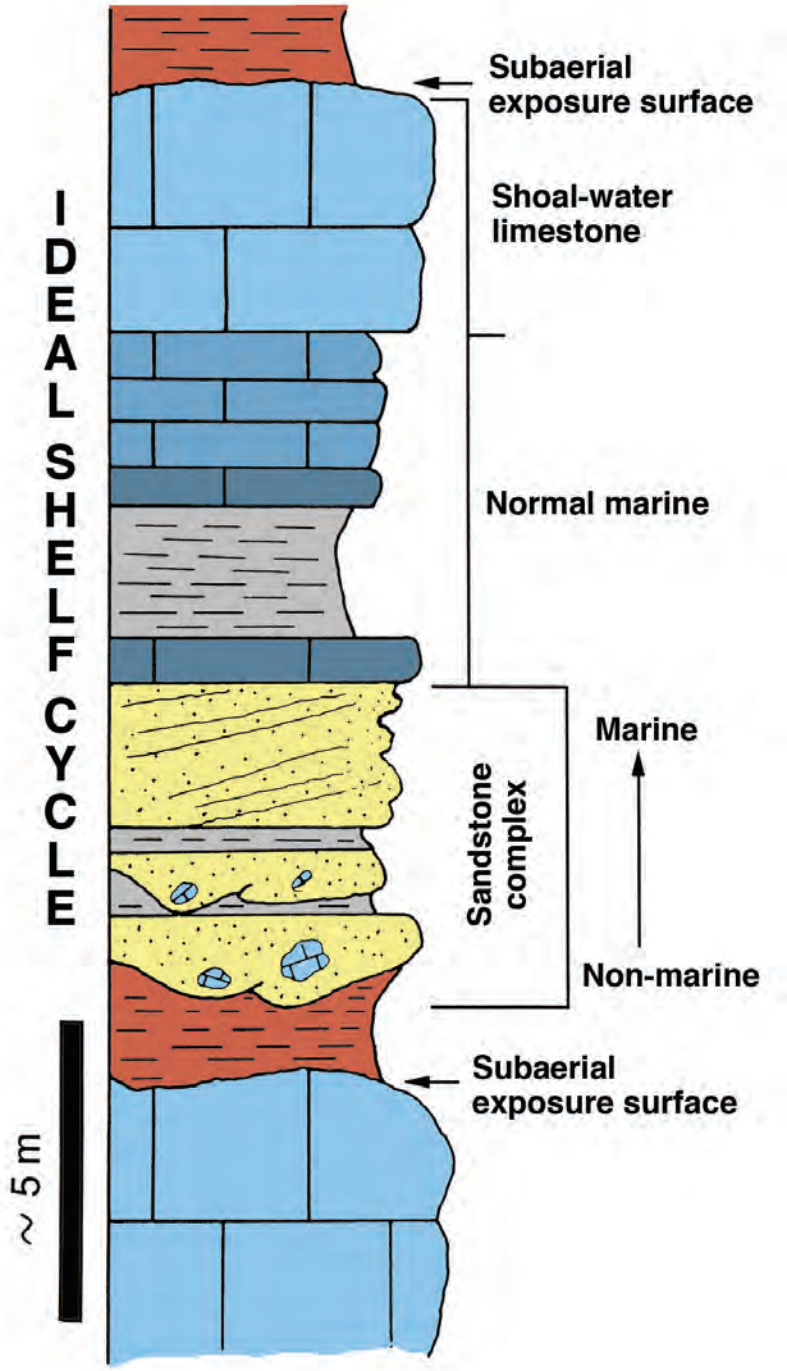

Figure 36 - Idealized shelf cycle of the Holder Formation (modified from Wilson, 1967 and Bowman, 1989).

the Holder Formation (up to about 25 meters above the base). Notice the beautiful paleosol capping the first major cycle. Does the paleosol form on subtidal or peritidal deposits? What are the implications in terms of relative fall in sea level for the two alternatives?

Notice the limestone and chert pebble conglomerate in the next cycle up-section. The composition of clasts in the conglomerate suggest only moderate unroofing of the Pedernal Uplift. Higher in the section, notice the "ball" of reefal material and facies changes that occur in a traverse up through the cycle.

0.0	45.55	Continue west New Mexico highway 82
0.2	45.75	Exposures of the Beeman Formation. Notice on the right is the large "Virgil Mound" bioherm with flank beds dipping down towards us.
0.25	46.0	We are now approaching the crest of the La Luz anticline. Above your left you see another large bioherm, about 2/3rd of the way up the cliff.
0.55	46.55	**STOP 7 - VIRGIL MOUND OVERLOOK** - Turn off to the left, in front of the Lincoln National Forest sign. Do not go past it, stay in front of it.

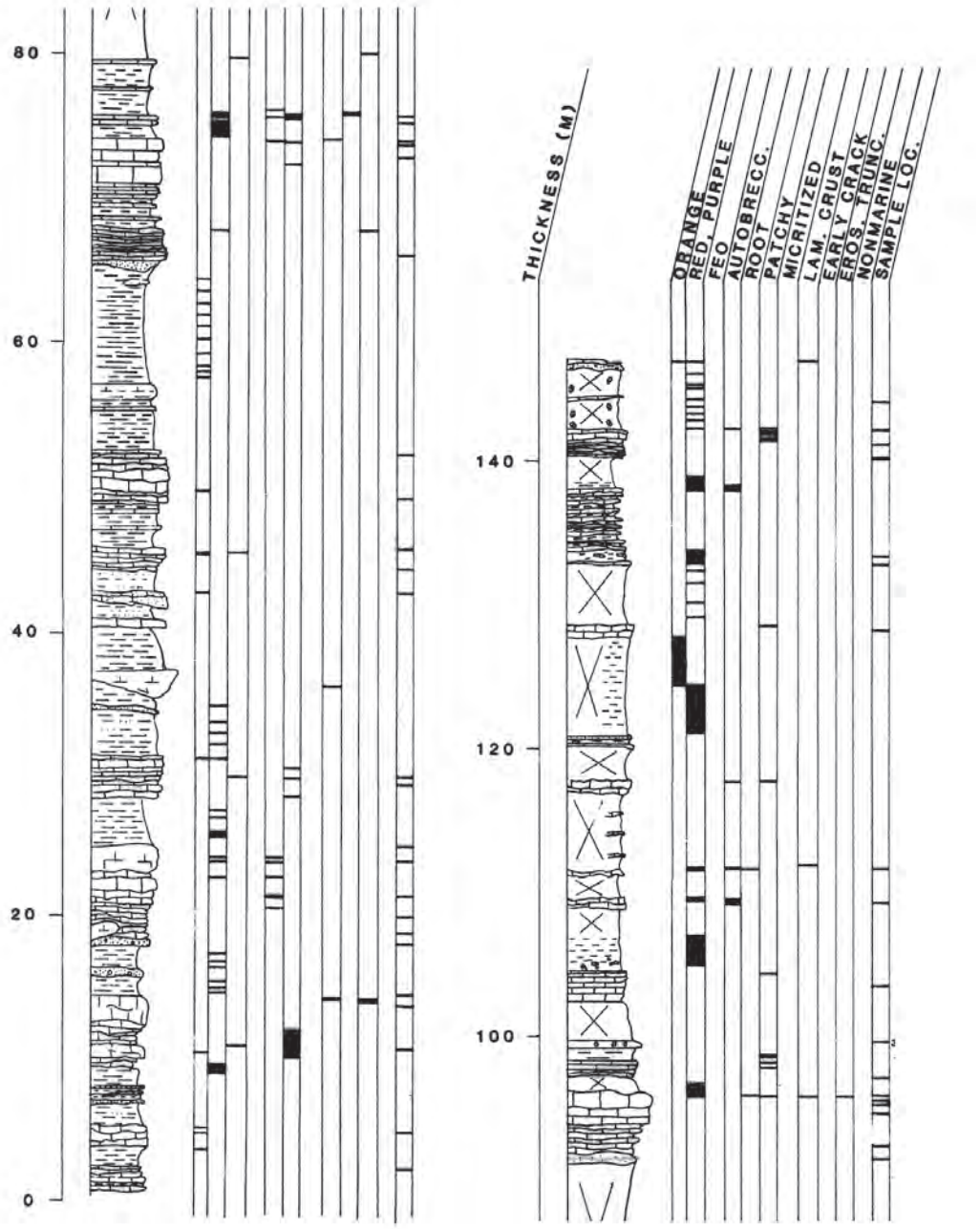

Figure 37 - Stratigraphic section of Holder Formation exposed along roadcut of New Mexico Highway 82. Stop 6 traverses from about 0 to 25 meters above the base of the stratigraphic section. Position of evidence indicative of subaerial exposure is recorded on log.

A careful look at the Holder Formation bioherm above reveals that it is largely composed of steeply dipping flank beds (Figs. 38, 39) composed of phylloid algal wackestone, packstone and other lithologies. The unit is about 20 meters thick. Also, notice the stacked mounds at a slightly higher stratigraphic level exposed west of the large bioherm above. Notice how normal looking limestone beds of even thickness build abruptly into the bioherms.

Pray (1961) defined the La Luz anticline, which runs approximately NNW through this area and had a pronounced local influence on Late Pennsylvanian sedimentation (Wilson 1969). Bioherms developed with long axes approximately parallel to the axis of the La Luz anticline, which was a subtle structural feature at the time.

Plumley and Graves (1953) first described the Virgilian bioherms and emphasized their geometry, orientation and biological origin. They appear as elongate bodies up to 1.6 km (1 mi.) long and 60 m (200 ft.) thick. They tend to parallel the mountain front. Parks (1958; 1962; 1977), Wray (1959; 1963) and Konishi and Wray (1961) established the importance of platy algae in these limestones and refined the taxonomy of the platy or phylloid (leaf-shaped) algae (Pray and Wray 1963). Phylloid algal limestones are widespread in the United States (Wray 1963; Wray 1968), and bioherms composed of such algal limestones are widespread in Late Pennsylvanian and Wolfcampian strata of southern New Mexico (Wilson 1977).

We will study the bioherms closely at a later stop. The bioherms are composed in large part of mud (micrite) and phylloid algal plates. The phylloid algae are usually poorly preserved as molds or replaced by blocky calcite with all traces of original microstructure

Figure 38 - Field photograph of Virgil mound above New Mexico highway 82. Note the steeply dipping flank beds which are making up most of the mound.

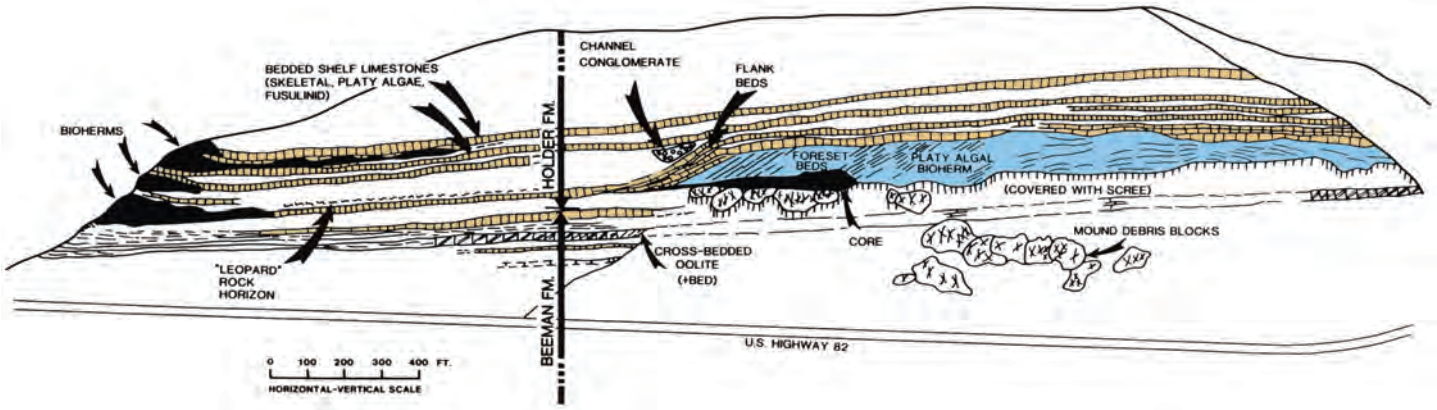

Figure 39 - Sketch illustrating the stratigraphic relationships of Virgil Mound to surrounding shelf cycles and later bioherms. Note how later bioherms postdate deposition of the Virgil mound. This could be interpreted as progradation of the shelf edge (after Toomey and Babcock 1983).

lost. They are probably of diverse origin, some being green calcareous algae and some being red calcareous algae. Their poor state of preservation suggests they were originally aragonitic, a conclusion that was confirmed in the 1990's through discovery of phylloid algae from this general locality that still have preserved primary aragonite (Kirkland et al. 1993). Wray (1975; 1977) has suggested that the closest living analogues to some of the phylloid algae may be a family of red calcareous algae known as the Squamariacean algae. Today, "squamies" are subtle but widespread coral reef inhabitants.

A great many other organisms are evident in the biohermal rocks, including stromatolites, sponges, tubular encrusting Foraminifera, stromatoporoids, and corals, all of which are capable of producing reef structures. Volumetrically, mud is the most important constituent of the bioherms. Wray (1959) suggests the mud had been trapped by a thicket of phylloid algae, probably in a relatively low-energy setting. Ball et al. (1977) question the mound-building capabilities of phylloid algae. Parks (1977) briefly reported that algal plate mudstones were uncommon in four cores taken through the bioherms and that true frame-building organisms were responsible for mound formation.

0.0	46.55	Continue west on NM highway 82.
0.65	47.2	Cross under power lines and end of the guard rail. To the north, is the entrance to Yucca Mound Canyon.
0.15	47.35	**STOP 8 - YUCCA MOUND AND SACRAMENTO SHELF TO OROGRANDE BASIN TRANSITION** - Turn off onto the left side of the road (mi. marker 3.0) and park the vehicle.

Look to the north at the basal bioherms of the Holder Formation (Fig. 40). Notice their steep fall in elevation following them westward. This transition reflects a break in slope marking the early Virgilian shelf edge passing into the Orogrande Basin to the west, Pray (1959) documented the presence of the Orogrande basin by demonstrating Pennsylvanian and Permian facies and thickness changes from the Sacramento Mountains and westward (Figs. 41, 42).

Wilson drew on conceptual models of cyclic deposition and evidence from the Holder Formation to develop the idea of shelf and basin reciprocal sedimentation (Table 1). This important model promotes alternate sites of basin and shelf sedimentation during sea level low and high stands, respectively. During lowered sea level, most sediment bypasses the exposed shelves and is deposited in adjacent basins. During sea level high stands, these sediments are deposited on the shelves along with shallow-water limestones, while the basins receive little sediment and are "starved." The reciprocal sedimentation concept has been widely applied in shelf/basin sediment dynamics.

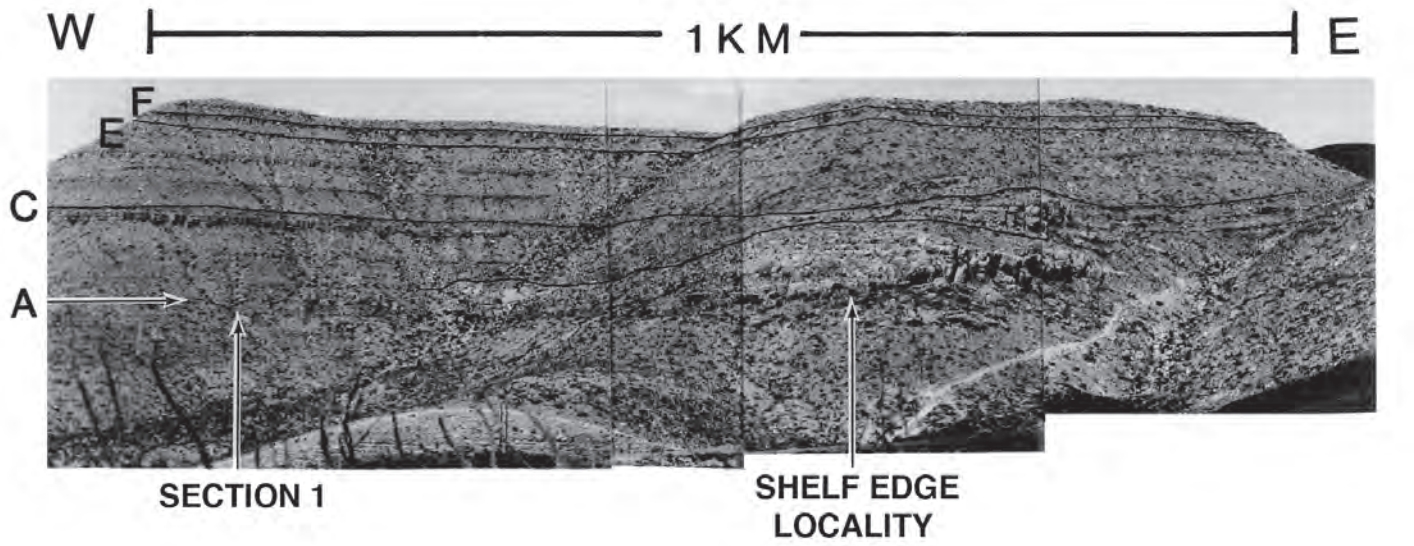

Figure 40 - Photomosaic of northwest wall of Dry Canyon illustrating stratigraphic relationships in the Holder Formation. Lower line of correlation (A) is stratigraphically above the basal bioherm horizon in the Holder Formation. Next higher line of correlation (C) outlines basinally restricted wedge of sediment, most of which was deposited basinward of the shelf edge during a lowstand of sea level (or several such lowstands).

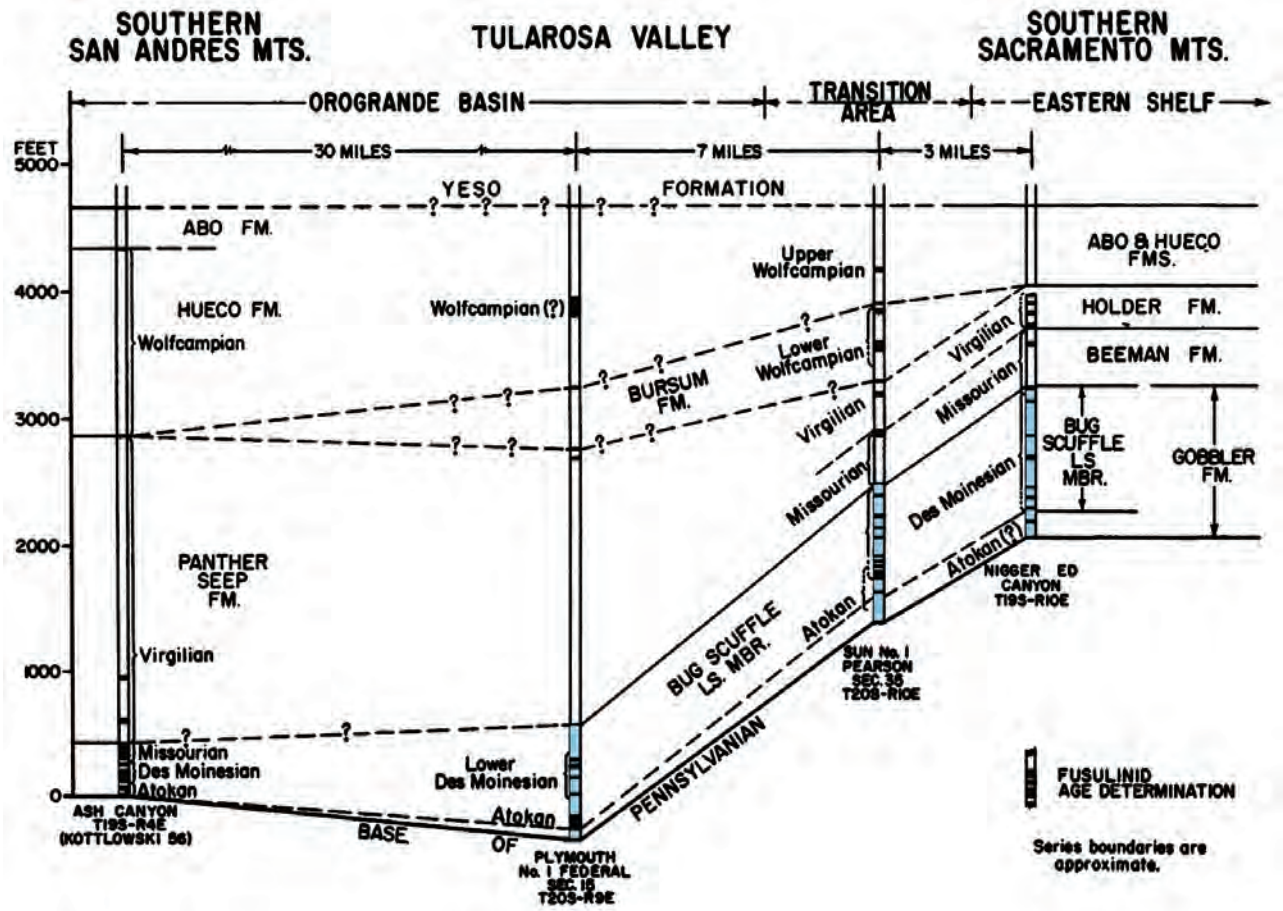

Figure 41 - East-West cross section illustrating thickness changes into the Orogrande Basin (after Pray 1959).

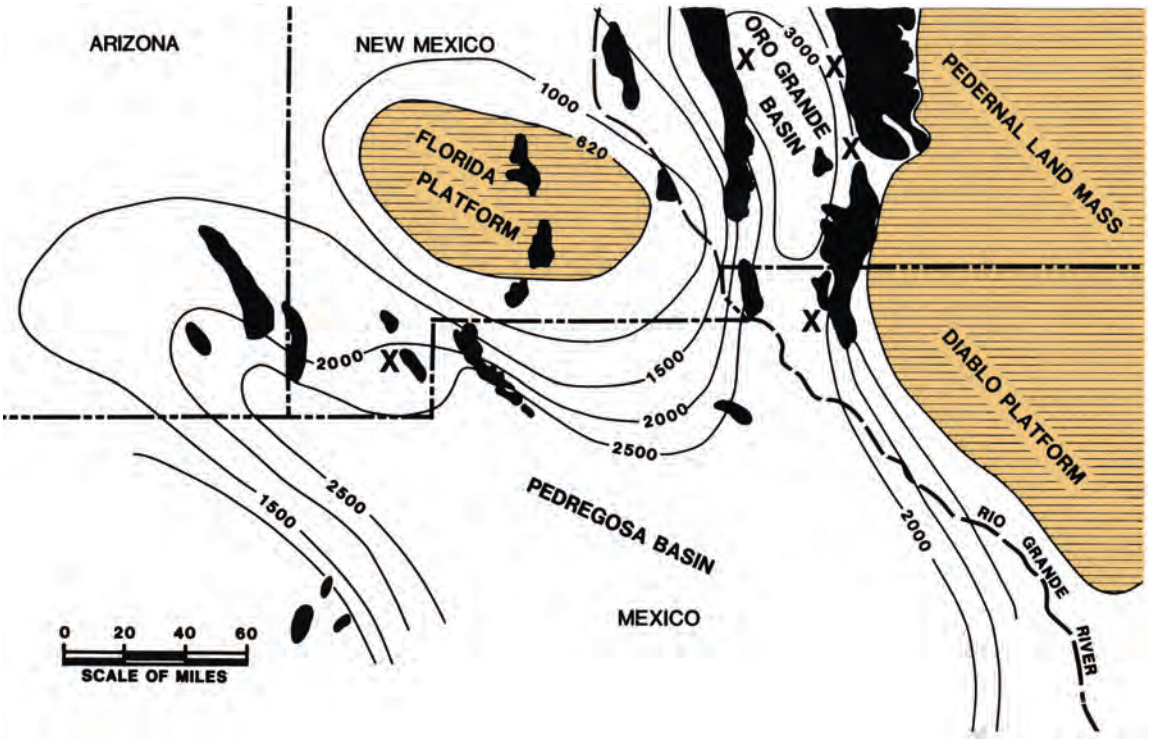

Figure 42 - Map illustrating thickness of Pennsylvanian strata (in feet) before Permian erosion (adapted from Toomey and Babcock 1983; after Wilson, 1977). Black areas indicate outcrop of late Paleozoic strata. X's indicate position of known late Paleozoic phylloid algal mounds.

TABLE 1. SUMMARY OF RELATIONSHIPS OF SHELF AND BASIN CYCLIC SEDIMENTATION

PROCESS	BASIN SEDIMENTATION	SHELF SEDIMENTATION
Regression or stabilized low stand of sea level	Euxinic tidal flat; limestone or gypsum	Exposure
Shoaling possibly beginning	Dark shale; possibly little deposition in a starved basin	Shoal limestone building out and up from shelf
Maximum inundation, water clearing	Dark shale but diminishing sedimentation	Normal marine limestones
Maximum inundation	Dark shale	Calcareous shale with abundant normal marine fauna
Deepening	Dark shale	Lower terrigenous member; either a transgressive sequence of channel fill or coarse gravel beach grading up to lagoonal sand and shale; or....
Shallowing or stailized sea level due to clastic infill		a regressive sequence of lagoonal shale grading up to bedded sands and conglomerate-filled channels
Transgression or sea level stabilized at a low stand	Cross-bedded lithic quartz sandstone	Exposure and downcutting of channels

The sequence stratigraphic geometries resulting from cyclic and reciprocal sedimentation are observable from this position. Stratigraphically above the basal bioherm horizon observable to the north, are other carbonate units that appear to diverge away from that basal bioherm surface, in a basinal direction (Fig. 40). The divergence is caused by a basinally restricted wedge of dominantly siliciclastic strata that laps out against the shelf edge and is confined to a basinal position. This lowstand systems tract (or series of them) is an important component of the sequence stratigraphy model.

Walk east up the highway, then turn left (north) on the dirt trail that is at the end of the guard rail. BEWARE OF TRAFFIC.

Traverse northeast up Yucca Mound Canyon on power line trail. Start observations where trail and telephone cable cross ravine.

We will traverse northeast through the canyon to observe facies of the lower Holder Formation. In doing so, we will traverse up significant paleoslope, investigate the bioherms, investigate aspects of cyclic sedimentation, and explore the importance of sequence stratigraphy in localizing reservoirs in such units. The stratigraphic sequence we are investigating is summarized from the 25 meter to the 75 meter position of Figure 43. The rough cross-section sketched on Figure 44 summarizes the geometric relationships of facies; this reconnaissance sketch of work in progress differs significantly from earlier reconstructions (Toomey et al. 1977a; Toomey et al. 1977b). Figure 45 summarizes the stratigraphic suc-

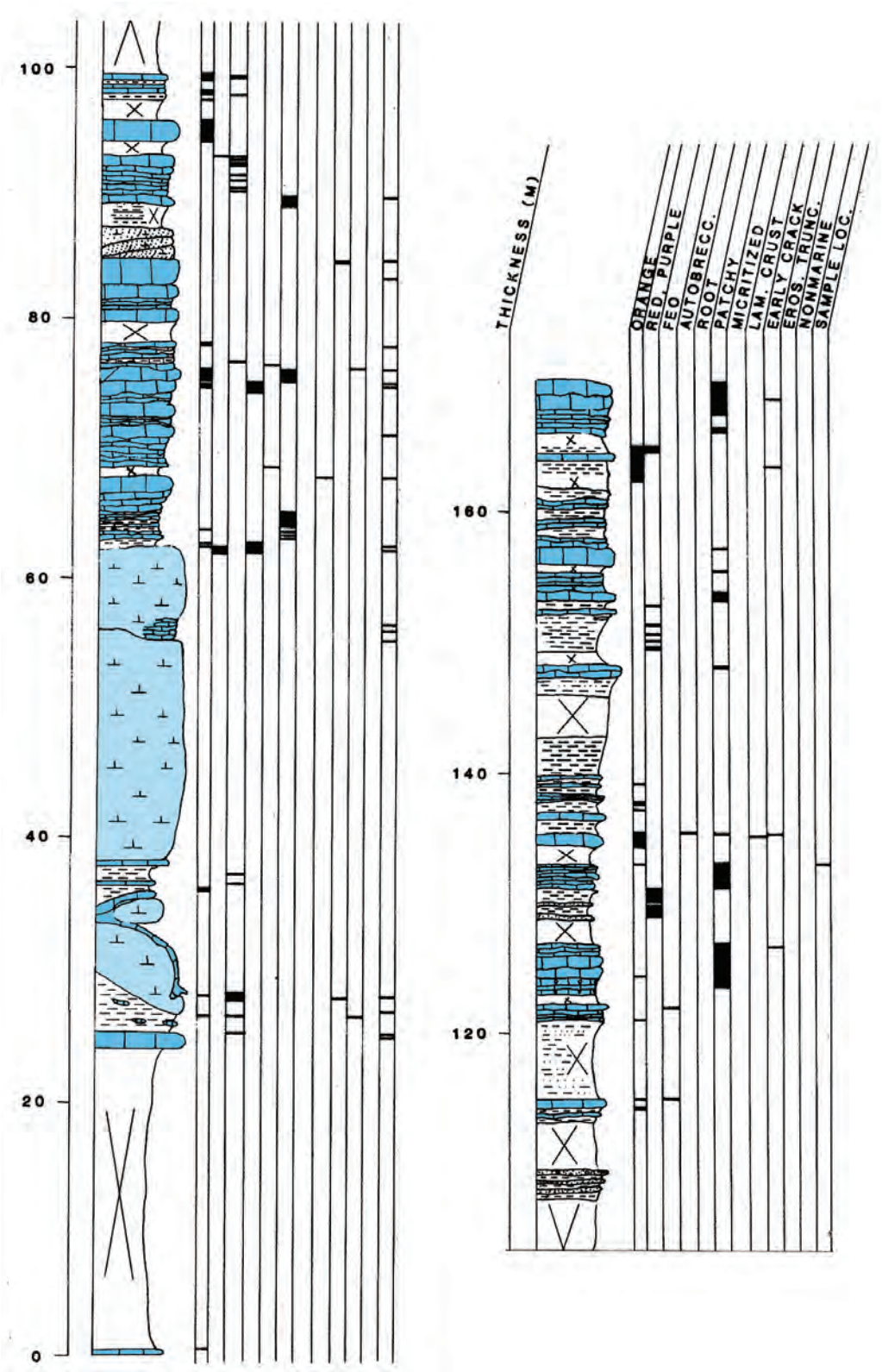

Figure 43 - Stratigraphic section of Holder Formation, Yucca Mound Canyon. Field trip traverse (Stop 8) covers 25 meter to 75 meter position. Light blue marks biohermal-limestone; darker blue marks other limestones. Evidence for subaerial exposure is logged.

cession (starting within Yucca lower) together with isotopic data (the 25 meter point on it is equivalent to the 75 meter point of Figure 43.

The position in which the trail crosses the ravine is point 1 (Fig. 44). The shales and nodular limestones here contain reworked fragments of paleosol material that includes random needle fibers of calcite and pendant cement. Thus, a surface of subaerial exposure apparently existed upslope during deposition of this unit. At eye level, notice the toe of a mound composed of sparry, black digitate masses of plumose algae and encrusting foraminifera. This mound framework lithology, colloquially known as "leopard rock", continues down slope. It is capped by a stromatolitic horizon. The top of the leopard rock horizon can be walked upslope along significant paleotopography through the ravine. Notice the dark, well-bedded limestones that drape and lapout against the leopard rock mound topography. Many of these units are fossil fragment, peloid grainstones and packstones.

Continue up the ravine to Leopard Knob. Leopard Knob is a body of reef framework that may have been displaced to some degree based on minor truncation at the base, deformation of some of the surrounding units and lack of actual flank deposits (Fig. 46). According to Toomey and Babcock (1983) the unit is an algal-foraminiferal boundstone. The beds overlying and lapping out against the Knob contain a restricted assemblage of fossils containing myalinid

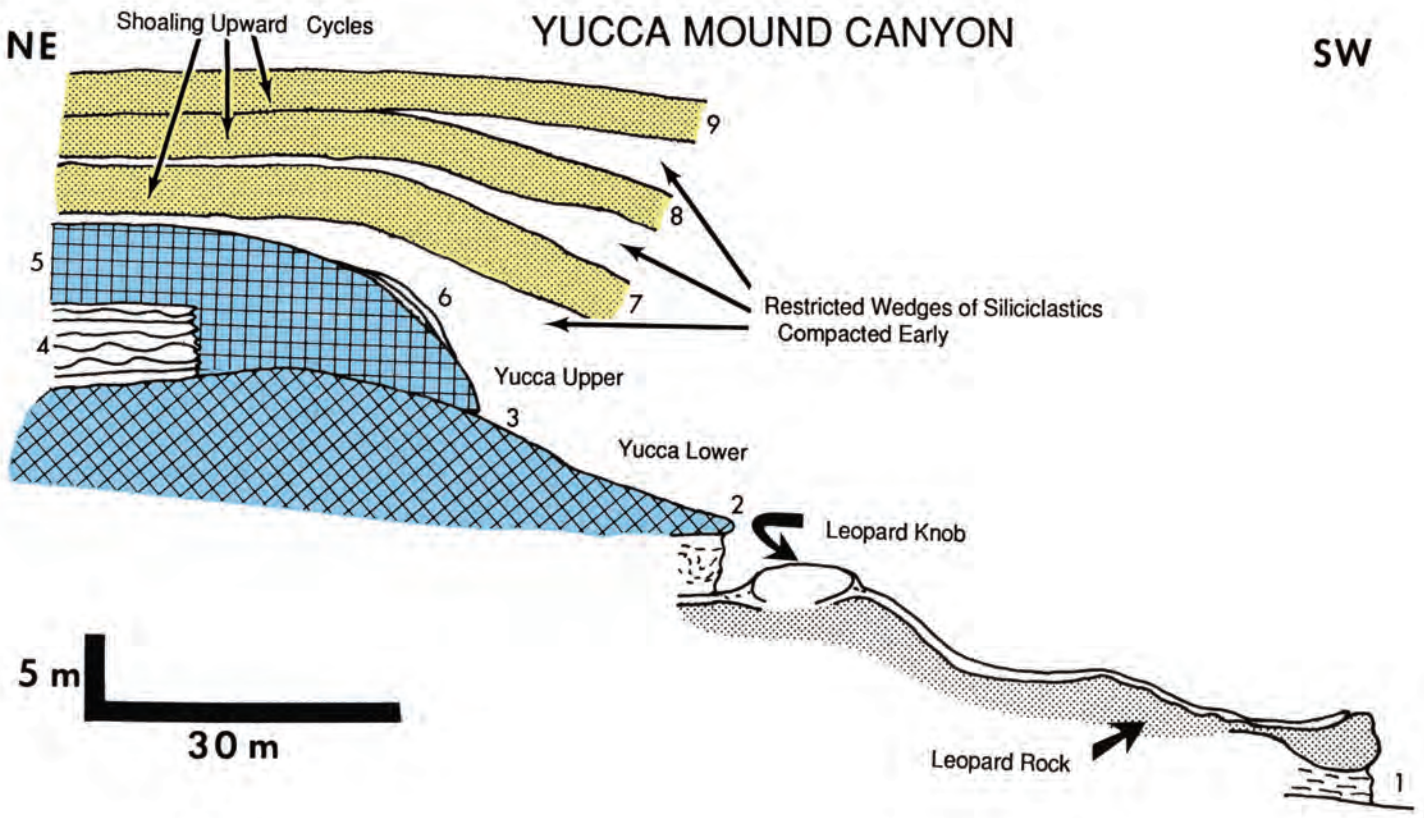

Figure 44 - Rough sketch of northeast - southwest cross section through Yucca Mound and overlying and underlying beds. Sketch illustrates retrogradation, progradation and basinally-restricted wedges of sediment.

bivalves, ostracodes, charophytes, and worm tubes.

Above Leopard Knob is a shaly sequence of strata displaying soft sediment deformation, possibly associated with downslope movement or compaction of the overlying Yucca Mound complex. Position 2 is where the lower mound of the Yucca Mound complex toes out. Climb onto the outcrop of the mound in the base of the ravine. Most of the lithology consists of a packstone of phylloid algae, however, some encrusting foraminiferal boundstone is also present. Climb southeastward out of the ravine and climb to the top of Yucca Upper.

This position provides a good vantage point of spectacular geometric relationships of stratigraphic units. The relationships illustrate the important sequence stratigraphic concepts of progradation and retrogradation. Application of such concepts is of importance in understanding the distribution and heterogeneity of reservoirs. Look across the canyon to observe bedded flank beds of Yucca Upper (position 4 of Fig. 44) that have apparently prograded basinward in relation to Yucca Lower. Notice that the upper part of Yucca Upper becomes massive above the flank beds, suggesting a period of retrogradation (position 5 of Fig. 44). A further thin veneer at position 6 (Fig. 44) suggests late progradation. The downslope toe of Yucca Upper appears to downlap onto Yucca Lower at position 3 (Fig. 44; best observed from other side of ravine). If this relationship is real rather that an artifact of the outcrop (the subject of further work), then a period of retrogradation is suggested from position 1 to position 2 to position 3 (Fig. 44). Also observable from this vantage point are cross-bedded grainstones of an overlying cycle and stacked mounds that form in the basinward direction. Cross the canyon to observe Yucca Mound from the northwest side of the canyon.

From this vantage point, observe the downslope toe of Yucca Upper downlapping onto

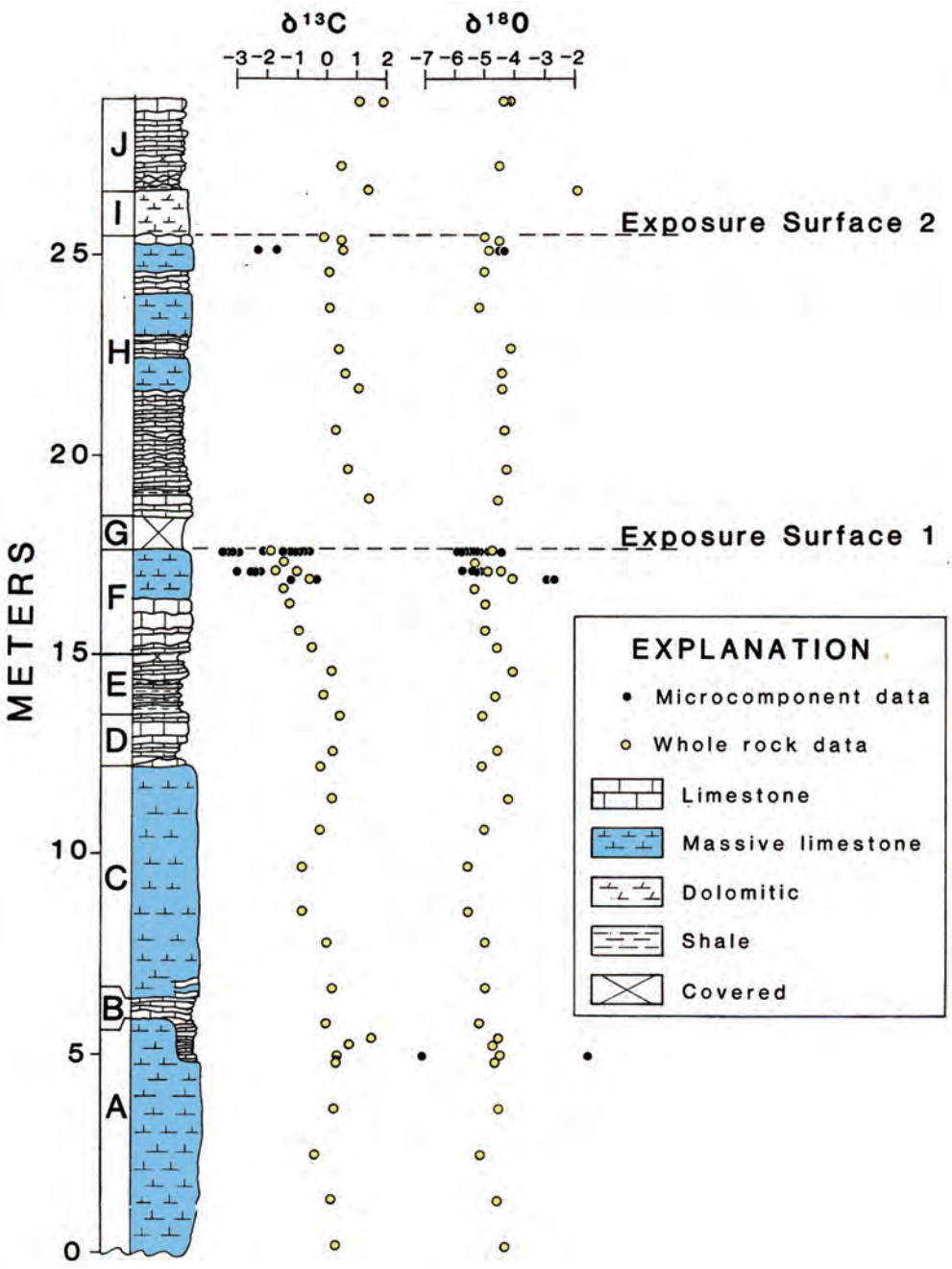

Figure 45 - Stratigraphic section with whole rock and micro-component stable isotope data for Yucca Mound Canyon (Stop 8). Position of two surfaces of subaerial exposure is documented. Base of stratigraphic section begins in lower part of Yucca Mound.

Yucca Lower (position 3 of Fig. 44). Look above the mound at the three limestone units (position 7, 8 and 9 of Fig. 44). Each of these shoaling upward cycles appear to dip downward off the flanks of the underlying mound, yet they appear to maintain their character and thickness throughout. Also, notice that the wedges of covered interval (probably siliciclastics) thicken off of the mound flanks and disappear above the mound. These "basinally restricted wedges" of sediment probably onlap and pinch out against the mound topography. This relationship provides another, smaller-scale example of cyclic and reciprocal sedimentation or lowstand systems tracts. It is interesting that the limestone units' character and facies do not reflect their present slope. Apparently the wedges of siliciclastic material compacted very early, before deposition of each overlying cycle.

To stand on the top of the lower mound, investigate the transition between flank beds and mound facies of the upper mound, and investigate the curious foraminiferal boundstone in the lower mound lithology, drop down to the top of the lower mound.

Climb through the next shoaling upward cycle by traversing up through the ravine (units D, B, and F of Fig. 45). The nodularly bedded units at the base of the cycle are fossil fragment wackestones and packstones. The more massive beds near the top of the cycle are fossil fragment packstones and grainstones. At the top of the cycle, notice laminated crust, blackened grain packstone, and root molds indicative of an event of subaerial exposure. What does each event of subaerial exposure indicate about the history of relative fall in sea level?

Small fractures and in-situ brecciation (compactional) are common in some portions of the limestones and are evidence of early lithification. Wilson (1975a) suggests this early cementation and vuggy leaching took place during sea level low stands and are the result of early meteoric diagenesis. This explanation seems particularly likely in light of the

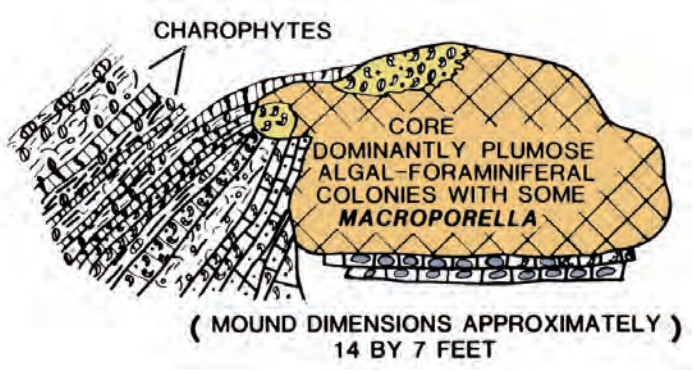

Figure 46 - Diagram illustrating size and relation to surrounding beds for Leopard Knob mound (after Toomey and Babcock 1983).

cyclic nature of Holder sediments overlying the bioherm and the transgression/regression model that explains their origin (Wilson 1977). More recent and more geochemically oriented work (Goldstein 1988a; Goldstein 1988b; Goldstein 1991a; Goldstein 1991b) has confirmed the repeated, complex nature of subaerial exposure effects in these strata. Sea level changes were of sufficient magnitude that meteoric waters penetrated through deposits of multiple prior cycles. Under such conditions, the degree and nature of diagenetic alterations depended on timing of exposure events, presence or absence of overlying aquicludes, and diagenetic susceptibility of the sediments. In total, fifteen events of intraformational subaerial exposure were responsible for calcite cementation in the limestones (Fig. 47). In general, lagoonal and basinal carbonates received little meteoric calcite cement and remained porous after deposition of the Holder cycles. In contrast, shelf edge and shelf crest carbonates were almost totally cemented during intraformational subaerial exposure. Limestones sealed off by shales or already cemented carbonates were also protected from extensive cementation during subaerial

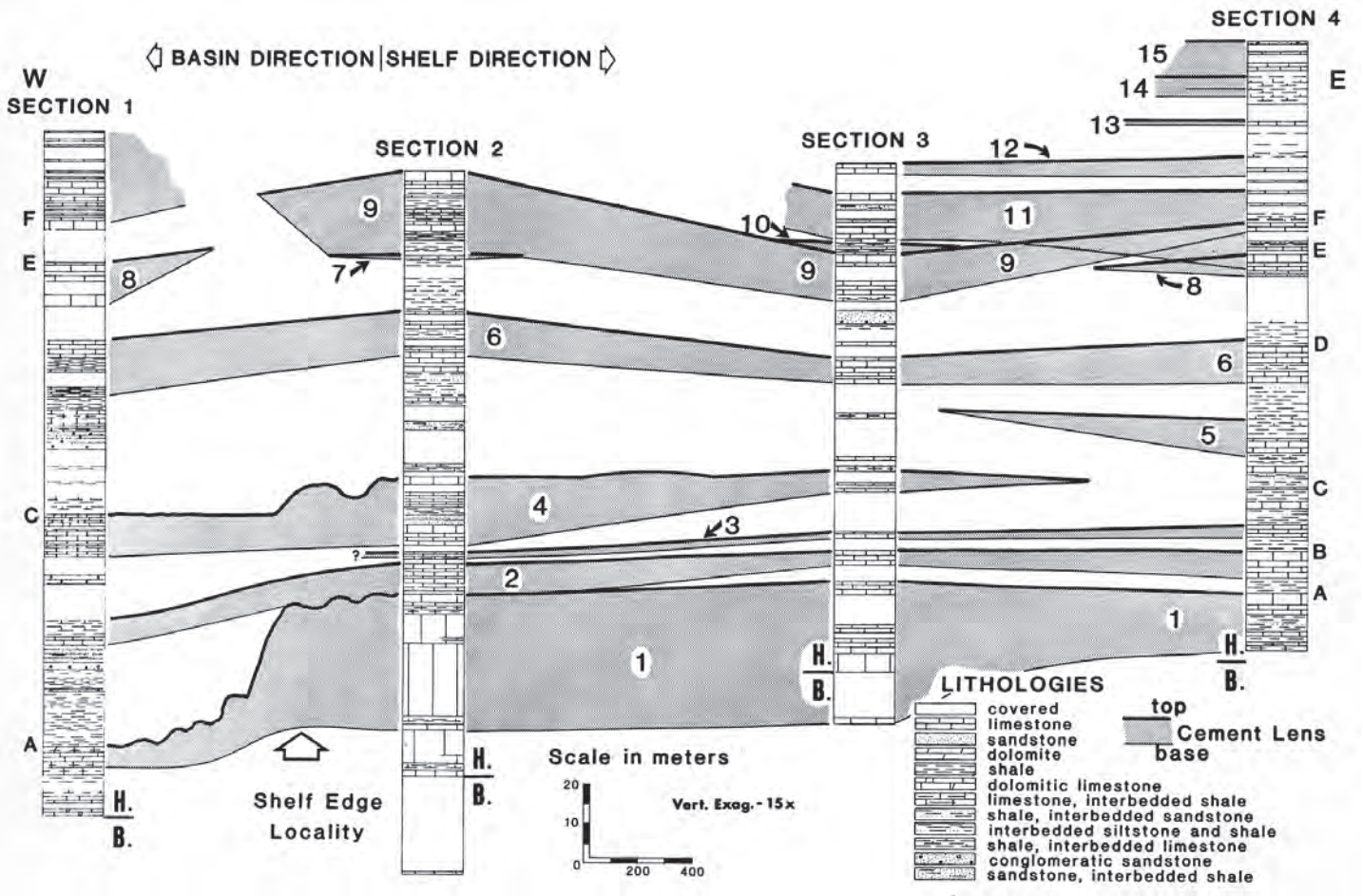

Figure 47 - Four stratigraphic sections in the Holder Formation. Section 2 is position of Yucca Mound Canyon (Stop 8); Section 4 is position of lagoonal Holder Formation at New Mexico Highway 82 roadcut (Stop 6). Numbered and shaded areas diagram the distribution of meteoric calcite cement that formed during 15 events of intraformational subaerial exposure.

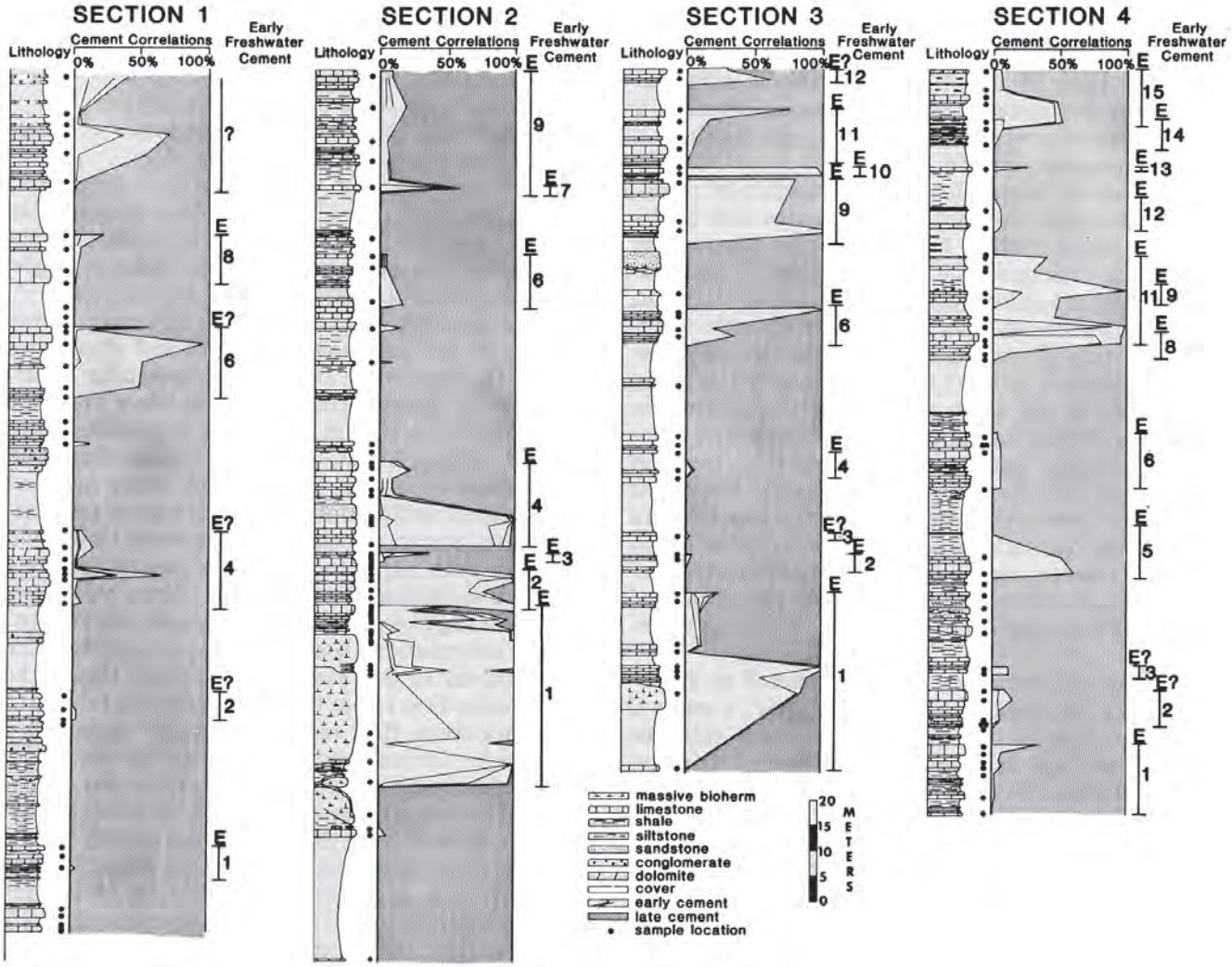

Figure 48 - Four stratigraphic sections in the Holder Formation. Section 2 is position of Yucca Mound Canyon (Stop 8); Section 4 is position of lagoonal Holder Formation at New Mexico Highway 82 roadcut (Stop 6). Cement stratigraphic diagram that illustrates the percent of meteoric calcite cement in white. Shelf and shelf-crest settings were almost totally cemented during intraformational events of subaerial exposure.

exposure (Fig. 48). Such relationships can be used in a predictive sense to better understand the distribution and heterogeneity of carbonate reservoirs. Return to vehicle.

0.0	47.35	Continue west on New Mexico highway 82 from the 3 mile marker.
3.4	50.75	Turn right (north) onto U.S. 54/70.
10.1	60.85	Turn right onto U.S. 70 East.
0.6	61.45	Turn left onto Bookout Road, going north.
0.7	62.15	The bioherms of the Laborcita Formation (Permian, Wolfcampian) can be seen to the east, capping the low hills on the frontal escarpment of the Sacramento Mountains.
0.1	62.25	Turn right (east) onto Bookout Road, northeast.
0.3	62.55	Observe style of mounding in Laborcita mounds, as we approach low hills. Notice alternating light-colored and dark-colored bands
0.25	62.8	Good scenic overlook of the mounding style. The mounds consist of alternating layers of dark, submarine cement-rich phylloid algal limestone and light-colored micrite-rich phylloid algal limestone (Figs. 49, 50). Topography on the upper surface of the mound is eliminated by "fill in" capping marine limestones that thicken into low areas (Fig. 51).

0.35 63.15 **STOP 9 MOUNDS OF THE PERMIAN LABORCITA FORMATION**

TULAROSA MOUNDS - Park vehicle just around the sharp curve in the road to the right. Julian Martinez, Rt. #2, Box 5058, Tularosa, NM, owns the ranch on which the outcrops are located. He has been kind to tidy and responsible geologists. Please check with him for permission before entering his land

From the parked vehicle (south curve on Bookout Road, past Martinez' Ranch house), look up (east) towards the southernmost massive capping limestone. This isolated buildup is called Scorpion Mound. Walk to the bioherms via a meandering route over beds of the Laborcita Formation of Otte (1959a; 1959b). Here, these beds (partial time-equivalents of the Abo and Hueco redbeds; Fig. 52) include red and green sandstones, siltstones and mudstones with some spectacular polymict conglomerates and thin limestones. At a few horizons, one can see brachiopods, cephalopods, sponges, algal-foraminiferal buildups, red algal buildups, and other grains concentrically coated by the red alga *Archaeolithophyllum lamellosum* Wray (Toomey 1983).

From the road, climb east directly along the trend of Bookout northeast road and then walk to the right (south) to reach the nose of the hill with an outcrop of limestone. It is only about a third of the way up the slope.

The sequence starting just below the limestone outcrop is summarized in Fig. 53. At the base, there are a couple of feet of greenish granulestone and sandstone overlain by several feet of calcrete (paleosol). In the calcrete, notice the laminated crusts, root molds,

Figure 49 - Field photograph of bioherm in the Permian Laborcita Formation. The mound (Vulture Mound) shows marked contrast between dark, submarine cement-rich and light, micrite-rich phylloid algal lithologies. Such layers are typical of the Laborcita bioherms.

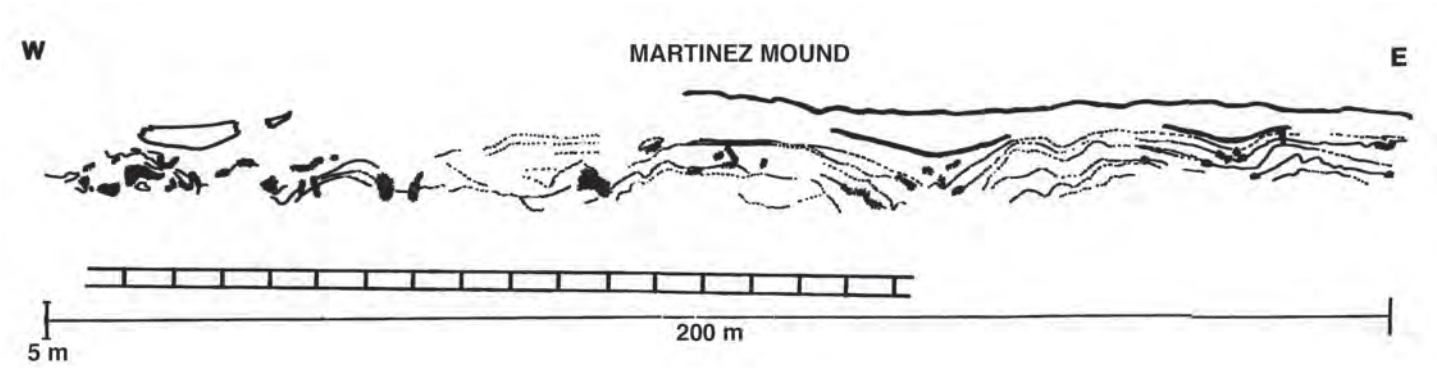

Figure 50 - Outcrop map of phylloid algal mound in the Laborcita Formation, Martinez Mound, northernmost south-facing exposure of Tularosa mounds, ravine with dam. Heavy lines with cross-marks denote location of abundant limestone filled fissures that cut across the mound fabric. Thin and dashed lines trace contacts between alternating light and dark-colored layers. Heavy solid lines outline marine limestone fill-in beds that reduce the topography on the tops of the mounds.

Figure 51 - Phylloid algal mounds of the Laborcita Formation. Notice the limestone beds that clearly fill in mound topography from above. The fill-in beds are normal marine limestones. They commonly make a V-shaped pattern as they fill in low areas. They both thicken into the lows and onlap against the highs.

and autoclastic breccia that provide strong support for an event of subaerial exposure at the top of this bed. It is overlain by one or two feet of a tan limestone unit containing possible fish debris, That is overlain by about a foot of black, possibly recrystallized algal fragment sandstone and conglomerate. That is overlain by a discontinuous 6-inch layer of ostracode wackestone. This is overlain by a 6-inch to 1-foot thick layer of leopard rock (plumose algal-foraminiferal) boundstone, which is overlain by in-place *Archaeolithophyllum lamellosum* (red algae) boundstone, and finally capped by *Archaeolithophyllum lamellosum* rhodoliths. These lithologies are best viewed by going up to the nose of the hill described, then down its dip slope, crossing the fallen fence to go north onto the next hill (go through the ravine) and to see the leopard rock, rhodoliths and the in-place

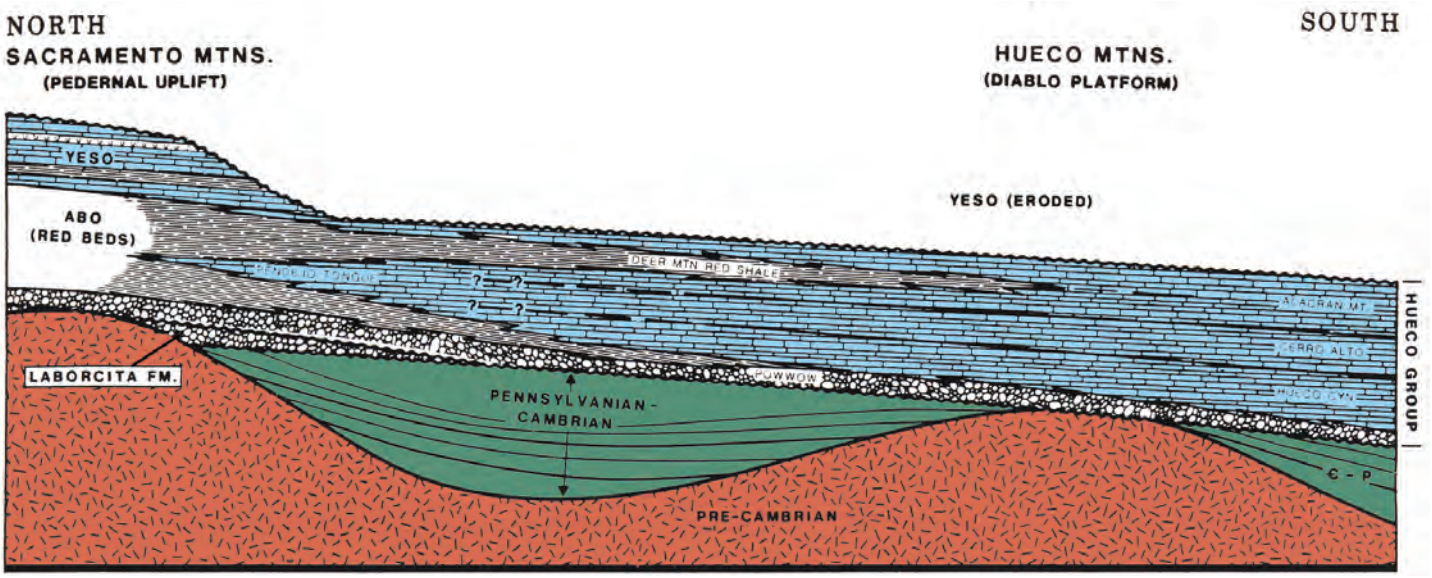

Figure 52 - North-South stratigraphic relationships of Laborcita Formation to other Wolfcampian stratigraphic units (after Candelaria 1988).

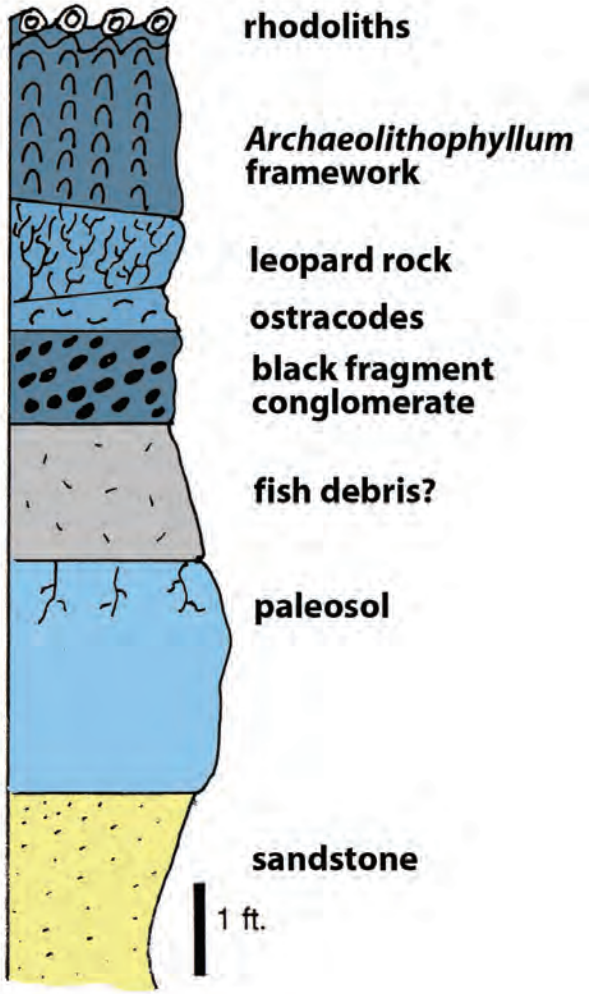

Figure 53 - Sketch of stratigraphic sequence in Laborcita Formation below Scorpion Mound. Sequence provides a record of transgression.

Archaeolithophyllum lamellosum boundstone. Toomey and Babcock (1983) have described these small mounds in some detail and noticed a capping sponge component. The mounds average about 3 feet in height and are 3-9 feet in diameter. The sequence of mound growth is interpreted (by Toomey and Babcock 1983) to represent initiation in quite shallow marine water and formation during progressive deepening to as much as 60 feet (Fig. 54). Overall, the sequence observed begins in the subaerial realm (paleosol), is overlain by limestones of restricted marine or freshwater, origin (ostracodes and fish debris) and is capped by a mound sequence that may record deepening upward. Hence, the sequence is one of transgression (Winchester 1976).

Climb under fence just north of where different fence trends meet. Climb up the hill through thick sequence of green and red siliciclastics to outcrop of conglomerate. Notice the composition of the clasts in the conglomerate are mostly chert, perhaps some quartzite, common rhyolite and some granite. These clast compositions are interesting to compare to those of the Pennsylvanian Holder Formation observed in Dry Canyon. The transition suggests progressive unroofing of the Pedernal uplift from Pennsylvanian to Permian time.

Continue up the hill, curving slightly to the southeast. About two-thirds of the way up, between the conglomerate and the major orange and grey limestone unit that crops out above us, there is a discontinuous leopard rock mound. It crops out especially well on the southeast side of the hill. Continue up the hill through siliciclastics and up onto the continuous limestone layer. Notice, immediately on top of the bed is debris of rhodoliths and fossiliferous limestone.

Continue up section and climb onto the southeastern gentle slope of Scorpion mound (Fig. 55). Notice the in-place phylloid algae, brecciation textures, and the laminated internal sediment. Climb

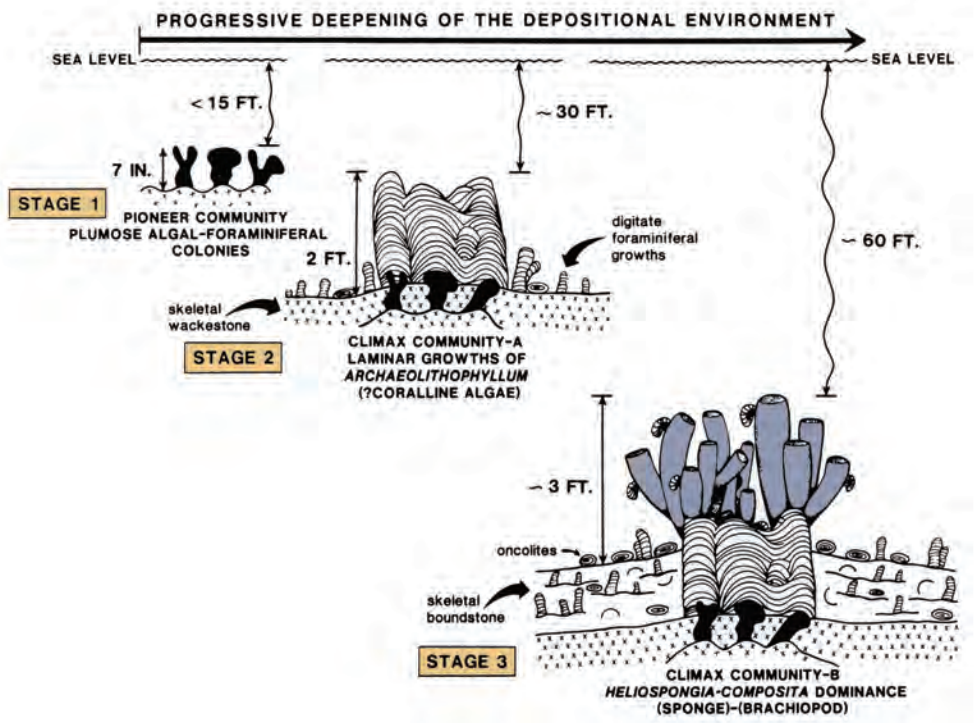

Figure 54 - Diagram illustrating the formation of Leopard Rock, *Archaeolithophyllum* boundstone, rhodoliths, and sponge mounds during progressive deepening (after Toomey and Babcock 1983).

to the top of Scorpion to the steep edge of the bioherm facing Bookout Road. Notice the rather gradational contact between the black submarine cement-rich facies and the cement-poor facies. Walk down from the top of the bioherm (east) and traverse downward along the front of Scorpion mound. On the northwestern end of the bioherm, (about 20 feet from the very edge of it) one can see beautiful exposure of upward-oriented black fans of submarine cement. Also, there is a fissure filled with muddy limestone. Note the upward transition from black (cement rich) to white (cement poor) is gradational, whereas the upward transition from white (cement poor) to black (cement rich) seems to be very sharp. Differences in such transitions may hold clues to the mechanism of mound growth and cement-rich to cement-poor alternation.

The bioherms have been described in increasing detail by Otte (1954; 1959a; 1959b), Otte and Parks (1963), Cys and Mazzullo (1977), Mazzullo and Cys (1979), and Shinn et al. (1983). Otte (1959a) estimates the bioherms to have stood as much as 20 m (60 ft.) above the surrounding bottom.

Weathering of these mounds has left internal structure easily visible. A number of components may be readily recognized in outcrop (Figs 56, 57). These include: (1) gray, commonly well-laminated lime mud; (2) dark calcite cement, which fractures to reveal a blocky structure but may be viewed in low angle light to reveal a relict fibrous habit and botryoidal form; (3) phylloid algal fragments; (4) fractures; (5) scattered sand pockets, some graded; (6) some coarsely crystalline, white pore-filling calcite; and (7) brown dolomite. The dark calcite cement derives its color from submicroscopic inclusions of organic matter, which is apparently not extractable (Plumley and Graves 1953). On outcrop, some areas of the lithoherms may be seen to be extremely rich in this dark cement. In places, it forms an anastomosing network with lighter-colored sediments infilling voids within the cement framework. Cys and Mazzullo (1977) and Mazzullo and Cys (1979) estimate that this cement accounts for 50-85% of the mound volume. They interpret the cement to be a marine precipitate that grew on the sea floor and within voids in the mound. However, study of polymud stratigraphy in polished slabs (Fig. 57) indicates initial accumulation of phylloid algae and mud was clearly followed by precipitation of dark marine cement in pore space. Cross and Klosterman (1981a; 1981b) interpreted some of the botryoids to have resulted from recrystallization of stromatolites.

A short core through this mound, taken by the U.S. Geological Survey in the early 1980's (Shinn et al. 1983), indicated that these mounds were localized on "thicks" in the underlying sandstone beds and that they were extensively brecciated during burial rather than because of subaerial exposure. The contrast between the highly cemented layers and

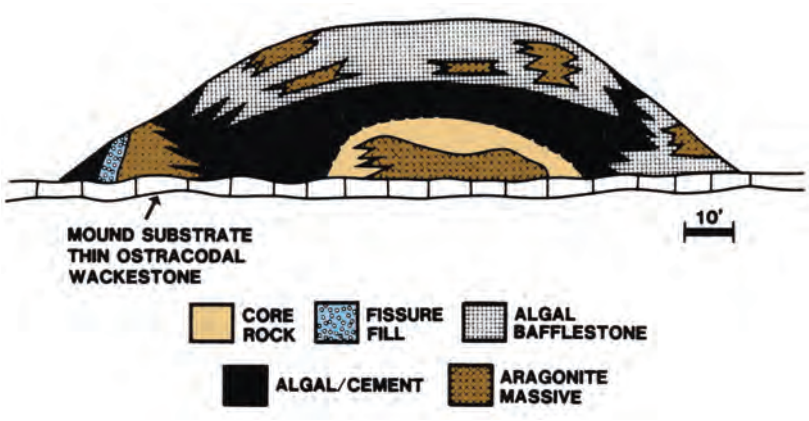

Figure 55 - Diagram illustrating the distribution of various lithofacies in Scorpion Mound (after Mazzullo and Cys, 1979).

Figure 56 - Negative print of thin section from mound in the Laborcita Formation. Notice dark phylloid algal blades, laminated internal sediments, and fibrous botryoid of submarine cement. Photo is about 0.75 centimeters across.

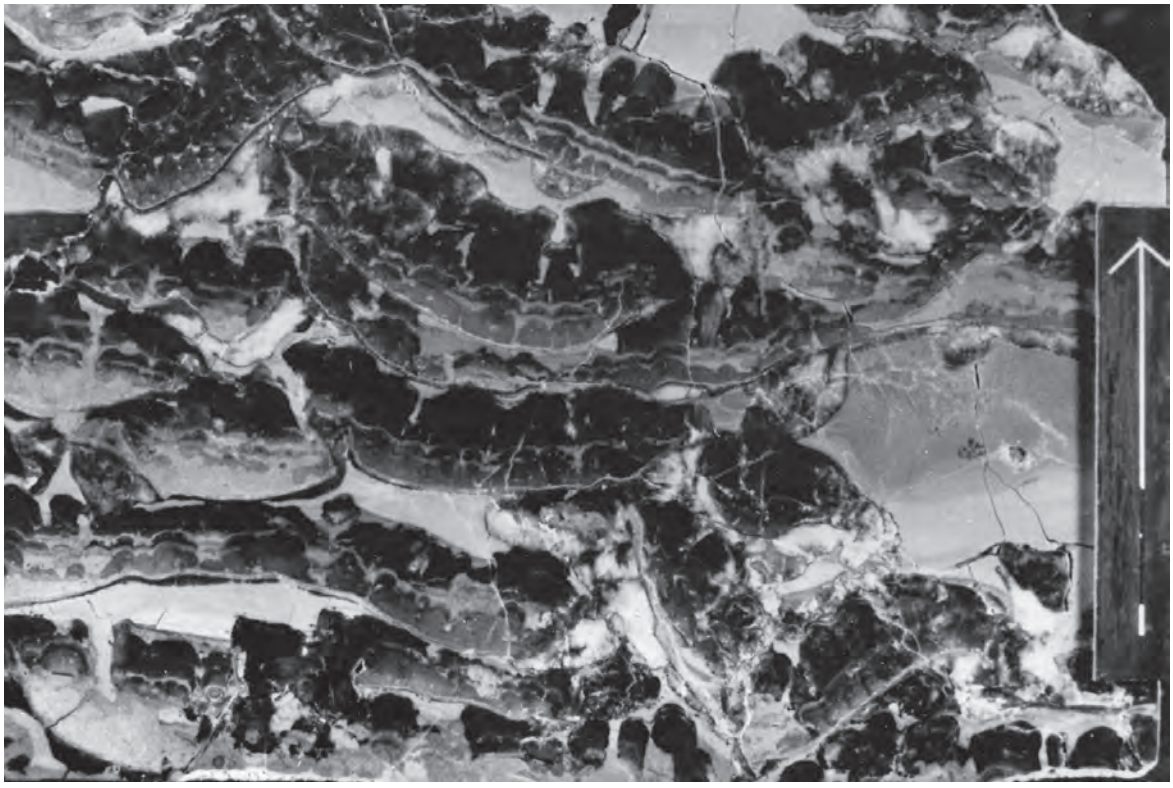

Figure 57 - Photograph of polished slab from mound in the Laborcita Formation. Note dark, upward oriented botryoids of submarine cement growing on various substrates at various levels. Internal sediment banding within botryoids is identical at all levels. Thus, submarine cement grew in pore space after accumulation of phylloid algae. It did not grow at the sediment-water interface. The preferred upward orientation was likely substrate controlled. Slab is about 10 inches across.

the mud-filled zones led, in their opinion, to intense grain breakage as a consequence of overburden stresses.

Return to vehicles. Reverse direction and drive west on Bookout Road northeast.

1.0	64.15	Cross Bookout Road and continue west on Bookout northeast.
1.1	65.25	Turn right (north) onto U.S. highway 54.
0.6	65.85	Just before mileage marker 81 and highway overpass, turn right (east) onto dirt road. Never take this road during a rain storm, as it and the outcrop could be inaccessible. Safety of the road also depends on how recently it has been graded. It is a county "harvest trail" and should be maintained. Note when driving, there are a couple of turn offs on this dirt road. When driving from U.S. 82 towards Coyote Canyon keep right whenever given a choice.
0.95	66.8	Pass old cable tool drill rig.
2.1	68.9	**OPTIONAL STOP 10 - COYOTE CANYON MOUND - LABORCITA FORMATION** - Park cars, making sure they are out of the way and out of the road. Walk down into Coyote Canyon and traverse upstream. As you walk up the canyon, the best outcrop is along the ravine wall on the south side of the canyon. The beds are dipping so you will climb section during the traverse. This locality has been described in detail by Fly (1986). The first major outcrop is of Otte's (1959a) bed 35 on which one can observe fenestral fabrics, root molds, and autoclastic breccia indicating an event of subaerial exposure. Above bed 35 are red shales interbedded with red sandstones. Continue up through the section to observe a conglomeratic unit with rhyolite clasts. A Tertiary dike complicates the stratigraphy directly above this. Above the conglomerate is a sequence of shales and sands, finely bedded, which pass upwards to marine limestones interbedded with shale, which are the basal units of Otte's bed 51 according to Fly. Bed 51 can be observed cropping out on both sides of the canyon. Above bed 51 are interbedded shales and some limestones that pass upward into a several foot thick bed of sandstone. This is overlain by shales and limestones underlying the Coyote Canyon bioherm complex.

The Coyote Canyon complex of phylloid algal mounds is exposed in the center of the canyon and on both sides. On the south side the mounds are cut by a Tertiary dike to provide a three dimensional exposure. The northeast-southwest face is mapped on Figure 58. Normal marine limestones cap the mound and fill fissures within it. In the mound, dominant components are phylloid algae, mud and submarine cement. Growth bands within the mound are defined by differences in amount of black, submarine cement.

Reverse direction and leave Coyote Canyon.

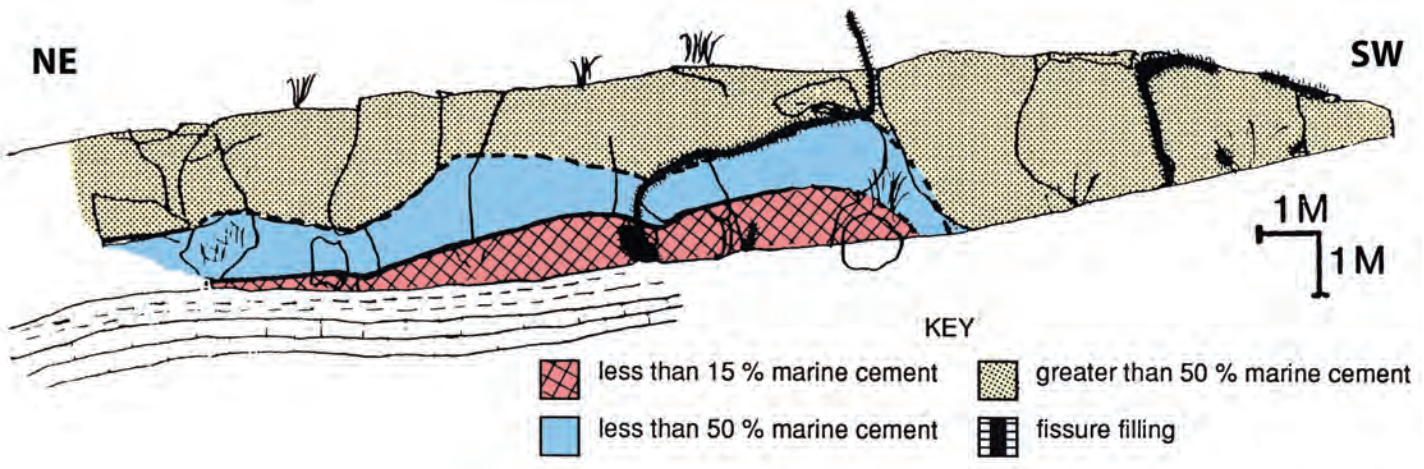

Figure 58 - Outcrop map of southernmost exposure of Laborcita mound in Coyote Canyon.

1.15	70.05	Cross cattle-guard
0.75	70.8	Cross cattle-guard
1.05	71.85	Reach intersection with dirt road and New Mexico highway 54. Now continue south (left) back to Alamogordo on New Mexico highway 54.
1.6	73.45	Pass intersection with New Mexico highway 70 and continue south on 70-54.
10.4	83.85	Pass intersection with New Mexico highway 82 and continue south on 54-70.
4.2	88.05	Pass Comfort Inn and continue toward El Paso.
0.75	88.8	Turn left (south) onto U.S. 54 to El Paso
10.0	98.8	Isolated buttes to the right are of varied origin. The closest is composed of Tertiary intrusives. Those beyond are outcrops of the Hueco and Yeso Formations. The San Andres Mountains are the prominent range in the background. This block-faulted range exposes a complete south-central New Mexico Paleozoic section from Precambrian basement on the east through Permian San Andres Formation on the west side of the range.
9.5	108.3	Stabilized reddish sand dunes in valley floor. Jarilla Mts. ahead on right expose Pennsylvanian and Permian sediments and Cretaceous and Tertiary intrusives. Southern end of the Sacramento Mountains and the Otero Mesa are in the distance to the left. The Otero Mesa is composed of the Yeso and Hueco Fms. and has been an area of great controversy in the early years of the 21st century. It has become a battleground between environmentalists and energy resource development interests. In 2004, New Mexico governor Bill Richardson put the entire area off limits to development, citing its uniqueness as an example of unspoiled desert grassland habitat.
122.8		Orogrande town limit. The town serves mostly to support the nearby McGregor and White Sands Missile Ranges. The lack of potable ground water in the Tularosa basin means that the town's water supply has to be piped in from the Sacramento Mountains.
123.0		Orogrande Post Office.
127.3		Directly west are the Organ Mountains, a southern extension of the San Andres Mountains. They expose large areas of Cretaceous and Tertiary volcanics and some Precambrian intrusives and Paleozoic sediments.
145.3		North end of Franklin Mountains at about 1 o'clock. To the right are the Hueco Mountains in the distance. The bulk of the Hueco Mountains section is Pennsylvanian and Permian, but its highest peaks are Cretaceous and Tertiary intrusives.
153.0		Texas state line and El Paso city limit. Note: we are really quite a way from the city of El Paso at this point.
161.7		Junction with Texas 2529. Take 45 left turn onto McCombs Street for airport or airport-area hotels. Continue straight ahead for downtown El Paso. We will follow the route that goes to the airport.
163.7		Bear right onto Railroad Drive.
166.8		Take overpass (Marshall Road).
170.1		Take left on Fred Wilson Road.
171.9		Fred Wilson Road makes a sharp right.
173.8		Left turn to entrance of El Paso airport. The El Paso area was first visited by the Spanish explorers in the 1500's and a mission was established here in 1959 by the Franciscans. By the mid to late 1700's the region (El Paso del Norte) was an established trading center and stopover for caravans. In 1848 El Paso (then known as Franklin) became part of the U.S.after the Mexican War was settled by treaty. Since then the town, with its sister city of Juarez, Mexico, has become a major center for commerce, especially manufacturing of clothing, leather goods, and other labor-intensive articles. Smelting and refining also once were major activities. The combined El Paso-Juarez population is now well over 2 million persons.

REFERENCES CITED

Ahlen, J.L., and Hanson.M.E., 1986, Southwest Section AAPG, Transactions and Guidebook of 1986 Convention (Ruidoso, New Mexico): Socorro, NM, New Mexico Bureau of Mines and Mineral Resources, p. 158.

Ahr, W.M., 1989, Sedimentary and tectonic controls on the development of an Early Mississippian carbonate ramp, Sacramento Mountains area, New Mexico, *in* Read, J.F., ed., Controls on Carbonate Platform and Basin Development: Tulsa, OK, SEPM Special Publication No. 44, p. 203-212.

Ahr, W.M., and Ross, S.L., 1982, Chappel (Mississippian) biohermal reservoirs in the Hardeman Basin, Texas: Transactions of the Gulf Coast Association of Geological Societies, v. 32, p. 185-193.

Armstrong, A.K., 1962, Stratigraphy and paleontology of Mississippian system in southwestern New Mexico and adjacent southeastern Arizona: Socorro, NM, New Mexico Bureau of Mines and Mineral Resources Memoir 8, 95 p.

Armstrong, A.K., 1967, Biostratigraphy and carbonate facies of the Mississippian Arroyo Peñasco Formation, north-central New Mexico: Socorro, NM, New Mexico Bureau of Mines and Mineral Resources Memoir 20, 80 p.

Bachman, G.O., 1975, New Mexico, *in* McKee, E.D., and Crosby, E.J., eds., Paleotectonic investigations of the Pennsylvanian System in the United States: Washington, D.C., U. S. Geological Survey Professional Paper 853-L, p. 233-243.

Bachtel, S.L., Rankey, E.C., Kaufman.J., and Mitchell, J.C., 1998, Field guide and discussion questions for Pennsylvanian Holder Formation, Dry Canyon, Sacramento Mountains, New Mexico, *in* Cox, D.M., ed., Upper Pennsylvanian and Wolfcampian Mixed Carbonate-Siliciclastic Systems, Sacramento Mountains, New Mexico: outcrop models for subsurface plays and reservoir development: Midland, TX, West Texas Geological Society Publication 98-104, p. 55-114.

Ball, S.M., Pollard, W.D., and Robert, J.W., 1977, Importance of phylloid algae in development of depositional topography, *in* Frost, S.H., Weiss, M.P., and Saunders, J.B., eds., Reefs and Related Carbonates - Ecology and Sedimentology: Tulsa, OK, American Association of Petroleum Geologists Studies in Geology No. 4, p. 239-260.

Boardman, D.R., II, Mapes, R.H., Yancey, T.E., and Malinky, J.M., 1984, A new model for the depth-related allogenic community succession within North American Pennsylvanian cyclothems and implications on the black shale problem, *in* Hyne, N.J., ed., Limestones of the Mid-Continent: Tulsa, OK, Tulsa Geological Society Special Publication No. 2, p. 141-182.

Bolton, K., Lane, H.R., and LeMone, D.V., 1982, Symposium on the paleoenvironmental setting and distribution of the Waulsortian facies (March 2-6, 1982): El Paso, TX, El Paso Geological Society and University of Texas at El Paso, p. 202.

Bowsher, A.L., 1948, Mississippian bioherms in the northern part of the Sacramento Mountains, New Mexico: The Compass, v. 25, p. 21-28.

Broadhead, R.F., 1984, Stratigraphically controlled gas production from Abo red beds (Permian), east-central New Mexico: Socorro, NM, New Mexico Bureau of Mines & Mineral Resources Circular 183, 36 p.

Butler, J.H., 1977, Geology of the Sacramento Mountains, Otero County, New Mexico: Midland, TX, West Texas Geological Society Publication 77-68, 216 p.

Candelaria, M.P., 1988, Synopsis of the Late Paleozoic depositional history of the Orogrande basin, New Mexico and Texas, *in* Robichaud, S.R., and Gallick, C.M., eds., Basin to Shelf Facies Transition of the Wolfcampian Stratigraphy of the Orogrande Basin: Midland, TX, Permian Basin Section-SEPM Publication No. 88-28, p. 1-4.

Carr, D.L., 1985, Depositional trends in Upper Paleozoic terrigenous clastic rocks, Sacramento Mountains, New Mexico: The Mountain Geologist, v. 22, p. 17-27.

Choquette, P.W., 1983, Platy algal reef mounds, Paradox basin, *in* Scholle, P.A., Bebout, D.G., and Moore, C.H., eds., Carbonate Depositional Environments: Tulsa, OK, American Association of Petroleum Geologists Memoir 33, p. 454-462.

Choquette, P.W., and Traut, J.D., 1963, Pennsylvanian carbonate reservoirs, Ismay field, Utah and Colorado, *in* Bass, R.O., and Sharps, S.L., eds., Shelf Carbonates, Paradox Basin (4th Field Conference Guidebook): Durango, CO, Four Corners Geological Society, p. 1-273.

Cline, L.M., 1959, Preliminary studies of the cyclical sedimentation and paleontology of upper Virgil strata of the La Luz area, Guidebook, Sacramento Mountains, New Mexico: Midland, TX, Permian Basin Section-SEPM, p. 1-306.

Cross, T.A., and Klosterman, M.J., 1981a, Autoecology and development of a stromatolitic-bound phylloid algal bioherm, Laborcita Formation (Lower Permian), Sacramento Mountains, New Mexico, USA, *in* Monty, C.L., ed., Phanerozoic Stromatolites: New York, Springer-Verlag, p. 45-59.

Cross, T.A., and Klosterman, M.J., 1981b, Primary submarine cements and neomorphic spar in a stromatolitic-bound phylloid algal bioherm, Laborcita Formation (Wolfcampian), Sacramento Mountains, New Mexico, USA, *in* Monty, C.L., ed., Phanerozoic Stromatolites: New York, Springer-Verlag, p. 60-73.

Crowell, J.C., 1978, Gondwana glaciation, cyclothems, continental positioning, and climate changes: American Journal of Science, v. 278, p. 1345-1372.

Cys, J.M., and Mazzullo, S.J., 1977, Biohermal submarine cements, Laborcita Formation (Permian), northern Sacramento Mountains, New Mexico, *in* Butler, J., ed., Geology of the Sacramento Mountains, Otero County, New Mexico: Midland, TX, West Texas Geological Society Publication 77-68, p. 39-51.

Davies, G.R., Edwards, D.E., and Flach, P., 1988a, Lower Carboniferous (Mississippian) Waulsortian reefs in the Seal area of north-central Alberta, *in* Geldsetzer, H.J., James, N.P., and Tebbutt, G.E., eds., Reefs, Canada and Adjacent Areas: Calgary, Canada, Canadian Society of Petroleum Geologists Memoir 13, p. 643-648.

Davies, G.R., Nassichuk, W.W., and Beauchamp, B., 1988b, Upper Carboniferous "Waulsortian" reefs, Canadian Arctic Archipelago, *in* Geldsetzer, H.H.J., James, N.P., and Tebbutt, G.E., eds., Reefs, Canada and Adjacent Areas: Calgary, Alberta, Canadian Society of Petroleum Geologists Memoir 13, p. 658-666.

Delgado, D.J., 1977, Paleocaliche textures from Wolfcampian strata of the Sacramento Mountains, New Mexico, *in* Butler, J.H., ed., Geology of the Sacramento Mountains, Otero County, New Mexico (Field Trip Guidebook, October 21-22, 1977): Midland, TX, West Texas Geological Society Publication 77-68, p. 102-108.

Delgado, D.J., and Pray, L.C., 1977, Stop "C-3" The Laborcita Formation, *in* Butler, J.H., ed., Geology of the Sacramento Mountains, Otero County, New Mexico (Field Trip Guidebook, October 21-22, 1977): Midland, TX, West Texas Geological Society Publication 77-68, p. 173-183.

Dix, G.R., and James, N.P., 1987, Late Mississippian bryozoan/microbial buildups on a drowned karst terrain: Port au Port Peninsula, western Newfoundland: Sedimentology, v. 34, p. 779-793.

Elias, G.K., 1963, Habitat of Pennsylvanian algal bioherms, Four Corners area, *in* Bass, R.O., and Sharps, S.L., eds., Shelf Carbonates, Paradox Basin (4th Field Conference Guidebook): Durango, CO, Four Corners Geological Society, p. 185-203.

Fly, S.H., III, 1986, Depositional environments of the Laborcita Formation (Wolfcampian), northern Sacramento Mountains, New Mexico, *in* Ahlen, J.L., and Hanson.M.E., eds., Southwest Section AAPG, Transactions and Guidebook of 1986 Convention (Ruidoso, New Mexico): Socorro, NM, New Mexico Bureau of Mines and Mineral Resources, p. 91-96.

Fly, S.H., III, and Speer, S.W., 1988, Day Three: Road Log Las Cruces-Alamogordo-Tularosa-La Luz-Cloudcroft, *in* Robichaud, S.R., and Gallick, C.M., eds., Basin to Shelf Facies Transition of the Wolfcampian Stratigraphy of the Orogrande Basin: Midland, TX, Permian Basin Section-SEPM Publication No. 88-28, p. 41-49.

French, J.A., 1987, Stratigraphy of a progradational unit, Pennsylvanian Holder Formation, Sacramento Mountains.

Füchtbauer, H., 1980, Composition and diagenesis of a stromatolitic bryozoan bioherm in the Zechstein 1 (northwestern Germany), *in* Füchtbauer, H., and Peryt, T.M., eds., The Zechstein Basin with Emphasis on Carbonate Sequences: Contributions to Sedimentology 9: Stuttgart, E. Schweizerbart'sche Verlagsbuchhandlung (Nägele u. Obermiller), p. 233-251.

George, P.G., and Ahr, W.M., 1986, The effects of paleotopography and substrate lithology on the origin of Waulsortian reefs: south-central Sacramento Mountains, New Mexico: Transactions of the Gulf Coast Association of Geological Societies, v. 36, p. 129-139.

Giles, K.A., and Soreghan, G.S., 2000, Lithofacies distribution and reservoir heterogeneity within Pennsylvanian bioherms, western Orogrande Basin, New Mexico, in Johnson, K.S., ed., Platform Carbonates in the Southern Midcontinent, 1996 Symposium: Norman, OK, Oklahoma Geological Survey

Circular 101, p. 269-274. Goldstein, R.H., 1988a, Cement stratigraphy of Pennsylvanian Holder Formation, Sacramento Mountains, New Mexico: American Association of Petroleum Geologists Bulletin, v. 72, p. 425-438.

Goldstein, R.H., 1988b, Paleosols of Late Pennsylvanian cyclic strata, New Mexico: Sedimentology, v. 35, p. 777-804.

Goldstein, R.H., 1991a, Practical aspects of cement stratigraphy with illustrations from Pennsylvanian limestone and sandstone, New Mexico and Kansas, *in* Barker, C.E., and Kopp, O.C., eds., Luminescence Microscopy and Spectroscopy: Qualitative and Quantitative Applications: Tulsa, OK, SEPM Short Course 25, p. 123-131.

Goldstein, R.H., 1991b, Stable isotope signatures associated with paleosols, Pennsylvanian Holder Formation, New Mexico: Sedimentology, v. 38, p. 67-78.

Heckel, P.H., 1980, Paleogeography of eustatic model for deposition of Midcontinent Upper Pennsylvanian cyclothems, *in* Fouch, T.D., and Magathan, E.R., eds., Paleozoic Paleogeography of West-Central United States [Rocky Mountain Paleogeography Symposium 1]: Denver, CO, Rocky Mountain Section-SEPM, p. 197-215.

Hunt, D., 2000, Platform architecture and sequence stratigraphy of the Lake Valley Formation, *in* Stanton, R.J., Jr., ed., Field Guide to the Carboniferous Geology of the Sacramento Mountains, New Mexico: Platforms and Mounds of the Lake Valley and Holder Formations: Tulsa, OK, SEPM (Society for Sedimentary Geology) and International Association of Sedimentologists Field Guide, p. 1-36.

Hunt, D., Kirkby, K.C., Allsop, T., Van Den Burgh, T.C., Simo, A.J., Pray, L.C., and Swarbrick, R., 1995, A one-day guide to Mississippian strata of Muleshoe Canyon, Sacramento Mountains, New Mexico, U.S.A.: Manchester, U.K., University of Manchester, 39 p.

Hurst, J.M., Scholle, P.A., and Stemmerik, L., 1988, Submarine cemented bryozoan mounds, Upper Permian, Devondal, East Greenland, *in* Geldsetzer, H.J., James, N.P., and Tebbutt, G.E., eds., Reefs, Canada and Adjacent Areas: Calgary, Canada, Canadian Society of Petroleum Geologists Memoir 13, p. 672-676.

Irwin, C.D., Jr., 1963, Producing carbonate reservoirs in the Four Corners area, *in* Bass, R.O., and Sharps, S.L., eds., Shelf Carbonates, Paradox Basin (4th Field Conference Guidebook): Durango, CO, Four Corners Geological Society, p. 144-148.

Jackson, W.D., 1983, A point source depositional model for Muleshoe Mound, a Mississippian (Osagean) spar-cemented carbonate buildup, Sacramento Mountains, New Mexico [abs.]: American Association of Petroleum Geologists Bulletin, v. 67, p. 488.

Jackson, W.D., and DeKeyser, T., 1984a, Microfacies analysis of Muleshoe Mound (Early Mississippian), Sacramento Mountains, New Mexico: a point-source depositional model. Part 1: West Texas Geological Society Bulletin, v. 23, p. 6-10.

Jackson, W.D., and DeKeyser, T., 1984b, Microfacies analysis of Muleshoe Mound (Early Mississippian), Sacramento Mountains, New Mexico: a point-source depositional model. Part 2: West Texas Geological Society Bulletin, v. 23, p. 6-9.

Jackson, W.D., and DeKeyser, T.L., 1989, Microfacies analysis of Muleshoe Mound (Early Mississippian), Sacramento Mountains: a point-source depositional model, *in* Mear, C.E., McNulty, C.L., and McNulty, M.E., eds., A Symposium on the Petroleum Geology of Mississippian Carbonates in North Central Texas: Fort Worth, TX, Fort Worth Geological Society and Texas Christian University, p. 21-31.

Jerome, S.E., Campbell, D.D., Wright, J.S., and Vitz, H.E., 1965, Geology and ore deposits of the Sacramento (High Rolls) mining district, Otero County, New Mexico: Socorro, NM, New Mexico Bureau of Mines and Mineral Resources Bulletin 86, 30 p.

Kerr, S.D., Jr., 1969, Algal-bearing carbonate reservoirs of Pennsylvanian age, West Texas and New Mexico [abs.]: American Association of Petroleum Geologists Bulletin, v. 53, p. 726-727.

Kirkby, K.C., and Hunt, D., 1996, Episodic growth of a Waulsortian buildup: the Lower Carboniferous Muleshoe Mound, Sacramento Mountains, New Mexico, USA, *in* Strogen, P., Somerville, I.D., and Jones, G.L., eds., Recent Advances in Lower Carboniferous Geology: London, Geological Society (London) Special Publication No. 107, p. 97-110.

Kirkby, K.C., Hunt, D., and Simo, J.A., 2000a, Guide to a Waulsortian buildup: Muleshoe Mound and associated strata; Sacramento Mountains, New Mexico, USA, *in* Stanton, R.J., Jr., ed., Field Guide to the Carboniferous Geology of the Sacramento Mountains, New Mexico: Platforms and Mounds of the Lake Valley and Holder Formations: Tulsa, OK, SEPM (Society for Sedimentary Geology) and International Association of Sedimentologists Field Guide, p. 1-47.

Kirkby, K.C., Simo, J.A., and Hunt, D., 2000b, Muleshoe mound: A possible 'Rosetta stone' for the interpretation of Waulsortian buildups [abs.], *in* Ahr, W.M., Harris, P.M., Morgan, W.A., Somerville, I.D., and Stanton, R.J., Jr., eds., Permo-Carboniferous Carbonate Platforms and Reefs — SEPM-IAS Research and Field Conference, Programs and Abstracts Volume: Tulsa, OK, SEPM (Society for Sedimentary Geology), p. 93.

Kirkland, B.L., Moore, C.H., Jr., and Dickson, J.A.D., 1993, Well preserved, aragonitic phylloid algae (*Eugonophyllum*, Udoteaceae) from the Pennsylvanian Holder Formation, Sacramento Mountains, New Mexico: Palaios, v. 8, p. 111-120.

Konishi, K., and Wray, J.L., 1961, *Eugonophyllum*, a new Pennsylvanian and Permian algal genus: Journal of Paleontology, v. 35, p. 659-666.

Kottlowski, F.E., 1960, Summary of Pennsylvanian sections in southwestern New Mexico and eastern Arizona: Socorro, NM, New Mexico Bureau of Mines and Mineral Resources Bulletin 66, 187 p.

Lane, H.R., 1982, The distribution of Waulsortian facies in North America as exemplified in the Sacramento Mountains of New Mexico, *in* Bolton, K., Lane, H.R., and LeMone, D.V., eds., Symposium on the Paleoenvironmental Setting and Distribution of the Waulsortian Facies: El Paso, TX, El Paso Geological Society and University of Texas-El Paso, p. 96-114.

Lane, H.R., and Ormiston, A.R., 1982, Waulsortian facies, Sacramento Mountains, New Mexico: Guide for an international field seminar, March 2-6, 1982, *in* Bolton, K., Lane, H.R., and LeMone, D.V., eds., Symposium on the Paleoenvironmental Setting and Distribution of the Waulsortian Facies: El Paso, TX, El Paso Geological Society and University of Texas-El Paso, p. 115-182.

Laudon, L.R., and Bowsher, A.L., 1941, Mississippian formations of the Sacramento Mountains, New Mexico: American Association of Petroleum Geologists Bulletin, v. 25, p. 2107-2160.

Laudon, L.R., and Bowsher, A.L., 1949, Mississippian formations of southwestern New Mexico: Geological Society of America Bulletin, v. 60, p. 1-88.

Lees, A., 1964, The structure and origin of the Waulsortian (Lower Carboniferous) "reefs" of west-central Eire: Philosophical Transactions of the Royal Society of London, Series B, v. 247 (no. 740), p. 483-531.

Lees, A., 1982, The paleoenvironmental setting and distribution of the Waulsortian facies of Belgium and southern Britain, *in* Bolton, K., Lane, H.R., and LeMone, D.V., eds., Symposium on the Environmental Setting and Distribution of the Waulsortian Facies: El Paso, TX, El Paso Geological Society and University of Texas-El Paso, p. 1-16.

Lees, A., Hallet, V., and Hibo, D., 1985, Facies variation in Waulsortian buildups, Part 1; A model from Belgium: Geological Journal, v. 20, p. 133-158.

Lees, A., and Miller, J., 1985, Facies variation in Waulsortian buildups, Part 2; Mid-Dinantian buildups from Europe and North America: Geological Journal, v. 20, p. 159-180.

LeMay, W.J., 1972, Empire Abo field, southeast New Mexico, *in* King, R.E., ed., Stratigraphic Oil and Gas Fields — Classification, Exploration Methods and Case Histories: Tulsa, OK, American Association of Petroleum Geologists Memoir 16, p. 472-480.

Lohmann, K.C., and Meyers, W.J., 1977, Microdolomite inclusions in cloudy prismatic calcites: a proposed criterion for former high magnesium calcites: Journal of Sedimentary Petrology, v. 47, p. 1075-1088.

Mack, G.H., and James, W.C., 1986, Cyclic sedimentation in the mixed siliciclastic-carbonate Abo-Hueco transitional zone (Lower Permian), southwestern New Mexico: Journal of Sedimentary Petrology, v. 56, p. 635-647.

Malek-Aslani, M., 1970, Lower Wolfcampian reef in Kemnitz field, Lea Co., N.M.: American Association of Petroleum Geologists Bulletin, v. 54, p. 2317-2335.

Mazzullo, S.J., and Cys, J.M., 1979, Marine aragonite sea-floor growths and cements in Permian phylloid algal mounds, Sacramento Mountains, New Mexico: Journal of Sedimentary Petrology, v. 49, p. 917-936.

McKinney, F.K., McKinney, M.J., and Listokin, M.R.A., 1987, Erect bryozoans are more than baffling: enhanced sedimentation rate by a living unilaminate branched bryozoan and possible implications for fenestrate bryozoan mudmounds: Palaios, v. 2, p. 41-47.

Meyer, R.F., 1966, Geology of Pennsylvanian and Wolfcampian rocks in southeast New Mexico: Socorro, NM, New Mexico Bureau of Mines and Mineral

Resources Memoir 17, 123 p.

Meyers, W.J., 1974, Carbonate cement stratigraphy of the Lake Valley Formation (Mississippian), Sacramento Mountains, New Mexico: Journal of Sedimentary Petrology, v. 44, p. 837-861.

Meyers, W.J., 1978, Carbonate cements: their regional distribution and interpretation in Mississippian limestones of southwestern New Mexico: Sedimentology, v. 25, p. 371-400.

Meyers, W.J., 1988, Paleokarstic features on Mississippian limestones, New Mexico, *in* James, N.P., and Choquette, P.W., eds., Paleokarst: New York, Springer-Verlag, p. 306-328.

Meyers, W.J., Cowan, P., and Lohmann, K.C., 1982, Diagenesis of Mississippian skeletal limestones and bioherm muds, New Mexico, *in* Bolton, K., Lane, H.R., and LeMone, D.V., eds., Symposium on the Paleoenvironmental Setting and Distribution of the Waulsortian Facies: El Paso, TX, El Paso Geological Society and University of Texas-El Paso, p. 80-95.

Meyers, W.J., and Lohmann, K.C., 1985, Isotope geochemistry of regionally extensive calcite cement zones and marine components in Mississippian limestones, New Mexico, *in* Harris, P.M., and Schneidermann, N., eds., Carbonate Cements: Tulsa, OK, SEPM Special Publication No. 36, p. 223-239.

Miller, F., 1969, The San Andres reef zone, *in* Summers, W.K., and Kottlowski, F.E., eds., The San Andres Limestone, a reservoir for oil and water in New Mexico, New Mexico Geological Society Special Publication 3, p. 27-31.

Neumann, A.C., Kofoed, J.W., and Keller, G.H., 1977, Lithoherms in the Straits of Florida: Geology, v. 5, p. 4-10.

Otte, C., Jr., 1954, Wolfcampian reefs of the northern Sacramento Mountains, Otero County, New Mexico [abs.]: Geological Society of America Bulletin, v. 65, p. 1291-1292.

Otte, C., Jr., 1959a, The Laborcita Formation of late Virginian-early Wolfcampian age of the northern Sacramento Mountains, Otero County, New Mexico, Guidebook, Sacramento Mountains, New Mexico: Midland, TX, Permian Basin Section-SEPM and Roswell Geological Society, p. 306.

Otte, C., Jr., 1959b, Late Pennsylvanian and Early Permian stratigraphy of the northern Sacramento Mountains, Otero County, New Mexico: Socorro, NM, New Mexico Bureau of Mines and Mineral Resources Bulletin 50, 108 p.

Otte, C., Jr., and Parks, J.M., Jr., 1963, Fabric studies of Virgil and Wolfcamp bioherms, New Mexico: Journal of Geology, v. 71, p. 380-396.

Parks, J.M., Jr., 1958, Plate-shaped calcareous algae in late Paleozoic rocks of mid-continent [abs.]: Geological Society of America Bulletin, v. 69, p. 1627.

Parks, J.M., Jr., 1962, Reef-building biota from late Pennsylvanian reefs, Sacramento Mountains, New Mexico [abs.]: American Association of Petroleum Geologists Bulletin, v. 46, p. 274.

Parks, J.M., Jr., 1977, Paleoecological evidence on the origin of the Dry Canyon Pennsylvanian bioherms, *in* Butler, J., ed., Geology of the Sacramento Mountains, Otero County, New Mexico: Midland, TX, West Texas Geological Society Publication 77-68, p. 27-32.

Parrish, J.T., 1993, Climate of the supercontinent Pangea: Journal of Geology, v. 101, p. 215-233.

Peryt, T.M., 1986, Zechstein *Stromaria* (=*Archaeolithoporella*)-cement reefs in Thuringia: Neues Jahrbuch für Geologie und Paläontologie, Monatshefte, v. 1986, p. 307-316.

Peterson, J.A., and Ohlen, H.R., 1963, Pennsylvanian shelf carbonates, Paradox Basin, *in* Bass, R.O., and Sharps, S.L., eds., Shelf Carbonates of the Paradox Basin: 4th Field Conference Guidebook: Durango, CO, Four Corners Geological Society, p. 65-79.

Plumley, W.J., and Graves, R.W., 1953, Virgilian reefs of the Sacramento Mountains, New Mexico: Journal of Geology, v. 61, p. 1-16.

Pol, J.C., 1982, Sedimentation and diagenesis of an Upper Pennsylvanian (Virgilian) mixed carbonate-clastic sequence, Hueco Mountains, El Paso County, Texas [unpublished Master's thesis]: University of Texas at Austin, Austin, TX, 212 p.

Pray, L.C., 1952, Stratigraphy of the escarpment of the Sacramento Mountains, Otero County, New Mexico [unpublished Ph.D. thesis]: California Institute of Technology, Pasadena, CA, 370 p.

Pray, L.C., 1958a, Fenestrate bryozoan core facies, Mississippian bioherms, southwestern United States: Journal of Sedimentary Petrology, v. 28, p. 261-273.

Pray, L.C., 1958b, Pennsylvanian sedimentation of the Sacramento Mountain area, New Mexico [abs.]: Midland, TX, Permian Basin Section-SEPM, Third Annual Meeting Abstracts, p. 7.

Pray, L.C., 1959, Outline of the stratigraphy and structure of the Sacramento Mountain escarpment of New Mexico, Guidebook, Sacramento Mountains, New Mexico: Roswell, NM, Roswell Geological Society and Permian Basin Section-SEPM, p. 86-130.

Pray, L.C., 1961, Geology of the Sacramento Mountains escarpment, Otero County, New Mexico: Socorro, NM, New Mexico Bureau of Mines and Mineral Resources Bulletin 35, 144 p.

Pray, L.C., 1965a, Clastic limestone dikes and marine cementation, Mississippian bioherms, New Mexico [abs.], Third Seminar on Sedimentation, Program: Midland, TX, Permian Basin Section-SEPM, p. 21-22.

Pray, L.C., 1965b, Limestone clastic dikes in Mississippian bioherms, New Mexico [abs.]: Boulder, CO, Geological Society of America Special Paper 82, p. 154-155.

Pray, L.C., 1969, Micrite and carbonate cement, genetic factors in Mississippian bioherms [abs.]: Journal of Paleontology, v. 43, p. 895.

Pray, L.C., 1975a, Mississippian Shelf-edge and Basin Facies Carbonates, Sacramento Mountains and Southern New Mexico Region: Dallas, TX, Dallas Geological Society Guidebook, 140 p.

Pray, L.C., 1975b, Muleshoe and South San Andres bioherms, supplemental notes and road log, *in* Pray, L.C., ed., Mississippian Shelf-Edge and Basin Facies Carbonates, Sacramento Mountains and Southern New Mexico Region: Dallas, TX, Dallas Geological Society Field Trip Guidebook, p. 129-134.

Pray, L.C., and Wray, J.L., 1963, Porous algal facies (Pennsylvanian) Honaker Trail, San Juan Canyon, Utah, *in* Bass, R.O., and Sharps, S.L., eds., Shelf Carbonates, Paradox Basin (4th Field Conference Guidebook): Durango, CO, Four Corners Geological Society, p. 204-234.

Ross, C.A., and Ross, J.R.P., 1987, Late Paleozoic sea levels and depositional sequences, *in* Ross, C.A., and Haman, D., eds., Timing and Depositional History of Eustatic Sequences: Constraints on Seismic Stratigraphy: Washington, D.C., Cushman Foundation for Foraminiferal Research, Special Publication No. 24, p. 137-149.

Schatzinger, R.A., 1983, Phylloid algal and sponge-bryozoan mound-to-basin transitions — a late Paleozoic facies tract from Kelly-Snyder field, west Texas, *in* Harris, P.M., ed., Carbonate Buildups — a core workshop (Dallas, Texas, April 16-17, 1983): Tulsa, OK, SEPM Core Workshop No. 4, p. 244-303.

Scholle, P.A., Stemmerik, L., and Ulmer, D.S., 1991, Diagenetic history and reservoir potential of Upper Permian carbonate buildups, Wegener Halvø area, Jameson Land basin, East Greenland: American Association of Petroleum Geologists Bulletin, v. 75, p. 701-725.

Schutter, S.R., and Heckel, P.H., 1983, Missourian (early late Pennsylvanian) climate in Midcontinent North America: Geological Society of America, Abstracts with Programs, v. 15, p. 681.

Shinn, E.A., and Robbin, D.M., 1983, Mechanical and chemical compaction in fine-grained shallow-water limestones: Journal of Sedimentary Petrology, v. 53, p. 595-618.

Shinn, E.A., Robbin, D.M., Lidz, B.H., and Hudson, J.H., 1983, Influence of deposition and early diagenesis on porosity and chemical compaction in two Paleozoic buildups: Mississippian and Permian age rocks in the Sacramento Mountains, New Mexico, *in* Harris, P.M., ed., Carbonate Buildups — a core workshop (Dallas, April 16-17, 1983): Tulsa, OK, SEPM Core Workshop No. 4, p. 182-222.

Smith, D.B., 1981, Bryozoan-algal patch-reefs in the Upper Permian Lower Magnesian Limestone of Yorkshire, northeast England, *in* Toomey, D.F., ed., European Fossil Reef Models: Tulsa, OK, SEPM Special Publication No. 30, p. 187-202.

Stanton, R.J., Jr., 2000, Field Guide to the Carboniferous Geology of the Sacramento Mountains, New Mexico: Platforms and Mounds of the Lake Valley and Holder Formations: Tulsa, OK, SEPM (Society for Sedimentary Geology) and International Association of Sedimentologists Field Guide, p. ca. 275.

Stanton, R.J., Jr., Jeffery, D.L., and Ahr, W.M., 2000a, Oxygen minimum zone and internal waves as potential controls on location and growth of Waulsortian mounds (Mississippian, Sacramento Mountains, New Mexico): Facies, v. 42, p. 161-176.

Stanton, R.J., Jr., Jeffrey, D.L., and Ahr, W.M., 2000b, Paleoclimatic setting of the Waulsortian mounds and ramp strata of the Alamogordo Member, Lake Valley Formation, Lower Mississippian of south central New Mexico [abs.], *in* Ahr, W.M., Harris, P.M., Morgan, W.A., Somerville, I.D., and Stanton, R.J., Jr., eds., Permo-Carboniferous Carbonate Platforms and Reefs

— SEPM-IAS Research and Field Conference, Programs and Abstracts Volume: Tulsa, OK, SEPM (Society for Sedimentary Geology), p. 139.

Stemmerik, L., Scholle, P.A., Henk, F.H., Di Liegro, G., and Ulmer, D.S., 1993, Sedimentology and diagenesis of the Upper Permian Wegener Halvø Formation carbonates along the margins of the Jameson Land Basin, East Greenland, *in* Vorren, T.O., Bergsager, E., Dahl-Stammes, Ø.A., Holter, E., Johansen, B., Lie, E., and Lund, T.B., eds., Arctic Geology and Petroleum Potential: Norwegian Petroleum Society (NPF) Special Publication 2: Amsterdam, Elsevier, p. 107-119.

Surlyk, F., Hurst, J.M., Piasecki, S., Rolle, F., Scholle, P.A., Stemmerik, L., and Thomsen, E., 1986, The Permian of the western margin of the Greenland Sea — a future exploration target, *in* Halbouty, M.T., ed., Future Petroleum Provinces of the World: Tulsa, OK, American Association of Petroleum Geologists Memoir 40, p. 629-659.

Thornton, D.E., and Gaston, H.H., Jr., 1968, Geology and development of the Lusk Strawn Field, Eddy and Lea Counties, New Mexico: American Association of Petroleum Geologists Bulletin, v. 52, p. 66-81.

Toomey, D.F., 1983, Early Permian coated grains from a lagoonal environment, Laborcita Formation, southcentral New Mexico, U.S.A., *in* Peryt, T.M., ed., Coated Grains: New York, Springer-Verlag, p. 259-269.

Toomey, D.F., and Babcock, J.A., 1983, Precambrian and Paleozoic algal carbonates, west Texas-southern New Mexico: Golden, CO, Colorado School of Mines Professional Contributions, v. 11, p. 345.

Toomey, D.F., Wilson, J.L., and Rezak, R., 1977a, Evolution of Yucca Mound complex, Late Pennsylvanian phylloid algal buildup, Sacramento Mountains, New Mexico: American Association of Petroleum Geologists Bulletin, v. 61, p. 2115-2133.

Toomey, D.F., Wilson, J.L., and Rezak, R., 1977b, Growth history of a Late Pennsylvanian phylloid algal organic buildup, northern Sacramento Mountains, New Mexico, *in* Butler, J., ed., Geology of the Sacramento Mountains, Otero County, New Mexico: Midland, TX, West Texas Geological Society Publication 77-68, p. 9-24.

Toomey, D.F., and Winland, H.D., 1973, Rock and biotic facies associated with Middle Pennsylvanian (Desmoinesian) algal buildup, Nena Lucia field, Nolan County, Texas: American Association of Petroleum Geologists Bulletin, v. 57, p. 1053-1074.

Tsien, H.H., 1985, Algal-bacterial origin of micrites in mud mounds, *in* Toomey, D.F., and Nitecki, M.H., eds., Paleoalgology: Contemporary Research and Applications: New York, Springer-Verlag, p. 290-296.

Tsien, H.H., 1994, The role of microorganisms and the origin of micrite components in algal reefs and micrite mounds: Mémoires de l'Institute Géologique de la Université de Catholique Louvain, v. 35, p. 123-135.

Vest, E.L., Jr., 1970, Oil fields of Pennsylvanian-Permian Horseshoe Atoll, west Texas, *in* Halbouty, M.T., ed., Geology of Giant Petroleum Fields - A Symposium: Tulsa, OK, American Association of Petroleum Geologists Memoir 14, p. 185-203.

Wanless, H.R., 1972, Eustatic shifts in sea level during the deposition of Late Paleozoic sediments in the central United States, *in* Elam, J.G., and Chuber, S., eds., Cyclic Sedimentation in the Permian Basin (2nd edition): Midland, TX, West Texas Geological Society Publication 72-60, p. 14-54.

Watney, W.L., French, J.A., and Franseen, E.K., 1989, Sequence Stratigraphic Interpretations and Modeling of Cyclothems: Lawrence, KS, Kansas Geological Society 41st Annual Field Trip Guidebook, 211 p.

Wilson, J.L., 1967, Cyclic and reciprocal sedimentation in Virgilian strata of southern New Mexico: Geological Society of America Bulletin, v. 78, p. 805-818.

Wilson, J.L., 1969, Influence of local structure in sedimentary cycles of Beeman and Holder Formations, Sacramento Mountains, Otero County, New Mexico, *in* Elam, J.G., and Chuber, S., eds., Cyclic Sedimentation in the Permian Basin: Midland, TX, West Texas Geological Society Publication 69-56, p. 100-114.

Wilson, J.L., 1972, Cyclic and reciprocal sedimentation in Virgilian strata of southern New Mexico, *in* Elam, J.G., and Chuber, S., eds., Cyclic Sedimentation in the Permian Basin (2nd edition): Midland, TX, West Texas Geological Society Publication 72-60, p. 82-99.

Wilson, J.L., 1975a, Carbonate Facies in Geologic History: New York, Springer Verlag, 471 p.

Wilson, J.L., 1975b, Regional Mississippian facies and thickness in southern New Mexico and Chihuahua, *in* Pray, L.C., ed., Mississippian Shelf-Edge and Basin Facies Carbonates, Sacramento Mountains and southern New Mexico: Dallas, TX, Dallas Geological Society Guidebook, p. 124-128.

Wilson, J.L., 1977, Regional distribution of phylloid algal mounds in Late Pennsylvanian and Wolfcampian strata of southern New Mexico, *in* Butler, J., ed., Geology of the Sacramento Mountains, Otero County, New Mexico: Midland, TX, West Texas Geological Society Publication 77-68, p. 1-7.

Winchester, P.D., 1976, Carbonate diagenesis and cyclic sedimentation in the Wolfcampian Laborcita Formation of the Sacramento Mountians, New Mexico [unpublished Ph.D. thesis]: Rice University, Houston, TX, 154 p.

Wray, J.L., 1959, Origin of some Pennsylvanian algal bioherms in southwestern United States, Guidebook, Sacramento Mountains, New Mexico: Midland, TX, Permian Basin Section-SEPM, p. 38.

Wray, J.L., 1963, Pennsylvanian algal banks, Sacramento Mountains, New Mexico, Geoeconomics of the Pennsylvanian Marine Banks of Southeast Kansas (27th Annual Field Conference): Lawrence, KS, Kansas Geological Society, p. 129-133.

Wray, J.L., 1968, Late Paleozoic phylloid algal limestone in the United States, International Geological Congress, Report of 23rd Session (Prague), Proceedings of Section 8 - Genesis and Classification of Sedimentary Rocks: Prague, International Geological Congress, Report of 23rd Session (Prague), Proceedings of Section 8, Genesis and Classification of Sedimentary Rocks, p. 113-119.

Wray, J.L., 1975, The puzzling Paleozoic phylloid algae: a Holocene answer in Squamariacean calcareous red algae [abs.]: AAPG-SEPM Annual Meeting Abstracts, v. 2, p. 82-83.

Wray, J.L., 1977, Origin of some Pennsylvanian algal bioherms in southwestern United States [abs.], *in* Butler, J., ed., Geology of the Sacramento Mountains, Otero County, New Mexico: Midland, TX, West Texas Geological Society Publication 77-68, p. 159-161.

Wright, F.W., 1962, Abo reef: prime west Texas target: Oil and Gas Journal, v. 60, p. 188-194.

Wu, Y., and Chafetz, H.S., 2002, ^{13}C-enriched carbonate in Mississippian mud mounds: Alamogordo Member, Lake Valley Formation, Sacramento Mountains, New Mexico, U.S.A: Journal of Sedimentary Research, v. 72, p. 138-145.